

Continuous-Flow Dynamic Dialysis and its
Application to Collagen-Ligand Interactions

by

Neil Arthur Sparrow

A Thesis Submitted to Rhodes University
in Partial Fulfilment
of the Requirements for the Degree of

Doctor of Philosophy

Leather Industries Research Institute,
Rhodes University,
Grahamstown

June, 1982

Acknowledgements

It gives me pleasure to acknowledge my indebtedness to the following people who have most generously contributed to this work.

Professor Leslie Glasser, mentor and supervisor, for his untiring enthusiasm, inspiration and knowledge.

Dr D.Cooper of the Leather Industries Research Institute Grahamstown, for placing at my disposal the facilities of the institute.

Dr A.E.Russell of the Leather Industries Research Institute in the capacity of local supervisor for his advice, valid and appreciated criticism.

Mr M.Lawrie and the staff of the Rhodes University Computer Centre.

Dr P.Terry of the Rhodes University Department of Computer Science for his assistance and advice in all aspects of computer programming.

Professor D.Glasser of the Department of Chemical Engineering of the University of the Witwatersrand, Johannesburg, for his freely given time, knowledge and advice.

Mr D.Bertossi of the Leather Industries Research Institute workshop for fabricating the prototype dialysis cell and subsequent modified versions.

Mrs N.Maher and Mr R.Kohl of the Leather Industries Research Institute for their practical assistance in the laboratory.

Mrs B.Vithal of the Rhodes University Computer Centre for frequent assistance.

Continuous-Flow Dynamic Dialysis and its Application to
Collagen-Ligand Binding

Abstract

Studies undertaken to investigate the binding of low molecular mass analogues of polyphenolic vegetable tannins to collagen have prompted the development of a new method to investigate protein-ligand interactions. This method, the continuous-flow dynamic dialysis method (CFDD), differs from conventional dialysis procedures used for protein-ligand binding studies. In this method, the ligand concentration in the diffusate is monitored automatically at successive closely spaced time intervals while being continuously eluted from the dialysis cell. The primary data obtained by this method consists of a series of spectrophotometric absorbance measurements representing the ligand concentration in the sink compartment of a dialysis cell. This primary data is recorded by means of a data logging device onto a punched paper tape for subsequent computer processing.

Two original methods are presented for analysing the primary data to extract the protein-ligand binding isotherm. The first of these is a direct analysis which relies on Fick's first law of diffusion. In this method it is necessary to establish, by means of a control experiment, a value for the ligand permeation constant. This is used in a subsequent analysis to establish a relationship between the measured rate of diffusion of the ligand from a protein-ligand mixture and the concentration of unbound ligand which is in equilibrium with the protein-ligand complex. The protein-ligand binding isotherm is obtained from parametric equations which give the quantity of ligand bound to the protein and the concentration of unbound ligand in the sample compartment as functions of time.

The second method, which is more general, utilizes the same primary data but is based on establishing a system transfer

function to characterise the dialysis and eluting processes. This analysis depends on the linearity of the system and utilizes numerical Laplace transforms of the primary data sets obtained from control and protein-ligand dialyses. Laplace transforms are used to effect a deconvolution of the transfer function from the primary data and yield the concentration of ligand in equilibrium with the protein-ligand complex. This procedure yields, simultaneously, both the total ligand concentration and the concentration of unbound ligand in the protein compartment of the dialysis cell. These quantities are used to establish the binding isotherm for the protein ligand system. Numerical inversion of the Laplace transforms in this analysis is effected by their reduction to Fourier series.

The experimental reliability of the continuous-flow dynamic dialysis method, and validity of the two analytical methods used to derive a binding isotherm from dialysis data are evaluated from studies of the binding of phenol red to bovine serum albumin (BSA) at 15°, 20° and 25°C, as well as from simulated binding curves generated by the numerical solution of the differential equations used to describe the dialysis and elution process in terms of a two-site Scatchard binding model.

The method is used to investigate the binding to collagen of a series of low molecular mass phenolic compounds which can be isolated from Wattle and Quebracho vegetable tannin extracts. These compounds can be considered as monomeric precursor analogues of the polymeric vegetable tannins. The binding of these ligands to collagen is shown to be characterised by high capacity, low affinity binding in which the uptake of ligand by the protein increases linearly with increasing ligand concentration. Collagen exhibits no indication of site saturation for these ligands over the experimentally accessible concentration ranges investigated.

Contents

| | | |
|---------------------|--|----------|
| Abstract | | iii |
| List of Figures | | xi |
| List of Plates | | xvi |
| List of Tables | | xvii |
| List of Appendices | | xix |
| Glossary of Symbols | | xx |
| | | |
| Chapter One | Ligand Binding to Collagen | 1 |
| | | |
| A | Introduction | |
| | 1.1 Collagen Occurrence | 1 |
| | 1.2 Skin Structure | 1 |
| B | Collagen-Tannin Interactions | |
| | 1.3 Hide-Tannin Affinity | 3 |
| C | Binding Studies on Collagen | |
| | 1.4 Experimental methods | 6 |
| | | |
| Chapter Two | The Chemistry of Collagen and the Vegetable Tannins | 9 |
| | | |
| A | Collagen Chemistry | |
| | 2.1 Scope of Collagen Research | 9 |
| | 2.2 Types of Collagen | 10 |
| | 2.3 Primary Structure | 10 |
| | 2.4 Single-Chain Components | 12 |
| | 2.5 Telopeptides | 12 |
| | 2.6 Fibril Structure | 13 |
| | 2.7 Solubility and Stability in Solution | 19 |
| | 2.8 The Collagen-Gelatin Transition | 19 |
| B | The Chemistry of the Vegetable Tannins and their Monomeric Subunits | |
| | 2.9 Occurrence | 23 |
| | 2.10 Hydrolysable and Condensed Tannins | 24 |

| | | |
|----------------------|--|-----------|
| Chapter Three | Protein-Ligand Interactions | 26 |
| A | Introduction | |
| 3.1 | Information Provided by Protein-Ligand Binding Studies | 26 |
| B | Mathematical Models for Protein-Ligand Binding | |
| 3.2 | Scope of Application | 33 |
| 3.3 | The Site-Binding Model | 37 |
| 3.4 | Stoichiometric Binding Constants | 40 |
| 3.5 | Binding site interaction due to Electrostatic Interaction | 46 |
| 3.6 | Binding site Interaction due to Steric Interference | 49 |
| 3.7 | Binding Site Interaction due to Conformational Change | 49 |
| 3.8 | A Generalized Approach to Equilibrium models | 52 |
| | | |
| Chapter Four | Experimental Methods for Obtaining the Binding Isotherm | 57 |
| A | General Methods | |
| 4.1 | Introduction | 57 |
| 4.2 | Experimental Methods | 58 |
| 4.3 | Direct Methods | 58 |
| 4.4 | Subtractive Methods | 60 |
| 4.5 | Dialysis Methods | 61 |
| B | Principles of Dialysis | |
| 4.6 | The Dialysis Process | 63 |
| C | Factors Affecting the Rate of Dialysis | |
| 4.7 | Factors relating to the Diffusion Process | 64 |
| 4.8 | Factors relating to Membrane Diffusion | 65 |
| D | Applications of Dialysis to Protein-Ligand Binding | |
| 4.9 | The Equilibrium Dialysis Method | 69 |
| 4.10 | Kinetic Dialysis Methods | 75 |

| | | |
|------|---|-----|
| E | The Meyer-Guttman Dynamic Method | |
| | 4.11 Experimental Procedure | 77 |
| | 4.12 Data Analysis | 78 |
| | 4.13 Limitations of the Meyer-Guttman Method | 81 |
| | | |
| | Chapter Five The Continuous-Flow Dynamic Dialysis Method and Data Analysis by the Permeation constant Method | 85 |
| | 5.1 Introduction | 85 |
| A | Experimental Procedures | |
| | 5.2 Apparatus | 86 |
| B | Mathematical Analysis | |
| | 5.3 The Two-Compartment Model System | 88 |
| | 5.4 The Control Dialysis (No protein present) | 90 |
| | 5.5 The Sample Dialysis (Protein present) | 91 |
| | 5.6 Use of Analytical Solutions of the System Differential Equations | 92 |
| | 5.7 Derivation of the Permeation Constant | 93 |
| | 5.8 Mass-Balance Method for Determining the Binding Isotherm | 94 |
| | 5.9 Fixed Initial Ligand Concentrations: A Special Case | 96 |
| C | Evaluating the Method of Analysis | |
| | 5.10 The Use of Synthetic Data | 97 |
| | 5.11 Experimental Evaluation | 99 |
| | 5.12 Computational Methods | 99 |
| | 5.13 Difficulties Associated with the CFDD method | 100 |

| | | |
|--------------------|--|------------|
| Chapter Six | Analysis of CFDD Data Using the System Transfer Function | 102 |
| 6.1 | Introduction | 102 |
| 6.2 | Linear Systems | 103 |
| 6.3 | Time Domain - Frequency Domain Relationships | 104 |
| 6.4 | Parametric Equations of the Binding Isotherm | 107 |
| 6.5 | Problems associated with Fourier Transformation Theory | 108 |
| 6.6 | Laplace Transform and Fourier Series Representation of the Elution Profile | 110 |
| 6.7 | The Unbound Ligand Concentration when Protein is Present | |
| 6.8 | The Total Sample Compartment Ligand Concentration when Protein is Present | 119 |
| 6.9 | The Quantity of Ligand Bound to the Protein | 122 |
| 6.10 | Evaluation of the Fourier Coefficients U_n , V_n , U_n^* and V_n^* | 123 |
| 6.11 | The Evaluation of the Parameters used to generate the Extended Data sets | 125 |
| 6.12 | The Number of Terms used in the Fourier Summation | 127 |
| 6.13 | The Laplace Convergence Parameter | 128 |
| 6.14 | The Gibbs Phenomenon: Effect on the Analysis | 129 |
| 6.15 | Evaluation of the Analysis | 131 |

| | |
|---|-----|
| Chapter Seven Applications | 132 |
| A Methods | |
| 7.1 The Dialysis Apparatus | 133 |
| B Materials | |
| 7.2 The Dialysis Membrane | 138 |
| 7.3 Binding Agents | 138 |
| 7.4 Proteins | 140 |
| C Extraction and Purification of Collagen | |
| 7.5 Extraction | 140 |
| 7.6 Purification | 141 |
| 7.7 Analytical Measurements on Collagen | 142 |
| 7.8 Preparation of Collagen Solutions | 144 |
| 7.9 Evaluation of the Effects of the Experimental Variables | 145 |
| 7.9 Data Treatment | 150 |
| | |
| Chapter Eight Results: Evaluation of the CFDD Method and Data Analysis by the Permeation Constant Method | 154 |
| 8.1 Phenol Red-BSA Interactions at 25 °C | 154 |
| 8.2 Phenol Red-BSA Interactions at 15 & 20 °C | 165 |
| 8.3 Discussion of Results | 170 |
| | |
| Chapter Nine Results: Evaluation of the CFDD Method using the Transfer Function Method of Data Analysis | 175 |
| 9.1 The Dialysis Cell as a Linear System | 175 |

| | | |
|------|---|-------------------------|
| A | Evaluation of the Method Using Hypothetical Data Sets | |
| 9.2 | Generation of Hypothetical Data Sets | 175 |
| 9.3 | The Use of the FFT to Evaluate the System Transfer Function | 177 |
| 9.4 | Use of Laplace Transforms to obtain the System Transfer Function | 182 |
| 9.5 | The Removal of Oscillations arising from the Gibbs Phenomenon | 188 |
| B | Application of the Transfer Function Analysis to Experimentally Determined Elution Profile Data | |
| 9.6 | Phenol Red-BSA Binding Studies at 25 °C | 191 |
| C | Discussion | |
| 9.7 | Comparisons of the Permeation Constant and Transfer Function methods of Data Analysis | 194 |
| | Chapter Ten Results: Application of the CFDD Method to Measure Collagen-Ligand Binding | 199 |
| A | Determination of Collagen-Plant Phenol Binding Isotherms | |
| 10.1 | Results | 199 |
| B | Discussion | |
| 10.2 | Physical Implications of the Collagen-Ligand Binding Isotherm | 207 |
| | Chapter Eleven General Discussion and Conclusion | 217 |
| | Appendices I - IX | pages 222 to 255 |
| | Bibliography | 256 |

List of Figures

| | | |
|------------|---|-----|
| Figure 1.1 | Structures of monomeric subunits of polyphenol tannins | 25 |
| Figure 3.1 | Commonly used transformations of the binding isotherms | 30 |
| Figure 4.1 | Scatchard plots of binding data obtained by fitting theoretical values of $C_1(t)$ from empirical mathematical functions to the general two-site Scatchard model. | 84 |
| Figure 5.1 | The continuous-flow dynamic dialysis cell (schematic) | 87 |
| Figure 5.2 | The continuous-flow dynamic dialysis apparatus (schematic) | 88 |
| Figure 5.3 | A two-compartment model system | 88 |
| Figure 6.1 | The dialysis cell as a linear system | 103 |
| Figure 6.2 | Time domain-frequency domain relationships | 106 |
| Figure 6.3 | Experimental and extended elution profile data sets | 111 |
| Figure 7.1 | The continuous-flow dynamic dialysis cell (plan) | 134 |
| Figure 7.2 | Flow-diagram of numerical procedures to extract the binding isotherm from elution profile data sets | 152 |

| | | |
|-------------|---|-----|
| Figure 8.1a | Elution profiles for the dialysis of phenol red at 25 °C | 154 |
| Figure 8.1b | Log-linear plots of phenol red elution profiles at 25 °C | 155 |
| Figure 8.2 | Variation in the permeation constant with time over the course of the dialysis experiment | 156 |
| Figure 8.3 | Elution profiles of duplicate control dialysis experiments at 25 °C showing the degree of reproducibility | 157 |
| Figure 8.4 | Time dependence of the sample compartment ligand concentrations at 25 °C. | 158 |
| Figure 8.5 | Bjerrum plot of the phenol red-BSA binding isotherm | 160 |
| Figure 8.6 | Linear transformations of the phenol red-BSA binding isotherm | 162 |
| Figure 8.7 | Variation of the phenol red permeation constants over the course of the dialysis at 15 and 20 °C | 165 |
| Figure 8.8 | Temperature dependence of the mean permeation constant for phenol red through Visking dialysis membrane | 167 |
| Figure 8.9 | Graph of $\log_{10} [D^*]$ vs $1/T$ | 168 |

| | | |
|-------------|---|-----|
| Figure 8.10 | Elution profiles and binding isotherms for phenol red to BSA at 15 & 20 °C | 169 |
| Figure 8.11 | Uncertainty in the phenol red-BSA binding isotherm at 25 °C | 173 |
| Figure 9.1 | Elution profiles and log-linear plots of the elution profiles to demonstrate the linearity of the dialysis cell | 176 |
| Figure 9.2 | Theoretical data sets used to evaluate the transfer function method of data analysis | 178 |
| Figure 9.3 | The phenol red-BSA binding isotherm obtained using the FFT algorithm to obtain the dialysis cell system transfer function | 179 |
| Figure 9.4 | The system transfer derived by the FFT algorithm | 180 |
| Figure 9.5 | The elution profile and log-linear plots of the elution profile showing the extension of the data sets by means of monoexponential decay function for the phenol red-BSA system | 183 |
| Figure 9.6 | Sample compartment ligand concentration vs time curves derived from the extended data sets of the elution profile | 184 |
| Figure 9.7 | The impulse response function | 185 |

- Figure 9.8 Sample compartment ligand concentrations curves and phenol red-BSA binding isotherm extracted from the extended data sets using values for the monoexponential parameters chosen to give the correct value of the total integral for $c_2^*(t)$ 187
- Figure 9.9 The phenol red-BSA binding isotherm re-extracted from the elution profile data sets by the transfer function method (data not smoothed) 187
- Figure 9.10 The effectiveness of the Lanczos sigma factors in smoothing the ligand escape curves and binding isotherm data 188
- Figure 9.11 The effectiveness of the Krylov ramp subtraction technique for removing the Gibbs phenomenon effects 189
- Figure 9.12 The effect of the number of terms in the Fourier series on the sample compartment ligand concentration and on the binding isotherm 190
- Figure 9.13 Comparison of the sample compartment ligand concentrations provided by the 'Permeation constant' and 'transfer function' methods of data analysis 191
- Figure 9.14 The influence of the Laplace convergence parameter on the sample compartment ligand concentrations and the binding isotherm 192

| | | |
|-------------|---|-----|
| Figure 9.15 | The power function of the transfer function | 193 |
| Figure 9.16 | The Fourier transform and power spectrum of the Fourier coefficients of the elution profile | 194 |
| Figure 10.1 | The variation of the permeation constants for the dialysis of the tannin precursor ligands at 15 °C with time | 202 |
| Figure 10.2 | Binding isotherms of the interaction of collagen to the plant phenols at 15 °C | 203 |
| Figure 10.3 | Bjerrum plots of the collagen-phenolic binding isotherms | 204 |
| Figure 10.4 | Scatchard plots of the collagen-phenolic ligand binding isotherms | 206 |

Appendix IV

| | | |
|-----------|---|-----|
| Figure i | The effect of the number of terms in the Fourier series on the Gibbs phenomenon associated with a discontinuity | 229 |
| Figure ii | (a) $\text{Log } [P_n^t]$ & $\text{Log } [P_n^t]$ vs $\text{Log } N$ | 233 |
| | (b) $1/P_n^t$ vs N | 233 |
| | (c) P_n^t vs $1/N$ | 233 |

List of Plates

| | Page |
|---|------|
| I Vertical cross-section of calf-skin | 2 |
| II Native type collagen fibrils | 14 |
| III Fibrous long spacing collagen fibrils | 15 |
| IV Segment long spacing collagen aggregates | 16 |
| V Dimorphic ordered aggregate of tropocollagen | 18 |
| VI Disruption of collagen fibrils by lyotropic agents | 21 |
| VII The continuous-flow dynamic dialysis cell | 135 |
| VIII The complete apparatus for investigating protein-ligand interactions by continuous-flow dynamic dialysis | 136 |
| IX Ultracentrifuge Schlieren pictures showing sedimentation of collagen in phosphate buffer, 0.11×10^{-2} M dihydroquercetin and 0.5 M urea | 213 |
| X Ultracentrifuge Schlieren pictures showing sedimentation of collagen in 0.4×10^{-2} M gallic acid, 0.1×10^{-2} M haematoxylin and 0.2×10^{-3} M phenol solutions | 214 |

List of Tables

| | | |
|-------------|---|-----|
| Table 7- I | Amino acid analysis of collagen extracted from calf-skin | 142 |
| Table 8- I | Initial phenol red concentrations used in successive dialysis experiments to determine a composite phenol red-BSA binding isotherm | 159 |
| Table 8- II | Equivalent mathematical transformations of the protein-ligand binding isotherm | 161 |
| Table 8-III | Comparison of the binding parameters for the phenol red-BSA interaction at 25 °C by the CFDD method with values obtained by other methods | 163 |
| Table 8- IV | A statistical re-analysis of binding isotherm data reported in the literature using the STEPIT regression routine to obtain values for the approximate errors | 164 |
| Table 8- V | Variation of the permeation constant and diffusion coefficient for phenol red through Visking dialysis membrane | 166 |

| | | |
|--------------|--|-----|
| Table 10- I | Experimental data for the dialysis of certain monomeric tannin precursors at 15 °C | 200 |
| Table 10-II | Permeation constants for certain monomeric tannin precursors at 15 °C | 201 |
| Table 10-III | Coefficients for the linear equation $\bar{v} = A_1C + A_0$ fitted to the binding isotherm data by regression analysis | 205 |

List of Appendices

| | | | |
|----------|------|---|-----|
| Appendix | I | The significance of back-diffusion in continuous-flow dynamic dialysis | 221 |
| Appendix | II | The calculation of the correction factor for the sink compartment volume of the dialysis cell, to correct for the change in volume due to membrane distension | 224 |
| Appendix | III | The Special Case: $n = 0$ in the Laplace transform of the mass-balance relationship between the sample and sink compartment ligand concentrations | 226 |
| Appendix | IV | The Krylov technique for removing oscillations due to the Gibbs phenomenon associated with the discontinuity at $t = 0$ in Fourier series representation of the sample compartment ligand concentration | 228 |
| Appendix | V | List of computer programs | 236 |
| Appendix | VI | FORTRAN program GAMMA | 238 |
| Appendix | VII | FORTRAN program DELTA | 243 |
| Appendix | VIII | FORTRAN program ZETA | 251 |
| Appendix | IX | FORTRAN program ETA | 253 |

Glossary of Symbols

| | |
|----------------------------------|--|
| a, b | : Exponential decay parameters in analytical expressions for the elution profile |
| A_n, B_n | : Fourier coefficients of Fourier series representation of the impulse response function |
| $C_1(t), C_1^*(t)$ | : Sample compartment ligand concentrations for the control and sample dialyses respectively |
| $C_1(t), C_1^*(t)$ | : Sink compartment ligand concentrations for the control and sample dialyses respectively |
| $C_q(t)$ | : Total sample compartment concentration (i.e., free and bound to the protein) |
| D | : The ligand permeation constant |
| E_n, H_n | : Fourier coefficients of the Fourier series which represents the variation of the permeation constant with time |
| F | : The eluting buffer flow rate |
| F, F^{-1} | : (Bold type) The Fourier and Inverse Fourier transform operators |
| $g_1(t), g_1^*(t)$ | : Sample compartment ligand concentrations derived from the product of the Laplace convergence function, $e^{-\alpha t}$, and the mass balance expression for the sample compartment ligand concentration |
| $g_1^t(t)$ | : The total sample compartment ligand concentrations derived from the product of the Laplace convergence function, $e^{-\alpha t}$, and the mass balance expression for the total sample compartment ligand concentration |
| $g_2(t), g_2^*(t)$ | : The functions defined as the product of the Laplace convergence function, $e^{-\alpha t}$, and the elution profiles for the control and sample dialyses respectively |
| $G_1(s), G_2(s)$ & $G_2^*(s)$ | : The Laplace transforms of $g_1(t), g_2(t)$ and $g^*(t)$ respectively |

| | |
|-------------------------------|--|
| k_i | :Binding constants used in the site binding model |
| K_i | :Binding constants used in the stoichiometric binding model |
| L | :Ligand concentration |
| $\mathbf{L}, \mathbf{L}^{-1}$ | :(Bold type) The Laplace and inverse Laplace transform operators respectively |
| p | :protein concentration |
| P_n, Q_n | :Fourier coefficients of the Fourier series |
| P_n^*, Q_n^* | :representation of sample compartment ligand concentrations as functions of time |
| P_n^t, Q_n^t | :Fourier coefficients of the Fourier series representation of the total ligand concentration in the sample compartment as a function of time |
| s | :Complex frequency term $s = \alpha + i\omega$ |
| $\tilde{v}(t)$ | :The ligand-protein molal binding ratio (i.e., mol ligand bound per mol protein) |
| U_n, V_n | :Fourier coefficients of the times series |
| U_n^*, V_n^* | :representation of the elution profiles for the control and sample dialyses respectively. |
| V_1, V_2 | :Sample and sink compartment volumes respectively |

Greek Symbols

| | |
|------------|--|
| α | :The Laplace convergence parameter |
| β | :Factor for varying the duration of the extended elution profile data sets |
| ϵ | :Molar extinction coefficients |
| λ | :Absorbance wave length |
| ω | :Frequency in Fourier and Laplace transforms |
| τ | :Dummy parameter used in integration |

Chapter One

Ligand Binding to Collagen

A Introduction

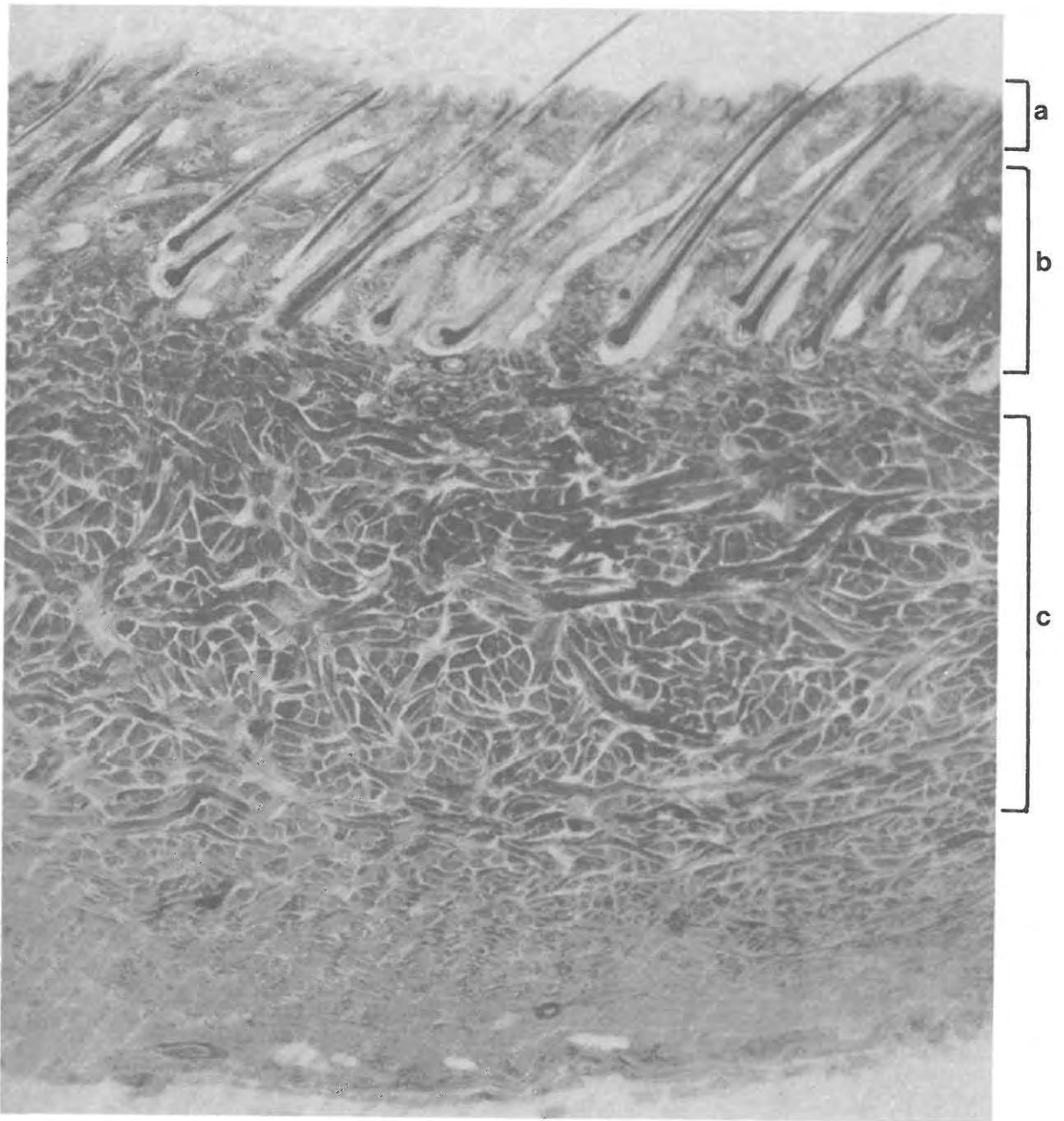
1.1 Collagen Occurrence

The collagens comprise a group of closely related proteins which occur widely throughout the animal kingdom. These proteins form the principal fibrous component of the skin, cartilage and tendon and are found in soft basement membrane and connective tissue. Calcified forms of collagen constitute the hard tissue of bone and the dentine of the teeth. The role of the collagens in nature is essentially a structural one and, as a consequence, this group of proteins displays a variety of unusual properties which distinguishes them from the globular proteins and the keratins. It has been estimated (Bear, 1952) that collagens make up 30% of the total organic matter of mammals and nearly 60% of their total protein content.

1.2 Skin Structure

In the skin (Plate I) collagen fibres are to be found in the corium minor or papillary layer, and in the fibrous network of the corium major of the dermis. The corium minor consists of mainly collagen fibres, some reticulin and a loose network of elastin. In this layer, the collagen fibrils are very closely packed. The corium minor passes almost imperceptibly into the fibre network layer of the corium major which consists almost entirely of collagen fibrils. The collagen fibrils of the corium major are organised into wavy bundles which interpenetrate to form a complex three-dimensional weave. The fibrils are mostly cylindrical in form with a uniform diameter of 100 nm. In the closely packed region of the papillary layer the fibrils broaden slightly and assume an hexagonal rather than circular cross-section.

Plate I



A vertical cross-section of calf-skin (magnification x 15)
showing (a) the epidermis, (b) the papillary layer and
(c) the corium major

(From Turley, 1926)

B Collagen-Tannin Interactions

1.3 Hide-Tannin Affinity

In leather manufacture, to convert the raw hide into leather, the skin collagen is made to interact with a variety of low molecular mass compounds. These compounds include biocides, bating agents, filling agents, lyotropic agents, surfactants, tanning agents and dyestuffs. Collagen-ligand interactions, because of their relevance to leather technology, are therefore of considerable economic importance.

The interactions with superficially adsorbed or penetrating dye-stuffs, and tannage with synthetic or vegetable tannins are probably the most important of these interactions. Tanning agents stabilize the hide against bacterial attack by introducing cross-links between the individual collagen molecules which make up the fibrous network of the dermis. In the vegetable tanning process, which is used to manufacture sole-leather, these cross-links are formed through the interaction of collagen and the polyphenolic constituents of vegetable tannin extracts. The polyphenolic tanning agents are multifunctional and form cross-links by bridging active binding sites on the collagen molecules.

The formation of cross-links produces marked changes in the physical properties of the hide and constitutes the fundamental process in the manufacture of vegetable tanned leather. However, despite its commercial exploitation and a history which extends to paleolithic times, many aspects of the vegetable tanning process are only partially understood. The complex nature of both the skin and the tanning materials obscures the fundamental details of the nature and mechanism of collagen-tannin interactions.

Solutions of vegetable tannin extracts are colloidal and are complex mixtures of polymeric compounds. Vegetable tannage, besides depending on hide-tannin affinity, also relies on the

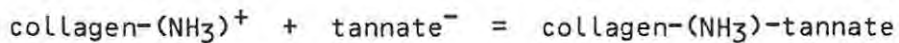
physical occlusion of colloidal particles of the tanning agent within the hide fibre matrix. These occluded particles act as a filling agent. The term tan-fixation is used to denote the permanency of the hide-tannin complex without specific regard to the nature of the hide-tannin interaction. Tan-fixation is influenced both by the ability of the tanning agent to penetrate into the hide fibre matrix and by its affinity for the hide collagen. Thus, besides chemical considerations, the physical properties of the hide also control tan-fixation. The accessibility of the binding sites on the collagen molecules depends on the degree of compactedness or looseness of the hide fibres. This, in turn, depends on the degree of hydration, the extent of swelling, pH, and the presence or absence of inorganic salts. Hydration and low pH cause the hide fibres to swell, and this adversely affects the penetration of the tanning agent. In addition to affecting the extent of swelling of the hide, pH also influences the hide-tannin affinity. Inorganic salts, which are used to suppress the acid-swelling, can also alter the intrinsic affinity of the hide for the tanning agent. The non-tannins of the vegetable tannin extracts can also indirectly affect the extent of tan-fixation; the hide-tannin affinity will be influenced by the quantity of organic acids present in the non-tannin components of the tannin extract.

Vegetable tannin fixation is greatest in acid solution with a pH between 2.5 and 3.5. As the pH is increased, the hide-tanning agent affinity decreases to a minimum at the isoelectric point (about pH 4). Further increase in pH causes the hide-tanning agent affinity to rise to a minor maximum near pH 7, which is followed by a further fall as the tanning solution is made alkaline.

The delicate balance between the affinity of the hide for the tannin and the ability of the tannin to penetrate into the hide matrix is shown by 'case-hardening'. This occurs under acid conditions where the tanning agent adheres to the outermost layers of the hide and impedes penetration of further tanning agent into the core of the hide which, consequently, remains

untanned. Thus, a judicious blending of acids and salts is necessary to achieve the desired level of penetration and fixation of the tanning agent.

The change in affinity for tanning agent with change in pH has been attributed to the variation in the charge profile on the collagen (Reed, 1966; Kühn, 1968). However, many aspects of the vegetable tanning reaction are still matters for speculation. In terms of the Proctor-Wilson theory (Proctor & Wilson, 1916), the collagen-tannin reaction involves an ionic mechanism which can be represented by:



In support of this theory, it has been observed that fixation of the tanning agent is greatly reduced by chemical action which removes or inactivates the positively charged ionizing groups on the protein. Such treatment, however, does not eliminate tan-fixation entirely. This indicates that other factors besides the ionic mechanism are involved in the tanning process. Efforts to distinguish between different modes of binding and to determine to what extent the collagen-tannin interaction involves an ionic mechanism, or is the result of physical occlusion and/or adsorption, also pose questions as to the nature and identity of the groups on the collagen fibres which participate in cross-link formation. A knowledge of the relative importance and contribution of each mode of bonding to the tanning process is of both academic and practical interest.

Binding between collagen and the tanning agent can include hydrogen bonding, hydrophobic bonding, and van der Waals attractions. It can be accepted that the binding of the tannin to the hide protein involves hydrogen bonding to the peptide bonds of the protein as well as polar interactions through active side-chain residues.

The role of hydrophobic bonding and its contribution to protein-tannin affinity is less clear-cut. At any rate, hydrophobic binding forces will only operate when, as a result of ionic attraction, the tannin has been brought into close proximity to the protein. The role of hydrophobic bonding in collagen fibril formation has been the subject of a recent review by Suarez et al. (1980). In addition to the secondary forces mentioned, there is the possibility that primary or covalent bonds between collagen and the tanning agent can be formed. Such covalent cross-links can result from Mannich-type reactions between basic side-chain residues of the protein, such as lysine or hydroxylysine, and quinone or aldehyde groups formed by partial oxidation of the phenols in the tanning agent. However, the vegetable tanning reaction is to a large extent reversible. This indicates that the participation by covalent binding in vegetable tanning is small.

C Binding Studies on Collagen

1.4 Experimental Methods

Experimental methods for the study of binding of low molecular mass ligands to soluble collagen, and to proteins in general, is the subject of the investigation reported in this thesis. Further, the interactions between collagen and certain low molecular mass plant phenols, which occur together with the polyphenolic tannins in vegetable tannin extracts, have been studied to provide some insight into the complexities of the vegetable tanning process. These low molecular mass plant phenols can be considered as the monomeric precursors of the polyphenol tannins. Thus their interaction with soluble collagen can be assumed to represent a simplification of the more complex hide-tanning agent interaction. It was anticipated that the results of binding studies, namely measurement of the protein-ligand association constants for the different classes of binding sites, would provide information about the nature of the

different classes of binding sites on collagen. From such information inferences about the relative contributions of the different modes of binding of the ligands to collagen can be made.

Binding studies on soluble collagen have not been undertaken to any great extent until fairly recently. A dissuasive factor has been the ready tendency of collagen to precipitate from solution. The formation of collagen fibrils while binding is being investigated provides an unwanted complication to the interpretation of experimental data. Fibrillogenesis can result from protein-ligand binding, or from changes in the collagen solution environment due to alteration of the pH or ionic strength.

Formerly, binding studies on insoluble fibrous collagen were carried out by measuring the ligand uptake by collagen from solutions containing different ligand concentrations. The insoluble collagen used in these studies was usually in the form of hide powder, limed or dried hide strips, or tendon. While such methods may be adequate for technical purposes, and do avoid complications in the interpretation of data due to fibrillogenesis, they are not very sensitive. At a more fundamental level, where binding studies are undertaken to investigate cooperativity phenomena or to differentiate between different classes of binding sites, this method is unsatisfactory.

Not only does the method ignore surface or interface phenomena, the results may be inconclusive because potential binding sites might not be utilized due to an inability of the ligand to penetrate into the fibre matrix of insoluble collagen. Problems arising from the inaccessibility of binding sites due to close packing of hide fibres, or dependence on the degree of hide hydration or the colloidal nature of the tanning agent are eliminated by carrying out the binding studies on soluble collagen.

More recently, binding studies on lathrytic soluble collagen (i.e., collagen which has fewer cross-links between fibres than

normal, a condition which can result from genetic defects or deficiency diseases, or can be induced by continued ingestion of chemical lathrogens such as β -propionitrile), have been reported using an equilibrium dialysis method (Deshmukh & Nimni, 1969, 1971). Kanfer (1976) has used a dynamic dialysis method to investigate the reactions and binding of anti-inflammatory corticosteroids to soluble collagen. Kanfer was able to delay sufficiently the onset of collagen fibrillogenesis (by the judicious selection of solution pH and ionic strength) to be able to undertake binding studies on soluble collagen. The dynamic dialysis technique used by Kanfer was very similar to a technique first reported by Meyer & Guttman (1968, 1970a, 1970b) to measure drug-protein binding.

A modification of the Meyer & Guttman dynamic dialysis procedure has been developed in the present study to measure the binding of the monomeric plant phenolic compounds to collagen. The method, however, is a much more general method which is applicable to most protein-ligand systems. It has several advantages over the classical equilibrium dialysis method (Klotz et al., 1946) and other dialysis methods which have been reported.

This method, which is here termed the continuous-flow dynamic dialysis method, utilizes a two-compartment dialysis cell. The protein-ligand mixture in the upper sample compartment is separated by a semi-permeable membrane from a lower sink compartment through which a constant flow of eluting buffer is maintained. The ligand concentration in the sink compartment is monitored at closely spaced intervals, and recorded automatically, to provide data from which a protein-ligand binding isotherm can be obtained. In this study, the experimental method and two different procedures by which the experimental data can be analysed to derive the binding isotherm are described.

Chapter Two

The Chemistry of Collagen and the Vegetable Tannins

A Collagen Chemistry

2.1 Scope of Collagen Research

The chemistry and biology of collagen have been studied extensively and, as a result, a vast and comprehensive literature relating to collagen structure, function, biosynthesis, metabolism and pathology has accumulated. Publications dealing with various aspects of the chemistry, biology and pathology of collagen are becoming increasingly specialised. A comprehensive account of the chemistry and structure of collagen is contained in the 'Treatise on Collagen', Volume I, edited by Ramachandran (1967). More recently published reviews which deal extensively with developments in collagen research subsequent to the 'Treatise on Collagen' include those by Baily (1968), Traub & Piez (1971), Bailey (1975), Arridge (1977), Jackson (1978), and Viidik & Vuust (1980).

A broad coverage of the biology, biosynthesis and pathology of collagen is provided in Volumes II Parts A & B of the 'Treatise on Collagen', edited by Gould (1968). This has been supplemented by the more recent and extensive survey of collagen biochemistry edited by Ramachandran and Reddi (1976). A more recent publication is the review on structure and function of collagen by Piez (1980), which provides a comprehensive coverage of the present developments in collagen research.

Aspects of the chemistry of collagen which are relevant to protein-ligand binding, and which relate mainly to collagen structure, solubility, stability in solution, and crosslink formation are reviewed briefly in this chapter.

2.2 Types of Collagen

There are slight species differences in collagen amino acid sequences and content, as well as differences in collagens extracted from different tissues in the same organism. A variety of collagen types which appear to be genetically distinct forms are designated collagen I, II, III and IV (Miller & Matukas, 1969). The distribution of these various forms of collagen is not uniform and the relative proportions of each type to be found in collagen extracts will vary according to the tissue from which the collagen has been extracted.

Type I collagen is the major collagen of the skin, and the only collagen of tendon and bone. Type II collagen is specific to hyaline cartilage. Type III collagen (Miller et al., 1971) is a minor constituent of the skin, but a major component of the walls of large blood vessels. Type IV collagen, which differs most markedly from the other three types, has a large non-collagenous component which contains a heteropolysaccharide and disulphide links (Olsen et al., 1973; Trueb et al., 1980).

2.3 Primary Structure

Amino acid sequencing of collagen, as a consequence of the large number of different types of collagen, is an on-going process. A review of early amino acid sequence studies on collagen has been provided by Hannig & Nordwig (1967). The more recent review by Miller & Matukas (1974) deals with the primary structures of the various types of collagen. Present knowledge relating to sequencing of different species of collagen is summarised in the 'Atlas of Protein Sequence and Structure' and its supplements (Dayhoff, 1972 - 1976).

Molecular mass and amino acid analysis studies indicate that 'tropocollagen', the soluble monomer and associating unit of collagen fibrils, consists of about three thousand amino acids residues, of which some 33% are glycine, 15% are proline and (usually) about 14% hydroxyproline. Sequence studies on the cyanogen bromide peptide fragments have shown a consistent

repetition of the gly-X-Y triplet, in which the residues designated by X and Y are frequently the imino acids proline and hydroxyproline. The tripeptide units gly-pro-R, where R is an amino other than proline or hydroxyproline, make up 35% of the collagen structure, and 75% of the proline in collagen is found in gly-pro-R links (Grassman, 1961).

Certain modifications to the side-chain residues of the amino-acids, which include hydroxylation of proline and lysine, glycosylation and aldehyde formation resulting from de-amination of lysine residues, occur after assembly of the collagen (Udenfriend, 1970; Prockop, 1973).

From chromatographic evidence, which shows that denatured collagen can be separated into three single-chain components, from amino acid analyses which show every third amino acid to be a glycine residue, and from X-ray diffraction studies, collagen was inferred to have a triple helix structure (Rich & Crick, 1955; Ramachandran, 1955). The triple helix structure consists of three non-coaxial helices, each with three residues per turn, arranged about a common central axis. Such an arrangement can accommodate a close-packing of the helical chains if the chains are staggered with respect to the glycine residues. The imino acids impart a stability to the structure by restricting the possibility of rotation about the bonds of the individual chains, and prevent the structure from collapsing. In addition, the strategically situated imino acids, by virtue of their rigid structures, provide a necessary helical curvature to the individual strands. The three strands comprising the triple helix are considered to be held together predominantly by a regular sequence of cooperative hydrogen bonds.

Collagen is a glycoprotein and has a glucosyl-galactosyl moiety attached to a hydroxylysine residue at position number 105 in the α_1 chain (nomenclature described in paragraph 2.4). The function of the carbohydrate at this position is not understood. It could serve as an anchor point for glycoprotein attachment to mucopolysaccharide tissue components such as chondroitin (Bailey et al., 1970).

2.4 Single Chain Components

Chromatographic evidence shows collagen to contain two types of single strand chains, the a-chains. These are designated a₁ and a₂ and occur in the ratio 2:1. The a₁ and a₂ chains, though not identical in composition, are similar to each other and have molecular masses in the range $9.2 - 9.5 \times 10^4$, and consist of about one thousand residues each.

Besides the a-single chain components, double chain b-components, triple-chain, and yet higher molecular mass components can be separated from denatured collagen by carboxymethylcellulose chromatography. This indicates the presence of covalent cross-links between the individual a-chains. These cross-links are formed by Mannich-type bond formation between lysine or hydroxylysine subunits of one a-chain and aldehyde groups formed by deamination of lysine or hydroxylysine groups on a second a-chain. Recently published reviews which deal with the isolation and chemistry of the cross-links in collagen are by Harlan et al. (1977), McClain (1977), and Fujii & Tanzer (1976).

2.5 Telopeptides

Amino acid sequence studies (Schmitt et al., 1964) show that, in both the a₁ and the a₂ chains, the first ten to fifteen residues from the N-terminal end do not have glycine at every third position. Since this is an absolute requirement for a collagen-type helical structure, it has been concluded that this portion of the molecule is non-helical. Similar evidence (Stark et al., 1971) indicates that short segments at the C-terminal end of the tropocollagen molecule are also non-helical. These regions, referred to as the telopeptides, are believed to be involved in cross-link formation between the a-chains, and to be responsible for the antigenic properties of collagen (Bornstein & Nesse, 1970; Furthmayr et al., 1971).

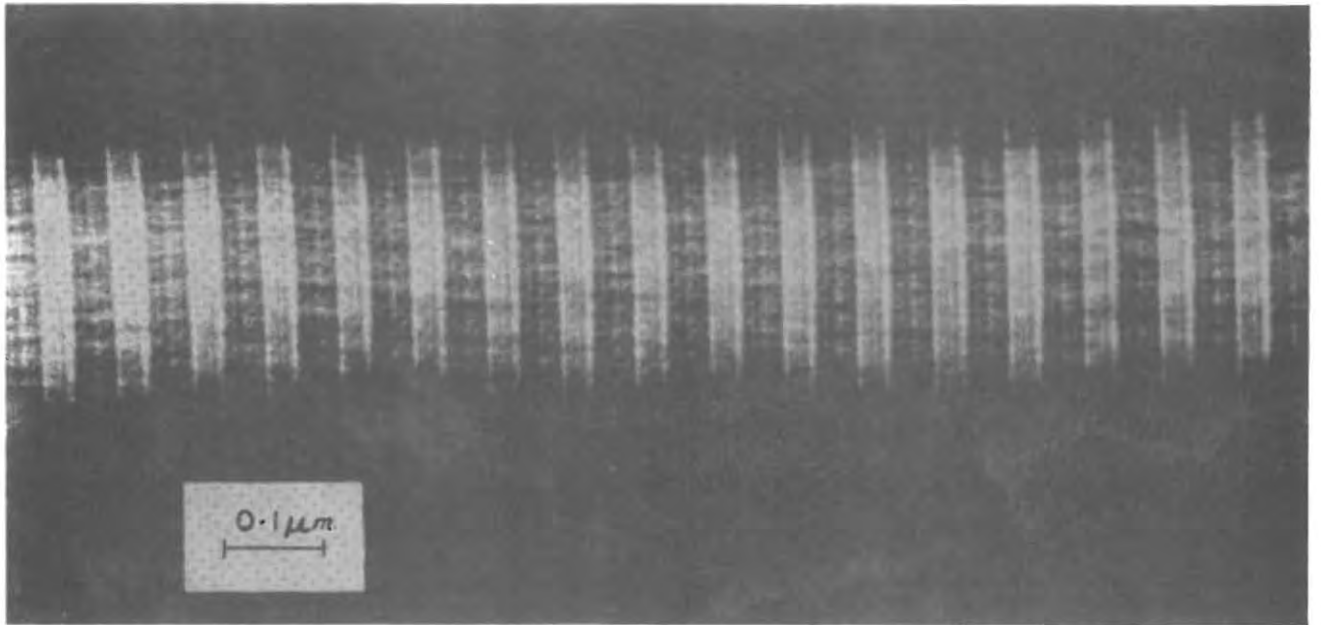
The term procollagen (Prockop, 1973) has been used to describe a collagen precursor which contains additional peptide extensions. These extensions are believed to render the procollagen soluble and prevent fibril formation during its biosynthesis (Fessler et al., 1975).

2.6 Fibril Structure

Tropocollagen molecules, 300 nm by 1.5 nm, are assembled in the fibroblasts. After extrusion from the cell, these molecules assemble spontaneously into cylindrical fibrils having fairly uniform diameters, which can vary from 5 nm to 200 nm depending on the nature and age of the tissue. Low-angle X-ray diffraction studies show the fibrils to have a repeat distance of 64 nm for dry collagen and 70 nm in the wet state. These fibrils, when stained with phosphotungstate or uranyl ions, show an asymmetric band pattern, or periodicity, under electron microscope examination (Gross & Schmitt, 1948). Collagen fibrils reconstituted from acid solution by the addition of salt or by dialysis against neutral phosphate buffer, and similarly stained, show the same banded structure when viewed under the electron microscope. These fibrils are referred to as native-type fibrils (Plate II).

In addition to the native-type aggregation mode, collagen fibrils with a repeat unit several times the length of the native fibril repeat unit can be formed. These consist of the fibrous long spacing (FLS) form which has a centrosymmetric band pattern (Plate III), and the segment long spacing form (SLS) (Plate IV), which is comparable in length to the FLS type but has an asymmetric band pattern. The FLS form is produced when soluble collagen is precipitated from solution by glycoprotein or chondroitin sulphate (Highberger et al., 1950; 1951). The SLS type is produced by precipitating soluble collagen with adenosine triphosphate or tripolyphosphoric acid (Schmitt et al., 1953). The three forms of fibrils are readily interconvertible by dissolution and readjustment of the solution environment (Gross et al., 1954). It is also possible to obtain outgrowths of SLS segments onto the native type fibrils by exposing reconstituted native-type fibrils to a solution of tropocollagen and ATP at a

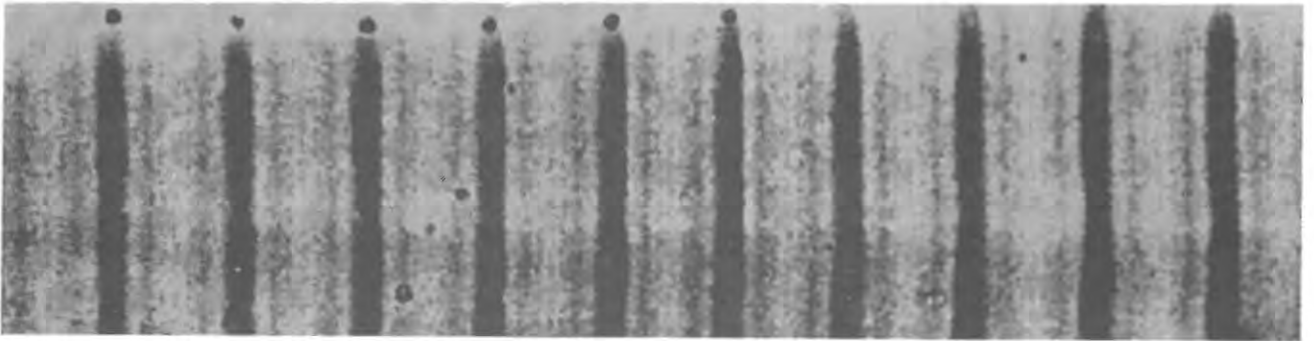
Plate II



Native type fibril from rat-tail tendon seen in negative contrast using sodium phosphotungstate, pH 7.0, as the contrast medium (magnification x 75 000)

(Hodge et al., 1965)

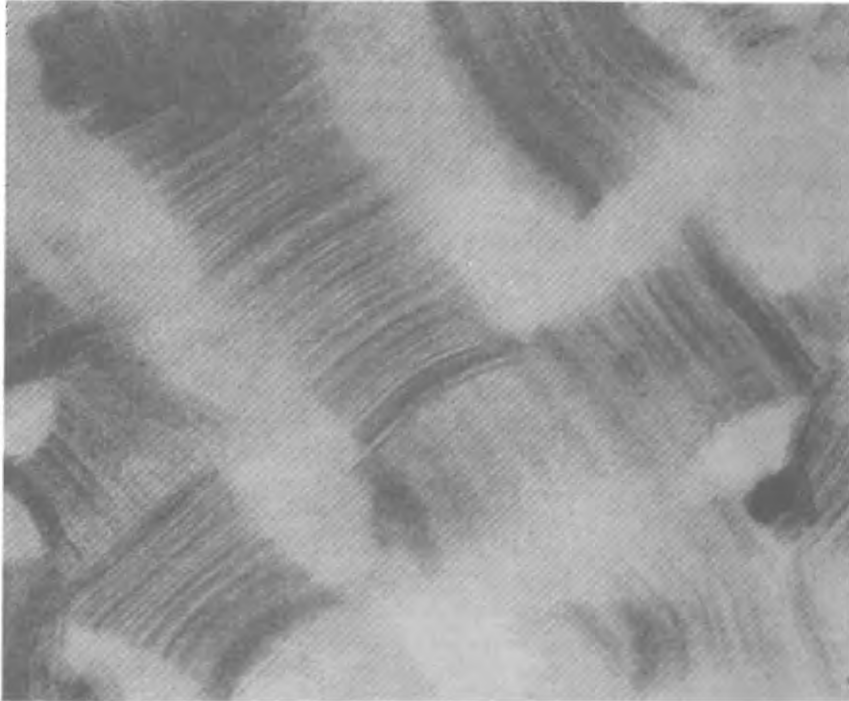
Plate III



Fibrous long spacing type fibril of calf-skin collagen
stained with phosphotungstic acid (the FLS fibrils were
produced by dialysis against distilled water from an acid
solution with added serum glycoprotein)

(magnification x 60 000)

(Hodge, 1967)

Plate IV

Segment long spacing collagen aggregates produced by the addition of 1% adenosine triphosphate solution to a tropocollagen solution (magnification x 120 000)

(Bowden, Chapman & Wynn, 1968).

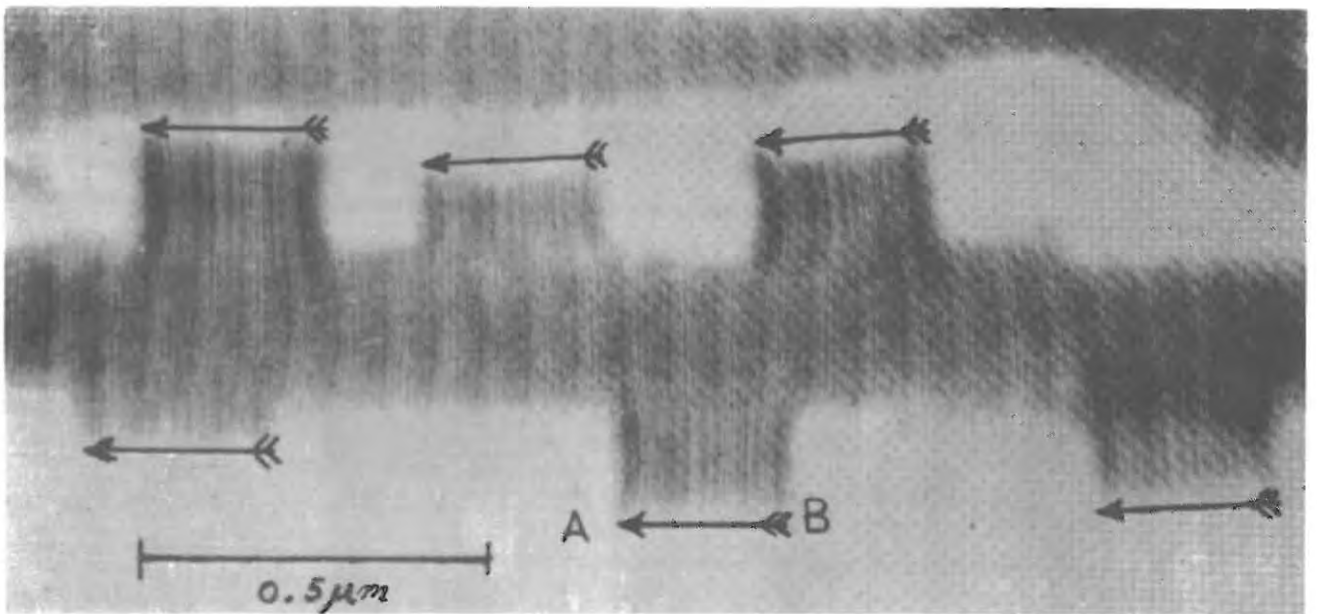
pH which favours the formation of SLS type aggregates. Electron micrographs of such stained fibrils (Plate V) show a direct continuity of the band patterns across the two fibril types. The SLS outgrowths on the native fibrils always exhibit a characteristic orientation with respect to the asymmetric pattern of the native type fibrils. The banded patterns of stained native collagen indicate that the surface of the molecule is divided into alternating zones of ionic and neutral side-chain residues. The bands represent the distribution of polar and apolar side-chain groups from the N- to C- terminal ends of the molecule.

Detailed studies of the band pattern show that the length of the tropocollagen molecule, taken to be the length of an SLS crystallite, is 4.4 times the repeat period of the native fibril. It was postulated (Hodge & Schmitt, 1960), that the FLS form consists of tropocollagen fibrils which have coincident ends, packed in antiparallel array, whereas in the SLS form, where the fibrils also have coincident ends, they have a parallel orientation.

On the basis of detailed studies, it has been proposed (Veis et al., 1967) that the native fibrils are composed of tropocollagen molecules which are displaced with respect to their nearest neighbours by one quarter of their length. This is referred to as the quarter stagger arrangement. According to this proposal, the fibrils are composed of tetrads of tropocollagen molecules in which there are regions of overlap interspersed with holes. In the fibrils these tetrads of tropocollagen molecules are linked together in head to tail fashion by cross-links in the regions of overlap.

It has been suggested (Piez et al., 1970; Morgan et al., 1970) that the carbohydrate situated on the hydroxylysine residue of the α_1 chain could play a role in determining the quarter stagger alignment of the tropocollagen molecules in the tetrads of the collagen fibrils. A recently published review of collagen primary and higher level structure is that of Piez & Trus (1979).

Plate V



Dimorphic ordered aggregate of tropocollagen produced by exposing reconstituted native-type fibrils to a solution containing tropocollagen molecules and ATP at a pH value favouring the formation of SLS type aggregates.

(Stained with phosphotungstic acid, magnification x 55 000)

(Hodge & Schmitt, 1960)

2.7 Solubility and Stability in Solution

Although largely insoluble in neutral aqueous solvents, it is possible to extract a proportion of collagen from the skin and connective tissue in the cold using acidic buffer solutions (acetate, tartrate and citrate) and/or neutral salt solutions, e.g., sodium chloride or calcium chloride. In terms of solubilization, collagen is classified as acid-soluble (ASC), neutral-salt soluble (NSC) or insoluble (ISC). All three types are essentially similar soluble precursor forms of the same basic material. Differences in solubility arise only with respect to degrees of incorporation into the insoluble fibres and extent of cross-link formation within molecular chains and between the individual monomeric soluble collagen units (Pinto & Bentley, 1974).

It has been proposed (Veis et al., 1959) that the rodlike tropocollagen repeating units associate laterally to form insoluble fibrous collagen. The repeating units are held together in aggregates in the polymeric network of the fibrous tissue by a variety of covalent bonds, polar and non-polar bonds. The solubility of collagen thus depends on the number of covalent bonds formed on maturation. A decrease in the solubility of collagen with the age of the tissue can be attributed to an increase in the number of covalent cross-links which form as the tissue ages (Pinto & Bentley, 1974). Even insoluble collagen can, however, be further solubilized without disruption of the peptide links by more drastic treatment with lyotropic agents such as urea, guanidine hydrochloride, or potassium thiocyanate. Such treatment does, however, cause denaturation of the triple helix structure.

2.8 The Collagen-Gelatin Transition

Collagen may be denatured and solubilized on treatment with hot water, when gelatin is formed. The collagen-gelatin transition occurs over a narrow temperature range. The transition

temperature represents the so-called melting temperature, and is the temperature at which the regular triple helix structure collapses into a random coil denatured form. The transition temperature for the collagen-gelatin conversion is a measure of the stability of the helical structure, and can be monitored by measuring changes in the optical rotation or viscosity as a function of temperature. The transition temperature depends on a number of parameters which include the rate of heating, solvent composition, amino-acid composition of the collagen, the degree of cross-linking, and the magnitude of specific interactions between collagen and solvent components.

Transition temperature measurements show that certain neutral salts, such as calcium chloride, lithium bromide and guanidine hydrochloride, have a profound effect on collagen stability.

Some substances, such as urea and the salts mentioned, have a destabilizing influence on collagen structure (Plate VI), while others (for example, potassium fluoride), stabilize the structure in solution. The study of the perturbation effects of various lyotropic or stabilizing agents on the transition temperature can be used to reveal the relative importance of various interactions, such as hydrogen and hydrophobic bonding, on collagen structure and stability in solution. These studies are also of interest in the broad field of chain folding because, in such studies, the backbone chain interactions can be investigated independently of side chain interactions. This subject has been reviewed in detail by von Hippel (1967) and by von Hippel & Schleich (1969).

The perturbant effects of alcohols and other organic compounds, and the thermal stability of collagen, has been the subject of several investigations (Russell & Cooper, 1969; Bianci et al., 1970). The dependence of the transition temperature on perturbant concentration and structure has been used to examine the roles of hydrogen and intermolecular hydrophobic bonding on the structural stability of collagen in solution.

(a)



(b)



Disruption of collagen fibrils by lyotropic agents
(a) disruption of native type fibrils by urea
(b) disruption of SLS collagen by Ca^{++} ions
(magnification x 125 500)

An indication that water has a significant role in the helix-coil transition is provided by the observation that substitution of water by other solvents has a substantial effect on the transition temperature. The affinities of the amino acid side chains for solvent water have been discussed by Wolfenden et al.(1981). It is probable that water contributes to the stability of the collagen structure through intramolecular hydrogens bonds, and also possibly by providing linkages between polar groups. This, however, also implies that the contribution of water to the stability of the collagen molecule is equivalent at all molecular locations. It is possible that water can destabilize structure at certain regions by interacting with specific residues. It is thus probable, that the amino acid sequence is the determinant of structural stability, not only through the structural limitations to rotational freedom imposed by imino acid content, but also through the contributions to stability by the interaction with water.

B The Chemistry of the Vegetable Tannins and their
Monomeric Subunits

2.9 Occurrence

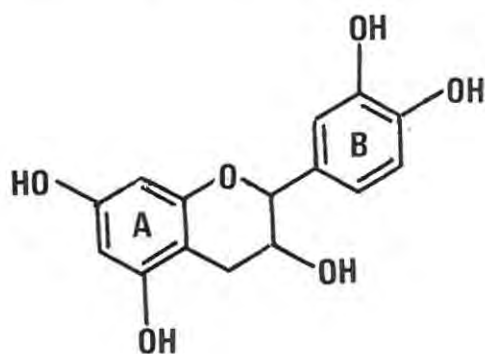
The vegetable tannins are complex polyphenolic compounds formed from tannic acid, gallic acid, and a variety of flavanoid subunits. They cannot be represented by any simple structural formula. A proportion of the polyphenolic tannins occur in the vegetable tannin extracts as the glycosides. An early review of the chemistry of these compounds is included in a publication on the naturally occurring plant phenolics (Ollis, 1961). A more recently published review which deals with the chemistry of the plant phenolics is that of Harborne et al. (1975).

The vegetable tannins occur in a variety of plants. Wattle (*Acacia mollissima*) and Quebracho (*Quebracho lorentzii*) constitute the two major sources of commercial vegetable tannins. Wattle extract contains 61 - 63% tannins and 18 - 20% non-tannins, while Quebracho extract has 63 - 70% tannin and 6 - 10% non-tannins. The non-tannins include the lower molecular mass polyphenolic components, sugars, hemicelluloses, pectin and lignin as well as organic acids and salts.

Wattle and Quebracho extracts are complex mixtures of flavanoid polymers based mainly on flavanol and flavanone structures with a more-or-less uniform molecular mass distribution over the range from 550 - 3250. The ability to tan manifests itself only in phenolic compounds consisting of at least four gallic acid, tannic acid, or flavanol subunits (Roux et al., 1965). The monomeric subunits which make up the vegetable tannins do not themselves exhibit the tanning reaction. It has been shown (Bose et al., 1976), however, that the flavanoids do have a stabilizing role on collagen. For example, catechin (a flavanoid precursor subunit found in vegetable tannin extracts, and itself a compound which does not tan) does render collagen resistant to degradation by trypsin, indicating some form of interaction with collagen (Kuttan et al., 1981).

2.10 Hydrolysable and Condensed Tannins

Depending on their response to acid hydrolysis, the vegetable tannins may be classified as condensed (catechol) tannins or as hydrolysable (pyrogallol) tannins. On acid hydrolysis, the condensed tannins polymerise into higher molecular mass compounds whereas the hydrolysable tannins disperse. On alkaline hydrolysis, the hydrolysable tannins produce predominantly pyrogallol as a breakdown product and the condensed tannins produce catechol or resorcinol. At a more fundamental level than chemical behaviour on hydrolysis, these two classes of tannins result from distinct biosynthetic pathways. It has been established that the benzenoid rings in the plant phenolic compounds are formed via two main biosynthetic pathways, namely, the shikimic acid pathway and by 'active acetate'. In catechin, for example, the ring A derives from an acetate biosynthesis and the ring B has a shikimic acid precursor.



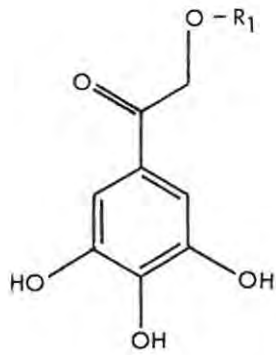
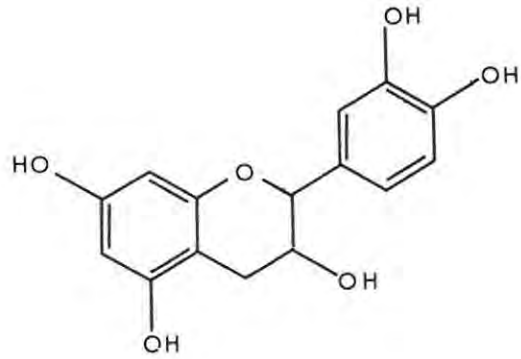
(+)-Catechin

The hydrolysable tannins are derived from shikimic acid biosynthesis. It is possible to distinguish between the two classes of tannins by their response to acid hydrolysis or by their reaction to iron salts or alkali. The hydrolysable tannins, which disperse on acid hydrolysis, develop deep blue colours in the presence of iron salts and show only a slight tendency to oxidise, with the formation of red compounds in alkaline solution. The condensed tannins, on the other hand, polymerise when heated with acid, develop green colours in the presence of iron salts, and are readily oxidised in alkaline solutions (which develop deep red colours).

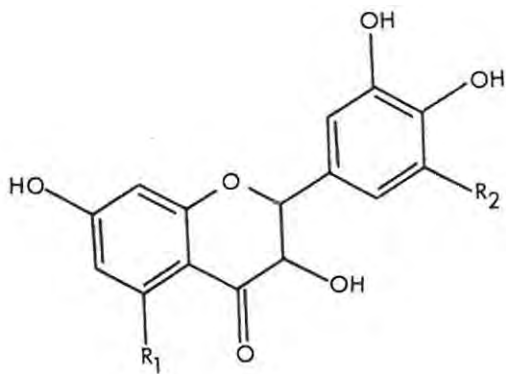
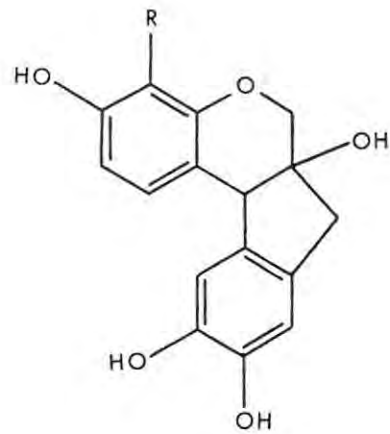
The monomeric analogues of the polyphenolic tannins used in the binding studies to investigate their binding ability to collagen are shown in the scheme below, together with their structures:

Figure 1.1

Structures of Monomeric Subunits of Polyphenolic Tannins

gallic acid $R_1 = \text{OH}$ n-propyl gallate $R_1 = \text{OC}_3\text{H}_7$ 

(+)-catechin

dihydrorobinetin $R_1 = \text{H}$ $R_2 = \text{OH}$ dihydroquercetin $R_1 = \text{OH}$ $R_2 = \text{H}$ brazilin $R = \text{H}$ haematoxylin $R = \text{OH}$

Chapter Three

Protein Ligand Interactions

A Information Provided by Protein-Ligand Binding Studies

3.1 Introduction

Protein-ligand interactions represent a prominent facet of protein chemistry. Several general aspects of protein-ligand binding are reviewed in this chapter. This includes a discussion on the type of information which protein-ligand binding studies can provide, particularly with respect to the nature of the binding site and the forces involved in protein-ligand complex formation. A number of mathematical methods, based on protein-ligand model systems, which are used to derive information from binding study data are examined. Much of the current interest in protein-ligand interactions derives from structure-activity relationships of pharmacologically active drugs (Cody, 1980; McElroy & D'Arcy, 1980) and because protein-ligand interactions provide the mechanisms for the control of biological activity at the molecular level. Binding studies are thus undertaken to provide insight into the mechanism of drug action, metabolism and drug elimination.

Publications which provide broad surveys of the field of protein-ligand binding are the reviews of Klotz (1953), Edsall & Wyman (1958), Tanford (1961), Feldman (1972), Klotz (1974), Heald & Sampat (1978), and Whitehead (1980). A standard text on protein-ligand binding, which provides a comprehensive survey of the subject, is 'Multiple Equilibria in Proteins' by Steinhardt & Reynolds (1969).

Apart from their biological importance, there are many reasons to justify protein-ligand binding studies. Protein-ligand binding studies attempt to characterize the protein-ligand interaction in terms of a binding isotherm. From the form of

the isotherm, it is possible to postulate a model to describe the binding. It is also possible, on the basis of the model selected, to evaluate binding parameters such as the number of binding sites on the protein molecule or protein-ligand association constants. These parameters provide information about the nature of the binding site, the energy changes associated with the protein-ligand interaction, and the kinds of bonds formed in the protein-ligand complex.

Proteins are almost invariably studied in a solution environment which contains, besides the solvent, a variety of salts or buffering acids. Thus the closely related aspects of protein structure and the forces which stabilize protein conformation in solution also fall within the scope of protein-ligand interactions. These features of binding are mutually interdependent. Depending on the conformational stability of the protein, binding may induce changes in the protein structure, or conversely changes in protein structure can bring about changes in ligand binding affinity. Changes in the protein conformation are brought about by the Gibbs function changes which result when internal bonds between protein segments and protein-solvent interactions are replaced by protein-ligand binding.

Measures of protein structural stability and propensity to undergo conformational change are reflected in the sensitivity of the binding isotherm to environmental variables. Studies which investigate changes in the binding isotherm with changes in temperature, pH, or ionic strength of the protein solution can provide information relating to the conformational stability of the protein.

The binding isotherm is usually expressed as the graphical plot of 'quantity of ligand bound to the protein' as a function of the concentration of non-bound ligand which is in equilibrium with the protein-ligand complex, or a statistically fitted mathematical representation thereof. Sometimes it is convenient to use equivalent transforms of the binding isotherm. These

transforms include the Scatchard plot (Scatchard, 1949), the Lineweaver-Burke plot (Lineweaver and Burke, 1934), the Linear-log plot (Bjerrum, 1941), the semi-reciprocal plot (Klotz, 1946), log-log plots, etc.

The simplest binding situation occurs when the protein possesses only a single class of binding sites which act independently of each other. In such a situation, a simple mass-balance relationship (Klotz et al., 1946; Klotz, 1953) yields an hyperbolic relationship between \bar{v} , the quantity of ligand bound to a unit mass of the protein and $[L]$ the concentration of ligand in equilibrium with the protein-ligand complex:

$$\bar{v} = Nk[L]/(1 + k[L]) \quad \dots \quad 3.1.1$$

where N is the number of binding sites on the protein molecule and k is the protein-ligand association constant.

Linear forms of equation 3.1.1, obtained by the Scatchard, Lineweaver-Burke and other transformations are convenient because they enable the binding parameters N and k to be obtained directly from measurement of the slope and axial intercepts. For example, in terms of the Scatchard variables $y = \bar{v}/[L]$ and $x = \bar{v}$ (Rosenthal, 1967) equation 3.1.1 reduces to:

$$\bar{v}/[L] = (N - \bar{v})k \quad \dots \quad 3.1.2$$

i.e., $y = Nk - kx$ which reduces to $x = N$ for $y = 0$, and $y = Nk$ for $x = 0$ with a slope of y against x equal to $-k$.

Other equivalent linear transformations of equation 3.1.1 are the double reciprocal Lineweaver-Burke plot:

$$1/\bar{v} = 1/(Nk[L]) + 1/N \quad \dots \quad 3.1.3$$

and the semi-reciprocal plot (Klotz, 1946):

$$[L]/\bar{v} = 1/Nk + [L]/N \quad \dots \quad 3.1.4$$

These graphs also provide graphical tests for differentiating

between protein-ligand interactions which involve only a single class of binding sites and more complex modes of binding. If the protein-ligand interaction is more complex due to, for example, binding site interaction or ligand induced conformational changes in the protein, these transforms of equation 3.1.1 will exhibit curvature. Curvature in these plots is usually interpreted as implying that the protein-ligand binding is heterogeneous, i.e., the protein possesses more than a single class of binding sites, each with its own association constant.

When the graphs of the linear transformations of equation 3.1.1 are not linear, it is still possible to use limiting slopes and extrapolated axial intercepts to derive estimates of binding parameters (see Figure 3.1). However, because there is a variety of factors which can contribute to the curvature in these plots, it is possible that this procedure can lead to a misinterpretation of the nature of the protein-ligand interaction. It is thus necessary to exercise caution in the assignment of particular binding models to protein-ligand interactions when the linear transforms of the isotherm display curvature.

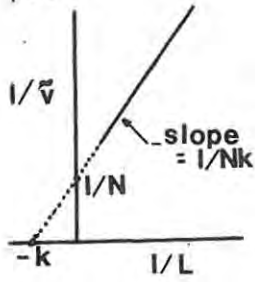
An evaluation of the use of the linear transformations of equation 3.1.1 to obtain binding parameters for multiple classes of binding sites on the protein has been given by Klotz & Hunston (1971) and by Kirdani et al., (1979). Comparisons of the efficacy of these graphical methods for determining binding parameters when the protein-ligand cannot be simply represented by equation 3.1.1 as well as the limitations of applying a simplistic model to more complex binding situations have been dealt with by Woosely & Muldoon, 1977; by Klotz & Hunston 1978; and by Peters & Pingoud 1979.

Frequently the binding parameters are obtained by least squares procedures which fit the binding isotherm data to an appropriate binding model incorporating the binding parameters. The binding parameters are usually obtained by iterative refining of initial estimates of parameters obtained from the Scatchard or Lineweaver-Burke plots.

A number of reports, which deal specifically with

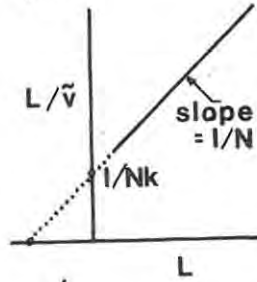
Figure 3.1

A Lineweaver-Burke plot



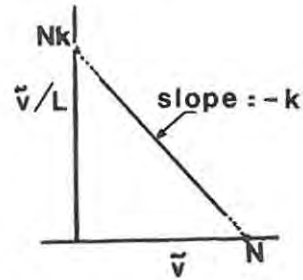
$$1/\tilde{v} = 1/N + 1/Nk \cdot L;$$

B Semi-reciprocal plot



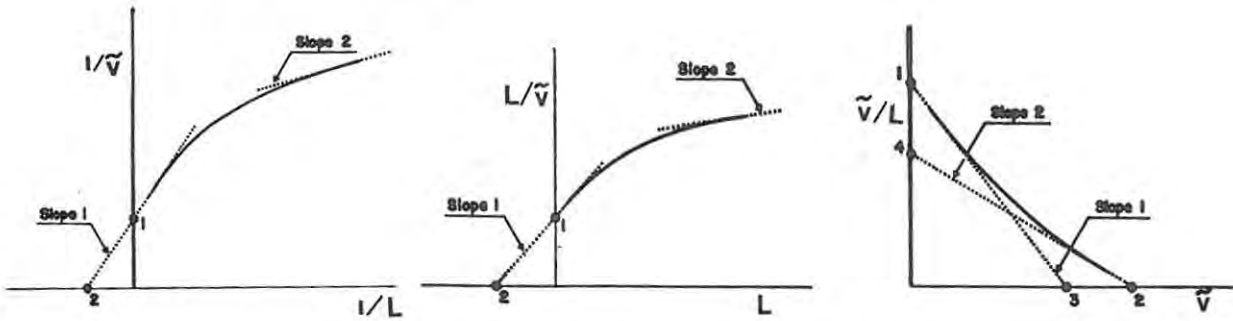
$$L/\tilde{v} = 1/Nk + L/N;$$

C Scatchard plot

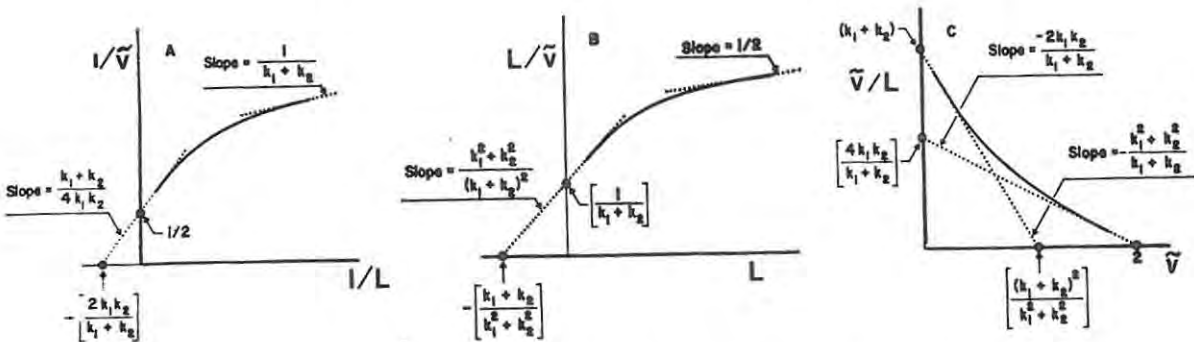


$$\tilde{v}/L = Nk - k \cdot \tilde{v}$$

Graphical representation of the three commonly used linear transformations of the binding equation for a single site or single class of sites



Schematic curves for each of the three pairs of transformed variables when m independent classes of binding sites are present



Schematic curves for each of the three pairs of coordinates for a system of only two independent binding sites
Intercepts and limiting slopes are indicated

from KLOTZ AND HUNSTON, 1971

mathematical methods and regression procedures to extract the binding parameters from binding isotherm data, have been published. These consider the statistical implications inherent in the methods, and discuss the reliability or otherwise of the parameters obtained using such methods. Included among these reports are the publications of Fletcher & Spector (1968), Sprague et al. (1980), Thakur et al. (1980), Duggleby (1980), Munson & Rodbard (1980), Whitlam & Brown (1980).

Once the binding parameters have been obtained, measures of the enthalpy changes associated with the protein-ligand interaction can be obtained from the change in values of the association constants with temperature. The energetics of protein-ligand binding represents an important product of binding studies. Often this can be used to establish the mode of binding in the protein-ligand complex. Thus, from energy considerations, it may be possible to propose that the binding is due to hydrogen bonding, hydrophobic, polar, or electrostatic attractions, or even whether covalent links are formed between the protein and the ligand.

Measures of the Gibbs function, enthalpy, and entropy changes of the protein-ligand interaction can be obtained by making use of thermodynamic relationships. The change in the Gibbs function, G^0 , for the protein-ligand association is given by the thermodynamic relationship:

$$\Delta G^0 = -RT \ln K_i \quad \dots \quad 3.1.5$$

where K_i is the protein-ligand association constant.

Enthalpies and entropies of binding are obtained by establishing the binding isotherm over a range of temperatures and using the thermodynamic relationships:

$$\Delta H^0 = R d[\ln K_i] / d(1/T) \quad \dots \quad 3.1.6$$

$$\Delta S^0 = (\Delta H^0 - \Delta G^0) / T \quad \dots \quad 3.1.7$$

The energy aspects of protein-ligand binding have been reviewed by Weber (1975), and recent reviews of the thermodynamics of ligand binding to macromolecules have been presented by Pohl (1978), Eftink (1980) and Kuchel & Dalziel (1980).

Together with a consideration of the energy-entropy changes, binding studies which investigate how the binding capacity and protein-ligand association constant of the protein vary with changes in ligand structure, also provide criteria whereby the mode of binding in the protein-ligand complex may be determined. Such studies provide information relating to the structure of the binding sites on the protein molecule. Studies of this nature are fundamental to the investigation of structure-activity relationships of pharmacologically active agents. For example, it has been shown that the acid association constant of the acidic group in the histamine receptor has a value which rules out carboxyl and phosphoric acid groups as active participants in the histamine receptor site. This indicates that the essential grouping of the histamine receptor might be the imidazole ring of an histidine residue (Rocha & Silva, 1960).

An important aspect of protein-ligand binding is the investigation of the interactions between binding sites. Binding site interactions may be the result of specific or indirect ligand involvement. Ligand binding at one site on the protein molecule may enhance or attenuate the binding of the same or a different ligand at a second binding site. This phenomenon, referred to as the allosteric effect (Monod 1963), may be the result of direct steric interference or electrostatic repulsion. It may also be a consequence of ligand-induced conformational change in the protein. Allosteric effects provide the 'feedback' mechanism for the control of biological activity, such as enzyme-substrate interactions. The term cooperativity is used to describe an increasing binding affinity with increasing site occupancy. This presumably results from an unfolding of the protein to make additional binding sites available for further binding.

B Mathematical Models for Protein-Ligand Binding

3.2 Scope of Application

In the following review of mathematical models used to describe protein-ligand interactions, a distinction is made between simple ligand binding of low molecular mass ligands to the protein chain, and those interactions which involve allosteric phenomena. A mathematical analysis of allosteric models is excluded from consideration because these models usually involve more than a single ligand species. Interactions which involve shifting equilibria due to protein subunit interactions in the presence of modifying reagents are also excluded from consideration. However, simple protein-ligand binding does not exclude the possibility of interaction between binding sites due to steric effects or electrostatic interactions resulting from the binding of charged ligand species. Nor are those situations excluded where cooperativity in binding may arise from binding induced configurational changes in the protein.

Early publications which can be considered as classical contributions to the subject of mathematical descriptions and models for protein-ligand interactions are by Langmuir (1918), Michaelis (1925), and Adair (1925). Klotz (1946), Scatchard (1949) and Goldstein (1949) have described methods to determine a protein-ligand equilibrium constant which can be assumed to have the same value for all binding sites on the protein molecule.

Methods to extend these models, by the use of limiting slopes and intercepts, to describe situations in which the equilibrium constant can not be assumed the same for all binding sites on the protein have been described by Karush (1952), Steiner (1953), and Edsall & Wyman (1958). Accounts which describe some of the various approaches to mathematical models for protein-ligand binding are by Hill (1960), Tanford (1961), Fletcher & Spector (1977), Klotz and Hunston (1975), and Steiner (1980).

Despite the variety of approaches, most mathematical models used to describe protein-ligand interactions utilize the following experimentally determined quantities:

- (i) the molal binding ratio, \bar{v} , which is defined as the average number of moles of ligand bound per mole of protein;
- (ii) the concentration or activity, L , of the ligand in equilibrium with the protein-ligand complex.

The graph of \bar{v} vs L for a fixed temperature constitutes the protein-ligand binding isotherm. Binding parameters such as n_j , the protein-ligand binding capacity, and k_j ,¹ the protein-ligand association constant for a particular class of binding sites, are usually obtained by assuming that the binding isotherm conforms to an hypothetical model. Thus, in order to extract the binding parameters from the isotherm, it is necessary to establish the functional relationship between \bar{v} and L in terms of the binding parameters, n_j and k_j . Values for the parameters are then obtained in terms of the model, by a curve-fitting (regression) analysis.

It is generally accepted that this procedure represents an oversimplification. There is usually some ambiguity associated with the quantity of protein used in the definition of \bar{v} . If the protein in the solution is non-homogeneous, i.e., does not have a unique structure, the protein will exhibit a spread of molecular mass. It is customary to assume (until results negate the assumption) that the protein is homogeneous in solution and possesses a unique molecular mass. In addition, the mathematical description is assumed to apply to the binding of a single ligand species to the protein. In practice, the simplest system encountered consists of the simultaneous equilibria of

¹ Footnote: See page 38 for definitions of n_j and k_j

protein, solvent, and at least two kinds of ions, besides the ligand in question.

In most cases, because of the difficulty in distinguishing between the effects of solvent and ligand, solvent interaction is disregarded. The binding parameters are usually quoted relative to a particular solvent (often water). Protein-ligand interactions are studied and results are quoted for a specific solution environment, in which pH, counter-ion composition and ionic strength are specified. Such a treatment is usually adequate for comparative studies involving an homologous series of ligands. It is also satisfactory for studies which examine the effects of how structural changes in the ligand influence its ability to bind to the protein, because studies of this nature are usually conducted in a common solution environment.

Kauzmann (1959), Nemethy & Scheraga (1962), Sinangolu (1968) and Chatterjee & Chatoraj (1978) have reported investigations which deal specifically with the effects of the solvent on protein-ligand interactions. These solvent effects include solvent binding, its effect on protein conformation, its contribution to internal binding in proteins, and solvent competition for binding sites.

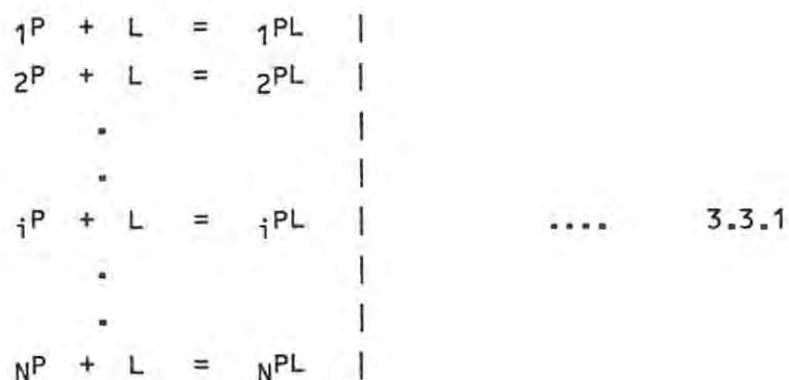
Frequently, the simplified treatment is inadequate and it is necessary to invoke the special considerations applying to allosteric phenomena. This requires an extended mathematical analysis to include the simultaneous binding of two or more ligands and to allow for the effects involving multiple interactions between different segments of the protein chain. Magar (1972) has reviewed several of these mathematical models. This review includes a discussion of a model which incorporates the allosteric effect in terms of the quaternary structure of the protein and molecular subunits (Monad, Changeaux & Wymann, 1965), as well as an allosteric model in which ligand-binding induces changes in the protein structure (Koshland, Nemethy & Filmer, 1966). Both these extended mathematical models are based on

geometrical models and consider linear, square or tetrahedral arrangements of the binding sites on protein units. A more recent review of allosteric cooperative binding has been given by Whitehead (1980). In an extended survey, Gäbler (1976) summarised theoretical models which range from formally descriptive to elaborate mechanistic models which deal with changes in protein-ligand affinity due to conformational changes in protein subunits. In a subsequent review, Gäbler (1977) presented a comprehensive survey of publications which dealt with cooperativity concepts in protein binding models. In this survey, thirteen distinct approaches to the problem were cited. The review by Steiner (1980) deals with the quantitative analysis of protein self-association when there is a significant mutual influence between ligand binding and protein association.

Magar (1972) has pointed out that, in terms of parameter extraction, a great deal of similarity between these models is evident. In situations where simple non-allosteric considerations are adequate, protein-ligand binding can be considered from two different approaches. These are the site binding model due to Scatchard (1949) and Karush (1950), and the stoichiometric binding constant model (Klotz 1946; 1953). A brief account of each of these models is given since these models provide a useful introduction to the generalized binding model which has been subsequently developed by Klotz (1974) and Fletcher and Spector (1977a). A recent review by Ferguson-Miller and Koppenol (1981) discusses the practical significance of the distinction between the stoichiometric and the site binding constants for macromolecules containing more than a single class of binding sites.

3.3 The Site-Binding Model

This model has been presented in slightly different forms by Scatchard (1949) and Karush (1950). The model is based on the assumption that the binding sites on the protein have a fixed affinity which does not change with the extent of site occupancy. The multiple equilibria between the ligand L and the protein P are represented by:



where the subscript i refers to the i^{th} binding site on the protein, and N is the protein-ligand binding capacity. A 'site-equilibrium' constant is defined for each site by:

$$k_i = [i^{PL}] / [i^P][L] \quad \dots \quad 3.3.2$$

The terms in the square brackets, $[i^{PL}]$, $[i^P]$ and $[L]$, represent the molar concentrations in the solution of the protein-ligand complex, protein, and ligand, respectively. In a rigorous analysis, activities should be used. However, because in practice the activity coefficients are not readily ascertainable, and also because in most cases binding studies are carried out at low ligand concentrations where the activity coefficients are approximately unity, molar concentrations can be used instead of the thermodynamically correct activities. In what follows, the activity coefficients are considered to be incorporated into the apparent association constants.

It follows from equation 3.3.1 that, for any site i , the number of moles of bound ligand per mole of protein is given by:

$$r_i = k_i [L] / (1 + k_i [L]) \quad \dots \quad 3.3.3$$

The total number of moles of bound ligand for all the binding sites is:

$$\bar{v} = \sum_{i=1}^N r_i = \sum_{i=1}^N \{k_i [L] / (1 + k_i [L])\} \quad \dots \quad 3.3.4$$

If the binding consists of a single class of binding sites of fixed affinity, equation 3.3.4 becomes

$$\bar{v} = N [L] / (1 + k [L]) \quad \dots \quad 3.3.5$$

where N represents the number of ligand binding sites on the protein molecule.

As has been noted previously, equation 3.3.5 can be subjected to a variety of mathematical transformations in which the transformed variables provide linear plots from which the binding parameters N and k may be determined from the slope and axial intercept. In the more complex protein-ligand binding situations, where the protein-ligand interactions are heterogenous, the quantity of ligand bound to the protein is represented by a summation of the binding at the different classes of binding sites.

Thus:

$$\bar{v} = \sum_{i=1}^m \{n_i k_i [L] / (1 + k_i [L])\} \quad \dots \quad 3.3.6$$

where n_i is the number of binding sites belonging to the particular class of binding sites which have an association constant k_i , and m is the total number of classes of binding sites on the protein molecule.

When the values of the k_i are separated by a factor of more than 10^4 , the individual terms in equation 3.3.6 corresponding to the different values of i will be well separated. The isotherm can then be considered to consist effectively of domains, in which \bar{v} within each domain is determined by a single k_i . It has been demonstrated that it is possible to obtain values relating to the n_i 's and k_i 's from limiting slopes and intercepts of the curvilinear functions equivalent to equations 3.1.2, 3.1.3 and 3.1.4 respectively, even when the binding system is more adequately described by equation 3.3.6 (Klotz & Hunston, 1971). However, if the binding is heterogenous and the k_i 's are not well separated, there is the risk of distorting or misinterpreting the data through using these reciprocal plots (Klotz & Thompson, 1971; Klotz, 1974).

The Scatchard general model has been criticised (Fletcher & Spector, 1977; Klotz & Hunston, 1979). The use of a linear combination of hyperbolic terms as in equation 3.3.6 will always yield corresponding parameters k_i , for $i = 1$ to m . However, these cannot correspond to true site-binding constants when binding sites are not independent. Also, curvature in the Scatchard plot (equation 3.1.2) is more likely to be a manifestation of interactions between initially identical binding sites than the less sophisticated view, that the protein has several independent classes of binding sites (Klotz & Hunston, 1979).

The site-binding approach can be generalized (Klotz & Hunston, 1975). A more generalized model provides an expression to describe the situation in which binding site interaction occurs. In this generalized approach, the equilibrium at the binding site is still governed by sets of binding constants.

However, additional site-binding constants are required in the analytical expression to describe the binding isotherm. In the general case, where binding affinity changes with the extent of site-occupancy, Klotz & Hunston (1975) have shown that $2^m - 1$ binding constants are required to describe adequately binding at m interacting binding sites.

3.4 Stoichiometric Binding Constants

An alternative approach (Fletcher et al., 1970), also based on a thermodynamic treatment originally due to Adair (1926), has been developed by Klotz (1946, 1953). According to this approach, stoichiometric equilibrium constants K_i are defined for the sequential macromolecule-ligand species PL_1, PL_2, \dots, PL_N . Capital letters are used to symbolise the stoichiometric constants K_i in this section to distinguish them from the site-binding constants discussed in the previous section. The stoichiometric model implicitly includes any cooperative or antagonistic interactions between successively bound ligands.

It is not necessary, in terms of this model, to consider the nature of the interactions between the binding sites. These can be due to steric interactions between ligands, electrostatic interactions arising from charged ligand species, or due to conformational changes in the protein. The model does, however, provide criteria for distinguishing between the various factors which cause the interaction between the binding sites. It is convenient to develop the model initially without considering the origins of site interaction and then to extend the analysis, as required, to cover the situations in which binding can be affected by steric considerations, electrostatic interactions, or protein conformational change.

The association between the protein and the ligand is assumed to be reversible (Fletcher, 1970; Klotz, 1974). The equilibrium between the ligand L and the protein P containing N independent, indistinguishable binding sites is given by:



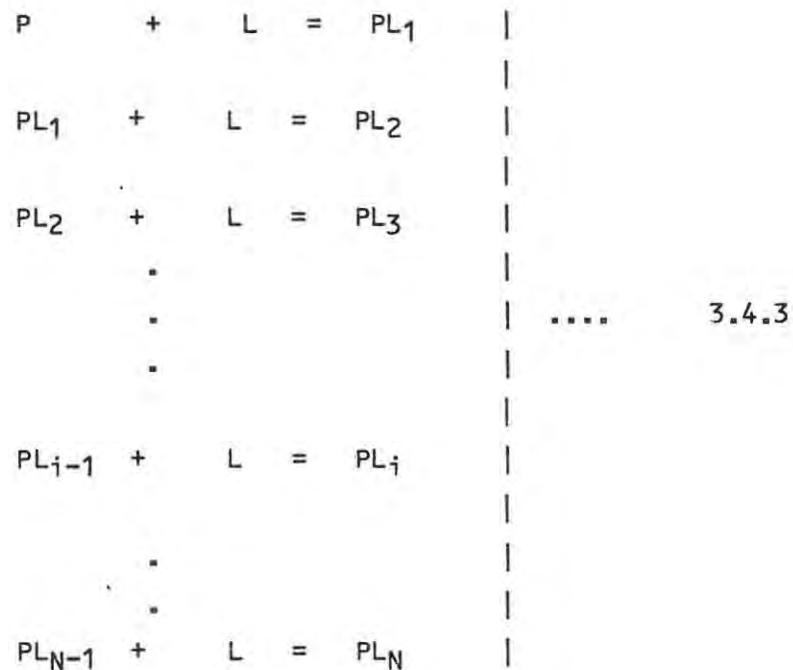
and has an overall protein-ligand association constant K_N' given

by:

$$K_N' = [PL_N] / [P][L]^N \quad \dots \quad 3.4.1$$

$$\text{where } \Delta G^0 = -RT \ln K_N' \quad \dots \quad 3.4.2$$

The stoichiometric binding site model deals with the totality of all the stoichiometric species PL_i , without regard to the possibility that the distribution of ligands among the i occupied binding sites may vary from molecule to molecule. In terms of the model, stoichiometric equilibrium constants are set up to describe an equilibrium for each of the stoichiometric species $PL_1, PL_2 \dots PL_{N-1}$. Thus the model makes no distinction between differences within the protein-ligand species due to ligands occupying different possible sites. The equilibria for each of the stoichiometric species are defined by:



where N represents the maximum number of binding reactions that can occur. The equilibria of equation 3.4.3 represent multiple equilibria even when binding induces allosteric changes in the protein binding sites.

The individual stoichiometric equilibrium constants are defined by:

$$K_i = [PL_i] / [PL_{i-1}] [L] \dots \quad 3.4.4$$

where the quantities $[PL_i]$, etc., are the molar concentrations approximating the activities of the ligand complex in question. The average number of ligand molecules bound to the protein is given by:

$$\begin{aligned} \bar{v} &= \frac{\text{Total no. of moles of bound ligand}}{\text{No. of moles of protein}} \\ \bar{v} &= \frac{[PL_1] + 2[PL_2] + \dots + i[PL_i] + \dots + N[PL_N]}{[P] + [PL_1] + [PL_2] + \dots + [PL_N]} \\ \bar{v} &= \frac{\sum_{i=1}^N i[PL_i]}{\sum_{i=0}^N [PL_i]} \dots \quad 3.4.5 \end{aligned}$$

in which $[PL_0] = [P]$

In terms of the stoichiometric equilibrium constants equation 3.4.5 can be expressed as:

$$\bar{v} = \frac{[PL_1] + 2[PL_2] + \dots + i[PL_i] + \dots + N[PL_N]}{1 + K_1[L] + \dots + K_1K_2 \dots K_i[L]^i + \dots + K_1 \dots K_N[L]^N}$$

$$\text{or } \bar{v} = \frac{\sum_{i=1}^N i \left(\prod_{e=1}^i K_e \right) [L]^i}{\left\{ 1 + \sum_{i=1}^n \left(\prod_{e=1}^i K_e \right) [L]^i \right\}} \quad \dots \quad 3.4.6$$

Equation 3.4.6 expresses the quantity of ligand bound to the protein in terms of the stoichiometric binding constants, and is the basis of the stepwise equilibrium model. These association constants, defined in terms of stepwise equilibria, specifically incorporate cooperativity or interaction effects between the ligand binding sites. If, however, the ligand binding sites are all considered to be equivalent, each site will be governed by the same intrinsic association constant K_0 in terms of which the stoichiometric constants K_i in equation 3.4.6 are given by:

$$\begin{aligned} K_i &= \left\{ \left[N C_i \right] / \left[N C_{i-1} \right] \right\} K_0 \\ &= \left\{ (N-i+1) / i \right\} K_0 \quad \dots \quad 3.4.7 \end{aligned}$$

where $\left[N C_i \right]$ is the number of possible combinations of N binding sites, taken i at a time. Substituting equation 3.4.7 for the K_i 's in equation 3.4.6 yields:

$$\bar{v} = \frac{\sum_{i=1}^N i \left(\prod_{e=1}^i \left\{ (N-i+1) / i \right\} K_0 \right)^i [L]^i}{\left\{ 1 + \sum_{i=1}^N \left(\prod_{e=1}^i \left\{ (N-i+1) / i \right\} K_0 \right)^i [L]^i \right\}} \quad \dots \quad 3.4.8$$

which on simplification reduces to:

$$\begin{aligned} \bar{v} &= \left\{ N K^* [L] (1 + K^* [L])^{N-1} \right\} / \left\{ 1 + K^* [L] \right\}^N \\ &= N K^* [L] / (1 + K^* [L]) \end{aligned}$$

$$\text{or } \bar{v}/(N-\bar{v}) = K^* [L] \quad \dots \quad 3.4.9$$

where K^* represents the product of the combined activity coefficients with K_0 . For systems in which the ligand concentration is small so that the activity coefficients can be taken as unity, $K^* = K_0$.

If the macromolecule possesses more than one class of binding sites, and each site is assumed to be independent, the total quantity of ligand bound per mole of protein can be expressed in the general case by the summation over the different classes of binding sites to give:

$$\bar{v} = \sum_{i=1}^N n_i K_i [L] / (1 + K_i [L]) \quad \dots \quad 3.4.10$$

where N is the total number of classes of binding sites, and n_i is the number of binding sites within a particular class of binding sites.

Equation 3.4.10 has the same form as the general Scatchard model (i.e., the two models reduce to the same mathematical form for the special case of independent binding sites). In both binding models, the molal binding ratio \bar{v} can be expressed as a sum of so-called "hyperbolic" terms.

Although equation 3.4.10 has been derived for the special case of N classes of binding sites which are mutually independent, this equation in its most general form (a form in which K_i may be complex) will contain sufficient parameters to describe adequately any binding system, irrespective of whether binding sites interact or not. The values assigned to the binding constants will not however correspond to association constants governing site-binding equilibria.

A useful feature of the analysis, which expresses the stoichiometric constants K_i in terms of an intrinsic association constant K_0 (equation 3.4.7), is that it provides a criterion to test whether in the successive binding (as depicted by the stepwise equilibrium model), the binding occurs cooperatively or antagonistically. It follows from equation 3.4.7 that, if the binding is non-interactive:

$$K_i = \{ (N-i+1) / i \} K_0 \quad \dots \quad 3.4.11$$

and the graph of $iK_i = (N+1)K_0 - iK_0$ (the affinity profile (Klotz, 1974)), should be linear. A non-linear affinity profile will indicate interdependence between binding sites. Moreover, it is possible to gauge from the changes in the slope of the affinity profile whether the binding sites are cooperative or antagonistic with increasing site occupancy as the ligand concentration is increased.

It is to be expected that the site-binding constants k_i of equation 3.3.6 and the stoichiometric constants K_i of equation 3.4.10, which allow for interaction between the binding sites, are related: Such a relationship is implied by the observation that \bar{v} and $[L]$ of equation 3.3.6 are the same experimentally observed quantities as in equation 3.4.6. The relationship between the two sets of constants has been formulated for multisite binding with fixed unchanged affinities (Klotz, 1974; Klotz & Hunston, 1975; Fletcher & Spector, 1977). The equations relating the two sets of constants are:

$$\begin{aligned}
 K_1 &= \sum_{j_1=1}^N k_{j_1} \\
 K_1 K_2 &= \sum_{j_1=1}^{N-1} \sum_{j_2=j_1+1}^N k_{j_1} k_{j_2} \\
 &\vdots \\
 &\vdots \\
 &\vdots \\
 K_1 K_2 \dots K_i &= \sum_{j_1=1}^{N-i+1} \sum_{j_2=j_1+1}^{N-i+2} \sum_{j_i=j_{i-1}+1}^N \dots k_{j_1} k_{j_2} \dots k_{j_{i-1}} \\
 K_1 K_2 K_3 \dots K_N &= k_1 k_2 k_3 \dots k_N
 \end{aligned}$$

..... 3.4.12

3.5 Binding with site interaction due to electrostatic repulsion

In general, there will be a decrease in binding affinity for charged species with increasing site occupancy due to charge repulsion between bound and free charged ligand species. A mathematical method to allow for the repulsive effects of charged ligands is based on a model proposed by Bjerrum (1923) and subsequently refined by Gane & Ingold (1931), Kirkwood & Westheimer (1938), and Tanford (1961).

The standard Gibbs function change for the reaction



is given by:

$$\Delta G' = -RT \ln K' \quad \dots \quad 3.5.2$$

where $\Delta G'$ contains an additional contribution due to electrical work done in increasing the charge on the protein by the binding of the charged ligand. This increase in Gibbs function is allowed for by defining a function $f(\tilde{v})$ such that $f(\tilde{v}) = 0$ when $\tilde{v} = 0$.

The modified association constants and expression for Gibbs function change are defined by:

$$K' = K \cdot e^{-f(\tilde{v})} \quad \& \quad \Delta G' = -RT \ln K + RT f(\tilde{v}) \quad \dots \quad 3.5.3$$

The equivalent expression for the equation 3.3.5 is now written as:

$$\tilde{v} = \frac{NK[LL]e^{-f(\tilde{v})}}{\{1 + Ke^{-f(\tilde{v})}\}} \quad \dots \quad 3.5.4$$

The evaluation of the function $f(\tilde{v})$ is made either on the assumption that the work done in bringing the ion to the surface of the protein is determined by the net charge on the protein, or by the calculation of the contribution of each charge on the protein surface to the electrical work of binding. In the former method (Güntelberg & Linderstrøm-Lang, 1949), the Debye-Hückel theory for the calculation of the work necessary to charge an ion in a continuous medium of given dielectric permittivity, is applied to the protein solution to yield the Linderstrøm-Lang equation:

$$\ln \{ \bar{v} / (n - \bar{v}) \} = \ln K + \ln L - 2 wZ \quad \dots \quad 3.5.5a$$

$$\text{or } \log_{10} \{ \bar{v} / (n - \bar{v}) \} = \log_{10} K + \log_{10} L - 0.868wZ \quad \dots \quad 3.5.5b$$

which is the more convenient form for use in binding studies which utilize pH measurement.

In equation 3.5.5a, the function $f(\bar{v})$ is thus given by:

$$f(\bar{v}) = 2 wZ$$

in which Z is the total charge on the protein surface and w is a composite constant, composed of electronic charge e , permittivity ϵ , temperature T , etc. From Debye-Hückel theory it is shown that w has the value:

$$w = (e^2 / 2\epsilon RT) \{ 1/b - \kappa / (1 + \kappa a) \} \quad \dots \quad 3.5.6$$

where b is the radius of the central ion and a is the closest distance to which a second ion can approach the central ion (Debye and Hückel, 1923). κ is the Debye-Hückel reciprocal length given by:

$$\kappa = (4 e^2 / \epsilon RT) \left(\sum_s c_s Z_s^2 \right)^{1/2} \quad \dots \quad 3.5.7$$

where c_s is the molar concentration, and Z_s the number of charges on the charged ligand species.

A more exact theory, due to Tanford & Kirkwood (1957), takes into account the location of charge density on a non-conducting surface. The charge density is calculated in terms of the distance between charged sites and the position of the sites relative to the interface between the binding surface and the solution medium in which it is immersed.

This theory is used mainly for performing calculations based on simple geometric arrangements of sites in hypothetical models.

A rigorous application requires a knowledge of the as yet unknown location of the binding sites on the protein. The method does permit certain generalizations to be made with respect to the binding of charged ligands (Ortung, 1968; Perutz, 1965). In a further refinement, Hill (1955) has provided a method for calculating the electrical contributions to the energy changes involved in the binding of ligands to cylindrical molecules in terms of the potential distribution for an infinite cylinder. In such a model, the electrical field at the ends of long molecules or molecular segments may be neglected.

Applications of the Lindestrøm-Lang theory to investigate the binding of ions to protein include studies by Steinhardt & Beychok (1964) and by Halfman & Steinhardt (1971).

3.6 Binding-site Interaction due to Steric Interference

Interactions between binding sites due to steric interference of the ligands can be accounted for in the same way as for electrostatic interaction. A steric component is added to the exponent in the Gibbs function expression:

$$\Delta G' = -RT \ln K + RTf(\bar{v}) \quad \text{or} \quad K' = Ke^{-f(\bar{v})}$$

.... 3.6.1

3.7 Site Binding Interaction due to Conformational Change

Changes in protein conformation brought about by ligand-macromolecule interaction may be due to one or a combination of:

- i) penetration of hydrophobic regions of the ligand into apolar regions of the macromolecule (Kauzman, 1959);

- ii) electrostatic repulsion between charges of bound ionic ligands (Hanstein, 1979);
- iii) energy considerations, in which the ratio of the number of binding sites (or association constants) in the native form to the unfolded form, favours an unfolded configuration over that of the native form (Steinhardt & Reynolds, 1969).

A two-state model has been proposed (Reynolds et al., 1967b) in which the protein can exist in native or unfolded state. In terms of this model, an expression for the binding isotherm is given by:

$$\bar{v} = \frac{[L]}{(1 + F[L])} \left\{ \frac{nK}{(1 + K[L])} + \frac{F[L]mJ}{(1 + J[L])} \right\}$$

.... 3.7.1

where $F[L]$ is the ratio of the amount of protein in the unfolded state to that in the native form. J and K are the association constants for the binding sites in the native and unfolded forms respectively. n and m are the ligand binding capacities in the two conformations.

A second approach is through the theory of linked functions (Wyman, 1964). This theory relates the binding of the ligand to each of the two protein conformers to changes in the equilibrium constant for the equilibrium between the native and denatured forms. If the ligand binds to both native and denatured forms of the protein then, according to this model, the equilibrium is given by:

$$\bar{v}_i P = \bar{v}_j D + (\bar{v}_i - \bar{v}_j)[L]$$

.... 3.7.2

where \bar{v}_i is the number of ligand molecules bound to the protein in its native state P, and \hat{v}_i is the number of ligand molecules bound to the protein in its denatured form D.

It can be shown that $\Delta \bar{v}$, the difference in the number of ligand molecules bound in each state, is related to the ligand concentration L by:

$$\Delta \bar{v} = d(\ln K^\ddagger) / d(\ln L)$$

.... 3.7.3

where K^\ddagger is the equilibrium constant governing the equilibrium between the two forms of the uncombined macromolecules. Thus, measurements of the equilibrium concentrations of the two forms of the protein (native and unfolded) for a given ligand concentration, carried out by absorbance, electrophoresis or gel-filtration, provide a direct measure of the difference in the number of molecules bound to the protein in each conformation. Alternatively, when the equilibrium concentrations of the native to unfolded form of the protein can be related to an environmental parameter (other than ligand concentration) for example pH, it is possible to relate \bar{v} to changes in this parameter.

Tanford (1969) has applied the method to include water as ligand in an examination of the effects of protein hydration on the transition between native and denatured states.

3.8 A generalized approach to equilibrium models

The generalized Scatchard model (equation 3.3.6), although widely used in protein-ligand binding studies, may be inappropriate when the Scatchard or Lineweaver-Burke plots display curvature. In such cases it is necessary to exercise caution in extrapolating from such data, and it is desirable to have available a method for testing whether the binding sites are independent. Although it can be inferred from the curvature in the Scatchard or Lineweaver-Burke plots that binding is heterogeneous, i.e., has more than a single class of binding site, this does not preclude the possibility of interdependence between the binding sites. The method of stepwise-equilibrium constants provides a model that is consistent with the possibility of cooperativity.

The use of stoichiometric constants (equation 3.4.10) explicitly allows for interaction between binding sites. The set of equilibria described by equation 3.4.3 identifies all constituent species having the same number of ligands as being represented by the same protein-ligand complex. However, these equations do not allow for the specific effects that binding at any particular binding site will have on further ligand binding. In terms of equation 3.4.3, the stepwise binding constants relate to the equilibria of sets of protein-ligand complexes rather than to specific binding sites.

A generalized binding model, based on the stoichiometric binding constants, which includes the Scatchard model as a special case, has been developed by Fletcher et al. (1970), and by Klotz & Hunston (1975) and Fletcher (1977). In this model, as in the generalized Scatchard model, the molal binding ratio is expressed as a sum of so-called "hyperbolic" terms. However, the generalized model allows for site interaction by considering the possibility of complex (in the sense of having real and imaginary parts) values for the binding constants. A complex value for a binding constant is interpreted to imply interaction between binding sites.

The stepwise equilibrium equation (equation 3.4.6) may be rewritten as:

$$\tilde{v}(L) = [L] \frac{d\{\ln R_n(L)\}}{d[L]} \quad \dots \quad 3.8.1$$

where $R_n(L)$ is the polynomial expression in the denominator of equation 3.4.6, i.e.,

$$\tilde{v} = \frac{\sum_{i=1}^N i \prod_{e=1}^i (K_e) [L]^i}{\left\{ 1 + \sum_{i=1}^N \prod_{e=1}^i (K_e) [L]^i \right\}} \quad \dots \quad 3.8.2$$

$$\text{i.e., } R_n = 1 + \sum_{i=1}^N \prod_{e=1}^i (K_e) [L]^i \quad \dots \quad 3.8.3$$

If R_n is written as the product of its N roots

$$\prod (Y_i) \quad i = 1, 2 \dots N$$

then:

$$R_n(L) = K_1 \dots K_N \left\{ \prod_{i=1}^N ([L] - Y_i) \right\} \quad \dots \quad 3.8.4$$

and equation 3.8.1 can be written as:

$$\tilde{v}(L) = \sum_{i=1}^N [L] / ([L] - Y_i) \quad \dots \quad 3.8.5$$

All the real roots Y_i of $R_n(L)$ are negative because the K_i are necessarily positive. Substitution of $-1/K_i$ for Y_i into equation 3.8.4 yields:

$$\tilde{v}(L) = \sum_{i=1}^N n_i K_i [L] / (1 + K_i [L]) \quad \dots \quad 3.8.6$$

the expression for the multiclass Scatchard model.

This is equivalent to the generalized Scatchard model except that n_i represents the multiplicity of the Y_i^{th} root of the polynomial $R_n(L)$, rather than a number of binding sites.

If the solution of the polynomial, $R_n(L)$, contains complex roots, these will occur as complex conjugate pairs, implying that binding at those sites is not governed by an invariable stoichiometric binding constant. The implication is that binding depends on the state of neighbouring binding sites. By grouping pairs of conjugate roots together, equation 3.8.5 may be written as:

$$\tilde{v}(L) = \sum_{j=1}^m n_j k_j [L] / (1 + k_j [L]) \quad \dots \quad 3.8.7$$

$$+ \sum_{j=1}^q \frac{m_j \cdot 2 [L] (C_j^r + C_j^m [L])}{\{1 + 2C_j^r [L] + C_j^m [L]^2\}}$$

$$\text{where } N = 2 \sum_{j=1}^q m_j + \sum_{i=1}^m n_i \quad \dots \quad 3.8.8$$

is the total number of binding sites. The real parameters C_j^r and C_j^m represent respectively the real part and the squared modulus of the complex pairs of constants k_1^j and k_2^j for which the superscript j is used to index these terms.

The binding parameters N_j , k_j , m_j , C_j^r and C_j^m in equation 3.8.7 are determined from the experimentally established isotherm by iterative least squares procedures. The experimentally determined isotherm is fitted to equation 3.8.6 or 3.8.7 using estimates for the initial values of these parameters. A variety of methods to extract these parameters from the binding isotherm has been described (Fletcher & Spector, 1968; Miller, 1979; Whitlam & Brown, 1980; Munson & Rodbard, 1980; Thakur et al., 1980).

In some of the methods, iterative refining of the binding parameters is based on initial estimates of parameters obtained from the limiting slopes and intercepts of the Scatchard plot or Lineweaver-Burke plots. If this procedure is adopted, and if free parameter regression procedures are used, this may give rise to non-integral values for the binding capacities, n_j . For example, Thakur et al. (1980) have described a method of continuous affinity distributions of arbitrary functions based on a numerical finite difference method.

Fletcher (1977) and Fletcher & Spector (1977), in the derivation of the generalized binding model, refer to the limitations of least squares procedures which permit non-integral values for binding capacities, n_j . These authors stress that non-integral coefficients may be inadequate for the interpretation of binding data, since these arise purely from the regression procedures. Consistent with the model, binding capacities should assume only integral values. Non-integral values can be taken to imply non-homogeneity of the protein, or the presence of a second ligand (which could be the supporting electrolyte) competing with the primary ligand for the same binding site, or experimental inaccuracy. On the other hand, it could also mean that the binding model is inappropriate. The model represented by a sum of hyperbolic terms which utilizes free-parameter least squares regression procedures may have an

excessive number of degrees of freedom. In such a case, a mathematical expression can indeed be derived using iterative least squares procedures; even though this may provide a satisfactory description of the binding isotherm, it does not necessarily mean that the binding isotherm will conform to the binding mechanism implied by the model. In such cases the model will provide misleading information relating to the binding process.

Klotz and Hunston (1979) have analysed the reliability of model interpretation and the significance that can be attributed to the parameters derived using this generalized model. The limited accuracy of the method used to measure protein-ligand binding can make the selection of a particular binding model, in preference to alternative models, a somewhat arbitrary procedure. Since the values of the binding parameters are derived using an assumed model it is optimistic to expect always to be able to distinguish between the subtleties of different binding models because of the limited accuracy of the experimental data. Although models incorporating a large number of binding parameters may provide equations which adequately match the experimentally determined isotherms, it is appropriate to bear in mind that such equations may have no physical significance with respect to the actual binding mechanism. The precision with which a given equation matches the measured binding isotherm, does not therefore automatically imply accuracy in the binding parameters because it is subject to the arbitrary choice of binding model.

Chapter Four

Experimental Methods for Obtaining the Binding Isotherm

A

General Methods

4.1 Introduction

A brief review of the methods available for measuring protein-ligand binding is presented in this chapter. The technique of dialysis and the factors affecting the dialysis process are examined and the application of dialysis methods to investigate protein-ligand binding is reviewed. The classical method of equilibrium dialysis (Klotz et al., 1946) is examined in some detail, since some of the limitations and pitfalls of this method are common to all of the dynamic dialysis methods.

A number of methods are referred to which represent various modifications of a dynamic dialysis method for investigating protein-ligand binding. In particular, the methods of Colowick & Womack (1969), and of Meyer & Guttman (1968; 1970a; 1970b) are discussed in some detail. These two methods offer several advantages over the classical equilibrium dialysis method. In addition, some of the principles of each of these methods are utilized in the continuous-flow dynamic dialysis method (CFDD) which is described in chapter 5. The CFDD method utilizes a dialysis cell similar to that of Colowick & Womack and is essentially a modification and refinement of the Meyer & Guttman method.

The mathematical analysis used by Meyer & Guttman to extract the binding isotherm from the experimental data obtained using their method is discussed. An alternative mathematical procedure due to Pedersen (1977; 1978) which can be used to extract a binding isotherm from experimental data obtained using the Meyer & Guttman technique is also discussed briefly.

4.2 Experimental methods

Many techniques have been reported for the measurement of the binding of ligands in solution to macromolecules. Usually, the methods are developed and applied to specific protein-ligand systems and are subsequently adapted or modified for application to other protein-ligand systems. It follows that methods suitable for a given protein-ligand system may have a limited range of application, and may be inappropriate for use in a different situation.

Reviews which classify the methods available for protein-ligand binding studies and which discuss, in general terms, the relative advantages and disadvantages of particular methods include publications by Klotz (1953), Steinhardt & Reynolds (1969), Bush & Alvin (1973), and Liao & Oehme (1980).

Experimental methods for measuring protein-ligand binding can be classified into direct methods and subtractive methods. In the former category, the quantity of protein-ligand complex is measured directly from changes in a physico-chemical property of either the bound ligand or macromolecule. The changes in properties which are utilized result from the binding process. Subtractive methods measure changes in the concentration of unbound ligand as a result of protein binding.

4.3 Direct methods

Direct methods can utilize any property of the macromolecule or ligand which changes on binding (Halfman & Nishida, 1972). Thus, recourse has been had to measurement of light absorbance (Wang et al., 1981), fluorescence (Tejima & Ozeki, 1979), optical rotation (Coleman, 1963), NMR (Botherby & Gassend, 1973), light scattering and spectroscopy (Amundsen et al., 1977), titration calorimetry (Sukow et al., 1980), and X-ray diffraction (Blake & Oatley, 1977). Direct methods are, in general, more accurate than the subtractive methods where the protein-ligand affinity is small and where subtractive methods would require the measurement of small differences in a ligand concentration. Where the

protein-ligand affinity is large, however, direct methods offer no advantage in accuracy over the subtractive methods.

It may be necessary, in the application of direct methods to measure protein-ligand binding, to establish by calibration a quantitative relationship between the concentration of the protein-ligand complex and the physical or chemical property by which it is to be monitored. The determination of the concentration of the protein-ligand complex may present difficulties because the measured changes in the physico-chemical properties used to detect the quantity of protein-ligand complex may not distinguish between allosteric and solvent effects. Alternatively, the physico-chemical property which is measured may be unsuitable for the determination of the protein-ligand complex concentration, because changes in the variable are non-linear with respect to the molal binding ratio. This may occur if the binding sites on the protein molecule become saturated at low ligand concentrations (Polet & Steinhardt, 1968), or it may be due to an inability to distinguish between protein-ligand complexes which contain differing amounts of ligand. Equations which relate the molal binding ratio \bar{v} to measured changes in some property X are usually based on a general relationship (Rossotti & Rossotti, 1961):

$$X = \theta(X_A[LL] + \sum_{i=1}^n X_i[PL_i]) \quad \dots 4.3.1$$

where X_A & X_i are the appropriate intensive factors for the ligand and the protein-ligand complex concentration $[PL_i]$ respectively. θ is a constant which depends on the measuring instrument. A survey of the applications of equation 4.3.1 to measure the interaction between small molecules and proteins has been presented by Rossotti & Rosotti (1961).

4.4 Subtractive methods

Subtractive methods usually depend on the distribution of the ligand between two phases, only one of which can accommodate the protein. The subtractive methods include partition equilibria between phases, gel-filtration (Braumbaugh & Ackers, 1971), ultrafiltration (Mihailova & Russeva, 1978), affinity chromatography (Nakano et al., 1979), electrical conductivity and polarography (Tanford, 1961) as well as dialysis methods. The most generally applicable subtractive methods are dialysis methods.

In addition to the methods referred to, a variety of methods which depend on the electrostatic theory of dilute solutions is available. Electrostatic methods include measurements based on changes in the conductivity of ligand solutions as a function of protein concentration (Klotz, 1953), and ionic mobility measurements (Waldmann-Meyer, 1980).

Alberty & Marvin (1951) have described a method to determine the extent of complex formation by comparing the constituent mobilities of the ligand and the protein-ligand complex with those of the free protein and ligand only, under identical conditions. The use of affinity electrophoresis to measure protein-ligand association constants has been described by Horejsi (1979).

Measurement of the permittivities of protein solutions at very high frequencies, to which the protein ions do not respond, have also been used to obtain information relating to solvent binding and to obtain estimates of protein hydration (Buchan et al., 1952).

An application of the Linderström-Lang theory, which depends on the measurement of changes in the pH of isoionic protein solutions by the addition of neutral salts (Scatchard & Black 1949), provides an easy and rapid method of determining binding of ions to proteins. This method relies on measurement of changes in pH from an unequal binding of cations and anions to de-ionized protein. In situations where the Linderström-Lang theory is applicable, the relationship between \bar{v}_i , the molal binding ratio for the salt ions of charge Z bound to the protein, and change in the pH of the protein solution is given by:

$$\Delta \text{pH} = -0.868w \sum_i \tilde{v}_i \quad \dots \quad 4.4.1$$

w is the composite constant derived from Debye-Hückel theory and \tilde{v}_i the number of salt ions of charge Z bound per mole of protein, which includes both cations and anions. When cation binding can be disregarded, and when only one kind of anion is present, equation 4.4.1 simplifies to:

$$\Delta \text{pH} = -0.868w\tilde{v} \quad \dots \quad 4.4.2$$

The accuracy of equation 4.4.2 depends on the applicability of the Lindeström-Lang equation and the validity of the assumptions used in its derivation. Cassel & Steinhardt (1969) have shown that this differential pH method underestimates the degree of binding when the value assigned to the constant w is obtained from Debye-Hückel theory (equation 3.5.6). However, when values of w are obtained by empirical methods using slopes of graphical plots (Halfman & Steinhardt, 1971), the method yields values for the binding constants which are in agreement with values obtained by equilibrium dialysis. A recent application of pH perturbations to measure the binding of positively ionized drugs to proteins has been described by Parsons & Vallner (1980).

4.5 Dialysis methods

Dialysis methods are essentially partition methods in which the distribution of the ligand between the protein and the solvent is achieved by means of a semipermeable membrane. The techniques of gel-filtration and ultrafiltration, which are similar in principle to dialysis, are useful complementary techniques. These techniques circumvent some of the problems associated with dialysis.

The gel-filtration method, which was introduced by Hummel and Dreyer (1962), uses a Sephadex column which has been equilibrated with the ligand. The protein-ligand mixture is applied to the column and the column eluted with a ligand solution. In this method, the surface of the gel is used as the interface to effect a distribution of ligand between the protein phase and the bulk solution. The ligand concentration in the eluting buffer is monitored, and after the emergence of the protein from the column a trough in the recorded ligand concentration signal reflects the abstraction of ligand from the gel by the protein. Fairclough & Fruton (1966) have given a description of the method, which includes a discussion of the procedures, calculations, and the corrections which have to be applied.

The method of ultrafiltration closely resembles the equilibrium dialysis method (to be discussed below). In this technique, the long time required to attain equilibrium between the protein and the ligand is reduced by using high pressure membrane filtration. High pressures are used to separate a fixed volume of protein-free solution from a protein-ligand mixture. This protein-free solution is then analysed to determine its free ligand concentration. Mihailova & Russeva (1978) have reported a method in which the filtration is performed under pressure produced by mechanical means.

The filtration membrane may be dispensed with by using an ultracentrifuge (Steinberg & Schachman, 1966). In this technique, the ligand concentration is depicted graphically as a function of protein concentration, from measurements of the migration of the protein under the influence of a centrifugal field. By extrapolating the linear plot of total ligand concentration to zero protein concentration, a value for the free-ligand concentration is obtained. The ligand-protein molal binding ratio \bar{v} can be determined from the slope of this linear plot. Refinements of the method, which measure sedimentation velocities of the protein and protein-ligand complex, have been described by Gilbert & Jenkins (1960), and by Nichol & Ogston (1965).

B Principles of Dialysis

4.6 The Dialysis Process

Dialysis methods to investigate protein-ligand binding can be applied to a wide variety of situations. Reviews which consider the relevant aspects of dialysis and factors which govern diffusion processes include the publications by Ferry (1936), Carr (1961), McPhie (1971), Crank (1956) and Hoch & Williams (1958). Friedman & McCally (1972) have dealt with quantitative aspects of dialysis while Barnes (1934) and Barrie et al. (1975) have provided the mathematical descriptions for the diffusional processes occurring within the diffusion membrane. A brief summary of the principles of dialysis is presented as background material for the subsequent discussion of the equilibrium dialysis method.

Dialysis may be defined as the separation of a mixture of macromolecules and low molecular mass compounds which can be effected by diffusion. A semi-permeable membrane permits diffusion of the small molecules (referred to as the dialysate or diffusate), and retains the macromolecules (the retentate). The diffusion of the small molecules occurs under the influence of a concentration gradient. A complete separation of the macromolecule and the low molecular-mass solute can be achieved by replacing the solution on the sink side of the membrane by fresh solvent, at regular intervals, to maintain the concentration gradient.

The rate of diffusion of the small molecules in a solution is governed by Fick's first law of diffusion, which is expressed by:

$$-dC/dt = D_f \text{ div } \{C\} \quad \dots \quad 4.6.1$$

where C is the solute concentration, and D_f is the ligand diffusion coefficient. The same law governs the diffusion of ligand through a semi-permeable membrane; however, in this case, a number of other factors can also affect the rate of diffusion.

C Factors Affecting the Rate of Dialysis

It is convenient to divide the factors affecting the rate of dialysis of the ligand into factors which are common to all diffusional processes, and those which are specific to membrane diffusion.

4.7 Factors Relating to the Diffusion Process

Diffusion occurs wherever there is a concentration gradient. As shown by equation 4.6.1, this is a three-dimensional process. In the general physical process of diffusion, the value of the diffusion coefficient D_f depends on physical variables such as temperature and particle size. The dependence of D_f on these factors is given by the Einstein equation (1908):

$$D_f = RT/6\pi Lr\eta \quad \dots \quad 4.7.1$$

where R is the universal gas constant, L the Avogadro number, T the solution temperature (absolute), η the solvent viscosity, and r is the radius of the ideal sphere equivalent to the molecular volume of the solute.

If Fick's law is applied to the diffusion of ligand through a semi-permeable membrane across which there is a concentration gradient, equation 4.6.1 reduces to:

$$- dC/dt = D_m A dC/dx \quad \dots \quad 4.7.2$$

D_m is now the ligand diffusion coefficient for the membrane and A is the effective membrane area. The effective membrane area is defined as the product of the total membrane area and the fraction available for solvent movement.

4.8 Factors Influencing Membrane Diffusion

Although membrane diffusion is influenced by both charge effects and solvent effects, where contributions to the overall dialysis mechanism have to be considered a simple approach can be adopted. This makes it possible to relate the diffusion rate of the ligand to its molecular dimensions, and to the effective area of the membrane available for diffusion. In this simplistic model, the membrane is considered as a mechanical sieve which consists of a series of cylindrical pores, normal to the membrane surface. Ferry (1936) derived the relationship:

$$A_{\text{eff}}/A_0 = (1 - r/a)^2 \quad \dots \quad 4.8.1$$

on the assumption that diffusion occurred when the solute molecule could pass through the channels without striking the edges. In equation 4.8.1, A_{eff} is the effective diffusion area for a spherical molecule to pass through an ideal cylindrical pore, a is the radius of the cylindrical pore, r is the radius of a spherical solute molecule, and A_0 is the cross-sectional area of the membrane.

A refinement of Ferry's equation which provides a better description of the observed diffusion of small molecules and which incorporates a drag term similar to that of capillary flow, is given by the Rencken equation (Rencken, 1955)

$$A_{\text{eff}}/A_0 = (1 - r/a)^2 \{ 1 - 2.104r/a + 2.09(r/a)^3 - 0.95(r/a)^5 \} \quad \dots \quad 4.8.2$$

The Ferry and Rencken equations demonstrate that the ability to differentiate between solute molecules of similar size on the basis of dialysis becomes greater as the radii of the solute molecules approach the pore radius. The experimental demonstration that the rate of diffusion of solute in the membrane is considerably slower than the diffusion of solute in

solution (Craig & Chen, 1972) also shows that the rate limiting factor in dialysis is the effective cross-sectional area of the membrane pore. This observation, together with the assumption that the physical forces underlying membrane diffusion are the same as those for free diffusion, permits a correlation between the diffusion coefficient, D , for ligand in the solvent, and the membrane diffusion coefficient, D_m . This correlation has been expressed (Stewart, 1977) in terms of the effective membrane area, A_e , and total membrane area, A_m , by:

$$D_m = (A_e / A_m) D_f \quad \dots \quad 4.8.3$$

It is useful to incorporate the Einstein equation (equation 4.7.1) into the Fick's law expression which governs the diffusion of ligand in the membrane, by expressing the proportionality between concentration gradient and rate of diffusion as a product of three factors. Thus equation 4.7.2 can be written as:

$$-dC/dt = k_1 k_2 k_3 (dC/dx) \quad \dots \quad 4.8.4$$

where

k_1 is the composite constant $k_1 = R/6 L$;

k_2 incorporates the effect of temperature and viscosity;

and k_3 is the term containing the effective membrane area and solute radii.

i) Pore shape

The effective diffusional diameter of the solute is, as a result of molecular tumbling, not the same as the diameter of the idealized molecular sphere. The effective diffusional diameter is directly related to the spherical volume described by the longest cross-sectional axes of the molecule. The critical dimension of a non-cylindrical membrane pore is thus its minimum

width. Unidirectional stretching of the membrane causes a distortion of the circular membrane pores to ellipses. This will thus adversely affect the rate of diffusion. Studies which examine the effect of stretching the membrane on the rate of ligand diffusion have been reported by Stewart (1977).

ii) Stirring

The apparent rate of diffusion of the solute through the membrane may be affected by concentration gradients within the solution. This factor will be especially noticeable when the volumes of the solution are very large relative to the membrane volume. It is thus necessary to agitate or stir the solution in contact with the membrane to ensure its homogeneity. The rate of diffusion has been shown (Meyer & Guttman, 1970b; Kanfer, 1976) to be independent of the rate of stirring, provided the stirring does not produce excessive turbulence or Joule heating, and is fast enough to maintain solution homogeneity.

iii) Ultrafiltration

The passage of the solute and solvent across the membrane is facilitated when the hydrostatic pressures on the two sides of the membrane differ. The effects of ultrafiltration can be appreciable, especially if large pressure differences develop due to osmosis. The effects of ultrafiltration on solute diffusion have been reported by Hoch & Miller (1966). It is preferable, where possible, to maintain the same hydrostatic pressure on both sides of the membrane.

iv) Osmosis

Osmotic effects can be severe at high concentrations. The ligand dialysis escape curve, which represents the ligand concentration on the sample side of the membrane as a function of time, can be affected by dilution of the solution due to osmosis (Carr, 1961; Shieh et al., 1975). Osmotic effects can be kept to negligible levels by the use of low macromolecular concentrations.

v) Membrane and solute charge

The rate of dialysis of charged solutes is usually less than or equal to that of uncharged solutes of similar size. Although the mechanism is not understood, this effect may be due to differences in hydrated molecular volumes. Membrane charge effects result in the formation of a membrane potential. This is a thermodynamic reflection of membrane polarization counteracting concentration gradients within the membrane (Tanford, 1961). Membrane potentials and the Donnan membrane effects are interrelated phenomena. In protein-ligand binding studies, membrane charge effects make their presence noticed mostly in the measurement of free ligand activity by EMF methods, and in the use of 'perm-selective' membranes (i.e., membranes which are only permeable to cation or anions but not both) (Carr, 1953; Parsons, 1958; Scatchard et al., 1957 & 1959).

vi) The Donnan membrane effect

A possible source of error in dialysis measurements is the unequal distribution of small ions across the semipermeable membrane separating a protein solution from a solution containing diffusible ions, even though the system is otherwise at equilibrium. This is the Donnan effect. It is common practice to minimize Donnan effects by having an excess of electrolyte on

both sides of the membrane. However, attempts to suppress Donnan inequalities by the addition of excess electrolyte is undesirable when dialysis methods are used to measure protein-ligand binding. A large excess of background ions may lead to competitive binding to the protein by these ions.

D The Application of Dialysis to Protein-Ligand Binding

4.9 Equilibrium Dialysis

The classical method of equilibrium dialysis (Klotz et al., 1946; Bush & Alvin, 1973) is the most commonly used procedure for measuring protein-ligand interactions. This equilibrium dialysis method still finds frequent application, because it is considered to possess several advantages over some of the more sophisticated methods. The equilibrium dialysis is in principle simple, inexpensive, thermodynamically valid, and can be made to approximate 'in vivo' conditions. The method consists of separating the protein in one compartment (the sample compartment) from a solution of the ligand in a second compartment (the sink compartment) by a membrane permeable to all components of the system except the protein. When the system attains equilibrium, the activities of all the components except the protein will be the same on either side of the membrane. The activity of the ligand in equilibrium with the protein-ligand complex may then be readily determined by assaying solution in the protein-free compartment of the system. Any appropriate analytical method can be used to assay the ligand concentration. Chemical potentials or activities can be determined directly by measurement of EMF using reversible electrodes (or measurement of partial pressures, if gases are involved). However, concentration measurements, determined by chemical analysis, are strictly valid only if it can be ascertained that the concentrations have the same relationship to chemical potential on each side of the membrane. This assumption is frequently taken for granted. Behm

and Wagner (1979) and Smith & Jubiz (1980) have questioned this assumption and commented on the possibility of obtaining incorrect results by the equilibrium dialysis technique by relying on this assumption when it is not valid.

The equilibrium dialysis method is subject to a number of sources of error and disadvantages (Steinhardt & Reynolds, 1969; Behm & Wagner, 1979). A major disadvantage is the length of time required for the system to attain equilibrium. In theory, an infinite time is required. The long times required to establish the equilibrium, apart from being undesirable in practical terms, increase the possibility of protein putrefaction or denaturation. The rate of attainment of equilibrium depends on the concentrations of both the protein and the ligand, the molecular volumes of the diffusate and retentate, the nature of the supporting electrolyte, membrane area, and membrane pre-treatment. The rate of attainment of equilibrium also depends on the temperature and viscosity of the solutions, and whether the solutions are stirred effectively. Competitive binding to the protein by cations and anions added to suppress the Donnan effect or to buffer the solutions against changes in pH may affect the equilibrium. The membrane also constitutes a possible source of error: binding to the membrane by the protein, the ligand, or the protein-ligand complex will lead to inaccuracies.

In general, optimum conditions require small solution volumes, large membrane areas, low temperatures, and agitation to ensure renewal of the solution layer in contact with the membrane. A quantity of ligand will be retained within the membrane. Attempts to reduce the time required for the system to attain equilibrium by increasing the surface area of the membrane (Craig & Chen, 1972) can therefore also introduce inaccuracies through the retention of larger quantities of ligand by the membrane. This effect is usually small and is generally disregarded.

Competitive binding by ions of the supporting electrolyte can be expected since it is usually not expedient, because of

Donnan effects and buffer requirements, to reduce the concentration of the supporting electrolyte to less than 0.03M. Thus the concentration of the supporting electrolyte may exceed that of the ligand by a factor of 10^3 . Klotz (1953) has shown that a variety of buffer anions, such as acetate, citrate, etc., can compete strongly as protein binders. Cassell & Steinhardt (1969) have shown that substitution of sodium chloride for phosphate buffer increases the time required for bovine serum albumin-hydrocarbon sulphonate system to attain equilibrium by more than 200%. This kinetic effect is due to the slow replacement of bound chloride by the ligand.

Inaccuracies due to competitive binding between the supporting electrolyte and the ligand can, however, be taken into account. Mathematical expressions which allow for competition between the ligand and the ions of the supporting electrolyte may be derived (Steinhardt and Reynolds, 1969). The mathematical correction for competitive binding by supporting electrolyte assumes that the protein molecule has available N binding sites and that the two competing ligands L_1 and L_2 will compete for the same binding sites. It is also assumed that the ligands L_1 and L_2 will have different association constants, k_1 and k_2 respectively. In terms of equivalent or identical binding sites, the molal binding ratios for the competing ligands are given by:

$$\bar{v}_1 = (k_1 [L_1]) (N - \bar{v}_2) / (1 + k_1 [L_1]) \quad \dots \quad 4.9.1$$

and

$$\bar{v}_2 = (k_2 [L_2]) (N - \bar{v}_1) / (1 + k_2 [L_2]) \quad \dots \quad 4.9.2$$

These equations represent the Scatchard equation for the single site binding model, for each ligand competing for the protein binding site. \tilde{v}_i is the molal binding ratio for a particular ligand, the k_i are the protein-ligand association constants ($i = 1, 2$) and N is the total number of binding sites available for ligand binding by either ligand. These equations can be solved for \tilde{v}_1 & \tilde{v}_2 , respectively, to give:

$$\tilde{v}_1 = Nk_1[L_1] / (1 + k_1[L_1] + k_2[L_2])$$

.... 4.9.3

and

$$\tilde{v}_2 = Nk_2[L_2] / (1 + k_1[L_1] + k_2[L_2])$$

.... 4.9.4

Equations 4.9.1 & 4.9.2 embrace the simplest model to describe ligand binding, viz., independence of the binding sites is assumed. It is therefore generally more convenient, in equilibrium dialysis studies, to use the minimum concentration of weak binding agents (such as phosphate) for the supporting electrolyte rather than to compensate for competitive binding by the use of mathematical corrections. It is also customary to carry out the dialysis with isoelectric protein, avoiding if possible the addition of neutral salts.

It has been shown (Ray et al., 1966) that the binding isotherm obtained by equilibrium dialysis can, in certain circumstances, be influenced by the protein concentration. Smaller values were obtained for the protein-ligand association constants with a variety of ligands at higher protein concentrations than for solutions of the same ligands at lower protein concentrations. Cassel and Steinhardt (1969) have postulated that this is a kinetic effect rather than a thermodynamic effect. These authors attribute the effect to a reduction in the membrane permeability at higher protein concentrations, due to coating of the membrane by protein, rather than to changes in the viscosity of the solution, or to the presence of weakly binding impurities in the protein.

However, more recent reports based on apparently anomalous binding isotherms indicate that a dependence on protein concentration can also be a feature of the ligand binding (Steiner, 1980). In these cases, Scatchard plots of the binding isotherms exhibit positive slopes. Protein-ligand binding systems which display positive slopes in the Scatchard plots have been examined by Shen & Gibaldi (1974) and by Bowmer & Lindup (1978). The latter have suggested several explanations to account for the phenomena. One explanation considers molecular association of the protein with an increase in the protein concentration. On the other hand, it has been pointed out (Noerby et al., 1980) that there is a widespread misinterpretation in the chemical literature of protein-ligand binding experiments. These authors discuss the commonly encountered errors due to faulty interpretation of curved Scatchard plots.

It has been established that adsorption of ligand onto the membrane can occur (Reed, 1973; Doluiso et al., 1974; Kinget et al., 1979). The quantity of ligand adsorbed onto the membrane will depend on the affinity of the ligand for the membrane and thus, in a general way, on the ligand structure. Consequently, the extent of adsorption to the membrane by the ligand will vary from ligand to ligand. This makes it difficult to evaluate the effect of ligand-membrane binding on the protein-ligand binding isotherm. Errors due to this source will be greatest when the protein-ligand coverage or ligand affinity for the protein is small.

A further source of error is the possibility of the release of interfering contaminants, such as plasticisers, etc., from the membrane (Cooney, 1980). Besides the possibility that these impurities may interfere with the measurement of the free ligand concentration, there is the further possibility that the impurities may induce conformational changes in the protein and thereby change the binding characteristics of the protein

(Reynolds et al., 1967a). This source of error in equilibrium dialysis can be eliminated by suitable pre-treatment of the dialysis membrane.

A discussion of the errors in the equilibrium dialysis technique which can result from the not always justifiable assumption that equilibrium in the post-dialysis sample is necessarily the same as existed before dialysis has been presented by Smith & Jubiz (1981). A discussion of possible errors in the interpretation of equilibrium dialysis data has also been given by Behm & Wagner (1979).

Despite its numerous hazards, in terms of experimental variables which require scrupulous attention, the equilibrium dialysis method is widely used, remains popular, and has been the preferred method in a number of recently published studies (Sukow et al., 1980; Romer & Bichel, 1979; Tipping et al., 1980).

Attempts to overcome some of the limitations of the method have led to the development of a variety of sophisticated dialysis techniques. Craig (1957) and Craig & Chen (1969) developed the thin-film dialyzer, in which a relatively large area of membrane is exposed to a small sink compartment. This apparatus has been used to measure protein-ligand binding by both equilibrium and kinetic dialysis methods (Ginsburg & Ireland, 1964; Russo and Engel, 1978). The advantage which a thin-film dialyzer offers over the classical equilibrium method is that the attainment of equilibrium is fairly rapid because of the large membrane surface area. Stein (1965) has described an automatic flow system for obtaining equilibrium dialysis data.

4.10 Kinetic Dialysis Methods

Most of the other dialysis techniques which have been used to investigate protein-ligand binding rely on the measurement of the rate of ligand diffusion rather than measurement of equilibrium ligand concentrations. These methods constitute the kinetic dialysis methods. Protein-ligand binding isotherms can be established from measurement of the differences in the rate of diffusion of the ligand in the presence and absence of protein. It is generally assumed that the diffusion of the ligand obeys Fick's first law of diffusion. One approach to the use of the kinetic dialysis method to investigate protein-ligand binding involves the removal of substantial quantities of ligand from the dialysis system during measurement (Hoch & Muller, 1966). The more commonly used methods, however, depend on the removal of only negligible amounts of ligand for analysis.

The theory developed for the former approach (Silhavy et al., 1975) shows that, when the protein concentration greatly exceeds the total ligand concentration, the exit diffusion rate of ligand follows quasi-first order kinetics. It has been shown that ligand retention has a half-life proportional to $(1 + C_p/K_d)$ where C_p is the concentration of binding sites and K_d is the protein-ligand dissociation constant.

All kinetic dialysis methods depend on the assumption that the formation of the non-diffusible protein-ligand complex is reversible, and very rapid. Klotz (1973) has discussed the validity of this assumption. On the basis of high-speed relaxation methods, such as temperature jump and magnetic resonance techniques, he has concluded that, in general, the rate of dissociation of the protein-ligand complex is sufficiently large that errors in subtractive methods due to this factor are unlikely. However, it is to be borne in mind that, with very strongly bound ligands, dissociation rates may be a limiting factor for subtractive methods.

Tanford (1961) has described a simple procedure whereby it is possible to test whether the protein-ligand equilibrium occurs rapidly. This consists of comparing the quantities of ligand bound to protein in a solution formed by the addition of ligand to protein, with those of a concentrated protein-ligand mixture which is diluted to the same final ligand concentration. If the same results are obtained in each case, it can be assumed that the protein-ligand dissociation is reversible and rapid.

A variety of other methods to investigate protein-ligand binding by kinetic or dynamic dialysis methods include the methods described by Meyer & Guttman (1969; 1970a,b), Colowick and Womack (1969), Lecureuil et al., (1974), Robertson & Madsen (1974) and Rachidy & Niazi (1978).

In the method described by Colowick & Womack, there is used a dialysis cell consisting of upper sample and lower sink compartments which are separated by a semipermeable membrane. A constant stream of eluting buffer is passed through the sink compartment. The method relies on a series of measurements of isotopically labelled ligand concentrations in the eluted sink compartment of the cell. However, these measurements are made only after steady-state conditions have been attained at each stage (i.e., only when the rate at which labelled ligand diffuses into the sink compartment is equal to the rate at which it is eluted). This necessitates regular additions of aliquots of unlabelled ligand to the sample compartment in order to promote a readjustment of the protein-ligand equilibrium, and give rise to a new steady-state condition.

In both this method and the method developed by Meyer & Guttman, ideal sink conditions are assumed to prevail. Back-diffusion of the ligand from the sink to the sample compartment is considered to be negligible. The Colowick & Womack method has not found wide application, although it has been proposed (Bush & Alvin, 1973), that the method can be readily adapted to kinetic studies to measure rates of ligand binding and release. A variation of the Colowick & Womack method which uses a similar type of dialysis cell has been described by Lecureuil et al. (1974). These authors have described two methods for

establishing a protein-ligand binding isotherm. In the one method, they obtained a binding isotherm in a discontinuous manner by varying the area of the membrane without varying the ligand concentration. In the second method, these authors described how the binding isotherm could be obtained in a continuous manner when the ligand concentration is changed. Farrell et al. (1971) have described an apparatus consisting of a closed loop system using radio-active tracers. This apparatus has been used to investigate the binding of metabolites to proteins.

As has been noted, each of these methods has been devised to obviate certain of the limitations of the equilibrium dialysis methods. Although each of these methods has specific advantages over the equilibrium method, which make them suitable for particular applications, they all share to a greater or lesser extent some of the limitations common to subtractive methods and dialysis processes. The major advantage of the dynamic or kinetic dialysis methods over the equilibrium dialysis method is in economy of time and material. A survey of the problems in the use of dialysis techniques to study the binding of drug molecules to macromolecules has been given by Kinget et al., (1979).

E The Meyer and Guttman dynamic method

4.11 Experimental Procedure

A brief synopsis of the experimental method and the principles of the Meyer & Guttman dynamic dialysis method is presented. This provides the background necessary for the development of the mathematical analysis used in the continuous-flow dynamic dialysis method.

In the Meyer & Guttman method, a solution containing known amounts of protein and ligand is introduced into a dialysis sac which is inserted into a jacketed beaker containing pure buffer solution. Aliquots of the external buffer are sampled at regular intervals for analysis, and replaced by equivalent

volumes of buffer to maintain a constant sink compartment volume.

Ideal sink conditions are assumed to prevail. The sink compartment ligand concentration is considered insignificant and back-diffusion of the ligand from the sink to the sample compartment is ignored in the calculation of the concentration gradient across the dialysis membrane. Thus in terms of Fick's first law of diffusion, which is assumed to govern the diffusion of the ligand both in the presence and absence of protein, the rate of diffusion of the ligand is directly proportional to the ligand concentration in the sample compartment of the dialysis cell. The concentration of the free ligand in the sample compartment can therefore be determined from the rate of ligand diffusion across the membrane. The proportionality constant relating the rate of ligand diffusion to the sample compartment ligand concentration (the permeation constant) depends on the area of the membrane, membrane thickness, membrane pore diameter and also on the nature of the ligand. The permeation constant is established from a control experiment where the rate of diffusion of the ligand in the absence of protein is monitored. A mass-balance relationship is used to establish the ligand concentration in the sample compartment as a function of time. This will be referred to as the ligand escape curve.

4.12 Data Analysis (Meyer & Guttman 1969; 1970a,b)

By Fick's law, the rate of loss of ligand from the sample compartment is given by:

$$-d[Q(t)]/dt = D C_1(t) \quad \dots \quad 4.12.1$$

where D is the permeation constant, $C_1(t)$ is the concentration of unbound or free ligand in the sample compartment, and $Q(t)$ is the total quantity of ligand (bound and free) in the sample compartment. Thus:

$$Q(t) = V_1 C_q(t) \quad \dots \quad 4.12.2$$

where V_1 is the volume of the solution in the sample compartment, and $C_q(t)$ corresponds to the total ligand concentration in the sample compartment.

For the control experiment, in the absence of protein:

$$C_q(t) = C_1(t)$$

and equation 4.12.1 has the solution:

$$\ln[C_1(t)] = -D/V_1 t + \ln[C_1(0)] \quad \dots \quad 4.12.3$$

where $C_1(0)$ is the total initial ligand concentration. From equation 4.12.3 it follows that the value for the permeation constant is given by :

$$D = V_1 \ln[C_1(0)/C_1(t)]/t \quad \dots \quad 4.12.4$$

The slope of a plot of $\ln[C_1(t)]$ vs t thus provides a value for D .

When protein is present in the sample compartment

$$C_q^*(t) = C_1^*(t) + p\tilde{v}(t) \quad \dots \quad 4.12.5$$

The asterisk is used to denote ligand concentrations in the presence of protein, p is the protein concentration, and $\tilde{v}(t)$ is the ligand-protein molal binding ratio.

When protein is present, a plot of $\ln[C_1^*(t)]$ vs t , now has a smaller slope because of the slower release of ligand to the sink. Depending on the nature of the binding, the plot can also display upward curvature. By equation 4.12.1

$$c_1^*(t) = -V_1/D \, d[C_q^*(t)]/dt \quad \dots \quad 4.12.6$$

which, on substitution into equation 4.12.5 and rearrangement, gives :

$$p\bar{v}(t) = \{C_q^*(t) + V_1/D \, d[C_q^*(t)]/dt\} \quad \dots \quad 4.12.7$$

The molal binding ratio is written as a function of time, and equations 4.12.6 & 4.12.7 constitute the parametric equations for the binding isotherm. $C_q^*(t)$ is obtained by mass balance as the difference between the total amount of ligand introduced into the sample compartment and the amount which has been lost to the sink.

Meyer & Guttman used a curve-fitting procedure incorporating the appropriate model (in this case, the Scatchard model) to obtain the protein-ligand binding parameters. An iterative least squares procedure was used to obtain refined values for the binding parameters from initial estimates which were obtained from the slopes and intercepts of Scatchard and/or double-reciprocal plots.

The advantages of the Meyer & Guttman method over the equilibrium dialysis method are that the method requires a minimal amount of sample preparation, is economical with respect to protein and time, and provides convenient means for temperature control. Since its introduction, the method has been successfully used to characterise the interactions of a number of compounds (including many drugs) to macromolecules. Reports of such use include those by Dearden & Tomlinson (1970), Crookes & Brown (1973), Tukamoto et al. (1974), Kanfer (1975), Judis (1980), and Kimura (1980).

4.13 Limitations of the Meyer & Guttman method

Meyer & Guttman (1970) investigated the influence of factors such as the viscosity of the solution, the rate of stirring, temperature, etc., on the reliability of the dynamic dialysis method. Apart from these practical aspects, the principal disadvantage of the method stems from the requirement to determine the rate of ligand diffusion, $d[C_q^*(t)]/dt$. The obvious method of determining the rate of ligand diffusion is by measurement of the slope of the $C_1(t)$ vs t or $C_q^*(t)$ vs t graphs. However, values of $d[C_q^*(t)]/dt$ obtained from such slopes, are subject to considerable uncertainty because of the paucity of data points. In a typical experiment by Meyer & Guttman, aliquots were withdrawn at half-hourly intervals over a period of about 9 hours, to yield only eighteen data points.

Uncertainties in the values for $d[C_q^*(t)]/dt$ are a serious limitation. Ashgar & Roth (1971) have shown that the isotherm is sensitive to slight variations in the slope of the $C_q^*(t)$ vs t curve. Practical difficulties which arise from increasing the sampling frequency prompted Meyer & Guttman (1968) to use a regression procedure to fit the ligand escape curve to an empirical function which was then differentiated analytically.

The selection of an empirical model is, however, a somewhat arbitrary procedure. The choice of model can vary both with respect to the nature of the function and the number of parameters used to specify the fit. Fitting data to an empirical function to determine the analytical derivative can also introduce various problems. There is a question of uniqueness, in that several different functions may provide equally suitable descriptions of the data in the sense of 'goodness of fit'. Although such functions may adequately describe the limited data set, could have different derivatives, especially near the limits of the data range. In addition, there exists the danger (especially when there is a limited number of observations, or if the data spans a limited concentration range) that the imposition of a particular mathematical model onto the data will bias the

interpretation according to the model chosen. A variety of model functions have been used, with varying degrees of success, to describe the ligand dialysis escape curve (Dearden & Tomlinson, 1972; Crookes & Brown, 1973). The utility and consequence of fitting a variety of empirical functions to the experimental data have been investigated by Kanfer & Cooper (1976). The effects on the Scatchard plots due to the choice of function, for a variety of functions, is shown in the graphs reproduced in figure 4.1. The solid curves represent the theoretical Scatchard plots, based on the published values for the n's and k's (Meyer & Guttman (1968, 1979b) while the symbols in each graph represent the binding data (\bar{v} and \bar{v}/C_1^*) obtained from the application of the particular function used to fit the curvilinear plot of C_1^* versus time.

Meyer & Guttman chose a six-parameter tri-exponential model. Kanfer (1975) was able to show, from a comparison of experimentally determined Scatchard plots using the Meyer & Guttman method with hypothetical data generated over the same concentration range, that this function gave the most satisfactory results for the systems involved. In terms of a tri-exponential function, the concentration of free-ligand in equilibrium with the protein is given by:

$$C_q^*(t) = \sum_{i=1}^3 A_i e^{-a_i b t} \quad \dots \quad 4.13.1$$

where A_i and a_i are the parameters obtained from the least-squares regression.

Substitution of equation 4.13.1 into 4.12.7 gives:

$$\bar{v}(t) = \sum_{i=1}^3 A_i (1 - V_1 a_i / D) e^{-a_i t} \quad \dots \quad 4.13.2$$

Despite the agreement between the generated and experimentally determined Scatchard plots obtained by Kanfer, a bi-exponential model and a tri-exponential equation with a negative value for the amplitude parameter, A_2 , provides an almost equally satisfactory description of the data in a Scatchard plot, as can be seen from Figure 4.1

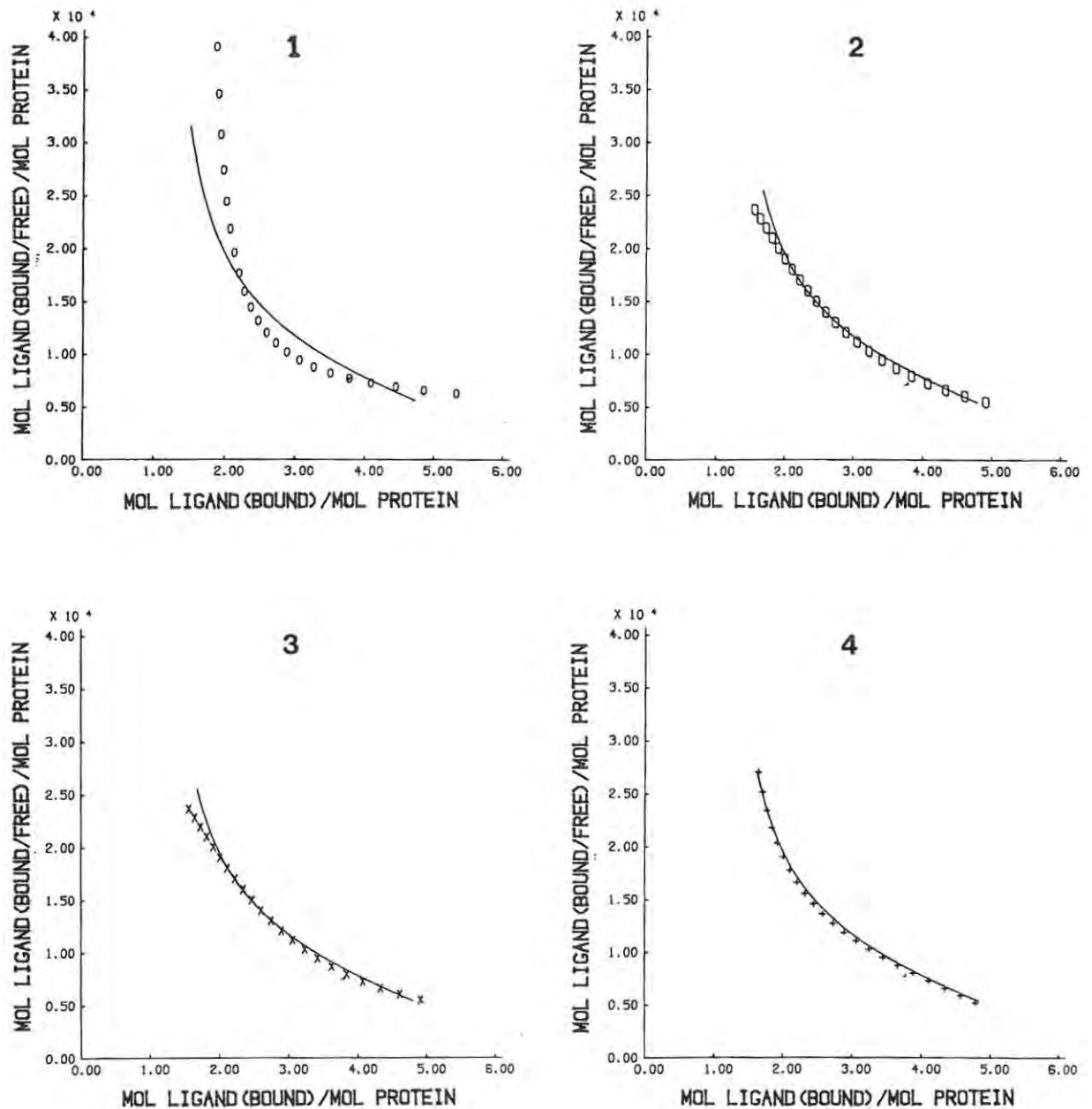
It has been pointed out by Lanczos (1967) that a variety of linear combinations of exponentials can be used to provide equally satisfactory fits to a given data set within the accuracy of the experimental measurements. However, because of the sensitivity of the amplitudes and exponents in a linear combination of exponentials to very small changes in the data, results derived from such a linear combination of exponentials by regression procedures will be subject to large uncertainties, and hence be unreliable.

4.14 Pedersen's analysis of the Meyer & Guttman method

Pedersen et al. (1977) have described a method for obtaining drug-macromolecule binding parameters directly from dynamic dialysis data. This method provides a pair of parametric equations in the parameter $s = -dC_q^*(t)/dt$ which are used to define a unique pair of values for $C_q^*(t)$ and t from which binding parameters are determined by non-linear regression analysis.

This approach offers several advantages over the original Meyer & Guttman method. It eliminates the need to determine a dialysis rate constant separately, is applicable to membrane-bound ligands, and does not require differentiation of the experimental data. The analysis does, however, depend on the assumption of a functional relationship between \bar{v} and the unbound ligand concentration. It is necessary, therefore, to incorporate a mathematical binding model into the analysis. Pedersen developed the method based on a single class of binding sites. Although this analysis can be expanded for use with molecules that display more complex binding behaviour, this not only complicates the analysis but is undesirable.

Figure 4.1



Scatchard plots of binding data obtained by fitting theoretical values of $C_1(t)$ from empirical mathematical functions to the general two-site Scatchard model

$$(1) C_1^*(t) = Ae^{-bt} + C$$

$$(2) C_1^*(t) = Ae^{-at} + Be^{-bt}$$

$$(3) C_1^*(t) = Ae^{-at} - Be^{-bt} + Ce^{-ct}$$

$$(4) C_1^*(t) = Ae^{-at} + Be^{-bt} + Ce^{-ct}$$

The solid curve in each graph was generated from the two-site Scatchard equation with binding parameters, $n_1 = 1$; $n_2 = 6$;

$$k_1 = 1.74 \times 10^5 \text{ and } k_2 = 1.97 \times 10^3 \quad (\text{from Kanfer, 1976})$$

Chapter Five

The Continuous-Flow Dynamic Dialysis Method and Data Analysis by the Permeation Constant Method

5.1 Introduction

As opposed to the Meyer & Guttman method for determining a binding isotherm by sampling and assaying the ligand concentration in the dialysate at regular intervals, a continuous-flow dynamic dialysis method (CFDD) has been developed to investigate protein-ligand binding. In this and the next chapter, the procedure and principles of the CFDD method are described, and mathematical methods of analysis to extract a binding isotherm from the dialysis data are presented. The CFDD method offers several advantages over the Meyer & Guttman method. The method does not ignore the small ligand concentration in the sample compartment of the dialysis cell. Rather, the analysis incorporates a term to allow for back-diffusion. This represents a more accurate recognition of Ficks' first law of diffusion than the Meyer & Guttman analysis. Unlike the Meyer & Guttman method which, by assuming ideal sink conditions to prevail, considers the rate of ligand diffusion to be directly proportional to the sample compartment ligand concentration, in the CFDD method the rate of ligand diffusion is taken to be proportional to the difference between the ligand concentrations on either side of the membrane. The significance of neglecting the finite sink compartment ligand concentration in the analysis and its effect on the binding isotherm is discussed in Appendix I.

Two different procedures are developed whereby the data obtained from dialysis experiments can be processed to extract a binding isotherm. In this chapter, a method of analysis which will be referred to as the "permeation constant method", is described. The permeation constant method is based directly on the assumption that ligand diffusion is governed by Fick's first law of diffusion, and that the permeation constant for the ligand, D , is independent of ligand concentration. By this

method, a value for the permeation constant is obtained from a control experiment. The control experiment is used to determine the relationship between sink compartment ligand concentration and the rate of diffusion of the ligand in the absence of protein.

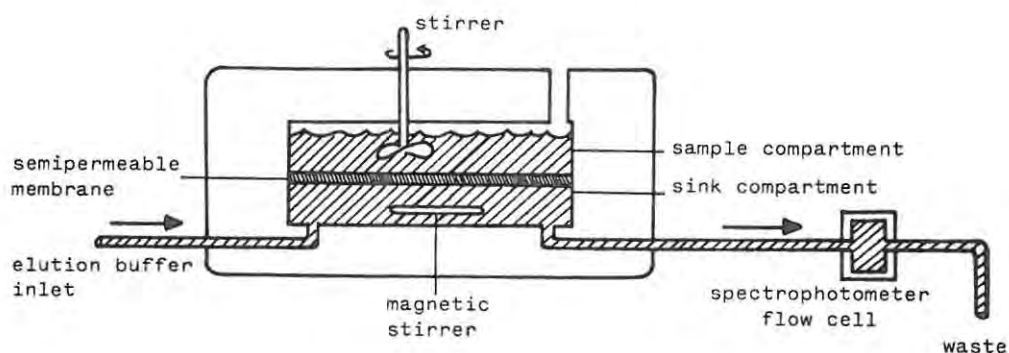
A more general method of analysis, which utilizes the concept of a system transfer function, is described in Chapter Six. In that more general analysis, the assumption of proportionality between rate of ligand diffusion and concentration gradient across the dialysis membrane is incorporated into a system linearity assumption by means of which a system transfer function may be developed. The same transfer function relates the sink compartment ligand concentration to the concentration of the free ligand in the sample compartment both in the control dialysis and when protein is present in the sample compartment of the dialysis cell.

A Experimental Procedures

5.2 Apparatus

The dialysis cell, which is similar to that of Colowick & Womack (1969), is shown in Figure 5.1. The cell is constructed of plexiglas (perspex), and consists essentially of an upper chamber (the sample compartment) and a lower chamber (the sink compartment). The two compartments are separated by the semi-permeable membrane, which can be clamped between the separable halves of the cell.

Figure 5.1

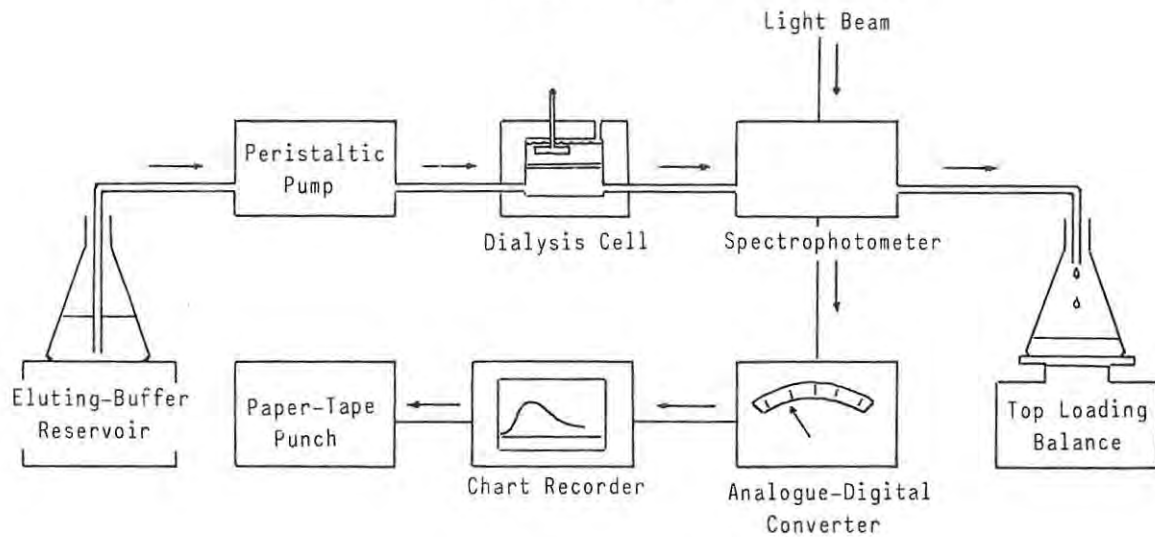


The Continuous-Flow Dialysis Cell

Eluting buffer is passed through the sink compartment at a constant rate by means of a peristaltic pump. The eluting buffer stream, after passing through the dialysis cell, flows through a spectrophotometer flow-cell where the ligand concentration is monitored. Spectrophotometric absorbance readings of the dialysate are determined automatically at equal, closely spaced, time intervals. The data is internally digitized and recorded onto paper tape for subsequent computer processing, by means of a data-logging device.

A schematic diagram of the entire apparatus is shown in Figure 5.2. The experimental data consists of a time series of measurements of the ligand concentration (recorded as absorbance) in the spectrophotometer cell. This data set is referred to as the elution profile; it is designated $C_2(t)$ for the control dialysis, and $C_2^*(t)$ for the sample dialysis, from a protein-ligand mixture. The corresponding sample compartment ligand concentrations are denoted by $C_1(t)$ and $C_1^*(t)$, respectively, and are referred to as the ligand escape curves of the control and sample dialyses.

Figure 5.2



The Continuous-Flow Dynamic Dialysis Apparatus

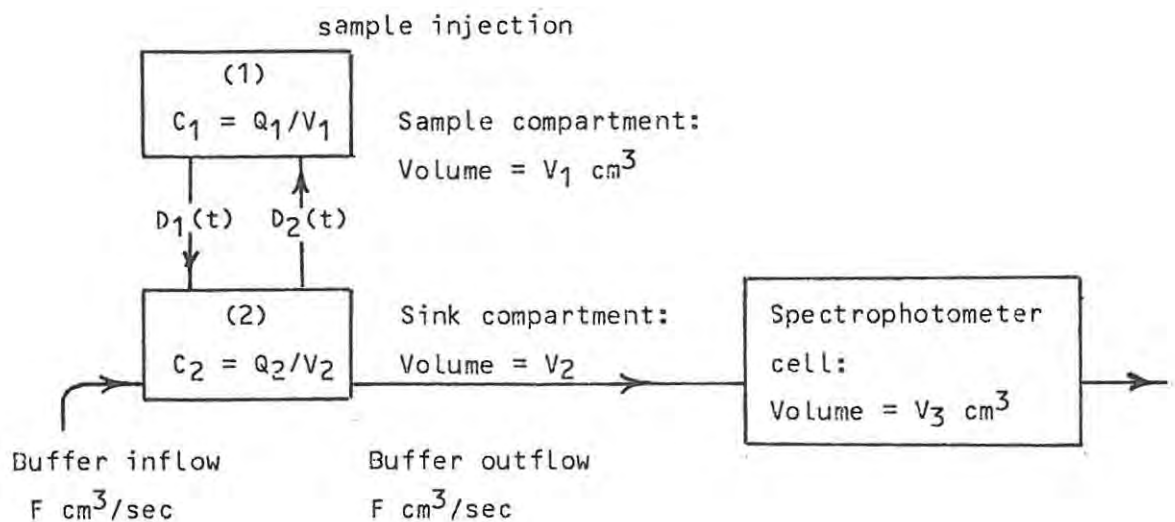
B Mathematical analysis

5.3 The Two Compartment Model System

The diffusion and elution flow processes in the dialysis cell can be described to a first approximation by a two-compartment situation (Simon, 1972).

This two compartment model system may be depicted thus:

Figure 5.3



A Two-Compartment Model System

The arrow labelled I, pointing into the sample compartment, represents the concentration-independent input. I may also represent a concentration-independent loss of material from the compartment, if it is given a negative value. $Q_1(t)$ and $Q_2(t)$ represent the quantity of ligand in each compartment at the time t; $D_1(t)$ represents the concentration dependent transfer of ligand from sample to sink compartment (diffusion); $D_2(t)$ represents the concentration-dependent transfer of ligand from the sink compartment to the sample compartment (back-diffusion)¹; F is the flow of the eluting buffer stream through the sink compartment; $C_1(t)$ and $C_2(t)$ are the ligand concentrations in sample and sink compartments, respectively.

$$\text{Thus } Q_1(t) = V_1 C_1(t) \quad \text{and} \quad Q_2(t) = V_2 C_2(t)$$

where V_1 and V_2 are the sample and sink compartment volumes respectively.

In terms of Fick's first law of diffusion, with permeation constant D , the differential equations for a two-compartment system relate the rate of ligand diffusion to the sample and sink compartment concentrations, and to the eluting buffer flow rate.

¹ Footnote

The term "back-diffusion" represents formal recognition of the presence of ligand in the sink compartment and its effect on the diffusion process. The only directly observable effect is the net process of diffusion from the sample to sink compartments. However, tracer studies would demonstrate the dynamic balance which gives rise to the observed process.

These equations are:

for the sample compartment,

$$d[C_q(t)]/dt = D[C_2(t) - C_1(t)]/V_1$$

.... 5.3.1a

and for the sink compartment

$$d[C_2(t)]/dt = \{D[C_1(t) - C_2(t)] - FC_2(t)\}/V_2$$

.... 5.3.1b

The subscript q in equation 5.3.1a is used to denote the grand total sample compartment ligand concentration. These equations apply to both the control experiment and the sample dialysis experiment (i.e., when protein is present). In the sample dialysis, $C_q(t)$ includes the quantity of ligand bound to the protein as well as the free, or unbound, ligand. For the control dialysis experiment, $C_q(t) = C_1(t)$.

5.4 The Control Dialysis

The differential equations include terms to allow for back-diffusion of the ligand if non-ideal sink conditions prevail (i.e., if there is a finite ligand concentration in the sink compartment).

For the control situation where $C_q(t) = C_1(t)$, the equations 5.3.1a and 5.3.1b can be solved analytically using Laplace transforms to give:

$$C_1(t) = C_1(0) \{ [a - (D+F)/V_2] e^{-at} + [b - (D+F)/V_2] e^{-bt} \} / (a-b)$$

.... 5.4.1

and $C_2(t) = DC_1(0) \{ e^{-bt} - e^{-at} \} / V_2(a-b)$

.... 5.4.2

$$\text{where } a = [x + \sqrt{x^2 - 4y}] / 2 \quad \dots \quad 5.4.3a$$

$$\text{and } b = [x - \sqrt{x^2 - 4y}] / 2 \quad \dots \quad 5.4.3b$$

$$\text{with } x = [(V_1 + V_2)D + V_1F] / V_1V_2 \quad \dots \quad 5.4.4a$$

$$\text{and } y = DF / V_1V_2 \quad \dots \quad 5.4.4b$$

from which it can be seen that $x = a + b$ and $y = ab$

5.5 The Sample Dialysis

In binding experiments, where protein is present

$$C_q^*(t) > C_1^*(t)$$

The superscript * is used to identify the presence of protein. In order to solve the differential equations for the two-compartment model when protein is present, it is necessary to incorporate into equation 5.3.1a a term which will allow for the quantity of ligand bound to the protein. Under these circumstances the quantity of ligand in the sample compartment is given by:

$$Q_1(t) = V_1 C_q^*(t) = V_1 [C_1^*(t) + p\bar{v}[C_1^*(t)]] \quad \dots \quad 5.5.1$$

where p is the protein concentration in the sample compartment and \bar{v} the ligand/protein molal binding ratio, expressed here as a function of the unbound ligand concentration.

The functional relationship between $\bar{v}(t)$ and $C_1^*(t)$, (i.e., $\bar{v}[C_1^*(t)]$), which is yet to be determined, constitutes the binding isotherm. Substitution of equation 5.5.1 for $C_q(t)$ in

equation 5.3.1a and rearranging gives

$$dC_1^*(t)/dt = \frac{-D \{ C_1^*(t) - C_2^*(t) \}}{V_1 \{ 1 + p \, d[\bar{v}\{C_1^*(t)\}]/dC_1^*(t) \}} \quad \dots 5.5.2$$

Equations 5.3.1b and 5.5.2 can only be solved analytically, (and in principle) only if an analytical relationship between \bar{v} and $C_1^*(t)$ is available.

5.6 Use of Analytical solutions of Differential Equations

Attempts have been made to obtain analytical solutions to equations similar to these (i.e., equations based on the Meyer & Guttman analysis rather than the continuous flow two-compartment dialysis system). In these attempts, analytical model isotherms containing the binding parameters were used (Kruger-Thiemer, 1966, Pedersen et al., 1977).

For example, if a binding model expressions such as the generalized Scatchard model:

$$\bar{v}[C_1^*(t)] = \sum_{i=1}^N n_i k_i C_1^*(t) / \{ 1 + k_i C_1^*(t) \} \quad \dots 5.6.1$$

is incorporated into equation 5.5.2, it may be possible under certain limited situations to obtain an analytical expression for \bar{v} in terms of $C_2^*(t)$ and the variables n_i and k_i . Values for the binding parameters n_i and k_i could then be obtained by an iterative least squares regression analysis. This could be achieved by fitting, to the sample elution profile, the

analytical expression which represents the solution to the system of differential equations when protein is present, and which contains n_1 and k_i as parameters. The expression which represents the analytical solution to the differential equations for the two-compartment model when protein is present will, however, be complicated. Moreover, depending on the complexity of the model binding expression, it may not be possible to obtain a direct analytical solution.

The analysis of Pedersen (1977), although not requiring an explicit solution to equations equivalent to equations 5.3.1b and 5.5.2, also incorporates a binding model into equations equivalent to 5.3.1a and 5.5.2. The method developed by Pedersen employed the simple single-site Scatchard binding model. Although the method is a general one which can incorporate more complex models, this entails complicated algebra.

These methods, because of the complicated analytical expressions involved, and because they involve the use of non-linear least-squares iterative procedures, cannot readily be adapted to different protein-ligand binding models. The complicated algebra that these methods entail, their dependence on an assumed binding model, and their lack of adaptability make them impractical, though symbolic manipulation will ease the algebraic problems.

5.7 Derivation of the Permeation Constant

While it is impractical to obtain analytical solutions to the system of differential equations for the protein-ligand dialysis, exact analytical solutions given by equations 5.4.1 and 5.4.2 for the control experiment are available and can be used to establish the permeation constant, D , for the ligand. One procedure to obtain D is to fit the data of the control elution profile to equation 5.4.2 by least squares regression procedures.

Difficulties are encountered in the application of this procedure, however, because the amplitude term $DC_1(0)/V_2(a-b)$ and the exponents a and b in equation 5.4.2 are not independent. Our experience has shown that iterative regression procedures to obtain estimates of these parameters converge at best very slowly, and more frequently do not converge.

The form of the analytical solution to equation 5.4.2 shows, however, that an approximate value for D can be obtained from a log-linear plot of $C_2(t)$ vs t . For large t , the analytical solution for $C_2(t)$ in equation 5.4.2 can be approximated by:

$$C_2(t) = Ae^{-bt} \quad \dots \quad 5.7.1$$

Estimates of the values of the amplitude A and exponent b can then be obtained from an extrapolated intercept and from the slope of the linear portion of the log-linear plot of $C_2(t)$ vs t for large t . The method must be regarded as both subjective and unreliable.

5.8 Mass-Balance method for determining the Protein-Ligand Isotherm

An alternative approach, not requiring explicit solutions for the system differential equations, is based on a mass balance relationship between the instantaneous sink compartment ligand concentration and the quantity of ligand lost from the sample compartment. This method can be employed both to derive a permeation constant from the control dialysis and a binding isotherm from the sample dialysis. By equation 5.3.1b, the rate at which the ligand is lost by diffusion from the sample compartment is given by:

$$D[C_1^*(t) - C_2^*(t)] = V_2 dC_2^*(t)/dt + FC_2^*(t) \quad \dots \quad 5.8.1$$

The analysis below applies to the situation when protein is present.

In an interval t the quantity of ligand diffusing out of the sample compartment will be given by:

$$D[C_1^*(t) - C_2^*(t)] t = \{V_2 d[C_2^*(t)]/dt + FC_2^*(t)\} t \quad \dots \quad 5.8.2$$

The total quantity of ligand lost from the time $t = 0$ to $t = t$ is, therefore, given by:

$$Q_1(t) = D \int_0^t [C_1^*(\tau) - C_2^*(\tau)] d\tau$$

$$Q_1(t) = V_2 \int_0^t d[C_2^*(\tau)]/d\tau d\tau + F \int_0^t C_2^*(\tau) d\tau$$

.... 5.8.3

where D is assumed to be independent of ligand concentration and F is independent of time.

Therefore $Q_1(t) = V_2 C_2^*(t) + F \int_0^t C_2^*(\tau) d\tau$

.... 5.8.4

if $C_2^*(0) = 0$ and no ligand is brought in with the flowing stream of buffer.

Since all the ligand lost from the sample compartment is lost to the sink (apart from the small amount retained in the membrane) it follows that the total quantity of ligand retained by the sample compartment at time $t = t$ is given by:

$$Q_r(t) = V_1 C_1^*(0) - \{ V_2 C_2^*(t) + F \int_0^t C_2^*(\tau) d\tau \}$$

.... 5.8.5

where $C_1^*(0)$ is the initial ligand concentration.

Since $Q_r^*(t) = V_1 \{ C_1(t) + p\bar{v}(t) \}$

it follows that:

$$p\bar{v}(t) + C_1^*(t) = C_1^*(0) - \{V_2 C_2^*(t) + F \int_0^t C_2^*(\tau) d\tau\} / V_1$$

.... 5.8.6

The values for $C_1^*(t)$ are obtained by rearranging equation 5.3.1b to give:

$$C_1^*(t) = C_2^*(t) + \{V_2 dC_2^*(t)/dt + FC_2^*(t)\} / D$$

.... 5.8.7

Equations 5.8.6 and 5.8.7 are the parametric equations of the binding isotherm, with parameter t .

The use of these equations, however, requires a value for the permeation constant D . The value of D is obtained from the control experiment elution profile data by setting $p = 0$ in equation 5.8.6 and substituting equation 5.8.7 for $C_1^*(t)$. Solving for D yields:

$$D = \frac{\{V_2 d[C_2(t)]/dt + F C_2(t)\}}{\{C_1(0) - [V_2 C_2(t) + F \int_0^t C_2(\tau) d\tau] / V_1\} - C_2(t)}$$

.... 5.8.8

5.9 Fixed Initial Ligand Concentration: A Special Case

The binding isotherm may be calculated directly in terms of the differences between the control elution profile $C_2(t)$ and the sample elution profile $C_2^*(t)$, provided that the initial ligand concentrations and the experimental variables V_1 , V_2 , $C_1(0)$, $C_1^*(0)$ and F , are the same in both the control and sample experiments. In such a situation, the binding isotherm

may be calculated directly by eliminating $C_1(0) = C_1^*(0)$ from equations 5.8.6 & 5.8.8 to give:

$$\begin{aligned} \bar{v}(t) = & \{ [V_t/V_1 + F/D] \Delta C_2(t) \\ & + (V_2/D) d[\Delta C_2(t)]/dt + F/V_1 \int_0^t \Delta C_2(\tau) d\tau \} / p \end{aligned} \quad \dots \quad 5.9.1$$

where $\Delta C_2(t) = C_2(t) - C_2^*(t)$ and $V_t = V_1 + V_2$

C Evaluating the Method of Analysis

The following paragraphs describe the methods of evaluation used; results will be presented in Chapters Eight and Nine.

5.10 The Use of Synthetic Data

Numerical solutions of the differential equations 5.3.1a and 5.3.1b for the control, and equations 5.3.1b and 5.5.2 for the sample dialyses (obtained using Runge-Kutta methods (Grove, 1966) applied to an assumed binding isotherm) represent synthetic protein-ligand binding systems. Such synthetic data sets may be used to establish the validity of the method by a comparison of the synthetic data sets obtained by the numerical solution of the differential equations with data obtained by experiment and for which the same binding isotherm is believed to apply; they may also be used to provide a reference for the Laplace transform method, as developed later in this report. These synthetic data sets can also be used to examine the effects of changes in experimental variables, such as eluting buffer flow rate, initial

ligand concentration, and ligand extinction coefficient, on the elution profile and provide estimates for the sensitivity of the binding isotherm to random errors in these variables. Synthetic elution profiles corresponding to the numerical solution of equations 5.3.1a and 5.3.1b for a simulated control, and equations 5.3.1b and 5.5.2 for a simulated protein-ligand binding experiment were obtained by means of a computer differential equation solving algorithm (Terry, 1978), and used to test the validity of the analysis. Values for the permeation constants used to generate the synthetic elution profiles were chosen to be the same as values of D determined experimentally from control dialysis elution profiles. A two-site binding model was chosen to simulate the binding of phenol red to bovine serum albumin (BSA) (Rodkey, 1961) and was used to generate synthetic elution profiles $C_2^*(t)$ for the sample experiments.

Reported values, obtained by difference spectroscopy (Rodkey, 1961) for the parameters n_i and k_i in the phenol red-BSA interaction were used in a Scatchard equation of the form:

$$\bar{v}(t) = \sum_{i=1}^2 n_i k_i C_1^*(t) / [1 + k_i C_1^*(t)]$$

.... 5.10.1

which was incorporated into equation 5.5.2.

A listing of a FORTRAN computer routine (program ETA) which can be used to generate simulated control and sample elution profiles, based on the general Scatchard binding model (equation 3.3.9) and appropriate values for experimental variables is given in appendix IX.

5.11 Experimental Evaluation

An experimental evaluation of the method was also performed in a series of experiments, by dialysing mixtures of phenol red and BSA at 15°, 20° and 25°C, for a systematic series of changes of both the initial ligand concentrations and the eluting buffer flow rates. The experimentally obtained elution profiles were compared with synthetic profiles in which the parameters V_1 , V_2 , F , and the extinction coefficient, ϵ , of the ligand were chosen to duplicate experimental conditions.

5.12 Computational Methods

The differentiation of the experimental elution profile data with respect to time, required for equations 5.8.6, 5.8.7 and 5.8.8 was performed numerically using a Savitzky-Golay polynomial smoothing and differentiating routine (Savitzky & Golay, 1964; Steinier, 1972; Madden, 1973). Numerical integration was performed using Simpson's rule. A listing of the computer program (program GAMMA -in FORTRAN) to evaluate the permeation constant or the binding isotherm from the elution profile data by means of the mathematical analysis developed in Chapter Five is given in appendix VI.

A non-linear least squares regression routine was used to derive values for the binding parameters n_i and k_i from the experimentally obtained isotherm, derived from the elution profiles by use of equations 5.8.5 and 5.8.6. For this purpose, a computer routine which permitted values for some of the parameters in the general binding model (equation 3.12.1) to be fixed (for example, integral values could be assigned to the n_i) was utilized. A copy of a computer driver routine, program ZETA, written in FORTRAN and used in conjunction with the least squares regression program STEPIT (Chandler, 1965), is listed in Appendix VIII.

5.13 Difficulties associated with the CFDD Method

The CFDD method and the procedure for deriving the binding isotherm from the dialysis data are not without inherent difficulties. Although the method provides a large number of data points from which the binding isotherm can be obtained, (usually about 1000 data points over a period of about seven hours in the CFDD method, as opposed to about 15-20 determined over the same period by the method of Meyer & Guttman) it is necessary, when using the permeation constant method, to discard a portion of the data. The data discarded represents the diffusion of ligand during an initial transient period during which the permeation constant has not yet attained a constant value. This transient phase is probably due to a hold-up of ligand in the membrane, and it is likely that during this transient phase the ligand in the membrane has not established a linear concentration gradient.

It was also observed, when computer generated elution profiles were compared with experimentally determined elution profiles, that at high eluting buffer flow-rates the experimentally determined permeation constant (calculated by means of equation 5.8.8) was influenced by the eluting buffer flow rate. The source of this influence on the permeation constant was traced to changes in the volume of the sink compartment of the dialysis cell. This change in volume occurred because of distention of the membrane at high eluting buffer flow rates, which resulted in doming of the membrane. The method for correcting the sink compartment volume to allow for this doming of the membrane is discussed in Appendix II.

As in other dynamic dialysis methods, several possible sources of error which stem from practical considerations need to be considered. The reliability of the method can be affected by experimental conditions. These include membrane effects, i.e., binding of protein, ligand, or protein-ligand complex to the membrane, Donnan effects, osmosis, viscosity of the protein

solution, temperature effects, or effects due to the rate of stirring. The influence of these factors on the accuracy of the method and means of minimizing their effects on the binding isotherm are discussed in Chapter Seven.

Chapter Six

Analysis of CFDD Data Using the System Transfer Function

6.1 Introduction

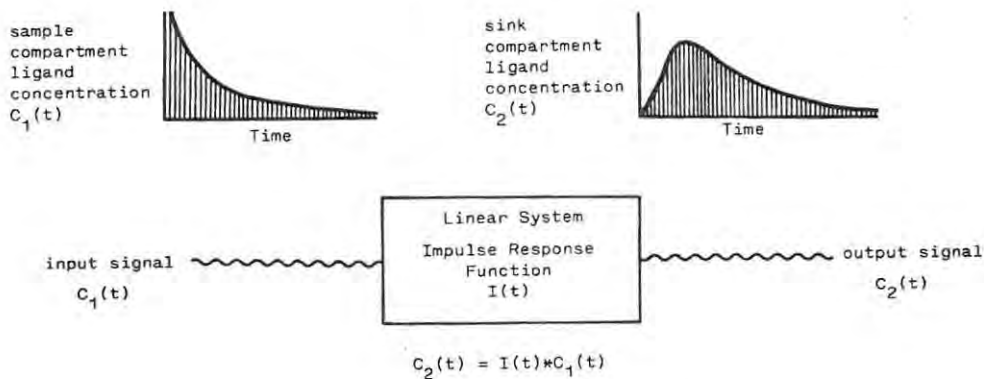
Comparisons of the binding isotherms derived from experimentally determined elution profiles and from theoretical elution profiles (generated by numerical solution of the system differential equations) show that for the phenol red-BSA system at least, the data analysis by the permeation constant method is adequate. However, considerations of model independence and generality have prompted the development of a more general analysis. This analysis, in addition to its generality, has the advantage over the permeation constant analysis that it is not necessary to discard the short-term data. In this general analysis, the relationship between the monitored ligand concentration in the sink compartment and the concentration of free ligand in the sample compartment is established by means of a system transfer function.

The use of a transfer function to relate an input signal to an output signal has many applications; the transfer function concept is used extensively in electrical network theory and in fields associated with the transmission of mechanical oscillations and vibrations using acoustical or mechanical transducers (Allen, 1973; Nicolson et al., 1972; Bancroft & Johnson, 1973; Reif et al., 1978). Tanaka (1978) has used transfer functions to obtain caloric power as a function of time, without having to make any assumption about their analytical form, by numerical analysis of a thermogram. Transfer functions are also used in image enhancement in optical systems (Gonzalez & Winz, 1977). Hühnerman & Mentzel (1979) and André (1979) have discussed applications which utilize the transfer function in radio transmission, etc., to effect a deconvolution of an impulse response function from an output signal to obtain the input signal.

6.2 Linear Systems

Since the concept of the system transfer function is used extensively in electrical network theory, it is convenient to use electrical network terminology to describe its application in the CFDD method. Accordingly, the dialysis cell is considered as a linear system or linear "filter" which has an input signal, $C_1(t)$, and an output signal signal, $C_2(t)$. The elution profile, $C_2(t)$, is thus visualized as the response of the filter to an input signal, $C_1(t)$, which arises from the release of ligand from the protein and the sample compartment of the dialysis cell to the sink compartment.

Figure 6.1



The Dialysis Cell as a Linear System

The fundamental assumption of the analysis is that the dialysis cell represents a linear system. In mathematical terms, if $C_2(t)$ and $C'_2(t)$ are the individual responses of the system to input signals $C_1(t)$ and $C'_1(t)$, then the system is linear if an input signal $a_1C_1(t) + a_2C'_1(t)$ generates an output signal $a_1C_2(t) + a_2C'_2(t)$, where a_1 and a_2 are constants. In the linear system representing the dialysis cell, the assumption of proportionality between the rate of diffusion of the ligand and the concentration gradient across the dialysis membrane is not explicitly made, only that the transport process is linear in the above sense.

6.3 Time Domain - Frequency Domain Relationships

In electrical network theory, "filtering" of the signal occurs because the proportionality constant relating the output signal to the input signal is not the same at all signal frequencies. The transfer function is thus expressed as a function of frequency. If the input and output signals are represented as frequency functions $S_1(\omega)$ and $S_2(\omega)$ respectively, where ω is the signal frequency, then:

$$S_2(\omega) = Z_T(\omega) S_1(\omega) \quad \dots \quad 6.3.1$$

in which $Z_T(\omega)$ is the system transfer function. In the corresponding time domain representation of these quantities, where the transformation from the time domain to the frequency domain is effected by means of the Fourier transform, the output signal is related to the input signal through an impulse response function, $I(t)$. The relationship between these quantities is one of convolution. The output signal signal, $C_2(t)$, is the convolution of the input signal and the impulse response function, which is the time domain representation of the frequency domain transfer function.

$$\text{Thus} \quad C_2(t) = I(t) * C_1(t) \quad \dots \quad 6.3.2$$

The asterisk denotes convolution, which is defined by:

$$C_2(t) = \int_{-\infty}^{+\infty} C_1(t - \tau) \cdot I(\tau) d\tau \quad \dots \quad 6.3.3$$

Deconvolution of the impulse response function from the data contained in the elution profile thus yields the concentration of

the free (or unbound) ligand in the sample compartment as a function of time.

The convolution theorem¹ (Papoulis, 1972) is used to effect the deconvolution, and in order to utilize the proportionality relationship (6.3.1) between the input and output signals in the frequency domain, it is convenient to transform the data contained in the elution profile from the time domain to the frequency domain by means of the Fourier transformation, F , which is defined by:

$$S(\omega) = F[C(t)] = \int_{-\infty}^{+\infty} C(\tau) e^{-i2\pi\omega\tau} d\tau \quad \dots \quad 6.3.4$$

where $i^2 = -1$ and ω is a frequency in radians.

Since $C_1(t)$ and $C_2(t)$ are causal functions (i.e., defined only for $t > 0$) equation 6.3.4 may be written for these functions as:

$$S_j(\omega) = F[C_j(t)] = \int_0^{+\infty} C_j(\tau) e^{-i2\pi\omega\tau} d\tau \quad \dots \quad 6.3.5$$

for $j = 1, 2$

¹ Footnote

The Fourier transform of the convolution of two functions $C_1(t)$ and $C_2(t)$ equals the product of the Fourier transforms, $S_1(\omega)$ and $S_2(\omega)$, of these two functions:

i.e., if $S_j(\omega) = F[C_j(t)]$ for $j = 1, 2$ (cf. equation 6.3.4)

$$\text{then } F\left[\int_{-\infty}^{+\infty} C_1(t-\tau) \cdot C_2(\tau) d\tau\right] = S_1(\omega) \cdot S_2(\omega)$$

The inverse transforms from the frequency domain to the time domain are obtained by the inverse Fourier transform, F^{-1} , as defined in equation 6.3.6:

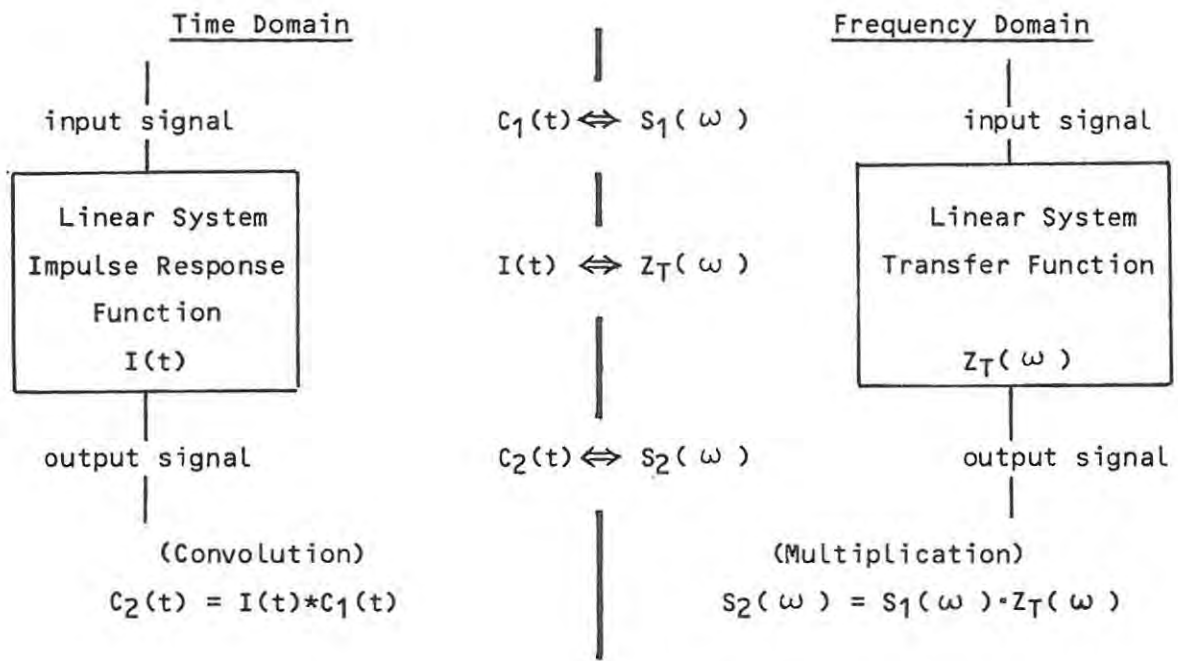
$$c_j(t) = F^{-1}[s_j(\omega)] = \int_{-\infty}^{+\infty} s_j(\omega) e^{i2\pi\omega t} d\omega$$

for $j = 1,2$

.... 6.3.6

The time domain - frequency domain relationships are shown in figure 6.2.

Figure 6.2



(Bracewell, 1965)

Time Domain - Frequency Domain Relationships

6.4 Parametric Equations of the Binding Isotherm

The system transfer function $Z_T(\omega)$ is obtained from a control dialysis experiment using the mass balance relationship between the sample and sink compartment concentrations.

Thus, by 6.3.1:

$$Z_T(\omega) = S_2(\omega) / S_1(\omega) = \text{FE } [C_2(t)] / \text{FE } [C_1(t)] \quad \dots \quad 6.4.1$$

where, from the mass-balance relationship (equation 5.8.5):

$$C_1(t) = C_1(0) - \{ V_2 C_2(t) + F \int_0^t C_2(\tau) d\tau \} / V_1 \quad \dots \quad 6.4.2$$

Thus

$$Z_T(\omega) = \text{FE } [C_2(t)] / \text{FE } [C_1(0) - \{ V_2 C_2(t) + F \int_0^t C_2(\tau) d\tau \} / V_1] \quad \dots \quad 6.4.3$$

Now, the Fourier transform of $C_1(t)$ is given by:

$$S_1(\omega) = \text{FE } [C_1(t)] \quad \dots \quad 6.4.4$$

$$S_1(\omega) = \{ C_1(0) - (F/V_1) \cdot S_2(\omega) \} / i\omega - (V_2/V_1) \cdot S_2(\omega)$$

Thus, $Z_T(\omega)$ can be expressed in terms of the Fourier transform, $S_2(\omega)$, of the elution profile.

$$Z_T(\omega) = i\omega V_1 S_2(\omega) / \{ V_1 C_1(0) - F S_2(\omega) - i\omega V_2 \cdot S_2(\omega) \} \quad \dots \quad 6.4.5$$

Since the transfer function establishes the relationship between the sample and the sink compartment ligand concentrations, both for the control and when protein is present:

$$Z_T(\omega) = F[C_2(t)]/F[C_1(t)] = F[C_2^*(t)]/F[C_1^*(t)]$$

.... 6.4.6

it follows that:

$$\begin{aligned} C_1^*(t) &= F^{-1}[S_2^*(\omega) / Z_T(\omega)] \\ &= F^{-1}[S_2^*(\omega) \cdot S_1(\omega) / S_2(\omega)] \text{ (cf. equation 6.4.1)} \end{aligned}$$

.... 6.4.7

This equation represents the essentials of the general mode of analysis which is described here. The quantity of ligand bound to the protein is obtained by substitution of equation 6.4.7 into the mass balance expression of equation 5.8.6 to give:

$$\begin{aligned} p\bar{v}(t) &= \{ C_1^*(0) - F^{-1}[S_2^*(\omega) \cdot S_1(\omega) / S_2(\omega)] \} \\ &\quad - \{ V_2 C_2^*(t) + F \int_0^t C_2^*(\tau) d\tau \} \end{aligned}$$

.... 6.4.8

Equations 6.4.7 and 6.4.8 constitute the parametric equations of the binding isotherm in terms of the parameter t .

6.5 Problems associated with Fourier Transformation Theory

In principle, the analysis to extract the binding isotherm from the elution profile data sets using the transfer function is direct and simple. In practice, several difficulties are encountered. These difficulties, which are inherent in the use of the Fourier transform, stem from:

- i) the use of sampled data sets;
- ii) the use of discrete Fourier transformation (DFT) to approximate the continuous Fourier transform, thus introducing an implied periodicity into the data set;
- iii) oscillations in the transformed data sets due to use of a finite number of terms in the Fourier summation;
- iv) oscillations in the transformed data sets due to discontinuities in the original data, arising from truncation of the dialysis after a finite time, and giving rise to the Gibbs phenomenon (Stuart, 1966).

Initial attempts to perform numerical transformation of the data from the time domain to the frequency domain (and the inverse transforms from the frequency domain to the time domain), by means of the Cooley-Tukey fast Fourier transform (FFT) algorithm (Cooley & Tukey, 1965; Brigham, 1974), were unsuccessful because the data set of the sampled elution profile is not time-limited (nor is its spectrum band-limited). The approximation to the continuous Fourier transform by the discrete transform, obtained using the FFT, is poor due to truncation and leakage errors (Brigham, 1974). Certain problems which arise from the use of the FFT to effect the transformation of the elution profile data from the time domain to the frequency domain, and the methods which were employed to eliminate or reduce truncation and leakage errors, are dealt with in greater detail in Chapter Nine.

The method which was adopted to circumvent the problems associated with the FFT algorithm is based on a proposal of D. Glasser (personal communication), and used by Greenberg (1969) to develop the transfer functions used in the process analysis and control of a gas-liquid chromatography system. This procedure provides a direct method for the calculation of the transfer function, by the use of the Laplace transform, and its numerical inversion by reduction to a Fourier series (Bryson et al., 1974). The use of the Laplace transform of the elution profile to derive the system transfer function removes the effects introduced into the discrete Fourier transform by the implied periodicity (Brigham, 1974).

6.6 Laplace Transform and Fourier Series Representation of the Elution Profile

Laplace transformation of the data from dialysis experiments circumvents the difficulties which are associated with Fourier transformation when the dialysis is truncated after a finite time. The discontinuity in the dialysis data is removed by extending the experimental data by means of an assumed monoexponential decay function (André et al., 1978). This extension is not conveniently done with the Fourier method for reasons which appear below.

The mathematical analysis described below follows that of Greenberg (1969) and Turner (1974). By first representing the data of the extended elution profile as a Fourier series, the numerical Laplace transform permits the transfer function, Z_T , to be expressed simply in terms of these Fourier coefficients. Since $C_1(t)$, $C_1^*(t)$, $C_2(t)$, and $C_2^*(t)$ are causal functions, the Fourier transform (equation 6.3.5) is replaced by the Laplace transform:

$$S_j(s) = L[C_j(t)] = \int_0^{+\infty} C_j(t) e^{-st} dt$$

for $j = 1, 2$

.... 6.6.1

where s is a complex frequency defined as:

$$s = \alpha + i\omega$$

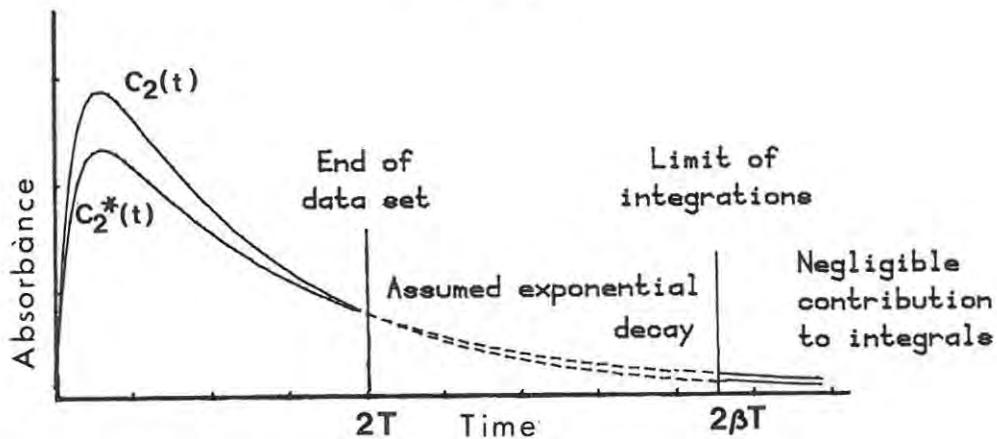
with α the decay parameter, and ω a frequency in radians.

In order to carry out the integration of equation 6.6.1 between the limits from $t = 0$ to $t = \infty$, the range of integration is divided into three parts, which correspond to:

- (1) the experimentally determined data set from $t = 0$ to $t = 2T$;
- (2) a mono-exponential function from $t = 2T$ to $t = 2\beta T$, and
- (3) a remainder from $t = 2\beta T$ to $T = \infty$.

Thus the elution profiles ($j = 2$ in equation 6.6.1) for both the control and sample dialysis experiments are partitioned as shown in Figure 6.3.

Figure 6.3



The Experimental and Extended Elution Profile Data Sets

The experimentally determined elution profiles, $C_2(t)$ and $C_2^*(t)$, which are truncated at $t = 2T$ are extended by means of monoexponential functions to remove the discontinuity at $t = 2T$.

The integral of the Laplace transform for the control profile ($j = 2$ in 6.6.1) can thus be partitioned:

$$\begin{aligned}
 L[C_2(t)] = S_2(s) = & \int_0^{2T} C_2(t)e^{-st}dt + \int_{2T}^{2\beta T} Y(t)e^{-st}dt \\
 & + \int_{2\beta T}^{+\infty} Y(t)e^{-st}dt \quad \dots \quad 6.6.2
 \end{aligned}$$

where $2T$ is the duration of the dialysis experiment and $Y(t)$ is the mono-exponential decay function, given by:

$$Y(t) = A e^{-bt} \quad \dots \quad 6.6.3$$

and chosen to approximate the elution profile in the extension of the data set over the interval for $t > 2T$. β is a positive multiplying factor, greater than unity, which allows the duration of the extended data set, over the interval $2T < t < 2\beta T$, to be varied at will. β is chosen such that the third integral term in equation 6.6.2 can be made arbitrarily small. A requirement of the analysis which follows is that the total duration of the data sets (i.e., which includes both the experimentally obtained data and the extension of that data set) be the same for both the control and the sample dialysis. The assignment of values to the parameters β , A and b in equations 6.6.2 and 6.6.3 is dealt with in Section 6.10.

Thus, with the appropriate value of β , A and b , the Laplace transformation of the extended data set (equation 6.6.2) may be written as:

$$\begin{aligned}
 L[C_2(t)] &= \int_0^{2T} e^{-at} C_2(t) e^{-i\omega t} dt \\
 &+ \int_{2T}^{2\beta T} e^{-at} \gamma(t) e^{-i\omega t} dt
 \end{aligned}
 \quad \dots \quad 6.6.4$$

alternatively

$$L[C_2(t)] = \int_0^{2\beta T} g_2(t) e^{-i\omega t} dt
 \quad \dots \quad 6.6.5$$

where $g_2(t)$ is defined to as the product of the elution profile and the Laplace convergence function e^{-at} , and has the form:

$$\begin{aligned}
 g_2(t) &= C_2(t) e^{-at} \quad \text{for} \quad 0 \leq t \leq 2T \\
 &= A e^{-(\alpha + b)t} \quad \text{for} \quad 2T < t \leq 2\beta T \\
 &= 0 \quad \text{for} \quad 2\beta T < t
 \end{aligned}
 \quad \dots \quad 6.6.6$$

A proper selection of parameters A and b ensures that $g_2(t)$ has the properties of continuity and of continuity of slope over the interval around $2T$. The function $g_2(t)$ satisfies the Dirichlet conditions (i.e., is single valued, finite, and sectionally continuous) and, therefore, can be expressed as a Fourier series over the interval $0 \leq t \leq 2\beta T$ (Stuart, 1966).

Thus,

$$g_2(t) = V_0/2 + \sum_{n=1}^{\infty} \{V_n \cos(n\pi t/\beta T) + U_n \sin(n\pi t/\beta T)\}
 \quad \dots \quad 6.6.7$$

The Fourier coefficients U_n and V_n are given by the Euler equations:

$$V_0 = (1/2\beta T) \int_0^{2\beta T} g_2(t) dt \quad \dots \quad 6.6.8a$$

$$V_n = (1/2\beta T) \int_0^{2\beta T} g_2(t) \cos(n\pi t/\beta T) dt \quad \dots \quad 6.6.8b$$

$$U_n = (1/2\beta T) \int_0^{2\beta T} g_2(t) \sin(n\pi t/\beta T) dt \quad \dots \quad 6.6.8c$$

and, since $g_2(t)$ satisfies the Dirichlet conditions, U_n and V_n will tend to zero for large n (Bracewell, 1978). It follows from the definition of $g_2(t)$ that for the extended range

$0 < t < 2T$:

$$C_2(t) = e^{\alpha t} \left\{ V_0/2 + \sum_{n=1}^{\infty} [V_n \cos(n\pi t/\beta T) + U_n \sin(n\pi t/\beta T)] \right\} \quad \dots \quad 6.6.9$$

Noting that $e^{-i\omega t} = \cos(\omega t) - i \sin(\omega t)$, and using the orthogonality properties of the sine and cosine functions it can be shown that²:

$$L_n[C_2(t)] = G_2(\alpha + i\omega) = \beta T(V_n - iU_n) \quad \dots \quad 6.6.10$$

where $\omega = n\pi/\beta T$ and the subscript n in the symbol L_n denoting the Laplace transform operator is used to show that only the n^{th} term of the transform is implied.

² Footnote:

$$G_2(\alpha + i\omega) = L[C_2(t)] = \int_0^{2\beta T} g_2(t) e^{-i\omega t} dt$$

where $\omega = n\pi/\beta T$

(continued)

It is necessary to define another function, $g_1(t)$, which represents the product of the sample compartment ligand concentration and the Laplace convergence function. Thus $g_1(t)$ is defined by:

$$g_1(t) = e^{-\alpha t} \cdot c_1(t)$$

.... 6.6.11

The Laplace transform of the function $c_1(t)$ may be expressed in terms of the Fourier coefficients of the Fourier series representation of $g_1(t)$.

continuation of footnote from previous page

$$= \int_0^{2\beta T} e^{-i\omega t} \left[V_0/2 + \left[\sum_{n=1}^{\infty} U_n \sin(n\pi t/\beta T) + V_n \cos(n\pi t/\beta T) \right] \right] dt$$

$$= \sum_{n=1}^{\infty} \int_0^{2\beta T} [U_n \sin(n\pi t/\beta T) + V_n \cos(n\pi t/\beta T)] \cdot [\cos(\omega t) - i \sin(\omega t)] dt$$

$$+ \int_0^{2\beta T} V_0/2 \cdot e^{-i\omega t} dt$$

$$\text{when } \omega = n\pi/\beta T \quad n = 0, 1, \dots$$

$$G_2(\alpha + in\pi/\beta T) = \int_0^{2\beta T} U_n \sin^2(n\pi t/\beta T) dt + \int_0^{2\beta T} V_n \cos^2(n\pi t/\beta T) dt$$

$$= \beta T (V_n - iU_n) \text{ for } n \neq 0$$

$$= \beta T V_0 / 2 \quad \text{for } n = 0$$

---o0o---

Thus, if $g_1(t)$, over the interval $t = 0$ to $t = 2\beta T$, is represented by a Fourier series of the form:

$$g_1(t) = Q_0/2 + \sum_{n=1}^{\infty} \{Q_n \cos(n\pi t/\beta T) + P_n \sin(n\pi t/\beta T)\} \quad \dots \quad 6.6.12$$

$$\text{then } \mathcal{L}[C_1(t)] = G_1(\alpha + i\omega_n) = \beta T(Q_n - iP_n) \quad \dots \quad 6.6.13$$

where $\omega_n = n\pi/\beta T$

It is possible to express the coefficients P_n and Q_n in terms of the Fourier coefficients U_n and V_n , because of the mass-balance relationship between $C_1(t)$ and $C_2(t)$ given by:

$$C_1(t) = C_1(0) - [V_2 C_2(t) + F \int_0^t C_2(\tau) d\tau] / V_1 \quad \dots \quad 6.6.14$$

Thus,

$$\mathcal{L}[C_1(t)] = \mathcal{L}[C_1(0) - \{V_2 C_2(t) + F \int_0^t C_2(\tau) d\tau\} / V_1] \quad \dots \quad 6.6.15$$

i.e.,

$$G_1(\alpha + i\omega_n) = [V_1 C_1(0) - F \mathcal{L}[C_2(t)]] / [\alpha + i\omega_n - V_2/V_1 \mathcal{L}[C_2(t)]] \quad \dots \quad 6.6.16$$

or

$$\begin{aligned} \beta T(Q_n - iP_n) &= [V_1 C_1(0) - F T(V_n - iU_n)] / [V_1(\alpha + i\omega_n)] \\ &+ \beta T V_2 (V_n - iU_n) / V_1 \quad \dots \quad 6.6.17 \end{aligned}$$

Q_n and P_n may be expressed directly in terms of the Fourier coefficients U_n and V_n by simplifying equation 6.6.17 and equating the real and imaginary parts. It is to be noted, however, that the coefficient Q_0 cannot be evaluated directly from the Laplace transform of $C_1(t)$ in this way, because of indeterminacy, and requires special treatment. The method of evaluating Q_0 is discussed in Appendix III.

Similarly, the transfer function, $Z_T(\alpha + i\omega_n)$, can be represented in terms of the Fourier coefficients of the Fourier series representation of the impulse response function, $I(t)$. Thus, if the impulse response function is represented by:

$$I(t) = B_0/2 + \sum_{n=1}^{\infty} \{B_n \cos(n\pi t/\beta T) + A_n \sin(n\pi t/\beta T)\} \quad \dots \quad 6.6.18$$

over the interval $t = 0$ to $t = 2\beta T$

$$\text{then } L[I(t)] = Z_T(\alpha + i\omega_n) = \beta T(B_n - iA_n) \quad \dots \quad 6.6.19$$

where again, $\omega_n = n\pi/\beta T$

From the definition of the transfer function in terms of the Laplace transform it follows that:

$$\begin{aligned} Z_T(\alpha + i\omega_n) &= L[C_2(t)]/L[C_1(t)] = \beta T(B_n - iA_n) \\ &= \beta T(V_n - iU_n)/\beta T(Q_n - iP_n) \quad \dots \quad 6.6.20 \end{aligned}$$

which, on simplifying and equating real and imaginary parts, yields:

$$A_n = [U_n Q_n - V_n P_n] / (\beta T [P_n^2 + Q_n^2]) \quad \dots \quad 6.6.21a$$

$$B_n = [V_n Q_n + U_n P_n] / (\beta T [P_n^2 + Q_n^2]) \quad \dots \quad 6.6.21b$$

$$\text{and } B_0 = (V_0/Q_0) / \beta T \quad \dots \quad 6.6.21c$$

Since the coefficients P_n and Q_n are functions of the U_n and V_n 's, the Fourier coefficients A_n and B_n of the transfer function may also be expressed directly in terms of the U_n and V_n 's by simplifying and equating the real and imaginary parts in the ratio:

$$\begin{aligned} \beta T (B_n - i A_n) &= G_2(\alpha + i\omega_n) / G_1(\alpha + i\omega_n) \\ &= \beta T [V_n - i U_n] / \{ [C_1(0) - F\beta T (V_n - i U_n) / V_1] / (\alpha + i\omega_n / \beta T) \\ &\quad - V_2 \beta T (V_n - i U_n) / V_1 \} \quad \dots \quad 6.6.22 \end{aligned}$$

In practice, the considerable algebra that the simplification of 6.6.22 entails can be avoided. The division and simplification of the ratio by equating real and imaginary parts to obtain the Fourier coefficients A_n and B_n is done internally by the computer routine used to process the data by making use of the FORTRAN facility for complex arithmetic.

6.7 The Unbound Ligand Concentration when Protein is Present

The same system transfer function, $Z_T(\alpha + i\omega)$, governs the relationship between the ligand escape curve and the elution profile, both for the control experiment and when protein is present. Thus

$$\begin{aligned} Z_T(\alpha + i\omega) &= \mathcal{L}[C_2(t)] / \mathcal{L}[C_1(t)] \\ &= \mathcal{L}[C_2^*(t)] / \mathcal{L}[C_1^*(t)] \quad \dots \quad 6.7.1 \end{aligned}$$

where the asterisk denotes functions when protein is present in the sample compartment. Hence

$$\beta T(B_n - iA_n) = (V_n^* - iU_n^*) / (Q_n^* - iP_n^*)$$

.... 6.7.2

Rearranging to solve in terms of Q_n^* and P_n^* by equating the real and imaginary parts yields:

$$Q_n^* = [B_n V_n^* + A_n U_n^*] / [\beta T(A_n^2 + B_n^2)]$$

.... 6.7.3a

$$P_n^* = [B_n U_n^* - A_n V_n^*] / [\beta T(A_n^2 + B_n^2)]$$

.... 6.7.3b

The free ligand concentration in the sample compartment when protein is present can thus be expressed in terms of the Fourier coefficients P_n^* and Q_n^* by:

$$c_1^*(t) = e^{\alpha t} \left\{ Q_0/2 + \sum_{n=1}^{\infty} [Q_n^* \cos(n\pi t/\beta T) + P_n^* \sin(n\pi t/\beta T)] \right\}$$

.... 6.7.4

in which the convergence parameter α is assigned the same value as in the control dialysis case.

6.8 The Total Sample Compartment Ligand Concentration when Protein is Present

In addition to providing an expression for the concentration of unbound ligand in the sample compartment as a function of time, the Laplace transform method provides a corresponding method for calculating the total quantity of ligand in the sample compartment as a function of time.

Thus, in the presence of protein

$$V_1 C_q(t) = V_1 p \bar{v}(t) + V_1 C_1^*(t) \quad \dots \quad 6.8.1$$

where again, p is the protein concentration and $\bar{v}(t)$ is the ligand/protein molal binding ratio, here expressed as a function of time. $C_q(t)$ represents the total ligand concentration (bound and free) in the sample compartment.

Corresponding to the definitions in the case of the control dialysis, the functions $g_1^t(t)$ and $g_2^*(t)$ are now defined over the range $0 \leq t \leq 2\beta T$ by:

$$g_1^t(t) = e^{-\alpha t} \cdot C_1^*(t) \quad \dots \quad 6.8.2$$

and

$$g_2^*(t) = e^{-\alpha t} \cdot C_2^*(t) \quad \dots \quad 6.8.3$$

$g_1^t(t)$ represents the product of the Laplace convergence function, $e^{-\alpha t}$, and the total ligand concentration in the sample compartment, derived from the mass balance expression (equation 6.6.14) incorporating the sample dialysis elution profile, $C_2^*(t)$. If $g_1^t(t)$ is represented by the Fourier summation:

$$g_1^t(t) = Q_0^t/2 + \sum_{n=1}^{\infty} [Q_n^t \cos(n\pi t/\beta T) + P_n^t \sin(n\pi t/\beta T)] \quad \dots \quad 6.8.4$$

then the Laplace transform of $C_1^t(t)$ is given by:

$$G_1^t(\alpha + i\omega_n) = L[C_1^t(t)] = \beta T(Q_n^t - iP_n^t) \quad \dots \quad 6.8.5$$

The Fourier coefficients P_n^t and Q_n^t are readily expressed in terms of the Fourier coefficients U_n^* and V_n^* of the Fourier series representation of $g_2^*(t)$.

Thus

$$L[C_1^t(t)] = L\left[C_1^*(0) - \{V_2 C_2^*(t) + F \int_0^t C_2^*(\tau) d\tau\} / V_1 \right] \quad \dots \quad 6.8.6$$

Thus,

$$\begin{aligned} G_1(\alpha + i\omega_n) &= L[C_1^t(t)] = \beta T(Q_n^t - iP_n^t) \\ &= \{C_1^*(0) - F\beta T(V_n^* - iU_n^*)/V_1\} / (\alpha + i\omega_n) \\ &\quad - V_2\beta T(V_n^* - iU_n^*)/V_1 \quad \dots \quad 6.8.7 \end{aligned}$$

in which V_1 and V_2 represent the sample and sink compartment volumes, respectively (as distinct from the bold face V_n which represents the Fourier coefficients of the sine terms in the Fourier series representation of $g_2^*(t)$).

Simplification of equation 6.8.7, by equating real and imaginary parts, yields

$$Q_n^t = \frac{[\alpha(V_1 C_1^*(0) / \beta T - F V_n^*) + \omega_n F U_n^*]}{[V_1(\alpha^2 + \omega_n^2)]} - V_2 V_n^* / V_1 \quad \dots \quad 6.8.8a$$

and

$$P_n^t = \frac{[\omega_n(V_1 C_1^*(0) / \beta T - F V_n^*) - \alpha F U_n^*]}{[V_1(\alpha^2 + \omega_n^2)]} - V_2 U_n^* / V_1 \quad \dots \quad 6.8.8b$$

where $\omega_n = n\pi / \beta T$

The evaluation of Q_0^t where $n = 0$ is again a special case, which is dealt with in Appendix III. The algebraic division and simplification of equation 6.8.7 to obtain values for the Fourier coefficients P_n^t and Q_n^t in terms of the U_n^* and V_n^* as shown in equations 6.8.8a and 6.8.8b, is not necessary since this can be carried out by making use of the FORTRAN facility for complex arithmetic.

The total ligand concentration in the sample compartment $\{ C_1^t(t) = C_q(t) \}$ as a function of time is given by:

$$C_1^t(t) = e^{*at} \{ Q_0^t / 2 + \sum_{n=1}^{\infty} [Q_n^t \cos(n\pi t / \beta T) + P_n^t \sin(n\pi t / \beta T)] \} \quad \dots \quad 6.8.9$$

for $0 < t < 2\beta T$.

6.9 The Quantity of Ligand Bound to the Protein

The difference between the total ligand concentration and the free ligand concentration in the sample compartment of the dialysis cell represents the quantity of ligand bound to the protein.

$$\text{Thus,} \quad p\tilde{v}(t) = C_q(t) - C_1^*(t) \quad \dots \quad 6.9.1$$

Represented as a Fourier series, this quantity is given by:

$$\begin{aligned} p\tilde{v}(t) = & e^{at} \{ (Q_0^t - Q_0^*) / 2 \\ & + e^{at} \{ \sum_{n=1}^{\infty} (Q_n^t - Q_n^*) \cos(n\pi t / \beta T) \} \\ & + e^{at} \{ \sum_{n=1}^{\infty} (P_n^t - P_n^*) \sin(n\pi t / \beta T) \} \} \quad \dots \quad 6.9.2 \end{aligned}$$

Equations 6.7.4 and 6.9.2 constitute the parametric equations of the binding isotherm.

6.10 Evaluation of the Fourier Coefficients U_n , V_n , U_n^* , and V_n^*

The Fourier coefficients U_n and V_n for the control dialysis, and U_n^* and V_n^* for the sample dialysis, are evaluated by means of the Euler equations (equations 6.6.8) using the appropriate data sets $g_2(t)$ and $g_2^*(t)$, respectively. The range of integration $t = 0$ to $t = 2\beta T$ is partitioned into the experimentally determined range from $t = 0$ to $t = 2T$, and the extended range from $t = 2T$ to $t = 2\beta T$, as mentioned before and as shown in figure 6.3

Thus

$$U_n = \int_0^{2T} c_2(t) e^{-\alpha t} \sin(n\pi t/\beta T) dt + A \int_{2T}^{2\beta T} c_2(t) e^{-(\alpha+b)t} \sin(n\pi t/\beta T) dt$$

.... 6.10.1a

and

$$V_n = \int_0^{2T} c_2(t) e^{-\alpha t} \cos(n\pi t/\beta T) dt + A \int_{2T}^{2\beta T} c_2(t) e^{-(\alpha+b)t} \cos(n\pi t/\beta T) dt$$

.... 6.10.1b

The integrals over the range $t = 0$ to $t = 2T$ in equations 6.10.1a and 6.10.1b are evaluated numerically by means of Simpson's rule or by Gaussian quadrature. The integrals over the extended range from $t = 2T$ to $t = 2\beta T$ are evaluated analytically using the identities:

$$\int e^{pt} \sin(qt) dt = e^{pt} \{p \sin(qt) - q \cos(qt)\} / (p^2 + q^2) + c$$

.... 6.10.2a

and

$$\int e^{pt} \cos(qt) dt = e^{pt} \{p \cos(qt) + q \sin(qt)\} / (p^2 + q^2) + C$$

.... 6.10.2b

where C is the constant of integration.

Substituting the appropriate values and integrating gives:

$$\int_{2T}^{2\beta T} e^{-(\alpha + b)\tau} \sin(n\pi\tau/\beta T) d\tau =$$

$$[e^{-2(\alpha + b)T} \cos(\theta - 2n\pi/\beta) - e^{-2(\alpha + b)\beta T} \cos(\theta)] / M$$

.... 6.10.3a

and

$$\int_{2T}^{2\beta T} e^{-(\alpha + b)\tau} \cos(n\pi\tau/\beta T) d\tau =$$

$$[e^{-2(\alpha + b)T} \sin(\theta - 2n\pi/\beta) - e^{-2(\alpha + b)\beta T} \sin(\theta)] / M$$

.... 6.10.3b

where $M = \sqrt{(\alpha + b)^2 + (n\pi/\beta T)^2}$ and $\tan(\theta) = (\alpha + b) / [n\pi/\beta T]$

The above analysis is applicable to both the control and sample dialyses.

6.11 The Evaluation of the Parameters Used to Generate the Extended Data Sets

It may appear that the extension of the experimentally determined elution profile data sets by means of a monoexponential function is an arbitrary procedure which could unduly bias the results, by forcing the analysis to conform to a model which is not necessarily the correct one. However, premultiplication of the data contained in the elution profiles by the Laplace convergence function, $e^{-\alpha t}$, will diminish to insignificance any discrepancies which could arise through the assumption of a monoexponential decay function to define the extended data set even if the elution profile were, in fact, to assume a more complex mode of exponential decay over the extended time interval. In addition, the Laplace convergence function ensures that the integrals used in the analysis are bounded. As has been noted, the extended control and sample dialysis experiments must contain the same number of observations. The value for the parameter, β , which governs the interval over which the data sets are extended, is derived from the control elution profile. It is necessary to use different methods to derive the parameters A and b in the monoexponential decay function for the control and sample dialyses respectively.

The value for β , is chosen such that the analytical integral for the control elution profile, which has been so far neglected:

$$I = A \int_{2\beta T}^{+\infty} e^{-bt} dt \quad \dots \quad 6.11.1$$

has a value of $< 0.1\%$ of the total area under the elution profile if the dialysis were continued for an infinite time. Thus, β is chosen such that:

$$A \int_{2\beta T}^{+\infty} e^{-bt} dt = 10^{-3} \int_0^{+\infty} C_2(t) dt \quad \dots \quad 6.11.2$$

The expected total area is known from mass balance considerations. It can be shown by integration of the analytical expression for $C_2(t)$ (equation 5.4.2) that:

$$\int_0^{+\infty} C_2(t) dt = V_1 C_1(0) / F \quad \dots \quad 6.11.3$$

For the control elution profile, values for the parameters A and b in equation 6.11.2 are obtained from the log-linear plots of the elution profile, or can be calculated from the elution profile by the computer in the routine used to process the data. Substitution of equation 6.11.3 for the integral on the right of equation 6.11.2, and integration of the left-hand side yields:

$$\beta = \ln [10^3 AF / \{ b V_1 C_1(0) \}] / 2bT \quad \dots \quad 6.11.4$$

Experience has shown that estimation of the values of the corresponding parameters A' and b' for the monoexponential decay expression for the extended **sample** elution profile, derived from the slope and intercept of the log-linear plot of the profile as above, introduces systematic errors in the values calculated for the concentration of free ligand in the sample compartment. Therefore, for the sample dialysis, values for the parameters A' and b' are chosen such that the integral

$$I' = \int_0^{2T} C_2^*(t) dt + A' \int_{2T}^{2\beta T} e^{-b't} dt \quad \dots \quad 6.11.5$$

is forced to yield the correct area according to mass-balance considerations

i.e.,

$$I' = \int_0^{+\infty} c_2^*(t) dt = \int_0^{+\infty} c_2(t) dt = V_1 c_1(0) / F \approx \int_0^{2\beta T} c_2^*(t) dt$$

.... 6.11.6

given that $c_1(0) = c_1^*(0)$

It should be noted that an error is introduced by the neglect of the last part of the elution profile, but that appropriate choice of β limits this error.

Equation 6.11.6 and the continuity condition:

$$c_2(2T) = A' e^{-b'(2T)} \quad \dots \quad 6.11.7$$

are sufficient to calculate the values of A' and b' .

6.12 The Number of Terms used in the Fourier Summations

In the description of the analysis, the Fourier series representing the ligand concentrations and transfer function were summed to infinity. In practice, it is necessary to select an upper value, N , for n . A sufficient number of terms have to be included in the series to ensure that the representation of the functions by a series is accurate. The functions representing the ligand concentrations and the impulse response function satisfy the Dirichlet conditions, therefore the Fourier coefficients converge to zero for large n . An optimum value for the number of terms to be included in the Fourier summations will contain sufficient terms to avoid inaccuracies in the representation of functions by series, but will not contain so many terms as to require excessive computer time for the data processing.

A cutoff term N can be chosen such that U_N/V_0 and $V_N/V_0 < \epsilon$ where ϵ can be made arbitrarily small, for example $\epsilon < 10^{-3}$. This procedure, however, may involve the inclusion of unnecessarily high frequency terms in the summation. The high frequency terms in the Fourier series representation of the elution profile contain contributions from high frequency noise components in the signal. These high frequency noise components, in which the contributions from noise are larger than those of the signal, may be usefully excluded without significant loss of information.

An optimum value for the cutoff frequency can be obtained from a computer generated plot of the power function. This is a plot of the modulus of the Fourier coefficients U_n and V_n i.e., $\sqrt{V_n^2 + U_n^2}$, as a function of the term n . Frequencies at which signal noise becomes appreciable are readily discernable from such a plot. The elimination of these high frequency components effects a "smoothing" of the data (Bracewell and Roberts, 1954; de Levie et al., 1978).

6.13 The Laplace Convergence Parameter

The Laplace convergence parameter, α , is given a non-zero value to ensure convergence of the integral terms used in the evaluation of the Fourier coefficients U_n^* , V_n^* , P_n^* ,

Q_n^* etc., in the event that the integral $\int_0^{+\infty} C_2^*(t)dt$ is unbounded.

At the same time, the convergence function, $e^{-\alpha t}$, ensures that, for large t , the sample elution profiles conform to a mono-exponential decay. This provides justification for the use of monoexponential expressions to describe the hypothetically extended data sets (especially for the sample dialysis) over the extended interval from $t = 2T$ to $t = 2\beta T$.

The analysis tolerates a certain latitude in the selection of α . However, if α is too large, the observed data in the latter part of the elution profile will be reduced to noise level. The contribution of observed data will decrease with increasing t , and the yield of reliable information from the dialysis will be correspondingly reduced. The analysis requires that the same value for α be used for both the control dialysis and the dialysis of ligand from the protein-ligand mixture. The convergence parameter is inversely correlated to the rate of diffusion and eluting processes (i.e., implicitly related to the half-life $t_{1/2}$ of the dialysis process). Thus, the more rapidly the sink compartment ligand concentration decays, the smaller the value that needs to be assigned to α . It was found, using computer simulated elution profiles based on the phenol red-BSA binding system incorporating appropriate binding parameters, that a value for α given by $\alpha < b/10$, where b is the slope of the log-linear plot of the control elution profile $C_2(t)$ for large times, gave satisfactory results.

6.14 The Gibbs Phenomenon - Effect on the Analysis

A test of the validity of the method, using computer-generated elution profiles to simulate the phenol red-BSA interaction, shows that the parametric equations 6.7.4 and 6.9.2 exhibit oscillations which increase in frequency with an increase in the number of terms used in the Fourier series. In addition, the graphs of $C_1(t)$ and $C_1^*(t)$, as functions of time, do not intersect the ordinate (at $t = 0$) at a value corresponding to the initial ligand concentration, $C_1(0)$ or $C_1^*(0)$. Rather, as seen in Figure 9.8 these graphs rise rapidly from the origin and, as shown by comparison with synthetic data which are generated from the analytical solution of the system differential equations (equations 5.3.1a & b and 5.5.2), overshoot the sample compartment ligand concentration curves. This effect is a consequence of the Gibbs phenomenon (Papoulis, 1962). The

oscillations and overshoot result from the discontinuities in $C_1(t)$ and $C_1^*(t)$ at $t = 0$, due to the injection of sample into the dialysis cell. The oscillations in the parametric equations 6.7.4 and 6.9.2 contribute to uncertainties in both the abscissa and ordinate of the binding isotherm when $\bar{v}(t)$ is plotted as a function of $C_1^*(t)$.

The oscillations in the parametric equations of the binding isotherm, due to the Gibbs phenomenon, can be smoothed using Lanczos' smoothing factors (Lanczos, 1967; Hamming, 1973). However, it was shown that, by incorporating Lanczos' smoothing factors into the analysis, although this technique effects smoothing of the oscillations, it does not eliminate the initial rapid rise and overshoot in $C_q(t)$ or $C_1^*(t)$ in the neighbourhood of $t = 0$.

A preferred method, which removes both the initial step and overshoot as well as the oscillations due to the discontinuity at $t = 0$, is due to Krylov (Kantarovich & Krylov, 1964). By this technique, the slowly converging components of the Fourier sum (which represent the step) are removed. The remainder is a rapidly convergent series which does not display the Gibbs phenomenon. The slowly converging part, which has an analytical sum to infinity, can be added back. Detailed description of this procedure to eliminate oscillations arising from the Gibbs phenomenon is given in Appendix 2.

6.15 Evaluation of the Analysis

It was found, while evaluating the analysis in terms of computer-generated data sets to simulate phenol red-BSA binding, that certain features in the analysis needed to be modified. These aspects concern mainly the zero frequency (initial) terms in the Fourier series representations of the Laplace transforms. For example, the initial terms Q_0 and Q_0^t cannot be evaluated directly because of indeterminacy and require special treatment.

In a full evaluation of the analysis it is also necessary to examine the validity of the assumption of a monoexponential decay function to represent the extended data set for the dialysis of ligand from the protein-ligand mixture. In addition, it remains to be shown that the dialysis cell does represent a linear system. The discussion and treatment of these points are deferred to Chapter Nine.

A computer program, written in FORTRAN, to process the data by establishing the transfer function from the control dialysis experiment and to evaluate the binding isotherm in terms of the parametric equations 6.8.9 and 6.9.2 (program DELTA) is presented in Appendix V.

Chapter Seven

Applications

In this chapter, certain experiments used to obtain binding isotherms by means of the CFDD method are described. These experimental procedures relate to:

- i) an evaluation of the methods of analysis developed to extract the binding isotherm from the dialysis data;
- ii) application of the CFDD technique to measure the binding of certain plant phenolic materials to soluble collagen.

In the former category, a study of the binding of phenol red to BSA at 15°, 20° and 25°C has been undertaken to obtain data which could be processed in terms of the analyses developed in Chapters Five and Six. A comparison of binding parameters for the phenol red-BSA binding system obtained by the CFDD method with values reported in the chemical literature and obtained by other techniques has been used to confirm the reliability of the method.

Besides the application of the CFDD method to measure collagen-ligand binding, the procedures to extract and purify collagen are described. Methods used to establish the quality of the collagen preparation and determine accurately the concentration of the collagen solutions in solution are also described.

A Methods

7.1 The Dialysis Apparatus

The essential features of the CFDD cell and schematic diagram of the complete apparatus including the flow-pump, monitoring and recording systems were shown in Figures 5.1 and 5.2 of Chapter Five. A plan of the cell showing dimensions and additional modifications, is shown in Figure 7.1. A Photograph of the dialysis cell and complete apparatus is shown in Plates VII and VIII.

In addition to the sample and sink compartments, a top chamber through which water from the constant temperature bath passes, was incorporated into the dialysis cell to achieve temperature control. This arrangement, however, was found to be inadequate and it was found necessary to immerse the entire cell, eluting buffer reservoir and flow-lines in the constant temperature bath in order to attain the necessary temperature control.

The contents of the sink compartment of the dialysis cell are stirred by means of glass beads and a bar magnet. Rotation of the bar magnet is effected by means of an axially mounted magnet in a chamber below the sink compartment. This magnet is rotated by means of a water turbine.

In order to avoid the possibility of abrading the surface of the dialysis membrane in the sample compartment by having a magnetic stirrer resting on the membrane surface, the contents of this compartment are stirred by means of a mechanically driven nickel stirrer. This stirrer, which does not come into contact with the membrane, has a vertically mounted axis situated off-centre to the cylindrical sample compartment to ensure mixing rather than merely imparting a rotational motion to the solution.

The sample is introduced into the dialysis cell by means of a calibrated gas-tight syringe. The channels leading to and from the sink compartment are 1 mm I.D. holes tapped to accommodate Luer fittings and 1 mm I.D. Tygon tubing. A peristaltic pump (Pharmacia P-3) is used to maintain a constant flow of eluting buffer through the sink compartment. Initial

Figure 7.1

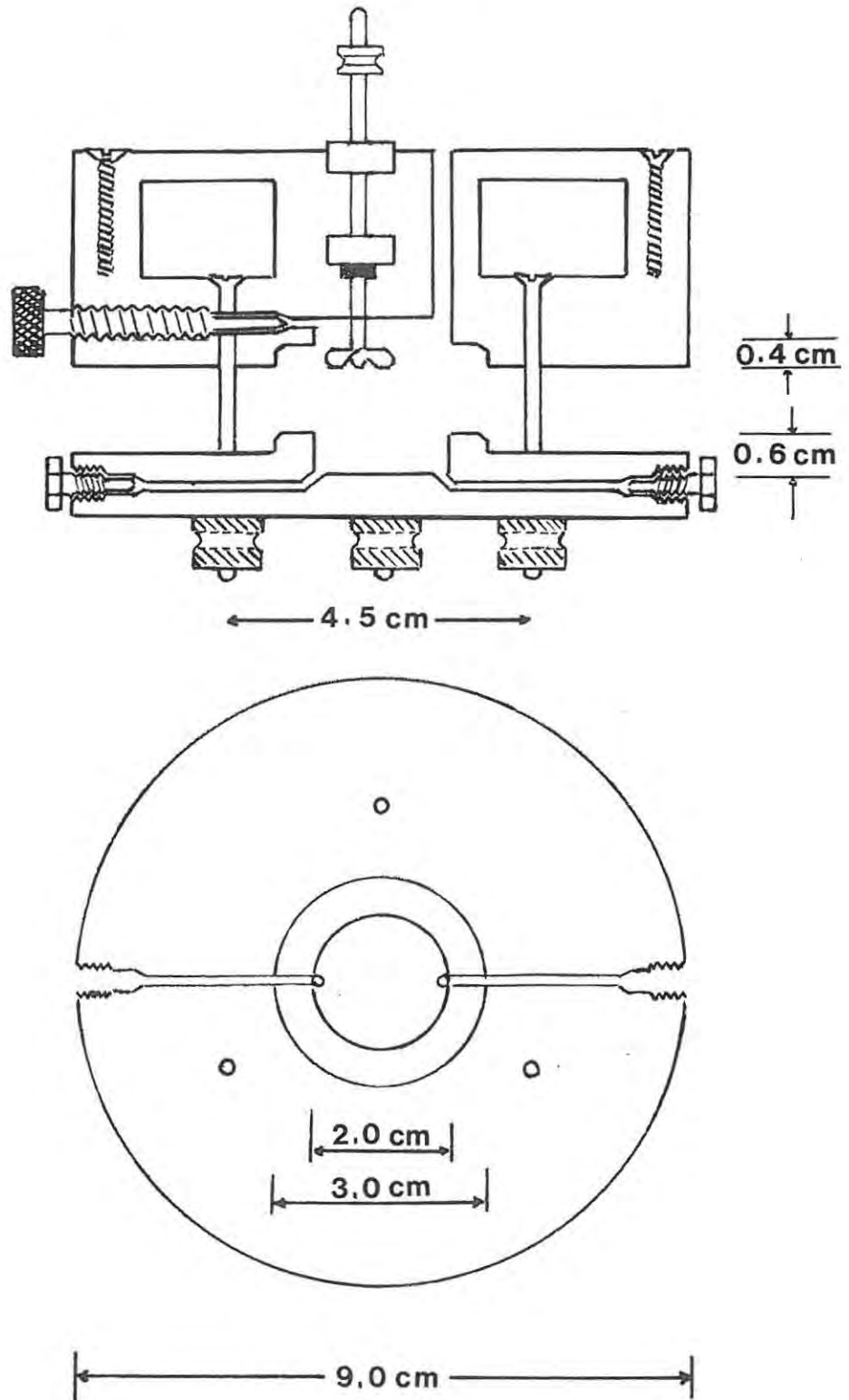
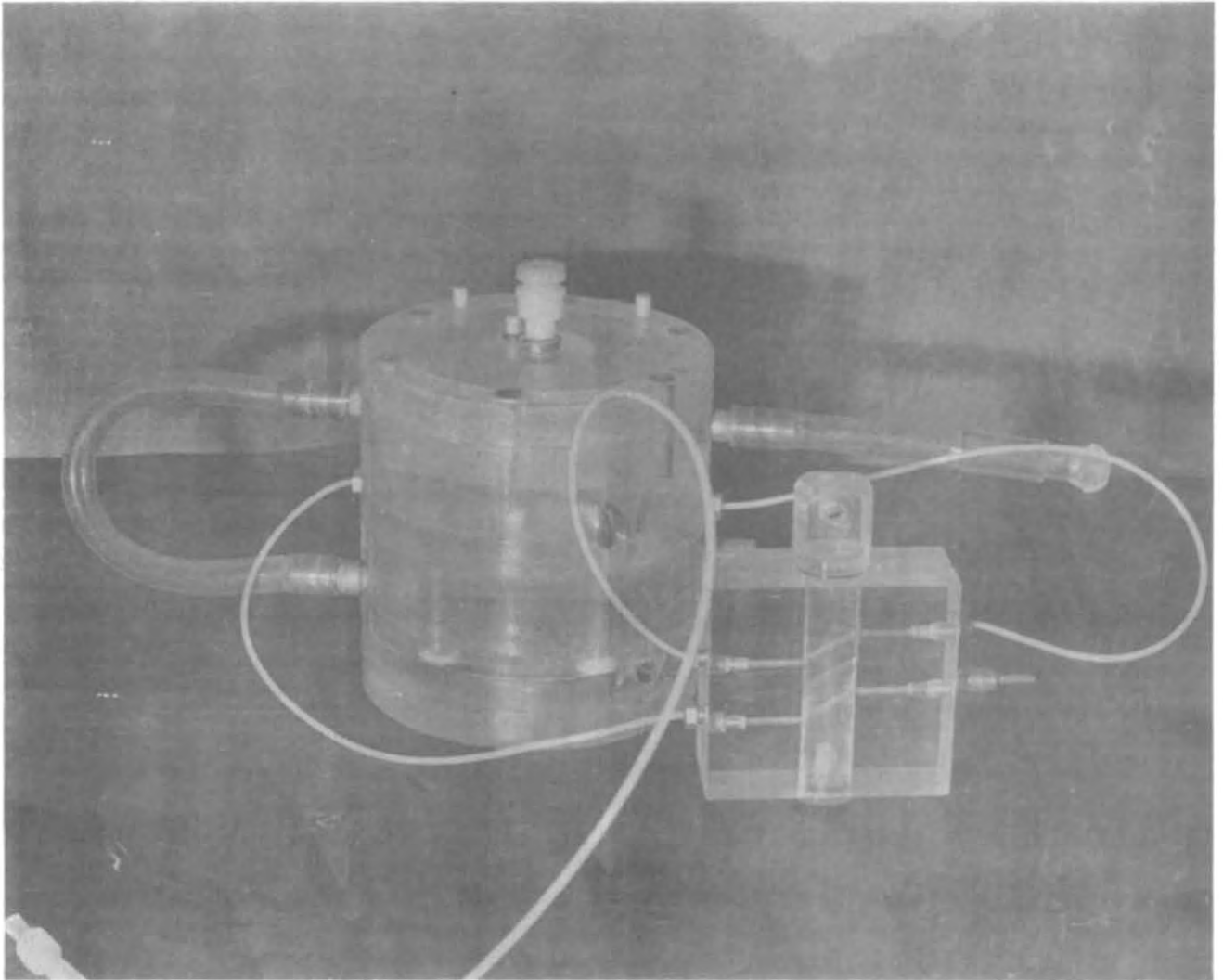
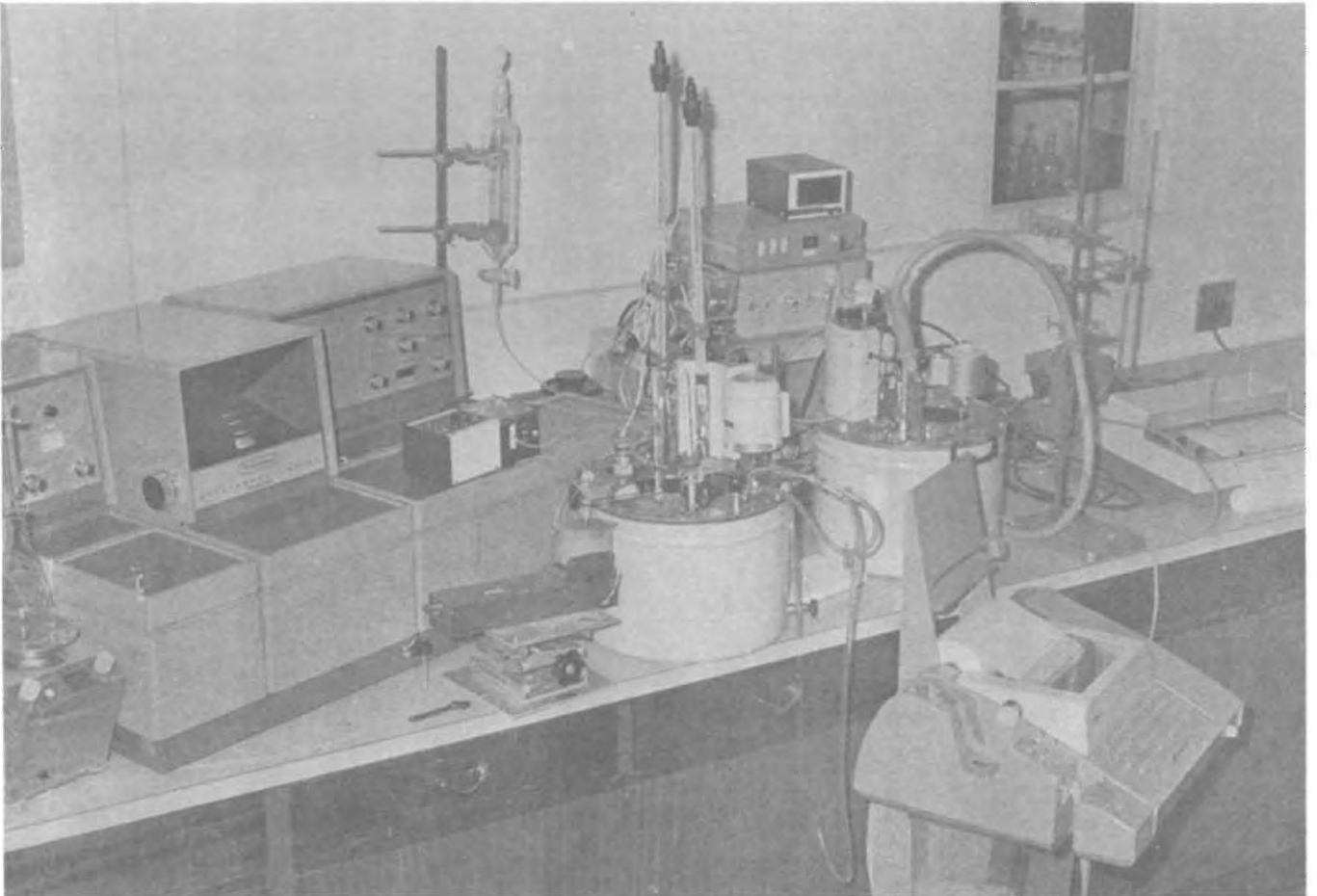


Plate VII



The Continuous-Flow Dynamic Dialysis Cell

Plate VIII



The complete apparatus for investigating protein-ligand binding by continuous-flow dynamic dialysis

attempts to obtain a constant flow using a Marriot flask and gravity feed proved unsatisfactory. Eluting buffer flow rates are monitored by recording at regular intervals (usually every 10 minutes) the mass of eluting buffer collected.

It is necessary to adjust the eluting buffer flow rate, depending on the extinction coefficient and/or initial concentration of the ligand. The eluting buffer flow rate was adjusted so that the value of the maximum absorbance in the elution profile for the control experiments was in the range from 0.4 to 0.7 absorbance units. Flow rates were varied between the limits of 0.2×10^{-2} to $0.1 \times 10^{-1} \text{ cm}^3 \text{ s}^{-1}$. An upper limit of the eluting buffer flow rate is imposed by the geometry of the flow cell. Too large a flow rate leads to inefficient mixing within the sink compartment and produces undulations in the elution profile.

Temperature control is achieved by means of a Colora Ultra thermostat used in conjunction with a Colora-Tauchk"uler cold-finger refrigerator system. The eluting buffer reservoir, the flowlines and dialysis cell are immersed into the constant temperature bath. The use of a thermostatically controlled relay and a 200 watt light bulb partially immersed into the constant temperature bath, as an auxiliary heat source, makes it possible to confine temperature variation in the dialysis cell to within $0.05 \text{ }^\circ\text{C}$. Temperatures in the sample compartment of the dialysis cell were determined using a digital display thermister.

Ligand concentrations in the eluting buffer flow stream were monitored spectrophotometrically using a Beckmann Acta CII spectrophotometer and a $60 \mu\text{L}$ spectrophotometer flow-cell. A W.W. chart recorder was used to provide a visual means of checking the course of dialysis.

Binding studies on the phenolic tannin precursor materials to collagen, as in the case of phenol red-BSA interactions, were carried out in duplicate for each compound. The ligand concentration range over which the binding was studied varied slightly from ligand to ligand depending on their solubilities and extinction coefficients. Upper concentration limits were imposed by the solubility of the compound in question.

B Materials

7.2 The Dialysis Membrane

The dialysis membrane consists of Visking cellulose dialysis tubing 4465-A2 (Union Carbide), with an average pore diameter of 480nm. In order to remove plasticisers and other membrane contaminants, the membrane is pretreated by boiling in 0.2M sodium carbonate solution for 30 minutes, then washed and boiled for a further 10 minutes in distilled water (Weiss 1976). Excess treated membrane was stored in distilled water in a refrigerator (0 - 4 °C) for further use.

7.3 Binding Agents

Phenol red

Phenol red (lot no. 737367) was supplied by Merck (Darmstadt) and recrystallized prior to use according to the method of Orndorff & Sherwood (1923). Control solutions were prepared in pH 7.3, 0.04M phosphate buffer using A.R. grade sodium dihydrogen phosphate and disodium hydrogen phosphate.

Mononuclear Phenols

Preliminary binding studies were carried out using phenol and the dihydric phenols catechol, resorcinol and dihydroquinone.

These materials were obtained from Merck (Darmstadt) and purified by sublimation prior to use. The solution concentrations were determined spectrophotometrically using the following reported values for the extinction coefficients (Pasto & Johnston, 1966).

| Compound | Wavelength | Extinction coefficient |
|----------------|------------|------------------------|
| | /nm | /M ⁻¹ |
| Phenol | 270 | 1450 |
| Catechol | 278 | 2630 |
| Resorcinol | 277 | 2200 |
| Dihydroquinone | 293 | 2700 |

Plant Phenolic Materials

The monomeric precursor materials of the hydrolysable wattle tannins gallic acid, $C_7H_6O_5$ (M.Mass 170) and isopropyl gallate, $C_{10}H_{12}O_5$ (M.Mass 212) used in binding studies were supplied by Merck (Darmstadt) and purified before use by recrystallization from water. The suppliers of the plant phenolic materials are listed below. These compounds were purified by recrystallization from water or water/ethanol mixtures.

| Compound | Formula | Supplier | Method of purification ^a |
|------------------|-------------------|--|-------------------------------------|
| Brazilin | $C_{16}H_{10}O_6$ | Fluka A.G.Chemiese Fabrik Germany Batch No. 53215 | w/e |
| Catechin | $C_{15}H_{10}O_6$ | Koch-Light laboratories Ltd. Colnbrooke England. Batch No. 57392 | w |
| Dihydroquercetin | $C_{15}H_{10}O_7$ | Fluka A.G.Chemiese Fabrik Germany Batch No. 158601/584883 | w |
| Dihydrorobinetin | $C_{15}H_{10}O_7$ | Supplied by Prof.D.Roux University of the O.F.S Bloemfontein. S.A. | - |
| Haematoxylin | $C_{16}H_{10}O_7$ | Hopkins & Williams Ltd. Chadwellheath England. Batch No. 75290 | w/e |

^a Recrystallized from water (w) or water/ethanol (w/e) mixture.
The materials were dried and stored under vacuum and over silica gel.

7.4 Proteins

Bovine Serum Albumin

Bovine serum albumin Fraction V (Batch No. B.P.E. 1572 Miles-Seravac Cape Town S.A) was used for the determination of the phenol red-BSA isotherm. Binding studies were carried out on BSA solutions of approximately 0.55% (m/v). To avoid errors in the measurement of the protein concentration due to hygroscopic absorption, BSA concentrations were standardised spectroscopically using a value of $E_{1\text{cm}}^{1\%} = 6.60$ (Clark et al., 1962; Chignall, 1969; Reynolds et al., 1970).

Collagen

Collagen was extracted from the skin of a six-week old Jersey bull calf, as outlined below.

C The Extraction and Purification of Collagen

7.5 Extraction

The method of extraction consisted of a modification of the extraction procedures described by Gross (1958) and Piez et al. (1963).

The skin from the freshly slaughtered calf was washed and immediately cooled in ice, macerated and extracted successively at 4°C for 48 hours with 0.15M sodium dihydrogen phosphate to remove the plasma proteins, 10% sodium chloride solution to remove the neutral-salt soluble collagen, and 0.5M acetic acid to extract the acid-soluble collagen. Each extraction procedure was repeated three times using about 10 volumes of solution based on macerated skin mass.

The solutions were stirred intermittently during the

extraction. The extracted liquors were vacuum-filtered successively through muslin, cotton wool, and Whatman No. 541 filter paper. The neutral-salt soluble collagen extract was precipitated by the addition of 5% m/v acetic acid and allowed to stand, with intermittent stirring, for 3 - 5 days at 4°C. The supernatant liquid was siphoned off and the precipitate subjected to centrifugation at 9 000 rpm for one hour at 5°C. The acid-soluble collagen extracts were precipitated by the addition of 5% m/v sodium chloride and treated in the same way as the neutral-salt soluble collagen extract.

7.6 Purification of collagen

Purification of acid soluble collagen was achieved by precipitation and dialysis (Gross, 1958; Bazin & Delauney, 1976). The combined precipitates of the acid-soluble collagen extracts were redissolved in the minimum quantity of 0.5M acetic acid. The solutions were centrifuged at 12 000 rpm for one hour and then dialysed against 0.2M disodium hydrogen phosphate, with frequent changing of the phosphate solution, until the collagen precipitated in the dialysis tubes.

The consolidated precipitates were redissolved in the minimum quantity of 0.15M acetic acid and dialysed against 0.15M acetic acid at 4°C for 24 hours. The reprecipitated collagen was again centrifuged, decanted, and finally lyophilized. The purity of the preparation was confirmed by ash, nitrogen and carbohydrate determinations. Molecular mass distributions were determined using a Beckman LB 52 ultracentrifuge. Amino acid analysis and separate hydroxyproline determinations using the method of Mitchell & Taylor (1970) were also carried out. The results of the amino acid analysis are tabulated in table 7-I. The results are the mean values of a triplicate analysis. For purposes of comparison, the results reported for an amino acid analysis of calf-skin collagen by Eastoe (1967) are also tabulated.

Table 7 - I
Collagen Preparation - Amino Acid Analysis

| | (a) | (b) | | (a) | (b) |
|----------------|-------|-------|---------------|-------|-------|
| | % | % | | % | % |
| alanine | 9.88 | 10.32 | methionine | 0.37 | 0.97 |
| glycine | 25.22 | 26.57 | aspartic acid | 5.89 | 6.95 |
| valine | 2.07 | 2.46 | phenylalanine | 2.06 | 2.35 |
| threonine | 1.98 | 2.26 | glutamic acid | 10.36 | 11.16 |
| serine | 3.61 | 4.27 | lysine | 3.84 | 3.96 |
| leucine | 3.18 | 2.73 | tyrosine | 0.56 | 0.90 |
| isoleucine | 1.32 | 1.88 | arginine | 8.89 | 8.22 |
| proline | 13.97 | 14.43 | histidine | 0.45 | 0.70 |
| hydroxyproline | 12.72 | 12.83 | | | |

(a) Present study

(b) from Eastoe (1967)

7.7 Analytical measurements on Total Protein

i) Determination of Ash

Ash determinations using the method of Eastoe & Courts (1963) were carried out in triplicate on 90 - 110 mg samples of the lyophilized collagen. The ash content was found to be less than 0.02%.

ii) Determination of Moisture

Moisture determinations were done in quadruplicate on 90 - 110 mg samples of lyophilized collagen, using the method of Eastoe & Courts (1963). The moisture content of the collagen was found to vary considerably due to its hygroscopic nature. For this reason, optical rotation measurements based on a predetermined specific rotation were used to standardize the concentration of collagen solutions used for dialysis.

iii) Nitrogen determinations

Nitrogen determinations were carried out on both pre-dried collagen samples as a check of the purity of the collagen preparation, and on collagen solutions to provide a method for accurately determining the concentration of the collagen in the solution. Nitrogen determinations were carried out on 100 mg samples which had been dried at 100°C for 4 hours over calcium oxide, using a modification of the method described by Eastoe & Courts (1963).

As in the Eastoe & Courts method, the modified method involved a Kjeldahl digestion of the protein in sulphuric acid, using a copper sulphate and mercuric oxide catalyst to convert the protein nitrogen to ammonium sulphate. The ammonia which was liberated from the ammonium sulphate by the addition of alkali was taken up by 0.1M boric acid and determined titrimetrically using a Metrohm-Heraeus E.436 potentiometric titrimeter. The mean nitrogen content on a dry ash-free basis determined from replicate experiments was $18.03 \pm 0.01\%$ which was consistent to within 0.6% of a published value of 18.6% for calf-skin collagen (Eastoe, 1967).

iv) Carbohydrate Analysis

A low carbohydrate content in collagen can be considered as a criterion of purity of the collagen preparation. Carbohydrate analyses were undertaken on an acid hydrolysate of the collagen preparation. The neutral sugars in the hydrolysate were separated from the hexosamine and amino acids using a 15 cm Dowex 50 chromatography column (Anastassiadis & Common, 1958) and the carbohydrate content of the eluate was determined using the method of Grant & Jackson (1968). The carbohydrate content, expressed as total hexose in terms of a galactose standard, was found to be $0.53 \pm 0.05\%$. This value is in close agreement with a reported value of 0.4% (Sharon & Li, 1980).

7.8 Preparation of Collagen Solutions

Collagen solutions were prepared by dissolving lyophilized collagen in the acid component of the phosphate buffer (0.05M phosphoric acid) at 5°C with continuous stirring over a period of 24 hours. This solution, the primary stock solution, contained approximately 2.5 mg/cm³ of collagen. After adjusting the pH of this solution to the desired value (pH 3.0) by the addition of sodium hydroxide solution, the solution was centrifuged at 15 000 rpm at 5°C, for one hour. The centrifuged stock solution was then mixed with sufficient volume of buffer solution to provide a stock concentration of 2.0mg/cm³. Aliquots of this, the secondary stock solution, were mixed with equal volumes of buffer solution for polarimetry measurements which were used to determine the exact protein concentration, or with equal volumes of double strength buffer solution, containing the ligand, for the dialysis experiments. This procedure ensured that the protein concentration in all the collagen solutions used for binding studies was 1.0mg/cm³.

The same double strength ligand solution, diluted with an equal volume of buffer solution, was used in the control dialyses, carried out without protein, to determine the permeation constant for the ligand. The concentrations of protein in the secondary protein stock solutions were determined by polarimetry measurements using a specific rotation calibrating factor for a 1.00 mg/cm³ collagen solution. This factor was determined from a 1.00 mg/cm³ solution, the concentration of which had been accurately established by comparison of its nitrogen content with that of dried lyophilized collagen.

The optical rotation of the collagen solutions were determined using water-jacketed polarimeter tubes at 15°C in a Perkin-Elmer model 141 polarimeter at a wavelength $\lambda = 365$ nm. Specific rotation values were calculated from a mean of 4

readings, each from 4 separate fillings of the polarimeter tube. Optical rotation measurements were taken one hour after filling the tubes, to ensure temperature equilibrium.

Using the 1.0mg/cm^3 collagen solutions, whose collagen concentration had been established from the nitrogen content, a standard optical rotation constant was calculated using the formula:

$$[\alpha]_{\lambda}^t = 100a/dc \quad \dots \quad 7.8.1$$

where:

- a is the observed optical rotation in degrees;
- d is the optical path-length in decimeters;
- and c is the collagen concentration in mg/cm^3

7.9 Evaluating the Effects of the Experimental Variables

The influence of experimental variables, such as pH, temperature, buffer concentration, stirring rate, viscosity, and sample solution volumes, on the rate of dialysis and on the shape of the escape curve have been reported by Meyer & Guttman (1970b). In the present CFDD method, standardized experimental conditions were employed. All binding studies were conducted at constant pH, temperature, and sample solution volume. Potential sources of experimental error, and methods adopted to limit their effect, are discussed below.

i) Viscosity

In an attempt to keep the viscosity of the sample solution constant, all binding studies were performed on protein solutions having the same protein concentration (approximately 1mg/cm^3). However, because of the difficulties associated with the solubilization of collagen and the hygroscopic nature of the

protein, protein concentrations did vary slightly from the standard value. This variation in protein concentration was, never, however, more than 1% in different binding experiments.

ii) The Dialysis Membrane

Although use of the dialysis cell ensures that the area of membrane exposed to the sample and sink solutions is constant in all experiments, values for the permeation constants for a given ligand were found to vary slightly when the membrane was changed. These effects are probably due to differences in stretching when the membrane is fitted into the dialysis cell. For this reason, control and binding experiments for a given ligand were carried out using the same piece of dialysis membrane, without remounting.

When duplicate binding studies were carried out for a given ligand, control and binding experiments were alternated to guard against the possibility that the permeation characteristics of the membrane would change as a result of ligand or protein adherence to the membrane. It was found that the permeability of the membrane could be affected by the presence or absence of the buffer background ions. This made it necessary, after rinsing the dialysis cell with distilled water at the end of a dialysis experiment, to re-equilibrate the membrane with the background buffer solution. Fresh membranes were used for each new ligand.

iii) Binding of the Ligand to the Membrane

Meyer & Guttman (1970a) stated that binding of the ligand to the membrane is indicated by curvature in the log-linear plot of the sample compartment ligand concentration as a function of time. A linear plot was interpreted by these authors to indicate an absence of ligand binding to the membrane. Stewart (1977), however, has shown (for systems such as that used by Meyer & Guttman) an upward curvature of the log-linear escape curve ($\log[C_1^*(t)]$ vs t), is a function of sampling frequency when back-diffusion is neglected, and that curvature in this plot

can be induced simply by increasing the time between sampling. This indicates that such curvature is caused by back diffusion of the ligand. An upward curvature of the log-linear escape curve can also be explained in terms of osmotic effects (Sheih, 1978).

These considerations do not apply to the CFDD method where the sink compartment is being continuously eluted. An alternative test to check whether ligand-membrane binding occurred was devised. Dialysis membrane, having been exposed to the ligand in a dialysis situation, was rinsed with distilled water, placed in a supporting frame and its UV spectrum scanned over the absorbance range of the ligand. A comparison of the spectrum of this membrane with that of membrane not exposed to ligand was used as a test for ligand binding to the membrane. Such comparisons showed that no significant binding to the membrane of the ligands investigated could be detected.

iv) Binding of Protein to the Membrane

The possibility of BSA or collagen binding to the membrane was investigated by removing the membrane from the dialysis cell after it had been exposed to the protein, rinsing gently with distilled water, and then hydrolysing the membrane in 5M hydrochloric acid. The hydrolysate was tested for the presence of amino acids by treatment with ninhydrin solution. This test showed no indication that either of these two proteins bound significantly to the membrane.

v) Osmotic Effects of the Protein Solutions

Meyer & Guttman (1970) and Kanfer (1976) considered the effect of osmosis by determining whether a change in the protein concentration in the sample compartment, due to osmotic uptake of solvent, occurred over the course of a dialysis experiment. Such a procedure could not be adopted in the present study because of

the small volume of protein solution used (1.5 cm^3), and the difficulties encountered in quantitatively removing this solution from the dialysis cell for protein assay.

An alternate procedure was adopted in which the sample solution was subjected to additional hydrostatic pressure to compensate for osmotic pressures. The results of these experiments were compared with the results obtained for dialysis experiments performed under atmospheric pressures. A theoretical value for excess hydrostatic pressure, P_i , to compensate for the osmotic pressure was calculated on the basis of the protein concentration by the formula:

$$P_i = MRT \quad \dots \quad 7.9.1$$

where M is the molarity of the protein solution, R the universal gas constant, and T the absolute temperature.

The excess pressure to compensate for osmosis was applied to the sample solution by fitting an hydrostatic U-tube arrangement to the dialysis cell. Dialyses carried out under increased pressure yielded the same results as dialysis at atmospheric pressure, from which it was concluded that, at the protein concentrations used and over the durations of the dialysis experiments, osmotic effects are not significant.

vi) The Effect of Stirring Rate

Although a standard stirring rate of 100 rpm was used in all binding study experiments, control experiments using phenol red were carried out using different stirring rates to test the efficacy of the stirring and to examine whether the rate of stirring had any effect on the elution profile or shape of the ligand escape curve, and to ensure that the experimental reproducibility of the CFDD method was independent of the choice of the stirring rate.

Successive dialysis experiments in which all the parameters except the rate of stirring were kept constant showed that, for the particular dialysis cell, the elution profile and escape curve are independent of the stirring rate, as long as the stirring does not produce frothing in the protein solution, and is sufficiently rapid to mix the contents of the protein compartment.

vii) Temperature Effects

The present study has shown that the CFDD method is very sensitive to temperature fluctuations. Binding studies over a temperature range from 15 - 25°C show that the ligand permeation constant increases with increasing temperature.

In order to achieve effective temperature control, it was found necessary to supplement the Colora temperature bath and thermostat with a fine control heat source. This consisted of a 200 watt light bulb which was partially immersed into the constant temperature bath. The light bulb was connected in series with a thermostatically controlled relay switch. A constant temperature heat sink was also provided by circulating water from a second Colora constant temperature bath, which incorporated a Colora-Tauchkühler cold finger refrigerator system, through a heat exchanger coil in the constant temperature bath containing the dialysis cell.

viii) Spectrophotometer Drift

The CFDD method is susceptible to the possibility of systematic errors which can result from a gradual drift in the spectrophotometer base line because of the lengthy duration of dialysis experiments (usually about 7 hours). In order to determine whether any such effect did occur, a two-way tap was incorporated into the system flow-stream so that the eluting buffer flow stream could be diverted to bypass the dialysis cell. At the end of the dialysis experiment, the tap would be set so that fresh eluting buffer solution could flow directly from the reservoir to the spectrophotometer flow cell.

A measure of the overall spectrophotometer base line drift was obtained by measuring the optical absorbance after allowing the eluting buffer to flush the flow lines and the spectrophotometer flow cell free of ligand. This was usually found to be within the specification limits of the spectrophotometer (0.005 in absorbance) and it was not necessary to make corrections for this source of error. The computer program written to process the data does, nevertheless, include a routine whereby if it is assumed that the baseline drift is linear with time over the course of the dialysis experiment, the drift-signal may be subtracted from the elution profile.

7.10 Data Processing

The data contained in the elution profiles was processed by means of a computer to extract the binding isotherms and binding parameters. This was facilitated by interfacing the spectrophotometer to a data-logging device, so that the elution profile could be recorded automatically onto paper tape in a computer readable format.

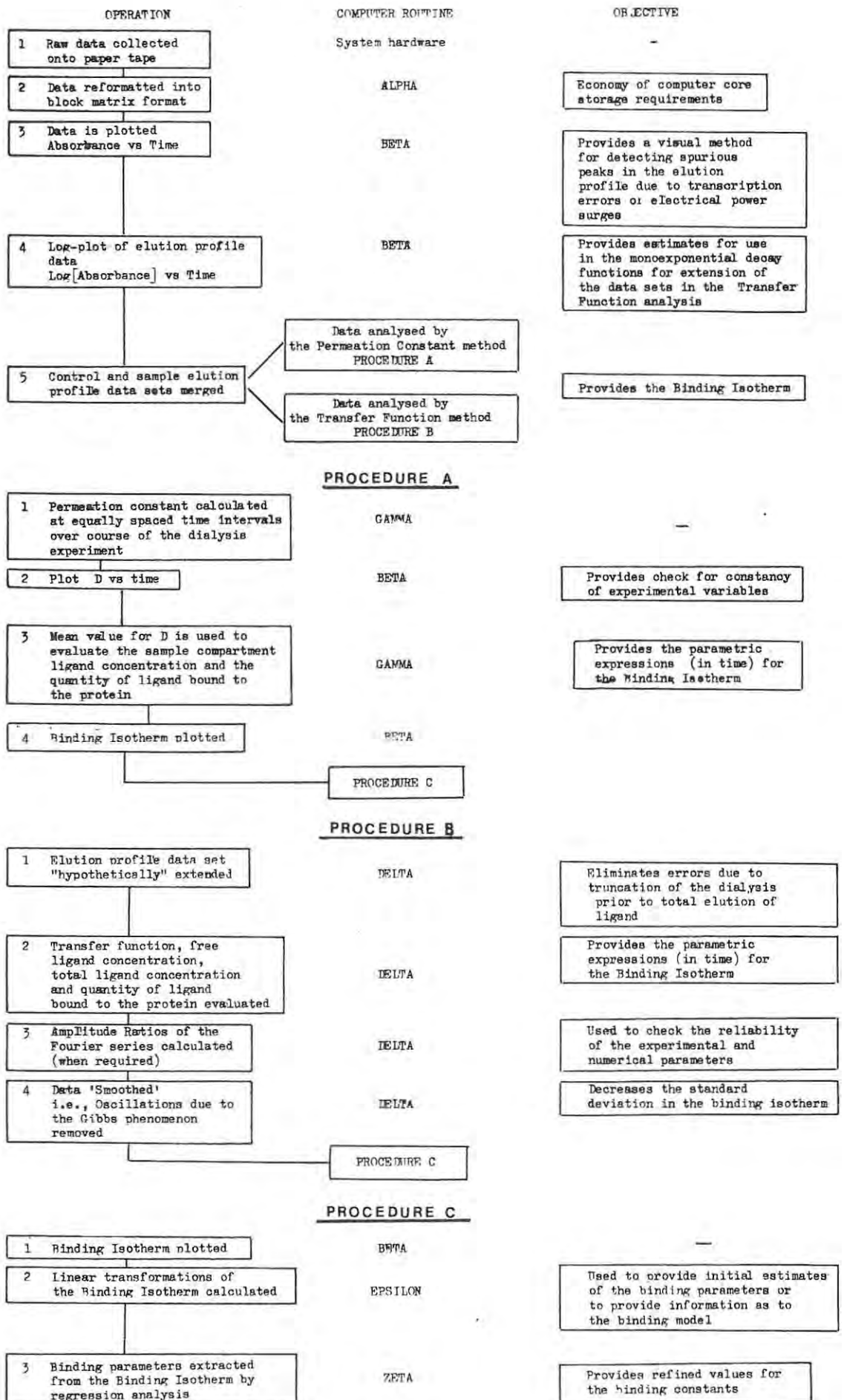
A general scheme for processing the raw data was adopted. This entailed obtaining computer drawn linear and log-linear plots of the elution profiles, to provide a check that the data was free of spurious peaks from electric impulses or transcription errors. After necessary editing of the data, a computer routine was used to provide values of the slope of the latter linear portion of the log-linear plot of the elution profile (i.e., that region of the curve after the profile had passed through its maximum) and a value for the extrapolated intercept of this linear portion of the curve with the ordinate. These parameters are subsequently used in the routine which calculates the transfer function. These values can also be used to check variation of experimental variables such as change in sink compartment volume resulting from distension of the membrane due to dynamic pressures of the eluting buffer flow (Appendix II).

The data of the control experiments can at this stage either be processed to extract the permeation constant, or be pooled with the data from protein-ligand dialysis experiments to be used in the computer routine which evaluates, simultaneously, the transfer function and the binding isotherm. If the option to evaluate a permeation constant is selected, a routine to calculate the mean value of the permeation constant and the within-run standard deviation for the permeation constant is utilized, together with a routine to provide a graphical plot of the variation of the permeation constant with time, over the course of the dialysis. The appropriate value of the permeation constant is incorporated into the data set of the protein-ligand dialysis and processed by the 'permeation constant' routine to derive the parametric equations of the binding isotherm.

Alternatively, the isotherm may be calculated by the transfer function routine. Once the parametric equations of the binding isotherm have been established, they can be used to generate a computer plot of the binding isotherm, or be subjected to transformations to obtain equivalent forms such as the Bjerrum plot, reciprocal plot, double reciprocal plot, etc. These plots are used to provide initial values for the binding parameters for the protein-ligand system. The initial estimates are subsequently used in an iterative non-linear least squares routine to obtain the refined values for the binding parameters. A flow diagram of the procedures used to extract the binding isotherm and binding parameters from the elution profile data is given in Figure 7.2

A listing of the computer routines used in the data analysis is given in Appendix V. The computer routine written to obtain the binding isotherm by the permeation constant method is given in Appendix VI, and the routine to derive the binding isotherm by the transfer function method is given in Appendix VII.

Flow Diagram of the Numerical Procedures to Extract a Binding Isotherm and Binding Parameters from the Elution Profile Data sets



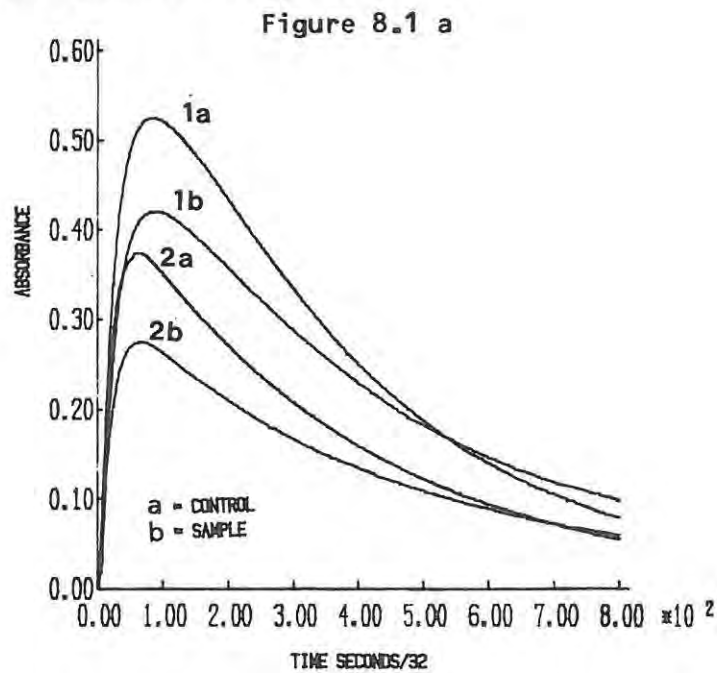
The iterative least squares procedure to derive the refined values of the binding parameters is that of Chandler (1965) which was found to be very stable. The subroutine which permits the binding parameters to be evaluated in terms of a binding-site model or the generalized model, which includes complex values for the binding constants, is listed in Appendix VIII.

Chapter Eight

Results: Evaluation of the CFDD method and Data Analysis
using the Permeation Constant method

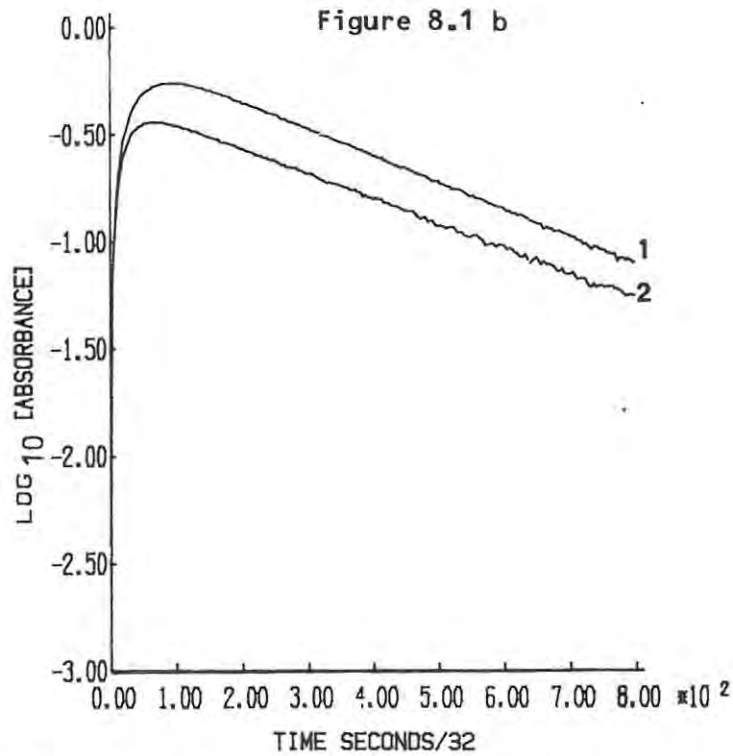
8.1 Phenol Red-BSA Interactions at 25 °C

Elution profiles depicting the dialysis of phenol red at 25 °C are shown in Figure 8.1 a. The profiles are shown for two sets of dialysis experiments, each set consisting of a control and a sample dialysis experiment. Log-linear plots of the elution profiles are shown in figure 8.1 b.



Elution profiles for the dialysis of phenol red at 25 °C

The elution profiles representing the sink compartment ligand concentration as a function of time are expressed in absorbance units at $\lambda = 269 \text{ nm}$ ($\epsilon = 10800 \text{ M}^{-1}$). The initial phenol red concentration for both the control and sample dialyses (Experiment 1) were $1.11 \times 10^{-3} \text{ M}$ with an eluting buffer flow rate $0.3 \times 10^{-2} \text{ cm}^3/\text{s}$. The initial ligand concentrations used in the sample and control dialyses (Experiment 2) were $4.98 \times 10^{-3} \text{ M}$ with an eluting buffer flow rate $3.42 \times 10^{-2} \text{ cm}^3/\text{s}$. BSA concentration in sample dialysis in both experiments was $7.55 \times 10^{-5} \text{ M}$. The durations of the dialysis experiments were 460 minutes. The sampling interval was 32 s.



Log-linear plots of phenol red elution profiles at 25 °C

The slope of the log-linear plot of the control profile for large t is used to provide an initial estimate of the permeation constant using the formula:

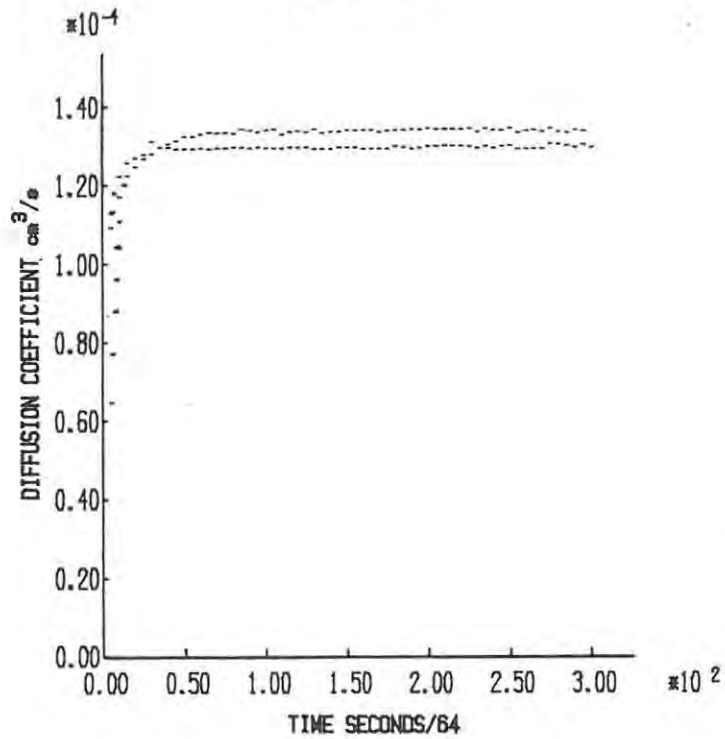
$$D = bV_1 \left\{ (bV_2 - F) / (bV_t - F) \right\} \quad \dots \quad 8.1.1$$

derived from equations 5.4.3b and 5.4.4a & b. Here, b is the slope of the log-linear plot of the elution profile, F the eluting buffer flow rate, V_1 and V_2 the sample and sink compartment volumes, respectively, and $V_t = V_1 + V_2$

If back diffusion is neglected, this reduces to $D = bV_1$. The initial value of the permeation constant obtained by substitution of the measured value of the slope ($0.8313 \times 10^{-4}/s$, figure 8.1b) into equation 8.1.1 is $D = 1.28 \times 10^{-4} \text{ cm}^3/s$. If back diffusion of the ligand is neglected the value for D is $1.30 \times 10^{-4} \text{ cm}^3/s$.

Values of the permeation constant computed at equally spaced time intervals (every 320 s) throughout the course of the dialysis, by means of equation 5.8.8, are shown in figure 8.2. These computations were performed by the FORTRAN computer routine GAMMA (Appendix VI).

Figure 8.2

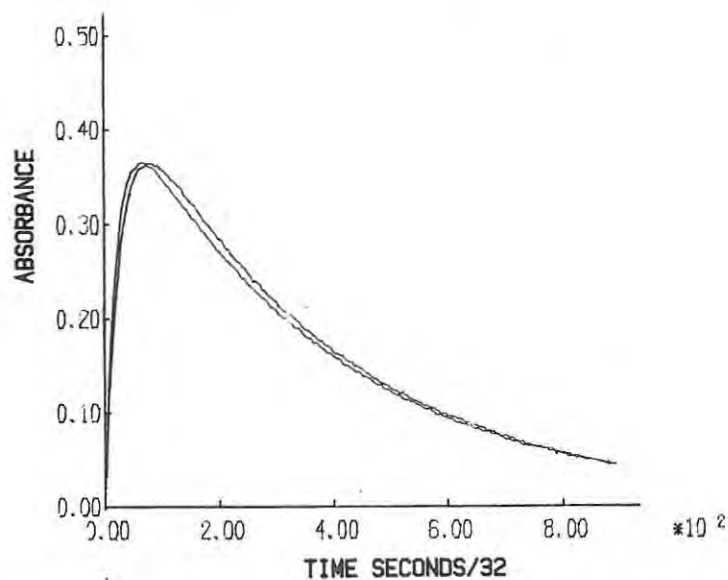


Variation in the permeation constant with time over the course of the dialysis experiment at 25 °C

It can be seen that, after an initial transient, the method yields a constant value for the permeation constant, apart from slight residual variations arising from experimental noise in the absorbance signal. The mean values of the permeation constants obtained from 200 values in each dialysis experiment were 1.299×10^{-4} and 1.311×10^{-4} cm³/s respectively. The

standard deviations were 0.007×10^{-4} and $0.006 \times 10^{-4} \text{ cm}^3/\text{s}$ respectively. The combined mean value for the permeation constant was $1.30 \times 10^{-4} \text{ cm}^3/\text{s}$. The differences in the mean values of the permeation constants observed for duplicate dialysis experiments (less than 2%), can be ascribed to the difficulty in reproducing exactly all the experimental conditions in separate experiments. For the same reasons, the standard deviation of the permeation constants obtained from different dialysis experiments is greater than the standard deviation within a single experiment. An indication of the degree of reproducibility provided by the CFDD method is given in figure 8.3, which shows the elution profiles obtained from duplicate control dialyses of phenol red.

Figure 8.3



Elution profiles for duplicate phenol red dialysis experiments

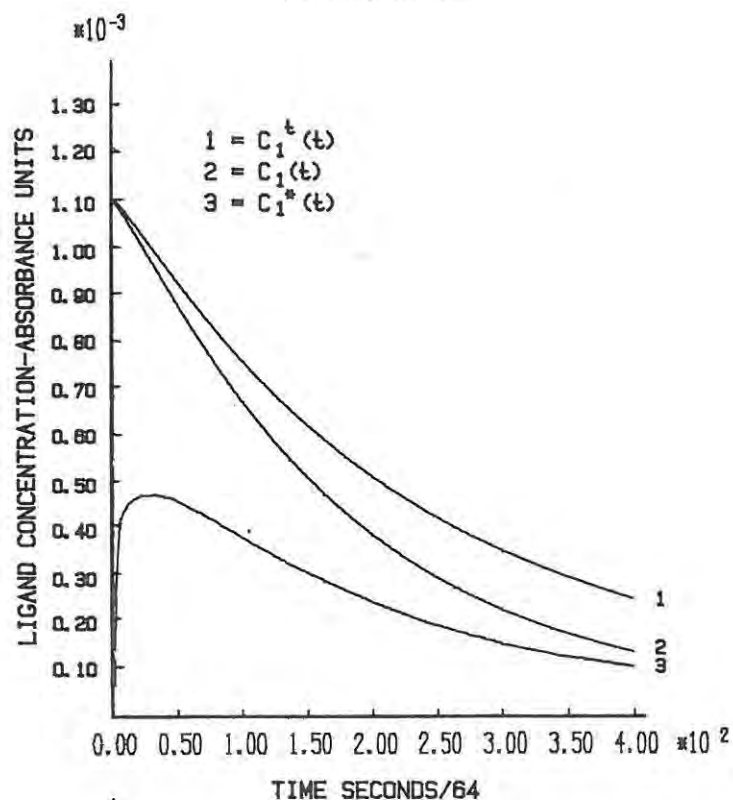
Elution profiles obtained from duplicate phenol red dialyses at 25°C
 Initial phenol red concentration $0.12 \times 10^{-3} \text{ M}$, eluting buffer
 flow rate $0.5 \times 10^{-3} \text{ cm}^3/\text{s}$.

A quantity of data is rejected in the calculation of the mean permeation constant because, during the initial transient period,

the permeation constant has not yet attained a constant value. This initial transient phase probably results from both the time taken for the ligand to establish a linear concentration gradient within the dialysis membrane and numerical rounding-off errors. These numerical rounding-off errors produce the largest inaccuracies during the transient phase, when only a small number of data points are as yet available for use in the Simpson and Savitzky-Golay numerical integrating and differentiating routines. During this phase, the slope and the rate of change of slope of the data with time are also greater than at subsequent stages of the elution process so that during this interval it is also likely that the inaccuracies in the Savitzky-Golay differentiating routine have their maximum values.

The variation in sample compartment ligand concentrations with time are shown in Figure 8.4. These curves were derived from the mass-balance expression (equation 5.8.5) for the control, and by equation 5.8.7 (which incorporates the measured value for the permeation constant) for the sample dialysis data.

Figure 8.4



Sample compartment ligand concentrations at 25 °C

Dialysis was usually discontinued after about 7 hours because of the possibility of decreasing accuracy due to accumulative errors, and drift in the recorder base-line. Experimental conditions were arranged such that, after this time, the ligand absorbance in the dialysate was about 0.01 and the sample compartment ligand concentration had fallen to about 30% of the initial value. Thus, in order to cover a wide enough range of ligand concentrations to establish the binding isotherm a series of dialyses were carried out in which the initial ligand concentration of each successive dialysis experiment was about 50% that of the preceding experiment. In most cases the protein concentration would be kept the same. However, in dialysis experiments where the ligand concentration after dilution in the eluting buffer would have been too low to provide reliable results, larger protein and ligand concentrations were used to obtain equivalent low values for the ligand/protein ratio. In this way, it was possible to establish the phenol red-BSA binding isotherm over a 100-fold concentration range, from 2.15×10^{-5} to 2.23×10^{-3} M.

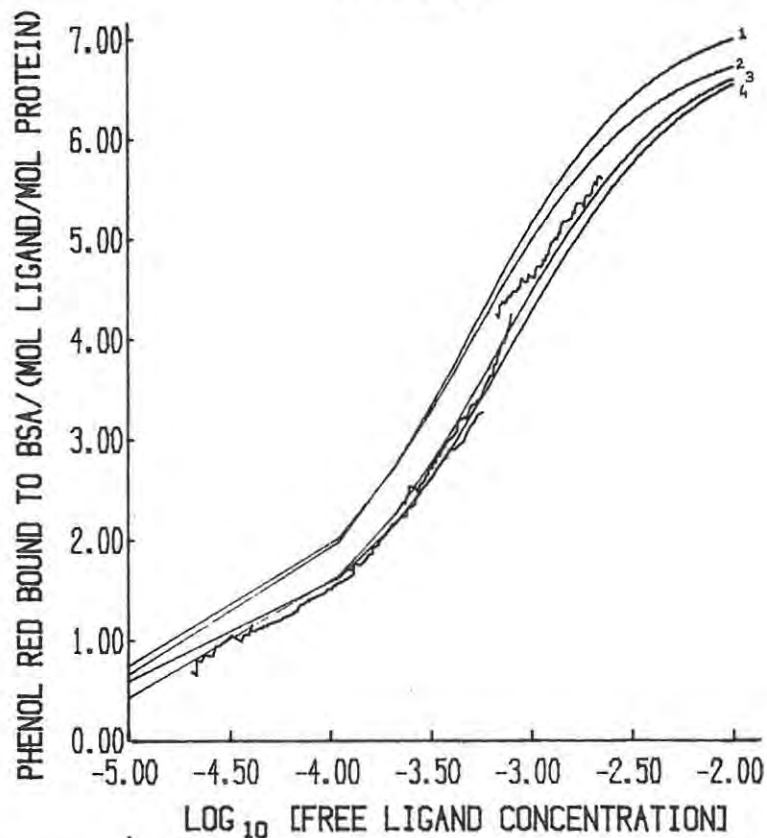
The series of phenol red concentration ranges covered in the separate dialysis experiments, in order to obtain the composite binding isotherm, are listed in table 8 -I

Table 8 -I

| Experiment Number | Initial ligand Concentration /M | Final ligand Concentration /M |
|-------------------|---------------------------------|-------------------------------|
| 1 | 2.23×10^{-3} | 7.45×10^{-4} |
| 2 | 8.31×10^{-4} | 2.74×10^{-4} |
| 3 | 2.87×10^{-4} | 1.10×10^{-4} |
| 4 | 1.61×10^{-4} | 4.22×10^{-5} |
| 5 | 4.20×10^{-5} | 2.15×10^{-5} |

The data from these elution profiles were processed using the FORTRAN program GAMMA. This computer routine yields the binding isotherm from the parametric equations in time for $\tilde{v}(t)$ and $C_1^*(t)$ (equations 5.8.6 and 5.8.7). The composite log-linear plot of the binding isotherm (Bjerrum plot) over the entire ligand concentration range is shown in figure 8.5. Included for comparison are the computer generated isotherms based on the Scatchard two-site binding model (equation 5.10.1) using the binding parameters reported by other authors.

Figure 8.5



Bjerrum plot of the phenol red-BSA binding isotherm

- 1 - Binding isotherm based on binding parameters of Kanfer (1976)
- 2 - Binding isotherm based on binding parameters of Meyer & Guttman (1970).
- 3 - Binding isotherm obtained by CFDD
- 4 - Binding isotherm based on binding parameters of Rodkey (1961)

The binding isotherm obtained by the CFDD method coincides more closely with the isotherm generated using the Scatchard two-site model and the binding parameters reported by Rodkey (1961) than with the pair of isotherms of Meyer & Guttman (1970) and Kanfer (1976). The isotherms of the latter are in fairly close agreement. Both of these isotherms were obtained using similar dynamic dialysis techniques; in both cases ideal sink conditions were assumed to prevail and back-diffusion was neglected. Since the Rodkey isotherm was obtained using difference spectroscopy, and because the CFDD method allows for back diffusion, the difference between these two sets of isotherms may reflect the effects of back-diffusion.

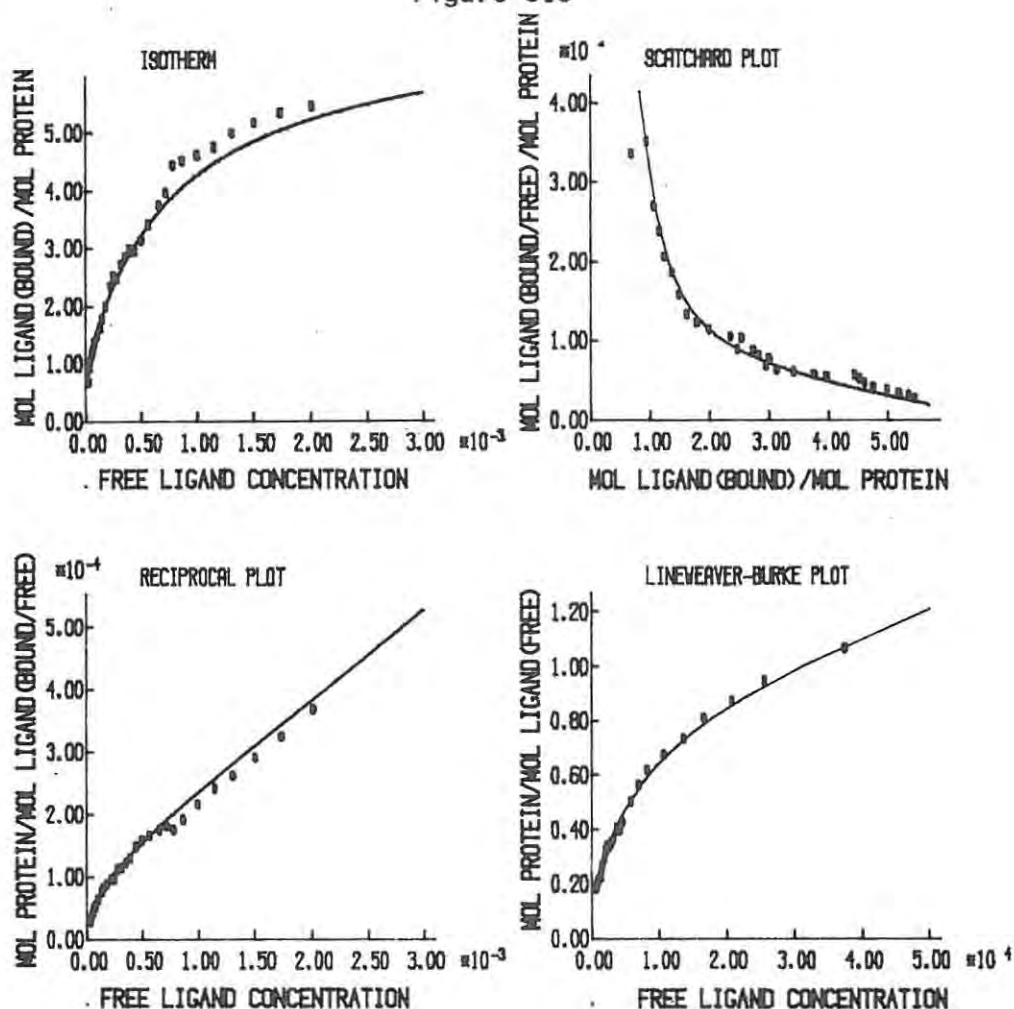
In order to evaluate the binding parameters for the isotherm determined by the CFDD method, computer plots for a variety of linear transformations of the isotherm were generated using the FORTRAN routine EPSILON. The equations to effect these transformations are tabulated in table 8 - II.

Table 8 - II

| | |
|--|----------------------------------|
| Bjerrum Plot | $\bar{v} = k (\bar{v} + n) 10^x$ |
| | where $x = \log_{10}[L]$ |
| Scatchard plot | $\bar{v}/[L] = k(N - \bar{v})$ |
| Reciprocal plot | $[L]/\bar{v} = 1/Nk + [L]/N$ |
| Lineweaver-Burke (Double reciprocal plot) | $1/\bar{v} = 1/N + 1/(Nk[L])$ |

The corresponding transformations of the binding isotherms are shown in figure 8.6.

Figure 8.6



Linear Transformations of the Phenol Red - BSA Binding Isotherm

The solid line in each diagram represents the appropriate transformation of the theoretical isotherm based on the Rodkey (1961) binding parameters.

The Scatchard two-site binding equation (equation 5.10.1) was incorporated into a least squares iterative curve fitting routine (program STEPIT by Chandler, 1965) to obtain refined values of the binding parameters n_i and k_i from initial estimates. The binding parameters n_i (for $i = 1$ and 2) which represent the number of bound molecules in the different classes of binding sites, were constrained to integer values. Values of the binding parameters obtained using the Scatchard two-site binding model in the regression analysis are tabulated in table 8 - III. For purposes of comparison, the binding parameters obtained by Rodkey, Meyer & Guttman, and Kanfer are also listed.

Table 8 - III

Binding Parameters for the Phenol Red - BSA interaction at 25 °C

| Source | n_1 | k_1 litre/m | n_2 | k_2 litre/m |
|------------------------|----------------|--|----------------|--|
| Rodkey (1961) | 1 ^a | 1.1×10^5 | 6 ^a | 1.2×10^3 |
| Meyer & Guttman (1970) | 1 ^a | 1.74×10^5 | 6 ^a | 1.97×10^3 |
| Kanfer (1976) | 0.9 | 1.5×10^5 | 6.4 | 1.96×10^3 |
| Present Study | 1 ^a | 0.56×10^5 $\pm 0.05 \times 10^5$ | 6 ^a | 1.37×10^3 $\pm 0.05 \times 10^3$ |

^a constrained to integer values

It is seen that the value for k_1 as determined by the CFDD method is smaller than the values reported by these investigators. This difference, however, is not statistically significant. The experimental data from which the binding parameters were determined by these investigators, were re-analysed using the STEPIT regression program to obtain estimates for the approximate errors. When these data sets representing the binding isotherm include the origin (consistent with the assumption of zero ligand binding at zero ligand concentration) the values yielded by STEPIT for the binding parameters, together with values for the approximate error, are given in table 8 - IV.

Table 8- IV

Binding Parameters for the Phenol Red-BSA Interactions at 25 °C
and their Approximate Standard Errors

| Method | No. of data points | n_1^a | k_1 | n_2^a | k_2 |
|--|--------------------|---------|-------------------------------|---------|-------------------------------|
| Difference Spectroscopy ^b | 12 | 1 | $(0.92 \pm 2.7) \times 10^5$ | 6 | $(1.29 \pm 0.47) \times 10^3$ |
| Dynamic Dialysis ^c | 38 | 1 | $(3.64 \pm 5.8) \times 10^5$ | 6 | $(1.52 \pm 0.37) \times 10^3$ |
| Dynamic Dialysis ^d | 32 | 1 | $(0.57 \pm 1.1) \times 10^5$ | 6 | $(2.05 \pm 0.42) \times 10^3$ |
| Continuous-Flow Dynamic Dialysis ^e | >500 | 1 | $(0.56 \pm 0.08) \times 10^5$ | 6 | $(1.37 \pm 0.02) \times 10^3$ |

^a Constrained to integer values.

^b Data from Rodkey (1961); parameters recalculated, using STEPIT,
in order to estimate standard errors.

^c Data from Meyer & Guttman (1970a). See footnote ^b and text for comment on statistics.

^d Data from Kanfer (1976). See footnote ^b and text for comment on statistics.

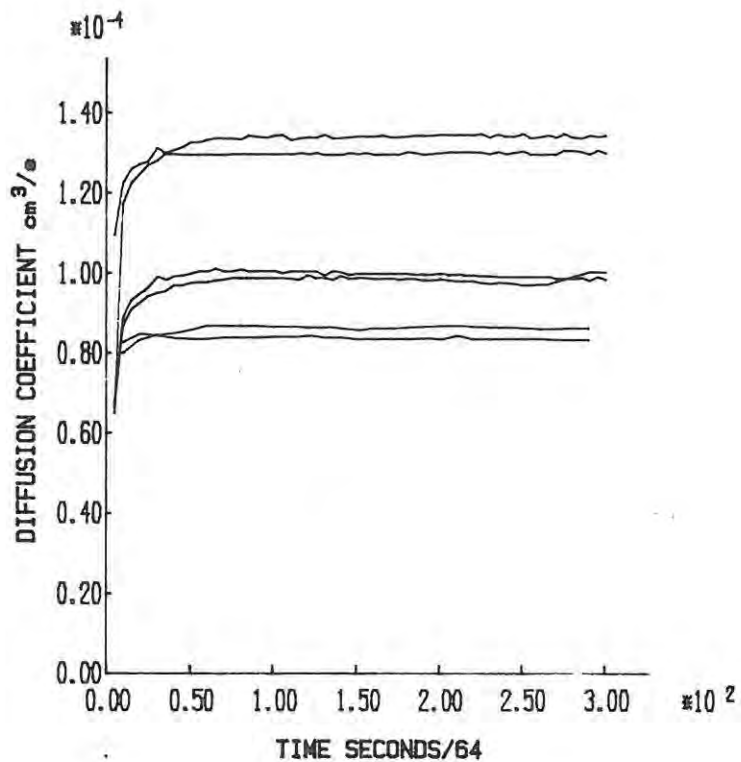
^e Data from present study; 15 point running smooth
used to obtain derivatives.

8.2 Phenol Red - BSA interactions at 15 & 20 °C

Initial experiments on the binding of phenol red to BSA using the CFDD method showed the method to be very sensitive to temperature changes. Since the temperature sensitivity could be a reflection of changes in either the binding characteristics of the protein or the rate of diffusion of the ligand through the membrane, binding studies on the phenol red-BSA system were also undertaken at 15 & 20 °C.

The binding of phenol red to BSA at these two temperatures was investigated over a phenol red concentration range from 1.0×10^{-5} to 2.0×10^{-4} M. The variation in the rate of diffusion of phenol red with temperature as reflected by the change in permeation constants with temperature is shown in figure 8.7.

Figure 8.7



Variation of the phenol red permeation constants over the course of the dialysis at 15 & 20 °C

Computer generated plots show the values of the permeation constants calculated from the control elution profiles at equally spaced time intervals throughout the course of the dialysis experiments at 15, 20 & 25 °C. The values for the permeation constants were calculated using the computer program GAMMA.

The mean values of the permeation constants determined at each temperature are listed in table 8 - V together with the corresponding values of the diffusion coefficient, D^* . The diffusion coefficient, D^* , is related to the permeation constant D by the formula $D^* = Dd/A$ where d is the membrane thickness and A the surface area of the membrane available for diffusion. The values of the diffusion coefficients were calculated using a value of 3.15 cm^2 for the membrane surface area and a value of 0.013 cm for the thickness of the swollen membrane. The wet membrane thickness was measured using a micrometer.

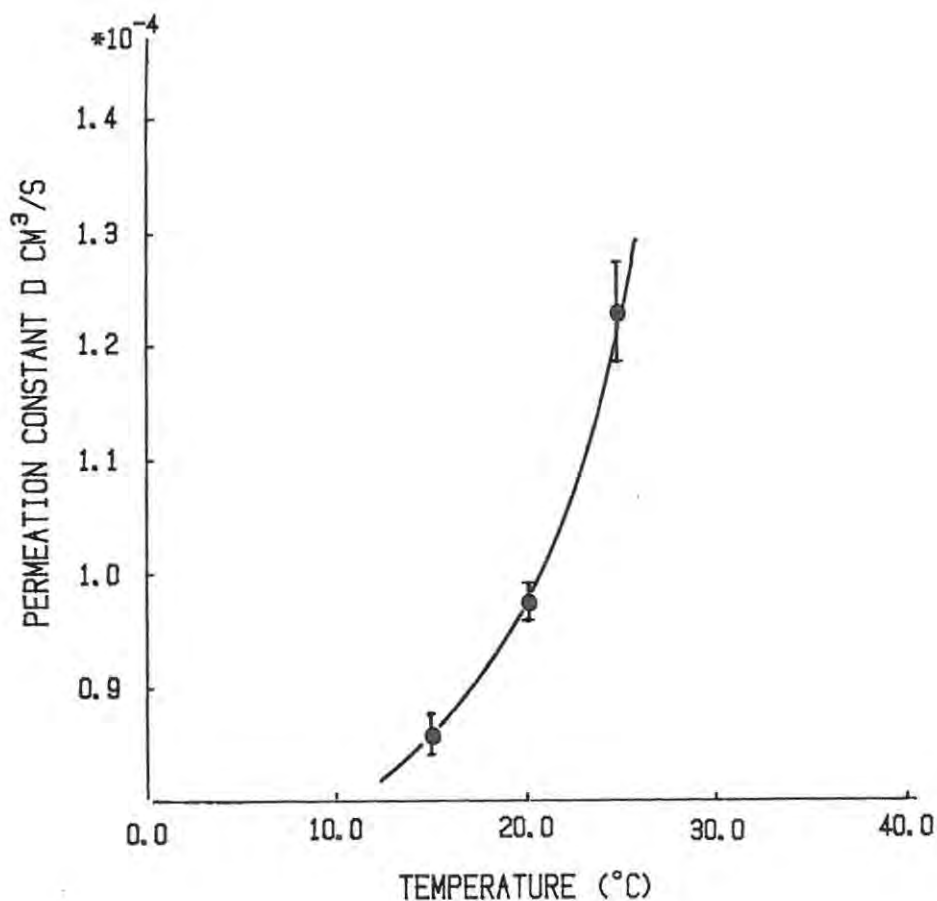
Table 8 -V

Variation with temperature of the permeation constant and diffusion coefficient for phenol red through Visking dialysis membrane

| Temperature | Mean Permeation Constant | Standard Deviation | Diffusion Coefficient |
|-------------|------------------------------|------------------------------|------------------------------|
| °C | $\text{cm}^3 \text{ s}^{-1}$ | $\text{cm}^3 \text{ s}^{-1}$ | $\text{cm}^2 \text{ s}^{-1}$ |
| 15 | 0.903×10^{-4} | 0.009×10^{-4} | 1.14×10^{-7} |
| 20 | 0.980×10^{-4} | 0.006×10^{-4} | 1.24×10^{-7} |
| 25 | 1.311×10^{-4} | 0.007×10^{-4} | 1.64×10^{-7} |

The temperature dependence of the mean permeation constant is depicted in Figure 8.8

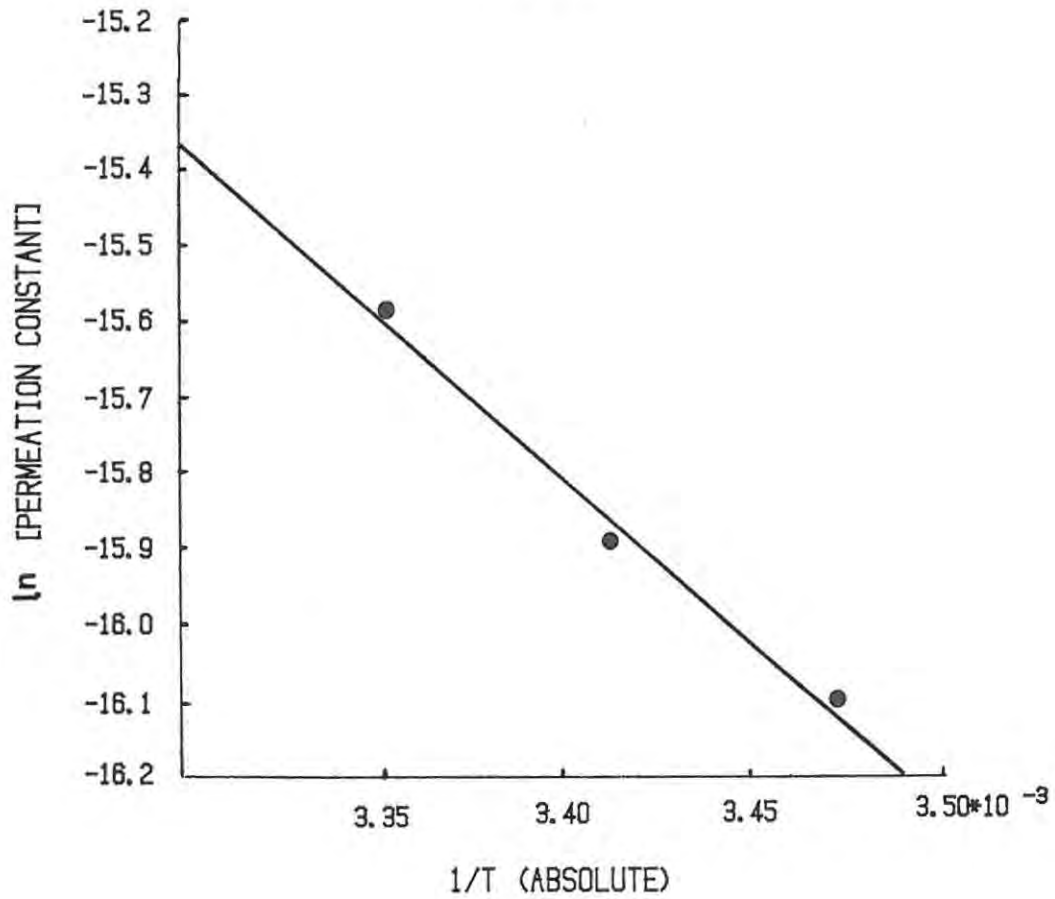
Figure 8.8



The Temperature dependence of the mean permeation constant for phenol red through Visking dialysis membrane

The average rate of change in the value of the mean permeation constant with temperature over the range from 15 to 25 °C is $0.041 \times 10^{-4} \text{ cm}^3 \text{ s}^{-1} \text{ K}^{-1}$, or about 4% per degree. An approximate value for the activation energy of the permeation process, based on the Arrhenius equation, can be obtained from the slope of a plot of the logarithm of the diffusion coefficient vs $1/T$ (Absolute). The log-linear plot of D^* vs $1/T$ (Figure 8.9) is linear, and yields a value of 26 kJ/mol for the activation energy of the diffusion of phenol red through Visking dialysis membrane.

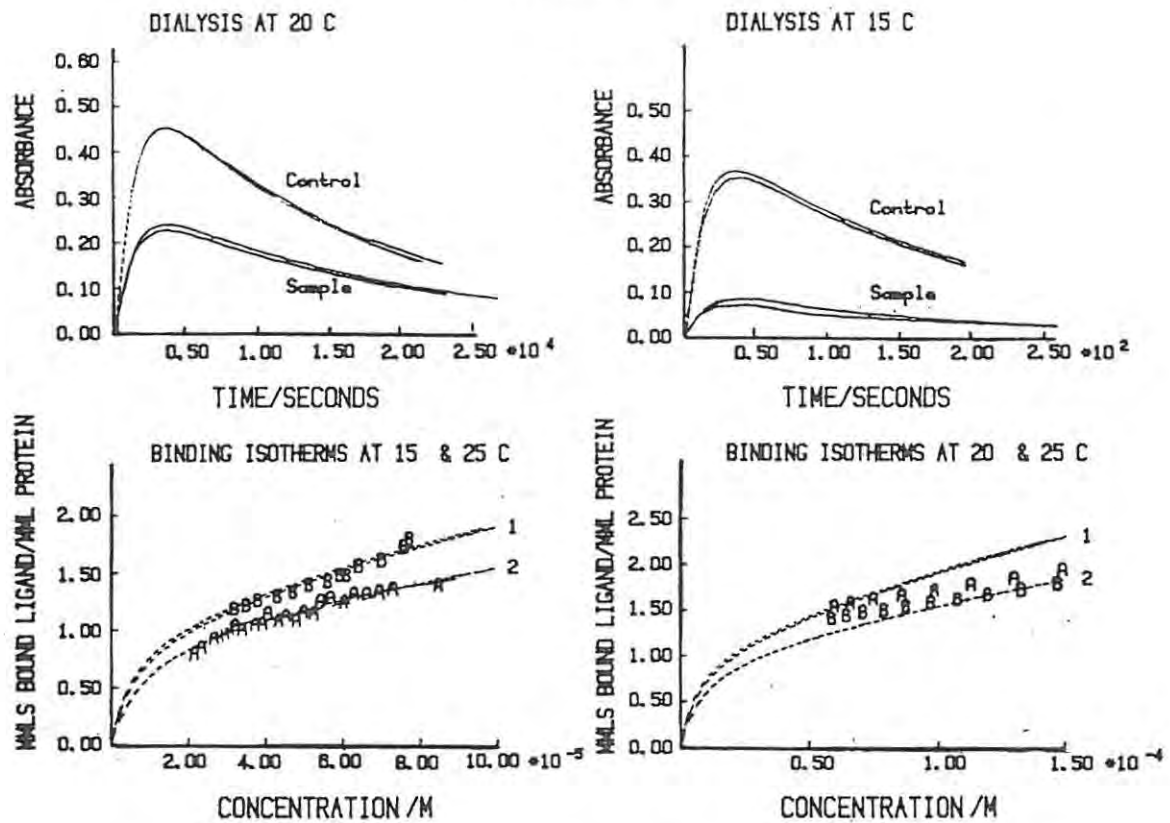
Figure 8.9



Graph of $\ln [D^*]$ vs $1/T$

Duplicate elution profiles and the binding isotherms for the binding of phenol red to BSA at 15 and 20 °C, derived using the appropriate values for the permeation constants, are shown in Figure 8.10. The binding isotherms of Rodkey (1961), Meyer & Guttman (1970), and that obtained in the present study, for the binding of phenol red to BSA at 25 °C, are also shown.

Figure 8.10



Elution profiles and binding isotherms for the phenol red-BSA interaction at 15 and 20 °C

Plotted points

A = Phenol red-BSA binding isotherm at 25 °C } bottom left
 B = Phenol red-BSA binding isotherm at 15 °C }

A = Phenol red-BSA binding isotherm at 20 °C } bottom right
 B = Phenol red-BSA binding isotherm at 25 °C }

- 1 Theoretical isotherm at 25 °C based on Meyer & Guttman parameters
- 2 Theoretical isotherm at 25 °C based on parameters derived by the CFDD method

---oOo---

From a comparison of the isotherms obtained at the lower temperatures with those determined at 25 °C, it can be seen that the effect of temperature on the binding characteristics of BSA for phenol red is negligible over this temperature range. The

sensitivity of the CFDD method to temperature in the case of the phenol red-BSA interaction is thus due to its influence on the diffusion of the ligand rather than on the interaction itself.

8.3 Discussion of Results

A comparison of the phenol red-BSA binding isotherm obtained by the CFDD method with the isotherms of Rodkey, Meyer & Guttman and Kanfer, shows the CFDD method to be valid. In contrast to the isotherms reported by these other investigators, the isotherm obtained by the CFDD method is based on a large number of data points. For example, in experiments of equal duration (about 7 hours) the CFDD method provides nearly a thousand measurements of the ligand concentration as opposed to about 15 measurements provided by the methods of Meyer & Guttman or Kanfer. The availability of a large number of data points means that the derivative of the data over the full data range may be obtained more easily and more reliably by the use of a numerical differentiating routine rather than by graphical methods. This constitutes a major advantage of the method over alternative dialysis methods used to investigate protein-ligand binding. Binding parameters derived by regression analysis from an isotherm defined for a large number of ligand concentrations have obviously a greater precision than the parameters derived from limited data sets.

Values of the permeation constant can be readily computed throughout the course of the control dialysis experiment. The standard deviation of these computed values within a single dialysis experiment, because of the reduced possibility of changes in experimental variables, and because of the large quantity of data, is expected to be small. Thus, changes in the permeation constant over the course of a dialysis experiment can provide a sensitive test for checking the degree of control over experimental variables (for example temperature and eluting buffer flow-rate) throughout the course of the dialysis

experiment.

The plot of D vs t is a sensitive test for the validity of the mass balance because the denominator in the formula used to obtain the value of the permeation constant (equation 5.8.8) represents the time dependent difference in ligand concentration between the sample and sink compartments of the dialysis cell. The difference between the ligand concentrations in the two compartments is given by:

$$C = C_1(0) - [V_2 C_2(t) + F \int_0^t C_2(\tau) d\tau] / V_1 - C_2(t)$$

.... 8.3.1

In this expression, any small discrepancies in this concentration difference due to change in experimental conditions, (i.e., filming of the membrane) will accumulate in the integral term, producing a rise or fall in D with time.

A computer generated plot of the permeation constant D as a function of time over the course of the dialysis, can thus be used to show that experimental variables such temperature or the eluting buffer flow rate are constant over the course of a dialysis experiment. Fluctuations in the value of D with time indicate inadequate temperature control or a change in the eluting buffer flow rate. Such plots showed, during the development of the CFDD method, that the use of a Marriot flask and gravity feed to maintain a constant flow of eluting buffer was not satisfactory and that it is necessary to use a peristaltic pump for reliable results.

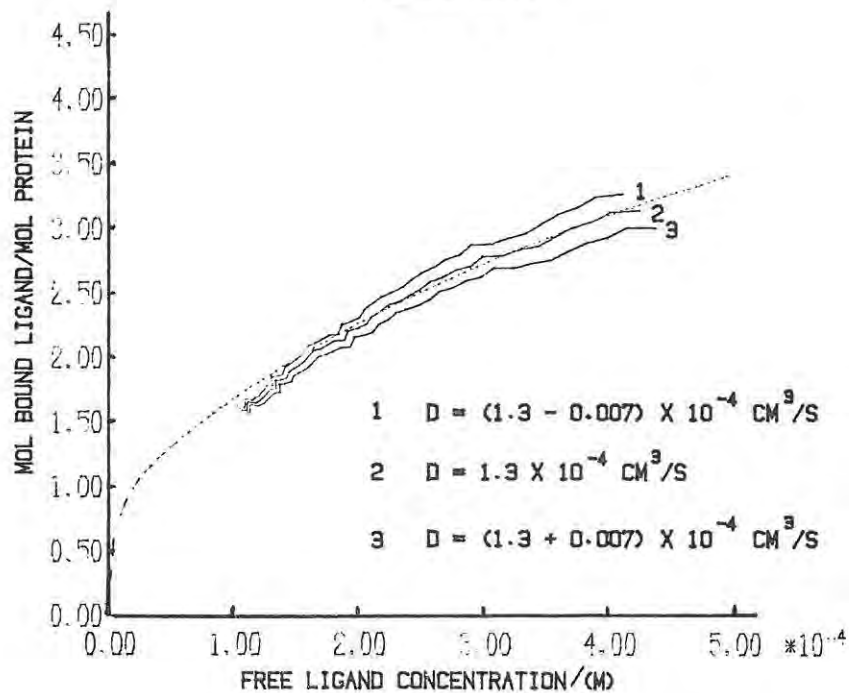
A continuous fall in the value of D with time could indicate binding of the ligand to the membrane or filming of the membrane by protein or protein-ligand complex. The plot of D as a function of time is a conveniently obtained diagnostic, and is a more sensitive test to indicate binding of the ligand to the dialysis membrane or filming by protein than the method adopted by Meyer & Guttman (1970) or Kanfer (1976).

Uncertainties in the measured value of the permeation constant provide the largest possibility for errors or inaccuracy in binding parameters obtained by dynamic dialysis methods. In the CFDD method, because this quantity is used in both of the parametric equations of the isotherm (equations 5.8.6 and 5.8.7), uncertainties in the value of D will produce uncertainties in both the abscissa and ordinate of the isotherm.

As has been noted, the accuracy of the method also depends on the ability to reproduce exactly the experimental conditions such as temperature, eluting buffer flow rate, etc. It is difficult to formulate a general measure for the specific or combined influence of these experimental errors on the binding isotherm. Experimental errors in these parameters affect the isotherm directly and also indirectly through their effect on the value of the permeation constant. In order to obtain an overall measure of the uncertainty in the phenol red-BSA binding isotherm, the isotherm was derived from the elution profile data using the measured value for the permeation constant, D , as well as for $D \pm$ the standard deviation. These limiting isotherms, which represent a measure of the uncertainties due to experimental error, are shown in Figure 8.11

Temperature fluctuation appears to be the most significant factor influencing reproducibility of the binding isotherm. However, from the observation that the isotherms at 15 and 20 °C coincide within the accuracy of the method to the 25 °C isotherm, it would appear that temperature sensitivity in this case must be attributed to the temperature effect on ligand diffusion rather than to changes in the binding characteristics of the protein. The observation that phenol red-BSA binding is not markedly susceptible to temperature change confirms the conclusion (Steinhardt & Reynolds, 1969), that enthalpy changes associated with BSA-ligand interactions are small, unless there were opposite influences at work on diffusion and complexation, which is most unlikely.

Figure 8.11



Uncertainty in the phenol red-BSA binding isotherm at 25 °C

The permeation constant analysis, although providing a binding isotherm and binding parameters which are consistent with those of other investigators, does not take into account the hold-up of ligand in the dialysis membrane. In this respect the method is no different from any other dynamic dialysis method so far reported. However, the initial transient phase during which the permeation constant has not yet attained a constant value (shown in figure 8.2) represents the time required for the ligand to develop a linear concentration gradient across the dialysis membrane. The occurrence of the transient phase means that some of the data of the dialysis experiment has to be discarded when using the permeation constant method of analysis. The first hundred or so observations of the elution profiles (both to establish the permeation constant and the binding isotherm), are included only in the calculation of the integral expression

$$\int_0^t c_2(t) dt \quad \text{used in equations 5.8.6, 5.8.7 and 5.8.8.}$$

These initial data points are not used to assess the mean value of the permeation constant nor for the computation of the binding isotherm. The computer routine to evaluate the permeation constant and binding isotherm was programmed to disregard the elution profile data (except for evaluation of the integrals by Simpson's rule) until the profile had attained its maximum value.

A more complete analysis would account for the hold-up of ligand in the membrane. An attempt was made to estimate the extent of hold-up of ligand in the membrane using Fick's second Law of diffusion with constant boundary conditions (Barnes, 1934; Barry et al., 1975; and Hoogervorst, 1978). It can be shown that the time dependent distribution of ligand across a semi-infinite membrane is given by:

$$N^*(x,t) = [N_0 / (A \pi D^* t)^{1/2}] \exp(-x^2 / 4D^* t) \quad \dots \quad 8.3.2$$

where N_0 is the number of molecules concentrated on the surface of the membrane, A is the surface area of the membrane and D^* the diffusion coefficient of the ligand in the membrane. An estimate for $N(d, 1800)$ where d is the membrane thickness, was obtained using equation 8.3.2, by assigning a value of $t = 1800s$, corresponding to attainment of steady state conditions, and a value to N_0 which corresponds to the amount of ligand in the sample compartment. The value assigned to D^* was the approximate value obtained from the control elution profile. With these values, equation 8.3.1 yields a value of 1% for the ratio $N^*V / (2N_0)$ where V is the volume of the membrane and the factor 2 allows for a linear concentration gradient within the membrane.

The estimated value of 1% is high, although no worse than the experimental error in the estimation of the permeation constant (2%). The value of 1% probably represents a gross overestimate. The initial transient phase also contains errors arising from the numerical methods used in the data processing. These errors are most significant when the the numerical methods are applied to small data sets.

Chapter Nine

Results: Evaluation of the CFDD method using the Transfer Function Analysis.

9.1 The Dialysis Cell as a Linear System

The transfer function analysis depends on the assumption that the dialysis cell represents a linear system. If the dialysis cell is a linear system, the sink compartment ligand concentrations for a series of dialysis experiments in which all the experimental conditions, except the initial ligand concentrations, are kept constant will be proportional to the initial ligand concentrations at corresponding points in time. The log-linear plots of the elution profiles ($\log[C_2(t)]$ vs t) should be linear and parallel after the profiles have attained their maximum values. The displacements of the parallel portions of these curves from each other should also represent the logarithm of the ratio of the initial ligand concentrations.

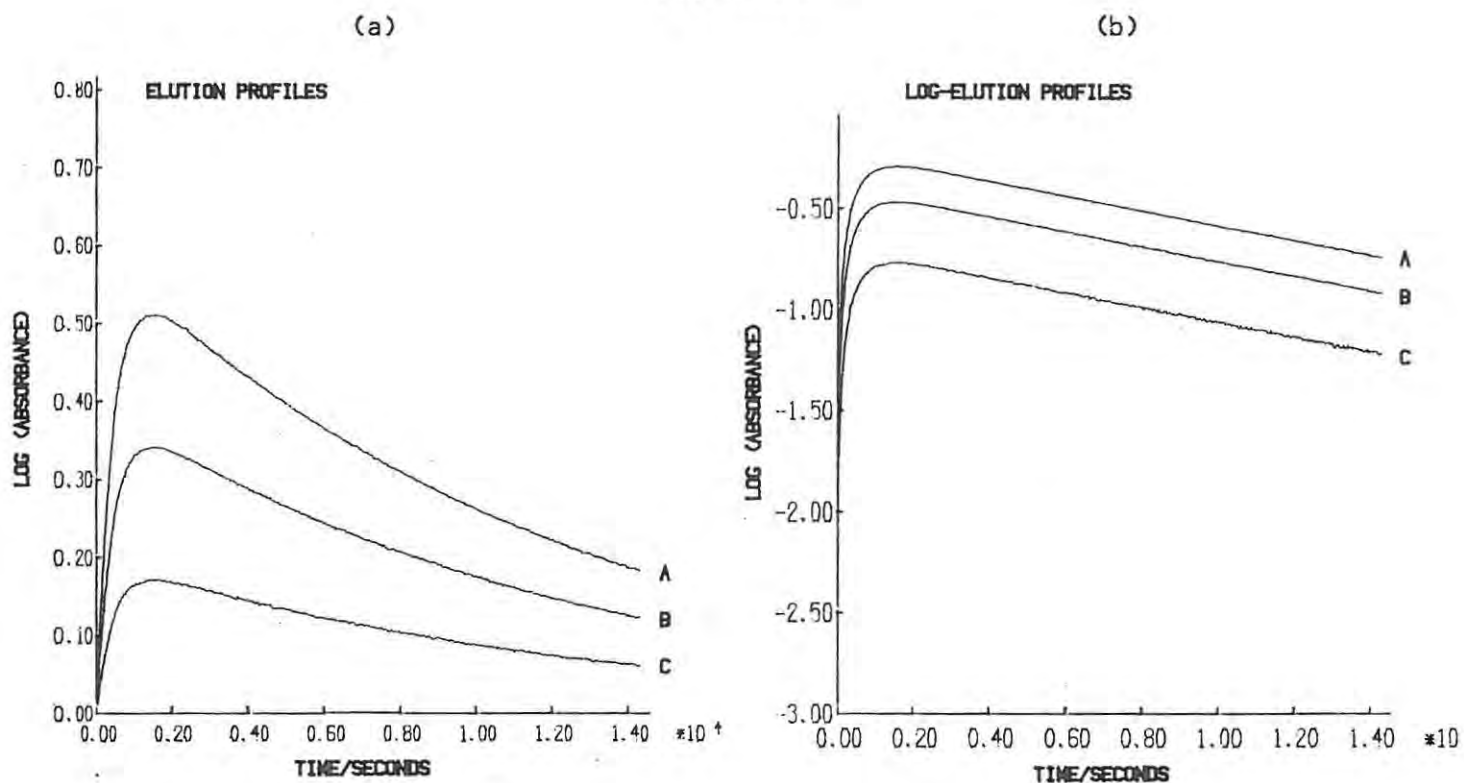
Elution profiles for the dialysis of 1.5 ml samples of phenol red solutions with different initial concentrations, dialysed and eluted under identical conditions are shown in Figure 9.1a. The log-linear plots of these elution profiles are shown in Figure 9.1b. It can be seen from these plots the the assumption that the dialysis cell is a linear system is acceptable.

A Evaluation of the Method Using Hypothetical Data Sets

9.2 Generation of Hypothetical Data Sets

Hypothetical elution profile data sets to simulate actual dialysis experiments were used for the initial evaluation of the transfer function method of analysis. This artificial procedure removes the contributions to the data from experimental errors and provides a means of examining how the controlled adjustment of the various parameters used in the analysis affects the accuracy and reliability of the method.

Figure 9.1



Elution profiles and Log-linear plots of the elution profiles to demonstrate the linearity of the dialysis cell.

Phenol red ligand concentrations were monitored at $\lambda = 269 \text{ nm}$ for which the extinction coefficient was 10800 M^{-1} with an eluting buffer flow rate of $1.5 \times 10^{-3} \text{ cm}^3/\text{s}$. Phenol red concentrations were:
 (a) 1.5×10^{-4} (b) 1.0×10^{-4} (c) $0.5 \times 10^{-4} \text{ M}$

The displacements of the curves (a) and (b) from the curve (c) at $t = 0.80 \times 10^4$ seconds are 0.17 and 0.30, which represent the logarithms of the ratios of the respective initial ligand concentrations to the initial ligand concentration used in curve (c) (3:1 & 2:1 respectively).

---o0o---

Data sets representing the control and sample elution profiles were generated by the numerical solution of the differential equations for the two-compartment dialysis cell (equations 5.3.1a & 5.3.1b for the control and equations 5.5.2 and 5.3.1b for the sample dialyses) using Euler or Runge-Kutta methods. The sample dialysis elution profiles were made to simulate phenol red-BSA binding by incorporating the Scatchard two-site binding model (equation 5.10.1) into equation 5.5.2. The binding parameters incorporated into the model were those of Rodkey (1961). The numerical solution of the differential equations was achieved using the FORTRAN routine ETA. A listing of this computer routine, which can be adapted for a variety of binding models, is given in appendix IX.

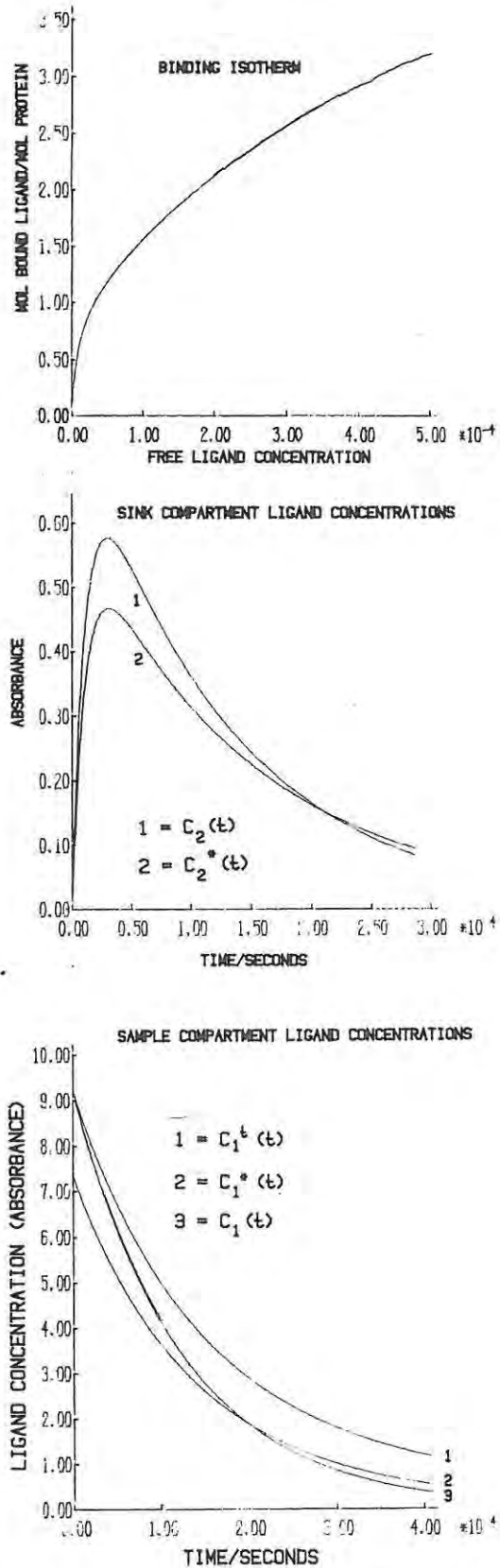
9.3 The use of the Fast Fourier Transform to evaluate the System Transfer Function

Hypothetical elution profiles were generated using a value of 5.0×10^{-4} M for the initial ligand concentration, 3.5×10^{-6} M for the protein concentration, and 1.5×10^{-3} cm³/s for the eluting buffer flow rate. A value of 18400 was used for the ligand extinction coefficient and an experimentally determined value of 1.31×10^{-4} cm³/s was assigned to D , the ligand permeation constant. The Rodkey binding parameters used in the binding model were:

$$\begin{aligned} n_1 &= 1; & k_1 &= 1.1 \times 10^5 \text{ litre/mol} \\ n_2 &= 6; & k_2 &= 1.2 \times 10^3 \text{ litre/mol} \end{aligned}$$

The graphs of the theoretical isotherm generated from the Rodkey binding parameters and the hypothetical sink compartment and sample compartment ligand concentrations are shown in Figure 9.2. Initially, the hypothetical elution profiles were generated for a time interval sufficiently long that the absorbance value representing the sink compartment ligand concentration attained a near zero value ($C_2(t) < 0.005$).

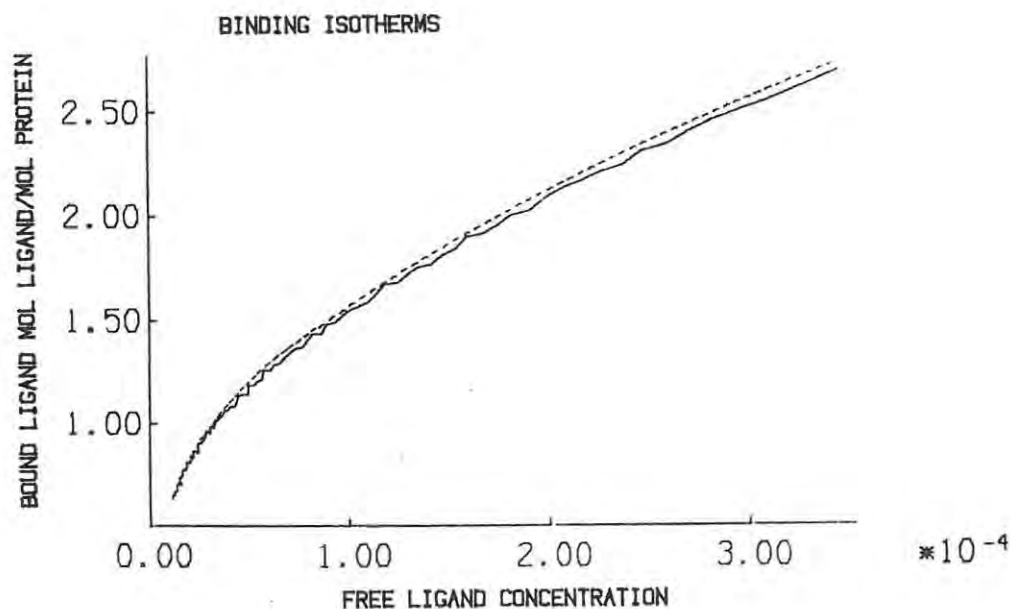
Figure 9.2



Theoretical data sets used to evaluate the transfer function
method of data analysis

These data sets were used to evaluate the system transfer function by forming the ratio of the Fourier transforms of the sink and sample compartment ligand concentrations for the control data set. Deconvolution of the impulse response function from the sample dialysis profile was achieved by division of the Fourier transform of the sample elution profile by the transfer function followed by the inverse Fourier transformation of this quotient. The transforms from the time domain to the frequency domain, and the inverse transformations from frequency to time domains were effected by means of the Cooley-Tukey Fast Fourier Transform algorithm (FFT). The binding isotherm which was obtained from this hypothetical data by deconvolution of the impulse response function from the elution profile $C_2^*(t)$ is shown in Figure 9.3

Figure 9.3

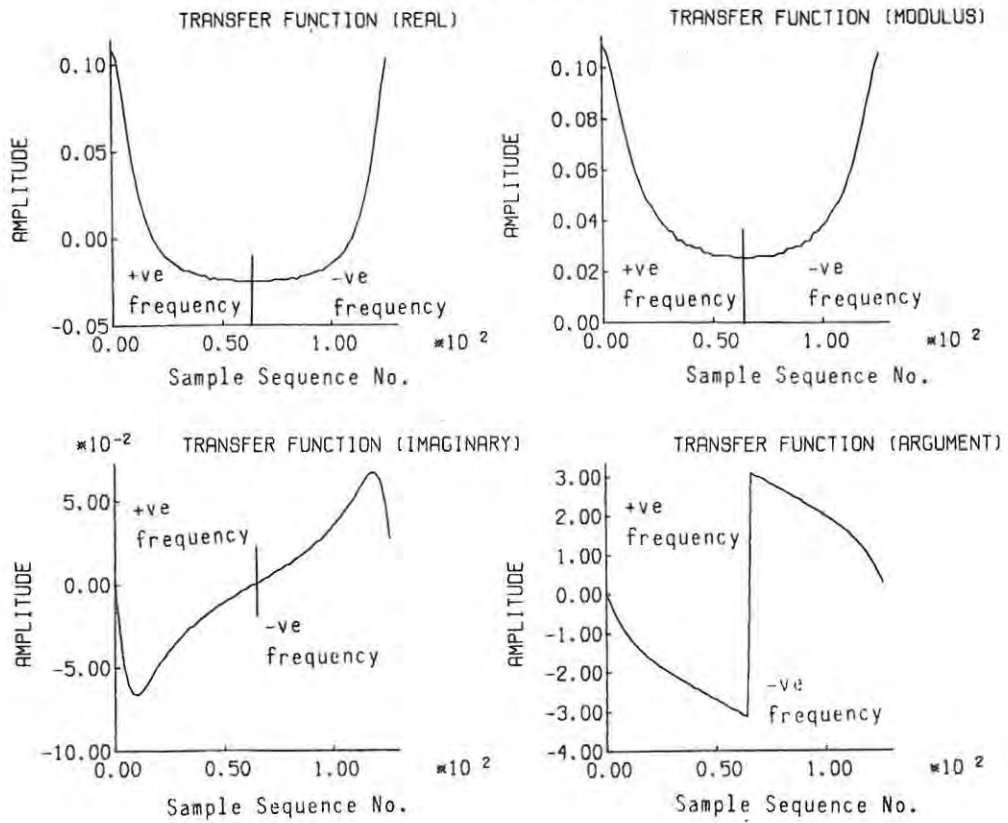


The phenol red-BSA binding isotherm obtained using the FFT algorithm to obtain the dialysis cell system transfer function

- (...) Theoretical binding isotherm based on Rodkey binding parameters (Rodkey, 1961)
- (---) Isotherm produced using the transfer function derived through the FFT.

The transfer function used to effect the deconvolution is shown in figure 9.4

Figure 9.4



System transfer function for phenol red dialysis derived by the FFT

The graphs are presented with the transfer function components in the sequence generated by the FFT. The horizontal axes have to be re-arranged to show the data in frequency order (Brigham, 1974).

---o0o---

As can be seen from the isotherms shown in Figure 9.3, apart from noise, the isotherm extracted from the elution profiles is a fair approximation to the theoretical isotherm. However, because practical considerations necessitate truncation of the dialysis before complete elution of the ligand, the analysis was repeated using the same elution profiles which were truncated when the absorbance signal was about 20% or more of the elution profile maximum. When the FFT algorithm was used with these truncated data sets, the results were unsatisfactory. In such situations, the discrete FFT approximation to the continuous Fourier transform is unsatisfactory because of 'leakage' and aliasing errors (Brigham, 1974; Kelly and Horlick, 1973). Such errors arise because the elution profiles are not time-limited functions. Although aliasing errors could be reduced by decreasing the sampling time interval to very small values relative to the duration of the dialysis, this requires large quantities of data in the elution profile data sets and this considerably increases the computer requirements for data processing.

Attempts to reduce the leakage errors by zero-filling the elution profile data sets (Horlick & Yuen, 1976; O'Halloran & Smith, 1978; and Comisarow & Melka, 1979) and by the use of window functions (Harris, 1978) to remove the discontinuity at the point of truncation, proved to be unsatisfactory. A method depending on the linear properties of the the Fourier transform (Bracewell, 1976) was also tested. This consisted of subtracting an analytical function (in this case, a biexponential function) from the elution profile to remove the discontinuity at the point of truncation. In this procedure, the subtraction of the biexponential function is finally reversed by adding the analytical transform of the subtracted function back to the transform of the difference elution profile, obtained using the FFT. This method also did not give satisfactory results. The technique probably fails because the difference function, obtained by subtracting the analytical function from the elution

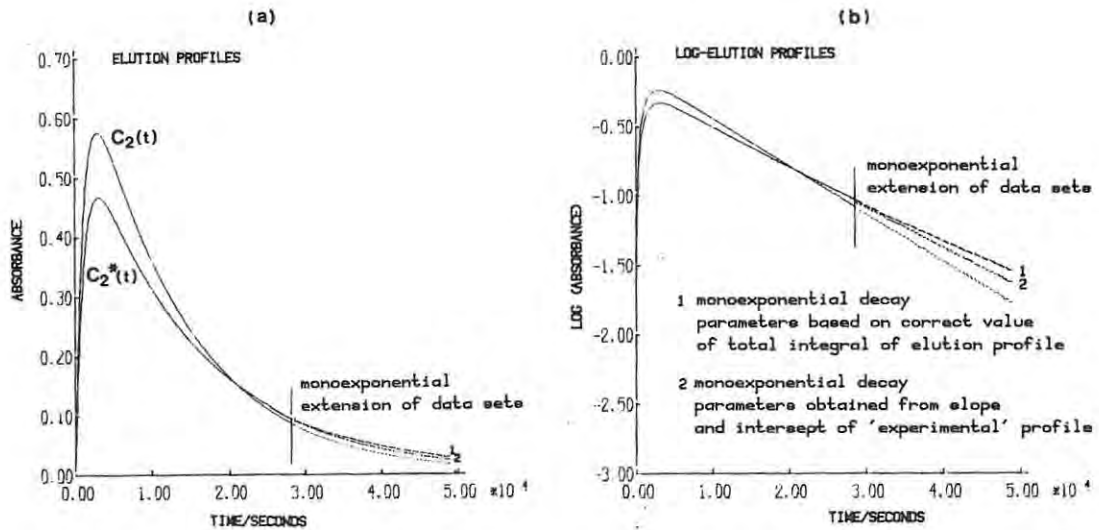
profile, tends to be small over the entire data set. The Fourier transform of such data sets consists of a number of very large low frequency components and many small high frequency components (Campbell & Foster, 1948). This means that the ratio of the transforms of elution profiles and ligand escape curve, although corrected to remove the discontinuities, is still considerably distorted.

Recently, a new FFT algorithm has been presented (Schutte, 1981) which, although still having the FFT characteristics, is no longer confined to band-limited functions. This may provide an alternative approach to solving the "leakage" problem. However, the application of this algorithm to obtain the Fourier transform was not attempted in this case. Instead, the procedure using Laplace transforms of data sets which are 'hypothetically' extended, was adopted to overcome the problems associated with truncated data sets.

9.4 Use of Laplace Transforms to obtain the Transfer Function

The analysis which uses the Laplace transforms of the data, and in which the data sets are extended by mono-exponential decay functions, gives satisfactory results. The hypothetical elution profiles for a phenol red-BSA system, shown in Figure 9.2 are truncated after 40960 seconds. At the point of truncation, the profiles $C_2(t)$ and $C_2^*(t)$ have the values 0.091 and 0.100 respectively (15.6% & 21.4 % of the respective elution profile maxima). The amplitude and exponent parameters for the mono-exponential decay functions, which were obtained from the log-linear plots of the profiles shown in Figure 9.5 are $A_1 = 0.7822$ and $b_1 = 0.7732 \times 10^{-4}$ for the control $C_2(t)$ and $A_2 = 0.6036$ and $b_2 = 0.6599 \times 10^{-4}$ for the sample $C_2^*(t)$. The extended elution profiles and linear-log plots of the extended profiles are also shown in figure 9.5.

Figure 9.5



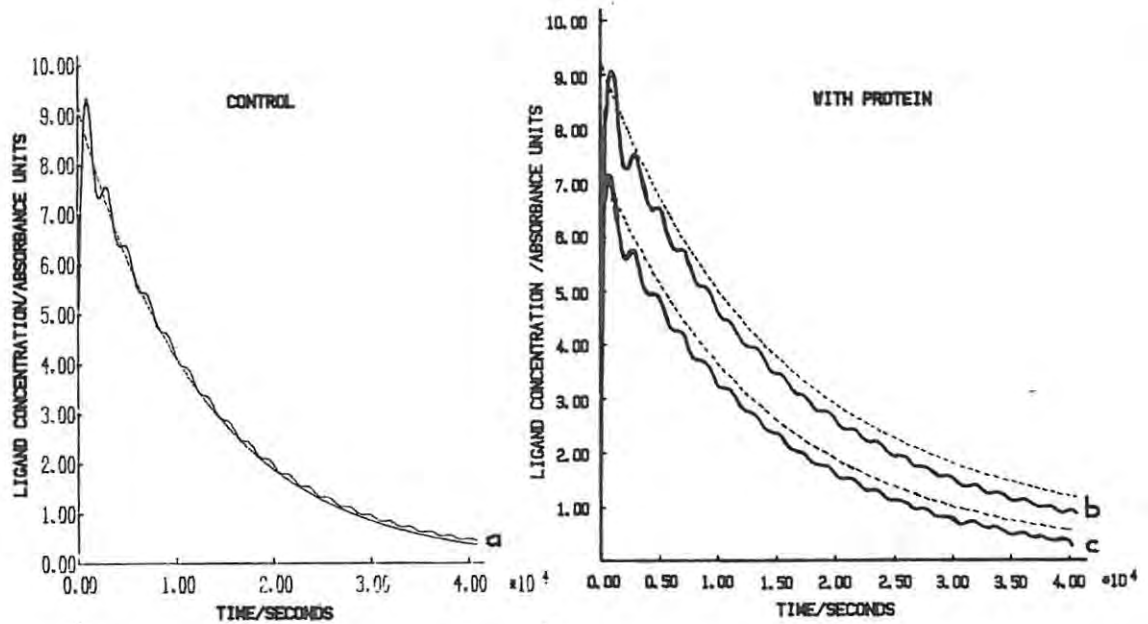
a) elution profiles of an hypothetical phenol red-BSA system, extended by means of mono-exponential decay functions profile.

b) log-linear plots of the extended data sets

The elution profiles are extended by means of mono-exponential decay functions over a period of five times the assumed duration of the dialysis.

The sample compartment ligand concentrations regenerated from the elution profiles by means of the transfer function for both the control and sample dialyses are shown in Figure 9.6. These curves are shown superimposed onto the curves obtained for the sample compartment ligand concentrations obtained by the numerical solution of the system differential equations.

Figure 9.6



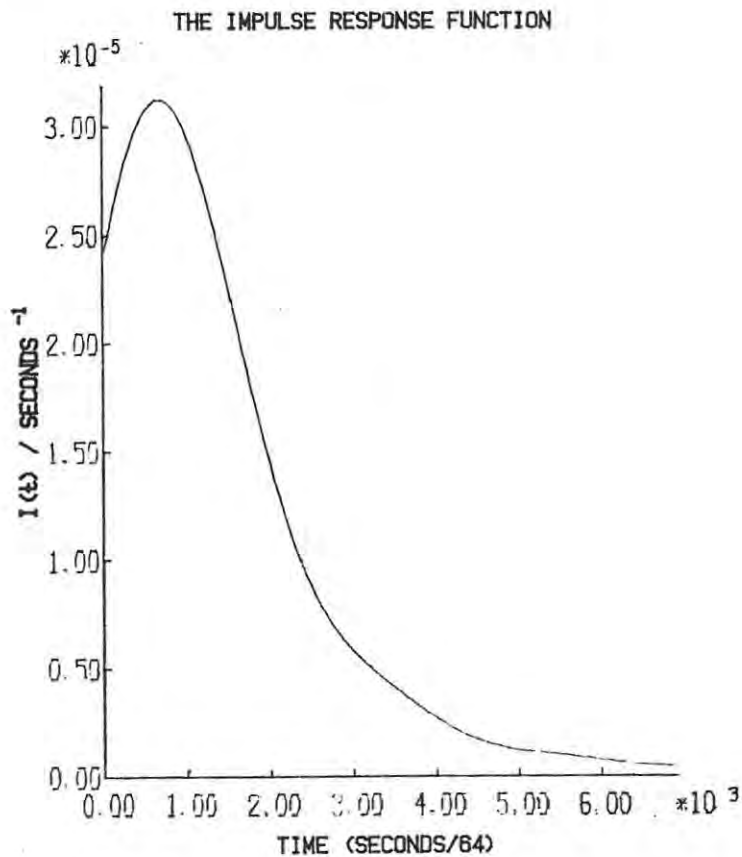
Sample compartment ligand concentrations derived from the hypothetical elution profiles shown in figure 9.5

- (a) Total ligand concentration, including ligand bound to protein;
- (b) Ligand concentration in control experiment;
- (c) Free ligand concentration in presence of protein.

---o0o---

The impulse response function of the dialysis cell, generated from the Fourier coefficients A_n and B_n (equation 6.8.1) is shown in Figure 9.7. In the calculations used to obtain the results shown in Figure 9.6 and 9.7 the Fourier series were summed over 100 terms. In the computation to derive the sample compartment ligand concentrations from the elution profiles (shown in figure 9.6) by the transfer function method, no attempt has been made to remove the oscillations due to the Gibbs phenomenon.

Figure 9.7



The impulse response function of the phenol red-BSA dialysis

It can be seen that, apart from the oscillations, the steep rise from the origin, and the 'overshoot' in the neighbourhood of $t = 0$, the agreement between the curves for the control dialysis is very good. The curves representing the total and free ligand concentrations which are computed from the sample dialysis elution profile by the transfer function although parallel to the theoretical curves, are displaced below them. This indicates that the first (or zero frequency) terms in the Fourier series representation of these functions (equations 6.9.4 & 6.10.5) are too small because of errors in the assessment of the areas under the elution profiles.

The zero frequency terms, Q_0^t and Q_0^* , are constants, and are measures of the integrals of $C_1^t(t)$ and $C_1^*(t)$ over the extended data set. The observation, that the zero frequency

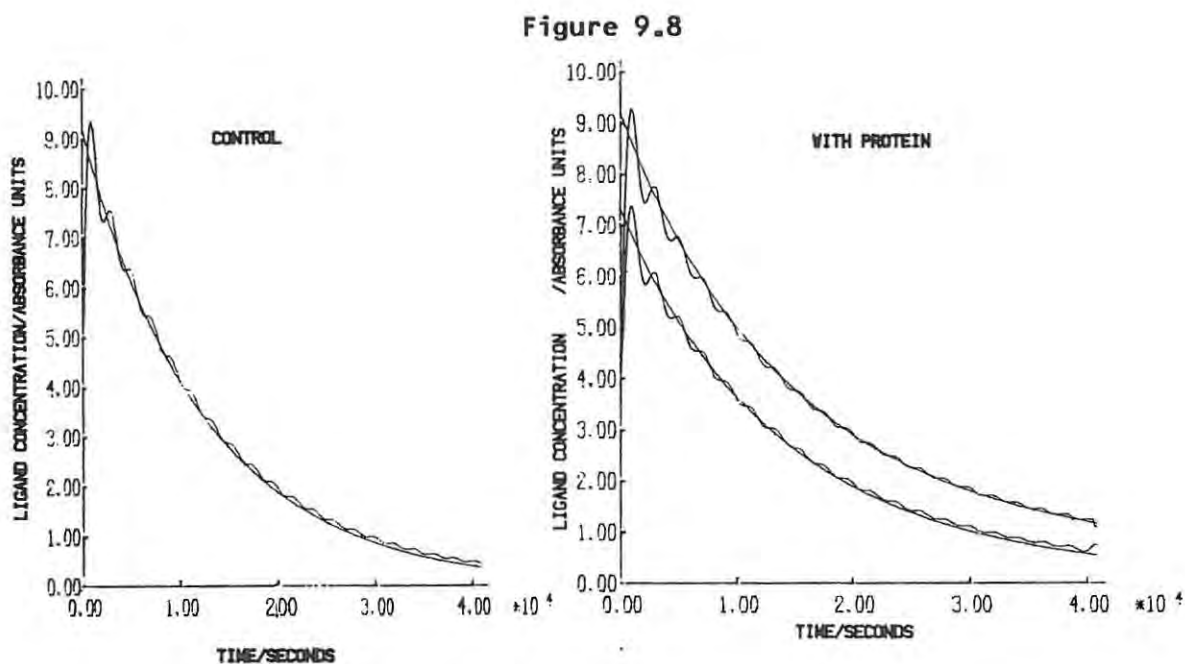
terms are too small only in the case of the sample dialysis and not the control, implies that the assumption of a mono-exponential decay for the extended data set of the sample dialysis may not be valid.

If the zero frequency terms Q_0^t and Q_0^* are corrected by selecting the parameters A_2 and b_2 for the mono-exponential decay of the extended sample profile data set such that the integral, I , is forced to yield the correct area according to mass-balance considerations:

$$I = \int_0^{2T} C_2^*(t) dt + \int_{2T}^{2T} A_2 e^{-bt} dt = V_1 C_1(0) / F$$

.... 9.4.1

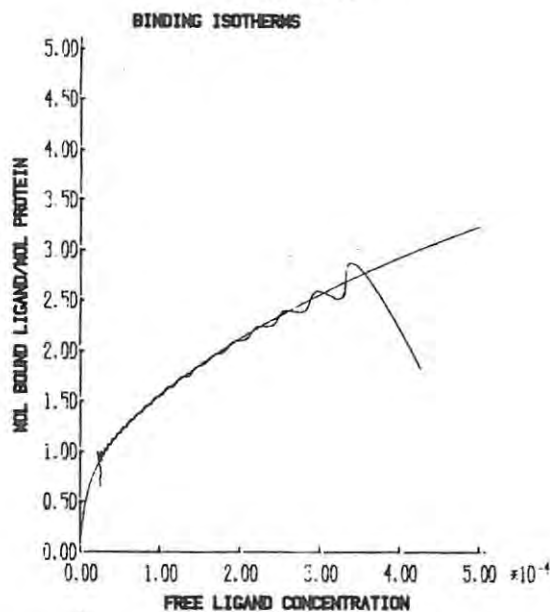
(equation A.III.16), then the agreement is considerably improved. The values of the parameters A_2 and b_2 which satisfy equation 9.4.1 are $A_2 = 0.6091$ and $b_2 = 0.5655 \times 10^{-4}$. (Compared with values $A_2 = 0.6036$ and $b_2 = 0.6599 \times 10^{-4}$, determined from the slope and extrapolated intercept of the linear portion or the log-linear plot of the elution profile.) The sample compartment ligand concentrations derived from the sample elution profile using these values for the parameters A_2 and b_2 are shown in Figure 9.8. The isotherm obtained by subtracting $C_1^*(t)$ from $C_1^t(t)$, shown in figure 9.8, at corresponding points in time, is shown in figure 9.9. The ripples in the isotherm are due to the Gibbs phenomenon.



Sample compartment ligand concentrations

Graphs of the sample compartment ligand concentrations derived from the sample elution profile, using the corrected parameters for mono-exponential decay expression of the extended data set. The oscillations in the curves are due to the Gibbs phenomenon.

Figure 9.9



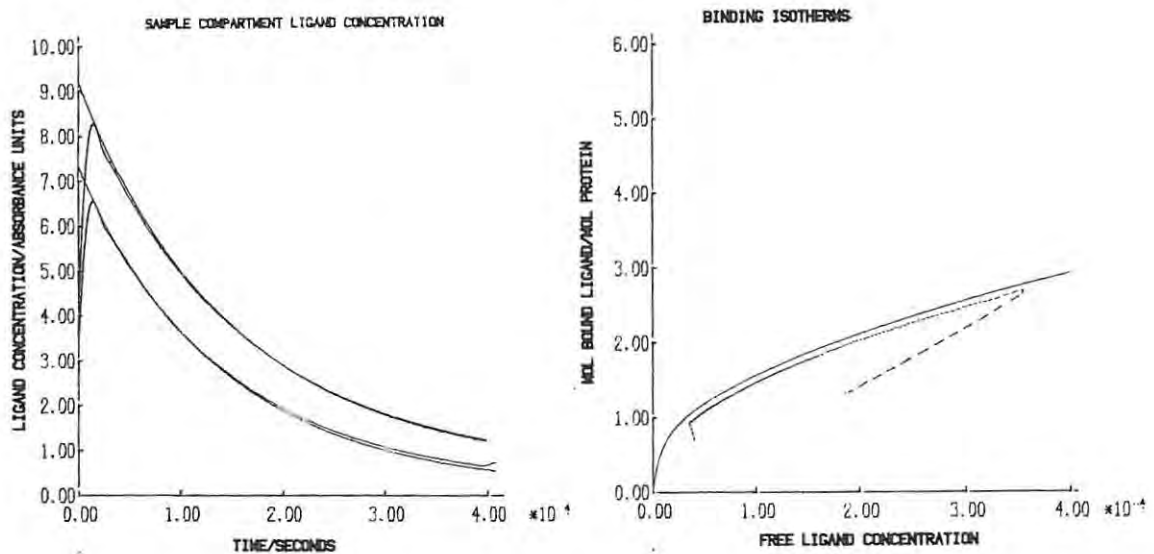
The phenol red-BSA binding isotherm re-extracted from the elution profile data sets by the transfer function method (Data not smoothed)

9.5 The Removal of Oscillations arising from the Gibbs Phenomenon

Although the successive terms in the Fourier series will converge to zero because the functions represented by Fourier series satisfy the Dirichlet conditions, the convergence is slow. The effectiveness of the Lanczos σ factors to effect a smoothing of curves obtained by summation of their Fourier Series is shown in figure 9.10

The more effective Krylov technique for smoothing the data, (Appendix IV) speeds up the convergence of the terms in the Fourier sums and simultaneously eliminates the initial step rise and overshoot of $C_1^*(t)$ and $C_1^t(t)$ in the neighbourhood of $t = 0$. The efficacy of this technique in removing the Gibbs phenomenon effects is shown in Figure 9.11

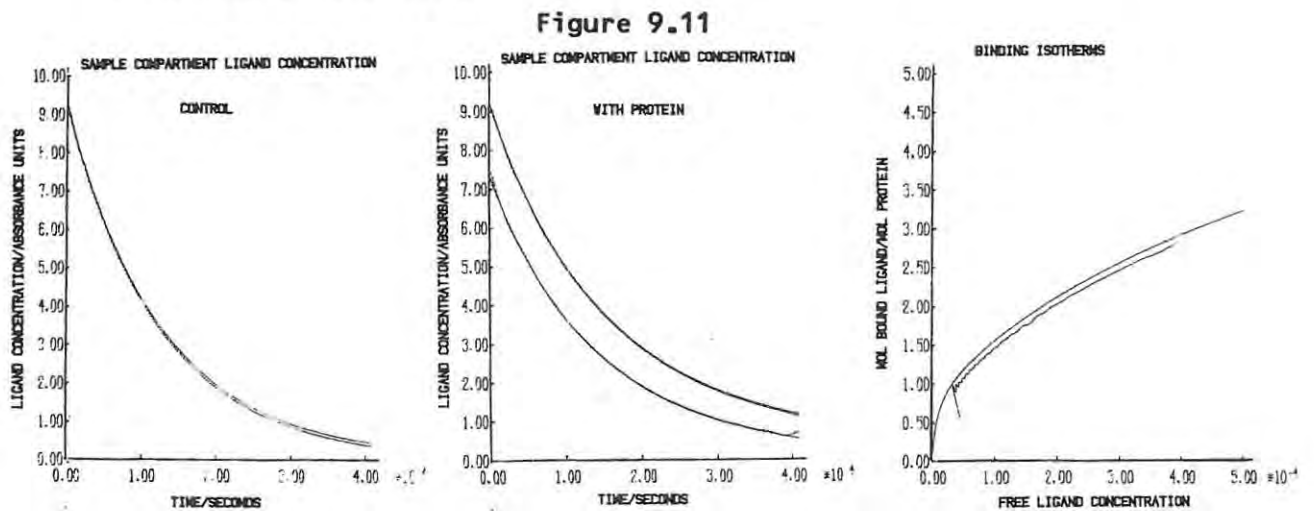
Figure 9.10



The effectiveness of the Lanczos σ factors in smoothing the sample compartment ligand concentration curves and the binding isotherm

The Krylov technique, involving the subtraction of a ramp function from a function and adding its analytical transform to the transform of the function, removes both the oscillations and

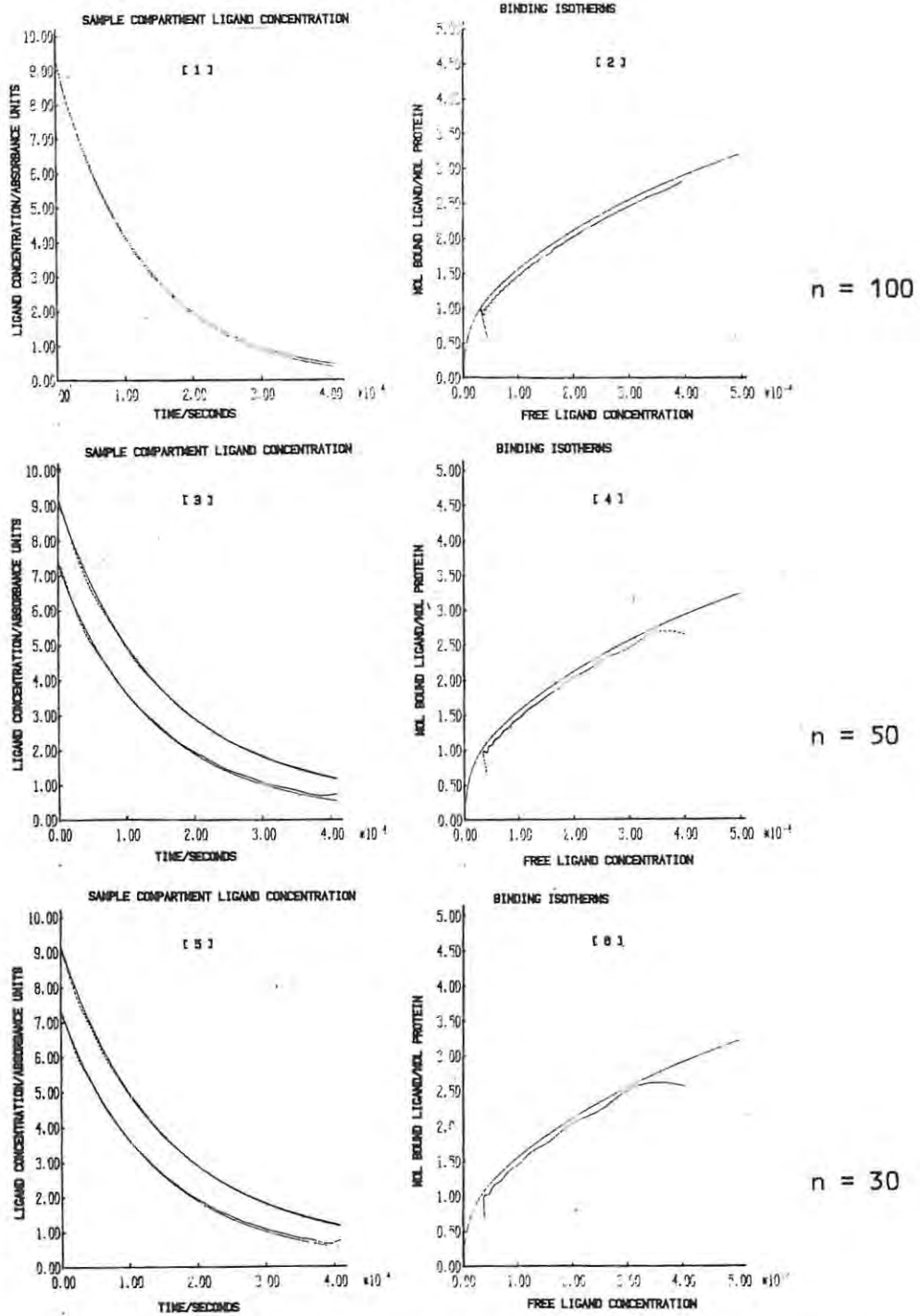
the initial steep rise in the $C_1^t(t)$ vs t and $C_1^*(t)$ vs t curves (Appendix IV). It can be seen in figure 9.11 that the regenerated isotherm although parallel to the theoretical isotherm is displaced slightly. This is probably the result of the small numerical discrepancies between the analytical or correct curves ($C_1(t)$, $C_1^t(t)$ and $C_1^*(t)$) and the curves derived using the transfer function. These small discrepancies are magnified in the conversion of the results from absorbance units to concentration units. Thus, the magnitude of this displacement will be related to the magnitude of the molar extinction coefficient of the ligand. It is noted that the remaining discrepancy lies within the 2% error of the experimental procedure.



The effectiveness of the Krylov ramp subtraction technique in smoothing the sample compartment ligand concentration curves and the binding isotherm

The effect of using different numbers of terms in the Fourier series summation is shown in figure 9.12. The graphs of the total and free sample compartment ligand concentrations with time, and the phenol red-BSA binding isotherm calculated using 30, 50 and 100 terms in the Fourier summations, are shown.

Figure 9.12



The effect of increasing the number of terms in the Fourier series on the sample compartment ligand concentration and binding isotherm

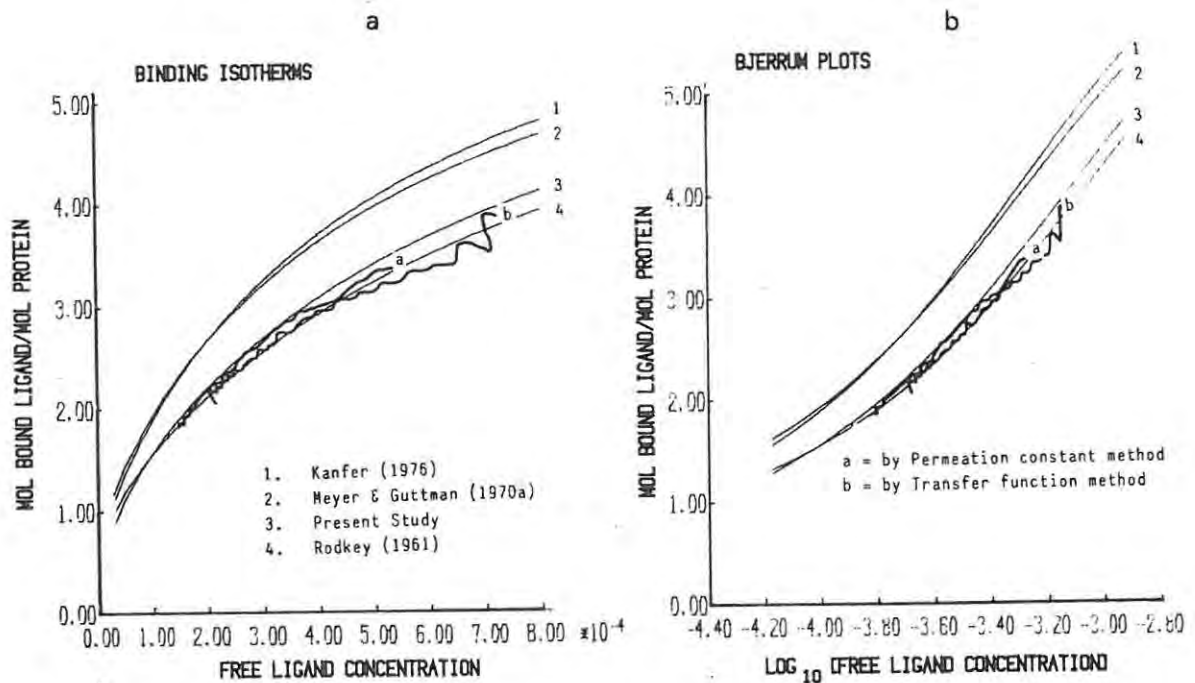
The effect of changing the value of the Laplace convergence parameter on the shape of the sample compartment ligand concentration curves and the binding isotherm is shown in figure 9.14

B Application of the Transfer Function Analysis to Experimentally Determined Elution Profile Data

9.6 Phenol Red-BSA Binding Studies at 25 °C

The results of the application of the transfer function method of analysis to experimentally determined data is shown in Figures 9.13a and 9.13b.

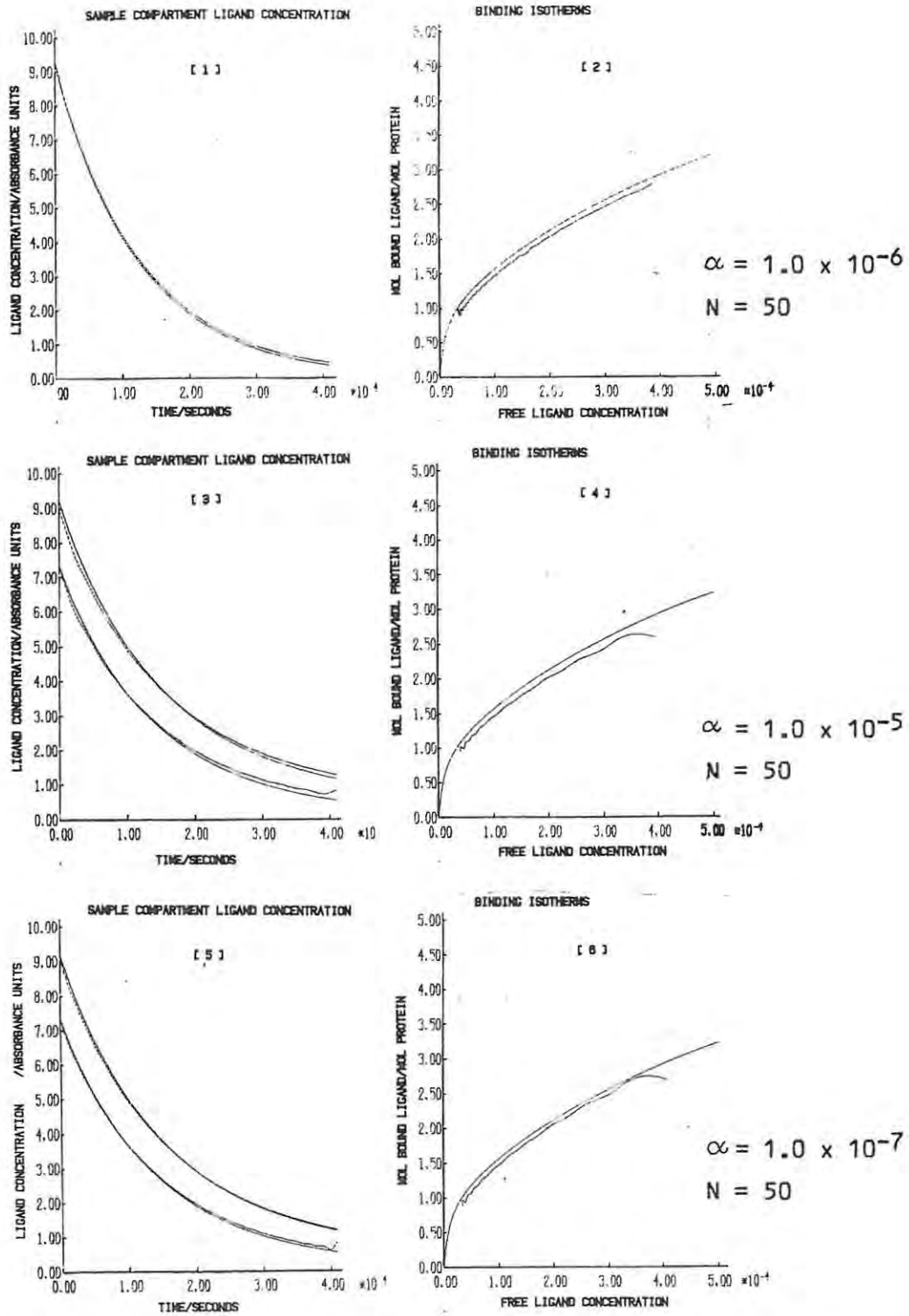
Figure 9.13



Comparison of the binding isotherms derived from experimentally obtained data sets by the permeation constant and transfer function methods

The experimentally determined elution profile shown in Figure 8.1 (experiment 1) was subjected to the transfer function method of analysis. The experimentally determined data sets obviously contain more signal noise than the hypothetical data sets.

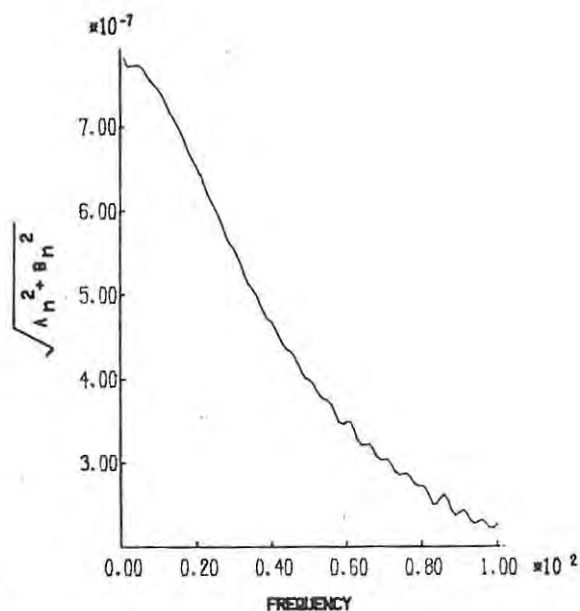
Figure 9.14



The Influence of the Laplace convergence parameter on the sample compartment ligand concentrations and the binding isotherm.

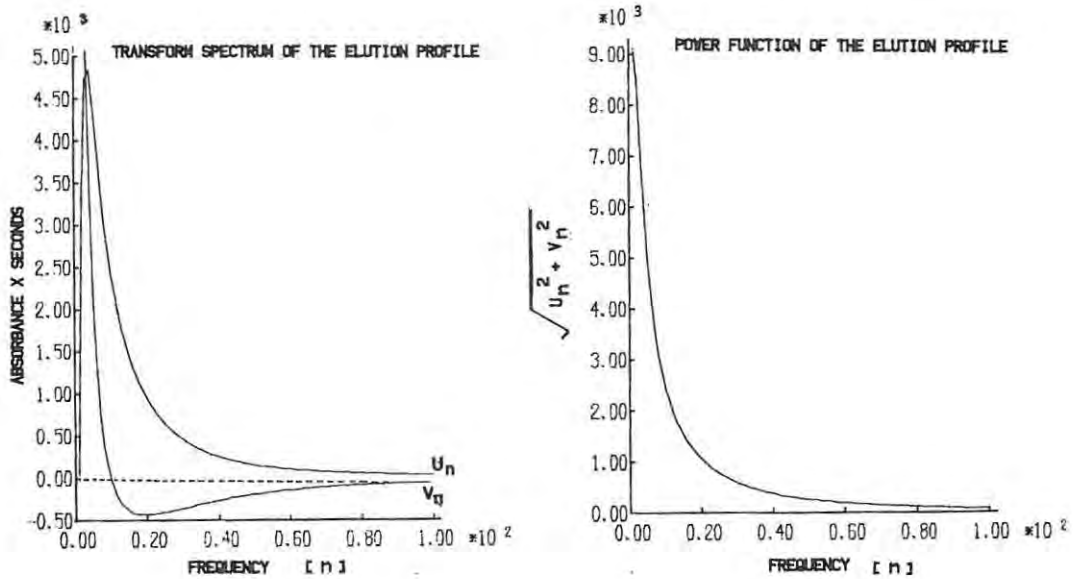
The power functions of the Fourier transform of the elution profile and the transfer function for the experimentally determined elution profiles are shown in figures 9.15 and 9.16. The high frequency components in which the signal noise is comparable to the signal, and which can be excluded from the Fourier summation without loss of information from the data are readily apparent, and determine the upper limit N_p of the number of terms over which the Fourier series should be summed. In the analysis used to extract the binding isotherm shown in Figure 9.13 the Fourier series were summed over $n = 100$ terms.

Figure 9.15



The power spectrum of the transfer function for phenol red dialysis

Figure 9.16



The Fourier transform and power spectrum of the Fourier coefficients the elution profile

C Discussion

9.7 Comparisons of the Permeation constant and the Transfer Function Methods of Data Analysis

It is seen from figures 9.13a and 9.13b that the binding isotherms obtained by both analytical methods, when applied to experimentally determined data for the phenol red-BSA system produce binding isotherms which are mutually consistent. Thus, on the basis of the ability of an analysis to reproduce binding isotherms, which are consistent with those obtained by other techniques, there are no obvious grounds for preferring one method over the other.

In terms of practical considerations, the 'transfer function' method entails some difficulties which are avoided in the simpler 'permeation constant' method. The transfer function method cannot be applied "mechanically" to extract the binding isotherm from the

elution profile data because it requires a judicious assignment of values to the parameters such as α , the Laplace convergence parameter, N , the number of terms used in the Fourier summations, and b , the exponential decay parameter. The transfer function method therefore, requires some degree of operator mediation.

In the transfer function method of analysis, however, it is unnecessary to discard the data collected during the initial transient phase. Thus, this method provides a greater number of data points over a greater concentration range of the isotherm for the same data set than does the permeation constant method. The additional points provided by the transfer function method can represent a considerable portion of the isotherm. The data discarded in the permeation constant analysis, although representing only a small fraction of the total duration of the dialysis experiment, can represent the loss of a considerable portion of the isotherm because the points on the binding isotherm which are represented by parametric equations in time are not uniformly distributed in time. Moreover, the ligand concentration and therefore quantity of ligand bound to the protein is greatest at the start of the dialysis. This can be seen by comparing the isotherms shown in figure 9.13. The upper limit of the isotherm derived by the permeation constant method occurs at a free ligand concentration of 0.42×10^{-3} M, whereas the upper limit of the isotherm extracted from the same data set by means of the transfer function method has a value of 0.8×10^{-3} M for the free ligand concentration. There is, however, a greater degree of uncertainty associated with the additional information provided by the transfer function method over that of the permeation constant method due to increased noise.

From the point of view of mathematical rigour, the transfer function method is the preferred method of analysis. The information content of each data point in the elution profile depends on the signal-to-noise ratio. The signal-to-noise ratio in the elution profile data decreases continuously as the signal

decreases. In the transfer function method, in which Laplace transforms of the elution profile are used, the noise component of the signal is effectively averaged over the entire elution profile data set and may be conveniently 'smoothed' by excluding the higher frequency components. This is in contrast to the permeation constant method of data analysis, where the quantity of ligand bound to the protein, and the sample compartment ligand concentration are evaluated over the entire dialysis data set on the basis of a single value of a permeation constant.

However, because the transfer function depends on the eluting buffer flow rate (cf. equation 6.3.4) in a way which has not been made explicit here, it is necessary to re-establish a transfer function, by means of a control dialysis experiment, each time a change of experimental parameters includes a change in the eluting buffer flow rate. In this respect the method is less convenient than the permeation constant method, in which, provided the eluting buffer flow rate is not so large to cause distortion of the dialysis membrane, the permeation constant is independent of the eluting buffer flow rate. This means that in the permeation constant method of analysis, once a value for the permeation constant has been established, this value may be used in a series of dialysis experiments in which both the initial ligand concentration and the eluting buffer flow rate are changed. In the transfer function method of analysis, the same transfer function, established in a control experiment can only be used for a number of dialysis experiments in which the initial ligand concentrations differ provided the flow rate of the eluting buffer is kept constant.

In the permeation constant analysis, a computer plot of the values of the permeation constant, determined at equally spaced time intervals over the course of the dialysis is used as a diagnostic to check the constancy of the experimental variables. A similar diagnostic can be obtained for the transfer function method. It is possible to obtain a parameter which is equivalent to the permeation constant D , in terms of a Fourier series. This parameter is represented as a function of time over the course of

the dialysis experiment as a Fourier series by making use of the system differential equations (equations 5.3.1a or 5.3.1b).

The Fourier coefficients used in the Fourier series representation of the permeation parameter as a function of time can be expressed in terms of the Fourier coefficients U_n and V_n of the Fourier series representation of the elution profile:-

Thus, equation 5.3.1b

$$\text{i.e.,} \quad V_2 dC_2(t)/dt = D[C_1(t) - C_2(t)] - F C_2(t) \quad \dots \quad 9.7.1$$

is re-arranged to give:

$$D(t) = [V_2 dC_2(t)/dt + F C_2(t)] / \{C_1(t) - C_2(t)\} \quad \dots \quad 9.7.2$$

where, in order to allow for the possibility of the permeation parameter varying with time, it is represented in equation 9.7.2 as a function of time.

The Laplace Transform to 9.7.2, assuming D a constant, yields

$$\begin{aligned} L[D] &= f(s) = \beta T(E_n - iH_n) \\ &= \{V_2 s L_2(s) + F L_2(s)\} / \{L_1(s) - L_2(s)\} \quad \dots \quad 9.7.3 \end{aligned}$$

where $L_1(s)$ and $L_2(s)$ are the Laplace transforms of $C_1(t)$ and $C_2(t)$ respectively, s is a complex frequency term, and E_n and H_n are the Fourier coefficients of the Fourier series representation of the permeation parameter as a function of time. $L_1(s)$ and $L_2(s)$ can be expressed in terms of the Fourier coefficients, U_n and V_n , of the control elution profile, as described in sections 6.5 and 6.6

Values for the coefficients E_n and H_n are obtained by simplifying and equating the real and imaginary parts of equation 9.7.3 in which $L_1(s)$ and $L_2(s)$ are expressed in terms of U_n and V_n . Again the tedious algebra that this involves can be avoided by using the complex arithmetic facilities of FORTRAN. Provided that the dialysis procedure is governed by Fick's law of diffusion, a computer plot of the $D(t)$ given by

$$D = E_0/2 + \sum_{n=1}^N E_n \cos(n\pi t/\beta T) + H_n \sin(n\pi t/\beta T) \quad \dots \quad 9.7.4$$

should show a value for D which does not vary with time and which can thus be used as a diagnostic in the transfer function method of analysis in the same manner as the plot of D vs t , where D is calculated by means of equation 5.8.8, is used in the permeation constant method. ¹

This reflects the essential similarity of the two methods of analysis both of which are derived from equations 5.3.1a and 5.3.1b, the differential equations describing the dialysis and elution processes in the dialysis cell.

---o0o---

¹ Footnote:

As pointed out by an examiner, it is unnecessary to actually perform the summations in 9.7.4; if D is indeed a real valued constant, then it has no imaginary components (i.e., all H_n 's are zero), and all E_n are zero except for a finite valued E_0 .

Chapter Ten

Results Application of the CFDD Method to Measure Collagen Ligand Binding

A Determination of collagen-plant phenol binding Isotherms

10.1 Results

Study of the binding to soluble collagen of the monomolecular phenols, i.e., phenol, catechol and resorcinol was initiated, but could not be measured by the CFDD method due to the rapid precipitation of collagen in the presence of these ligands. Attempts to overcome the precipitation of the collagen by these ligands, using very dilute solutions of the phenols, produced only very slight differences between the control and sample elution profiles. Despite the fact that these ligands cause a destabilization of collagen, which is indicated by their lowering of the collagen-gelatin transition temperature (Otto, 1953), the binding of these ligands to collagen is weak.

On the other hand, fibrillogenesis due to the presence of the flavanoid based plant phenols and gallic acid and its n-propyl ester could be delayed sufficiently in acid medium (pH = 3.0) to carry out binding studies using the CFDD technique. However, the range of concentrations over which the binding of these ligands to collagen could be studied was restricted because of the limited solubility of some of these compounds. Although these compounds are more soluble at higher pH, increasing the pH increases both the chance of collagen precipitation and the possibility of oxidation of the ligand.

The absorbance wavelengths, molar extinction coefficients and range in concentrations over which the binding of these compounds to collagen was investigated are listed in Table 10 -I. Since both the permeation constant and the transfer function

Table 10-I

Experimental Data for the Dialysis of Monomeric Tannin precursors at 15 °C

| Ligand | Molecular Mass | Absorbance Wavelength (nm) | Extinction Coefficient | Initial Ligand Concentration mol/L | Final Ligand Concentration mol/L | Eluting Buffer Flow-Rate $\text{cm}^3 \text{s}^{-1}$ |
|------------------|----------------|------------------------------|------------------------|------------------------------------|----------------------------------|--|
| (+)-catechin | 290 | 279 | 3800 | 0.306×10^{-2} | 0.08×10^{-2} | 3.6×10^{-3} |
| dihydroquercetin | 274 | 288 | 17500 | 0.108×10^{-2} | 0.02×10^{-2} | 1.8×10^{-3} |
| dihydrorobinetin | 274 | 273 | 18200 | 0.101×10^{-2} | 0.03×10^{-2} | 1.1×10^{-3} |
| brazilin | 286 | 287 | 6400 | 0.181×10^{-2} | 0.04×10^{-2} | 1.8×10^{-3} |
| haematoxylin | 302 | 292 | 4600 | 0.107×10^{-2} | 0.05×10^{-2} | 1.7×10^{-3} |
| gallic acid | 170 | 271 | 9600 | 0.402×10^{-2} | 0.05×10^{-2} | 4.0×10^{-3} |
| n-propyl gallate | 212 | 271 | 9800 | 0.350×10^{-2} | 0.04×10^{-2} | 3.5×10^{-3} |

methods of analysis yield almost identical isotherms except that the permeation constant method neglects the first part of the data, whereas the transfer function method uses essentially all of the data, the binding isotherms of collagen and the plant phenolic ligands were evaluated using the simpler permeation constant analysis. The dialysis experiments were carried out in duplicate for each ligand.

The mean values for the permeation constants obtained from the dialysis of these ligands through Visking dialysis membrane in control experiments and the standard deviations associated with these values are listed in Table 10- II.

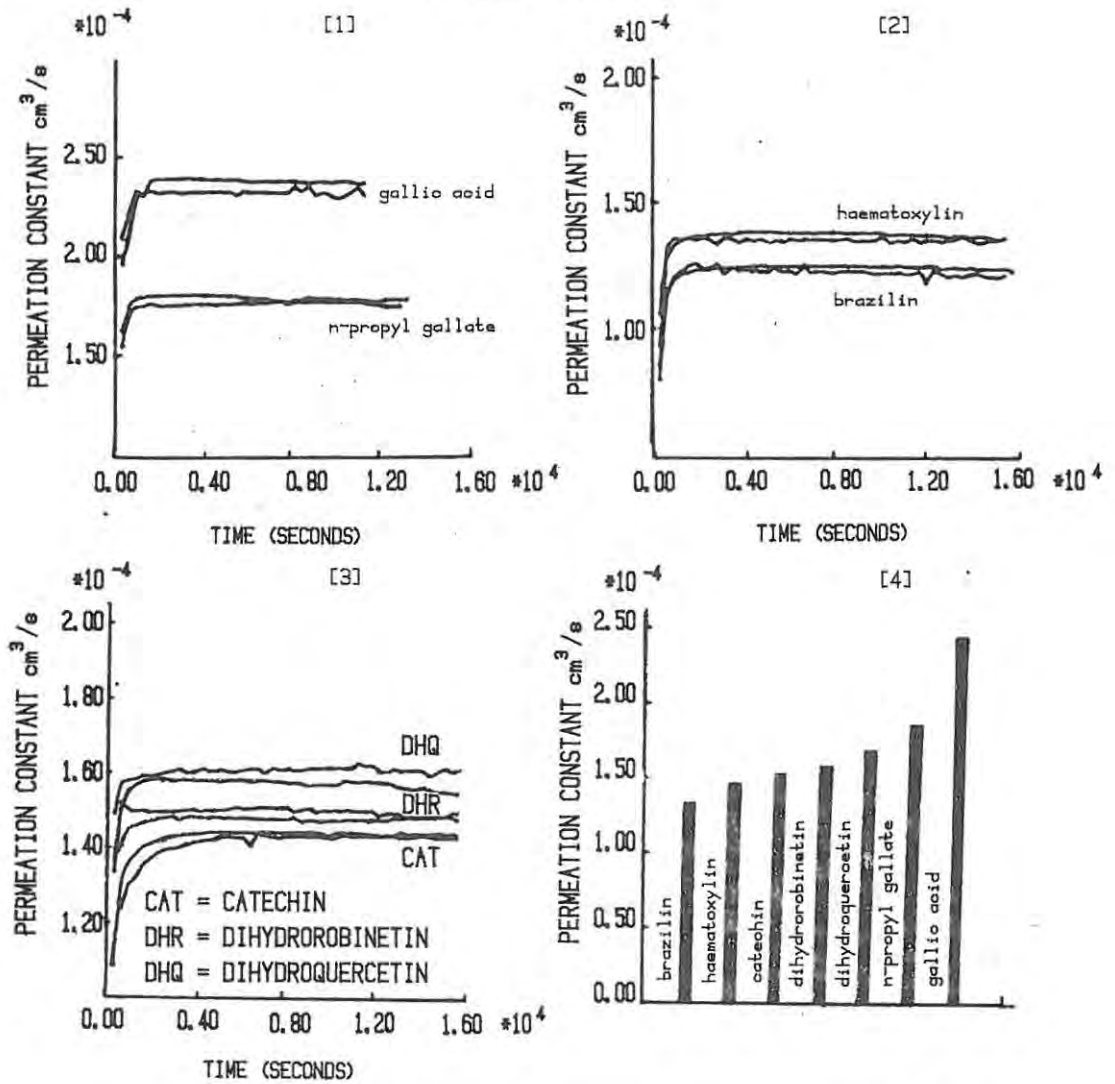
Table 10 - II

Permeation Constants for Plant Phenolic Ligands

| Ligand | Permeation Constant | Standard Deviation |
|------------------|------------------------------|------------------------------|
| | $\text{cm}^3 \text{ s}^{-1}$ | $\text{cm}^3 \text{ s}^{-1}$ |
| (+)-catechin | 0.143×10^{-3} | 0.0048×10^{-3} |
| dihydroquercetin | 0.158×10^{-3} | 0.0069×10^{-3} |
| dihydorobinetin | 0.148×10^{-3} | 0.0053×10^{-3} |
| brazilin | 0.122×10^{-3} | 0.0034×10^{-3} |
| haematoxylin | 0.138×10^{-3} | 0.0042×10^{-3} |
| gallic acid | 0.237×10^{-3} | 0.0068×10^{-3} |
| n-propyl gallate | 0.177×10^{-3} | 0.0068×10^{-3} |

The variations with time over the course of the dialysis in the values of the permeation constants for the respective ligands are shown in Figure 10.1.

Figure 10.1

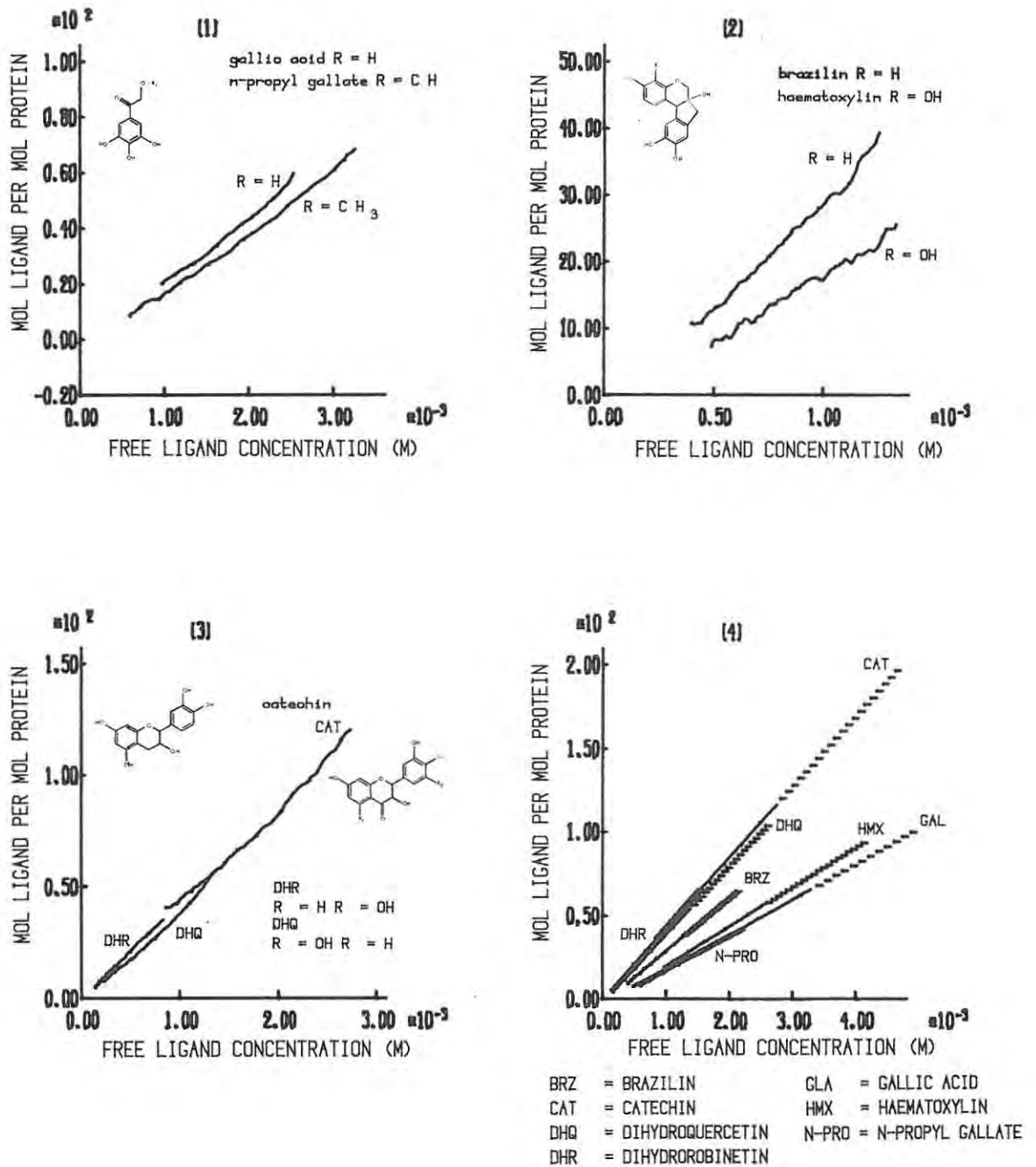


The variation of the ligand permeation constants with time

---oOo---

The complete set of binding isotherms for all the phenolic ligands investigated are shown in Figure 10.2 and for purposes of comparison, the Bjerrum plots of the isotherms are shown together in figure 10.3

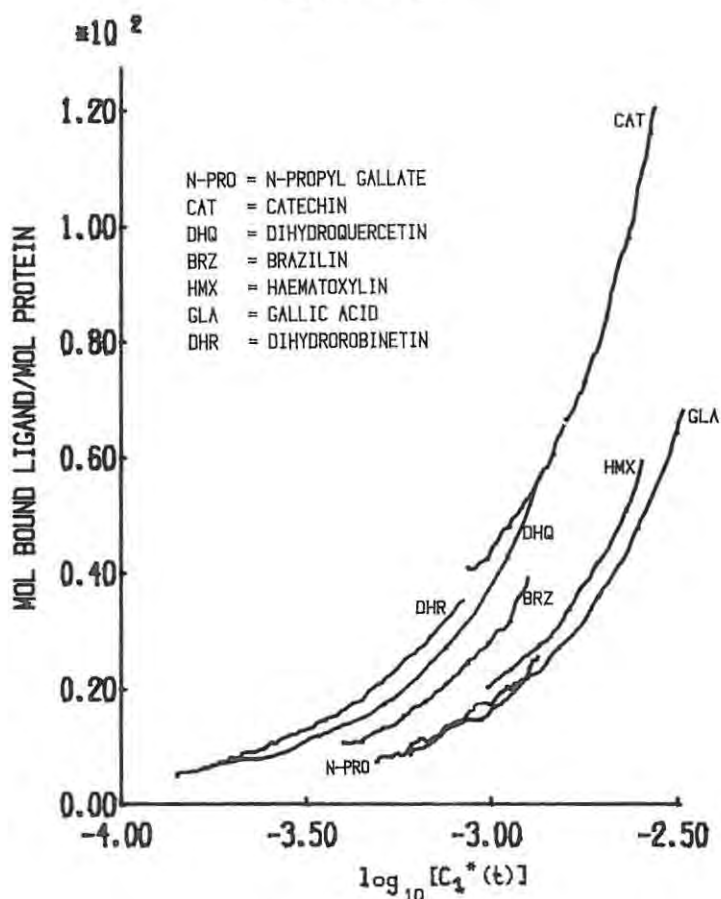
Figure 10.2



Binding isotherms of the interaction of collagen to the plant phenols at 15 °C

Figure 10.2 [4] shows the straight lines fitted by least squares to the binding isotherm data.

Figure 10.3



Bjerrum plots of the collagen-plant phenol
ligand binding isotherms

In each case, over the range of ligand concentration investigated, the quantity of ligand bound to the collagen varied linearly with free ligand concentration. The binding isotherms were fitted to a linear model $\bar{v} = A_1 C_1^*(t) + A_0$ by least squares regression. The graphs of these linear plots to represent the isotherms are shown in figure 10.2. It is to be noted that the binding of these ligands to collagen differs markedly from the binding of phenol red to BSA. The binding capacity of collagen for these ligands is large. Thus, in the case of catechin, when the free ligand concentration is 0.25×10^{-4} M, the number of ligand molecules bound to a collagen molecule is about 100, compared to about six phenol red molecules to BSA at the same ligand concentration. Furthermore, unlike the

phenol red-BSA interaction in which the binding isotherm exhibits a plateau at higher ligand concentrations, indicating an approach to saturation of the ligand binding sites, there is no indication of saturation of binding sites in the case of collagen and the phenolic ligands investigated. The binding isotherms appear to be linear over the ligand concentration ranges investigated. The values obtained for these parameters, A_1 and A_0 for the linear equations fitted to the binding isotherms are listed in Table 10 -III.

Table 10 - III

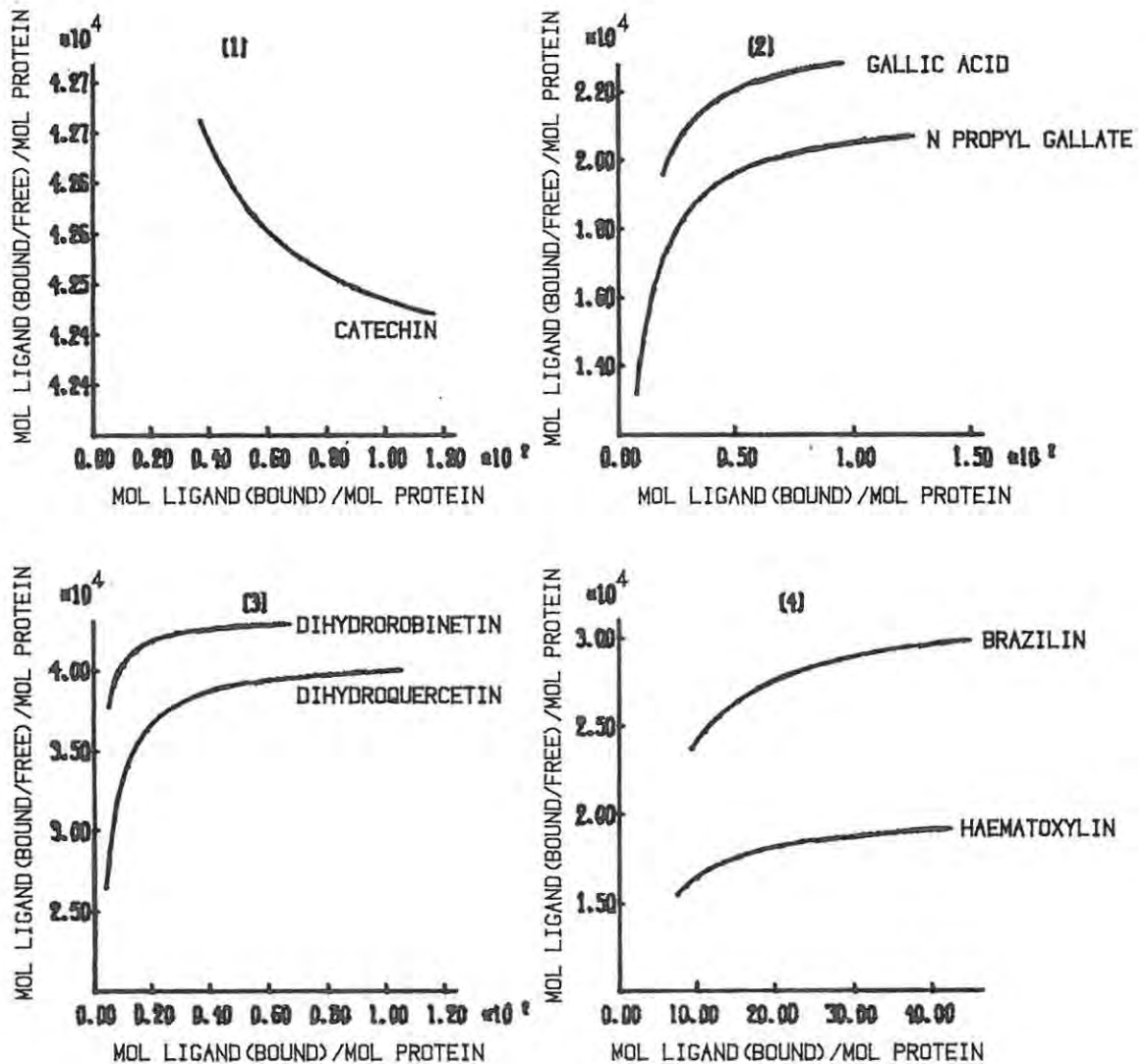
Coefficients for the linear equation $\bar{v} = A_1C + A_0$
fitted by least squares to the binding isotherm data

| Ligand | A_1 | Confidence Interval (95%) | A_0 | Confidence Interval (95%) |
|------------------|---------------------|---------------------------|-------|---------------------------|
| dihydrorobinetin | 0.435×10^5 | $\pm 0.38 \times 10^3$ | -0.81 | ± 0.15 |
| (+)-catechin | 0.424×10^5 | $\pm 0.76 \times 10^3$ | 0.24 | ± 1.31 |
| dihydroquercetin | 0.410×10^5 | $\pm 0.98 \times 10^3$ | -2.38 | ± 0.66 |
| brazilin | 0.322×10^5 | $\pm 0.53 \times 10^3$ | -3.34 | ± 0.42 |
| haematoxylin | 0.203×10^5 | $\pm 0.70 \times 10^3$ | -2.34 | ± 0.60 |
| n-propyl gallate | 0.239×10^5 | $\pm 0.52 \times 10^3$ | -4.17 | ± 0.90 |
| gallic acid | 0.216×10^5 | $\pm 0.33 \times 10^3$ | -4.99 | ± 0.60 |

It can be seen from Table 10 - III that the values for the intercepts A_0 are relatively small (though not identically equal to zero) as is to be expected when there is no curvature in the isotherm. The Scatchard plots of the binding isotherms are shown in Figure 10.4. Except in the case of (+)-catechin the

Scatchard plots are unusual. In contrast to the more familiar linear plots or hyperbolae with negative slopes, when binding involves more than a single class of binding sites, the Scatchard plots for these collagen ligand interactions are hyperbolae with positive slopes.

Figure 10.4



Scatchard plots for the collagen plant phenol binding isotherms

B

Discussion

10.2 Physical implications of the collagen-ligand isotherms

The application of the CFDD method to investigate soluble collagen-ligand interactions yields an isotherm which is expressed in terms of the number of molecules of ligand bound to a molecule of protein, as opposed to adsorption methods where the isotherm is expressed in less fundamental terms as mass of ligand bound per unit mass of hide substance. Binding studies by the CFDD method on collagen-ligand binding, in contrast to the phenol red-BSA system, show collagen to have an extremely high capacity for the flavanoid low molecular mass plant phenols. As has been noted, at similar ligand concentrations, the number of plant phenol ligand molecules per collagen molecule is about ten to fifteen times the number of phenol red molecules per BSA molecule. In terms of the respective molecular masses of the two protein molecules (Collagen M.Mass 300 000; BSA M.Mass 69 000) this shows the binding capacity of collagen to be considerably greater than that of BSA, since if all other influences were equal, the expected value for this factor is about five. Furthermore, unlike the phenol red-BSA system in which the binding isotherm levels out at higher ligand concentrations indicating that saturation of the ligand binding sites has been attained, there is no indication in collagen of any approach to saturation of the binding sites with these ligands. The high binding capacity of collagen for these plant ligands, relative to the small value for BSA and phenol red, may imply that the binding of these ligands to collagen involves participation of the peptide links rather than specific arrangements or sequences of amino acid side-chain residues, as indicated below.

The linear relationships between the amount of ligand bound to collagen and the high binding capacity of collagen for these ligands have several implications. Apart from gallic acid and n-propyl gallate, which have values of -5 ± 1 for the intercept A_0 when a linear function is fitted to the binding isotherms,

the values for the intercept for the remaining ligands are close to zero. This indicates that a proportionality exists between the quantity of ligand bound to the protein and the concentration of ligand in equilibrium with the protein-ligand complex over the experimental concentration range. In terms of a Scatchard binding model for a single class of binding sites:

$$\text{i.e., } \bar{v}(t) = n_j k_j C_j^*(t) / [1 + k_j C_j^*(t)]$$

.... 10.2.1

proportionality between $\bar{v}(t)$ and $C_1^*(t)$ implies a very small value for the protein-ligand association constant (i.e., $k_j C_1^*(t)$ is small compared with 1 and may be neglected in the denominator in equation 10.2.1). This inference, coupled with the observed high ligand binding capacity of collagen, indicates that binding between collagen and these ligands is relatively non-specific. In other words, the binding of these ligands to the collagen is not dependent on any particular amino acid sequence or protein configuration at the binding site. It is thus very likely that the binding of these ligands to collagen is by hydrogen bonding, and probably involves the numerous polar peptide links and polar side-chain residues which are present in collagen.

Although the parameters A_1 representing the proportionality between $\bar{v}(t)$ and $C_1^*(t)$ are not identical for each ligand, it can be seen from Figure 10.2 and 10.3 that, except for brazilin, the ligands fall into two categories with respect to the parameter A_1 . The value of this parameter for brazilin (0.32×10^5) falls midway between those of (+)-catechin and the flavanones dihydroquercetin and dihydrorobinetin on the one hand (mean value for $A_1 = 0.423 \times 10^5$) and that of gallic acid, n-propyl gallate and haematoxylin on the other (mean value for $A_1 = 0.219 \times 10^5$). This shows that, although the binding of these phenolic ligands to collagen is relatively non-specific,

the binding is influenced slightly by ligand structure. This is not surprising, since the ligands are multifunctional and each possesses several hydroxyl groups capable of participating in hydrogen bonding. However, in view of the similarity of the structures of catechin, dihydroquercetin, and dihydrorobinetin, the structure-affinity relationship appears to be more dependent on the skeletal structure of the ligand than on the positioning of the hydroxyl groups. In this context, it is of interest to note that for (+)-catechin, no evidence, apart from an ability to inhibit the enzymic degradation of collagen by mammalian collagenase (Kuttan et al., 1981), has been presented to demonstrate a binding reaction to collagen. The binding affinity of these ligands appears to increase with increasing structural complexity; it is relatively low in the monomolecular polyhydric structures, such as gallic acid, and highest in the polynuclear types, such as catechin and the flavanones, dihydroquercetin and dihydrorobinetin.

It is not possible to obtain any detailed information relating to the magnitude of the association constants for these interactions, because of the linearity of the binding isotherms for these protein-ligand systems. The Scatchard plots, which usually provide initial estimates of the binding parameters for subsequent least squares refinement, are also not very informative. As can be seen from Figure 10.4, these plots are hyperbolae with positive slopes, except for the negative slope in the case of catechin.

Scatchard plots with positive slopes are not unprecedented, and have been reported by Shen & Gibaldi (1974), and by Judis (1978) for alkaloid-albumin interactions. Protein-ligand systems which exhibit positive slopes in the Scatchard transformation of the binding isotherm have been reviewed by Bowmer & Lindup (1978), and a variety of explanations have been proposed to account for the phenomenon. These explanations have invoked both cooperativity and ligand induced self-association of the protein.

Steiner (1980) has reviewed a variety of model systems which report the influence of the ligand on self-association of the protein. Cann (1978) has generated curves to simulate protein-ligand interactions for a series of protein monomer-dimer systems

in an attempt to relate the shape of the Scatchard plots to model systems involving protein self-association.

Although it is possible to account for positive curvature in the Scatchard plot by means of model systems invoking ligand-mediated dimerization of the protein, in the case of the interactions between collagen and the plant phenols, the positive slopes in the Scatchard plots are readily explained, without having to invoke the concepts of cooperativity or ligand-induced association of the protein. It is easily shown that the slope of the Scatchard transformation of a linear isotherm will be positive or negative according as the parameter A_0 is positive or negative.¹

¹ Footnote:

The Scatchard expression for a single class of binding sites (equation 3.1.1) is substituted into a linear expression for the binding isotherm. In the resulting expression, \bar{v}/C is differentiated with respect to \bar{v} .

Thus, the linear expression, $\bar{v} = A_1 C + A_0$, is rearranged to give:

$$\bar{v}/C = A_1 + A_0/C \quad (a)$$

Rearrangement of the Scatchard equation for a single class of binding sites:

$$\text{i.e., } \bar{v} = nkC/(1 + kC) \quad (b)$$

$$\text{yields } 1/C = nk/\bar{v} - k \quad (c)$$

which is substituted into equation (a) for $1/C$ to give

$$\bar{v}/C = A_1 + A_0 \{ nk/\bar{v} - k \} \quad (d)$$

(continued)

Thus, in the case of the collagen-plant phenol interactions, the positive curvature in the Scatchard plots is an artifact due to the small, non-zero values for the parameter A_0 arising from experimental errors at low ligand concentrations. These examples show that care must be exercised in the extraction of a binding mechanism from the form of the Scatchard plot. This point has been emphasised by Noerby et al. (1980), who stress the possibility of misuse of the Scatchard plot, and discuss a variety of commonly encountered errors in the use and interpretation of Scatchard plots.

Although the Scatchard plots cannot be used in the present instance to provide values for the protein-ligand association constants, it is possible to draw certain conclusions about the magnitude of these parameters. If it is assumed that, in the CFDD method, deviations from linearity of the order of 5% to 10% can readily be detected in the binding isotherm, a linear trend would imply that:

$$k_1 C_1^*(t) < 0.05 \text{ to } 0.1$$

¹ Continuation of footnote to previous page

Differentiating (d) with respect to \bar{v} gives:

$$\frac{d[\bar{v}/C]}{d\bar{v}} = - A_0 \{ nk/\bar{v}^2 \}$$

$$\text{i.e., if } A_0 > 0 \quad d[\bar{v}/C] / d\bar{v} < 0$$

$$\text{and if } A_0 < 0 \quad d[\bar{v}/C] / d\bar{v} > 0$$

since the remaining terms are necessarily positive.

with reference to equation 10.2.1. Thus, the absence of detectable deviation from linearity in the binding of the plant phenols to collagen up to concentrations in the region of 10^{-3} M would imply a k_j value of 50 to 100 M^{-1}

$$\text{(i.e., } k_j = \{0.05 \text{ to } 0.1\} / 10^{-3} \text{ M}^{-1}\text{)}$$

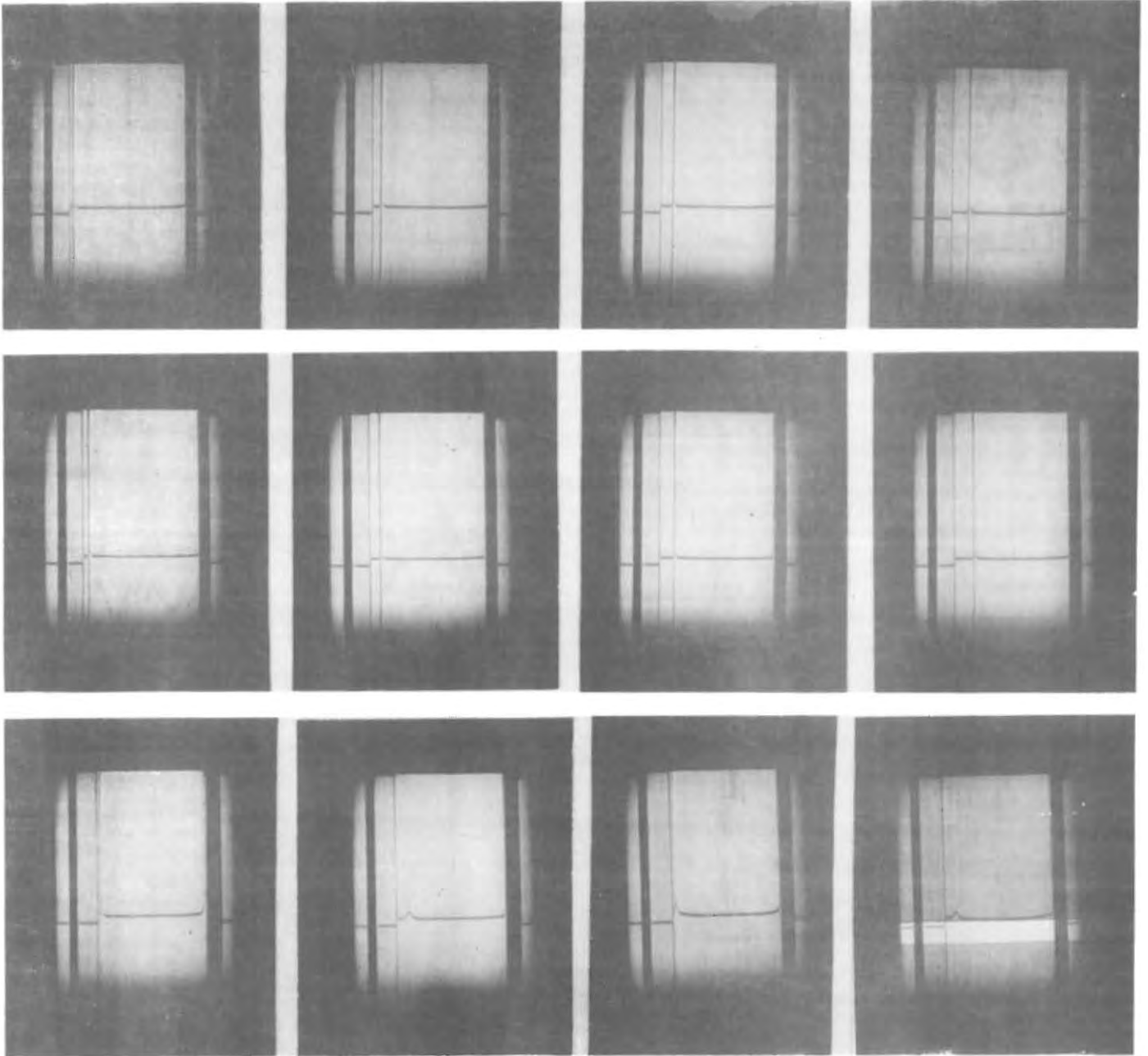
A corresponding approximate value for n , a value between 500 and 1000 mol/mol protein, is obtained from the gradients of the various isotherms ($nk_j = 0.5 \times 10^5 \text{ M}^{-1}$ approximately).

Although it is not necessary to use cooperativity of protein association to explain the positive curvature in the Scatchard plots, nevertheless, because the phenolic ligands examined in this study are multifunctional, it is possible that these ligands can promote association of the collagen molecules. In order to test this possibility, the sedimentation patterns of collagen, obtained by ultracentrifugation in the presence and absence of these ligands, were compared. The sedimentation patterns of collagen in 0.5 M urea, a hydrogen bond breaker, and 2% phenol were also determined for comparison.

The sedimentation patterns for collagen in the presence of the plant phenolics (Plates IX and X), except in the case of gallic acid and haematoxylin, show a single narrow peak which resembles the sedimentation pattern of collagen in the absence of any ligand. The sedimentation patterns in the case of gallic acid and haematoxylin show a slight broadening of the peak which could imply more than a single protein species. The sedimentation patterns of collagen in the presence of these ligands are similar to that of collagen in the presence of phenol (Plate X).

The binding of phenol to collagen has been investigated by measuring the adsorption of phenol by hide powder (Küntzel & Schwenk, 1940). This study showed that phenol binding to collagen neither obeys a common adsorption formula, nor, does phenol binding appear to involve the ionic groups on collagen, since the binding of mineral acids and bases by collagen is unchanged in the

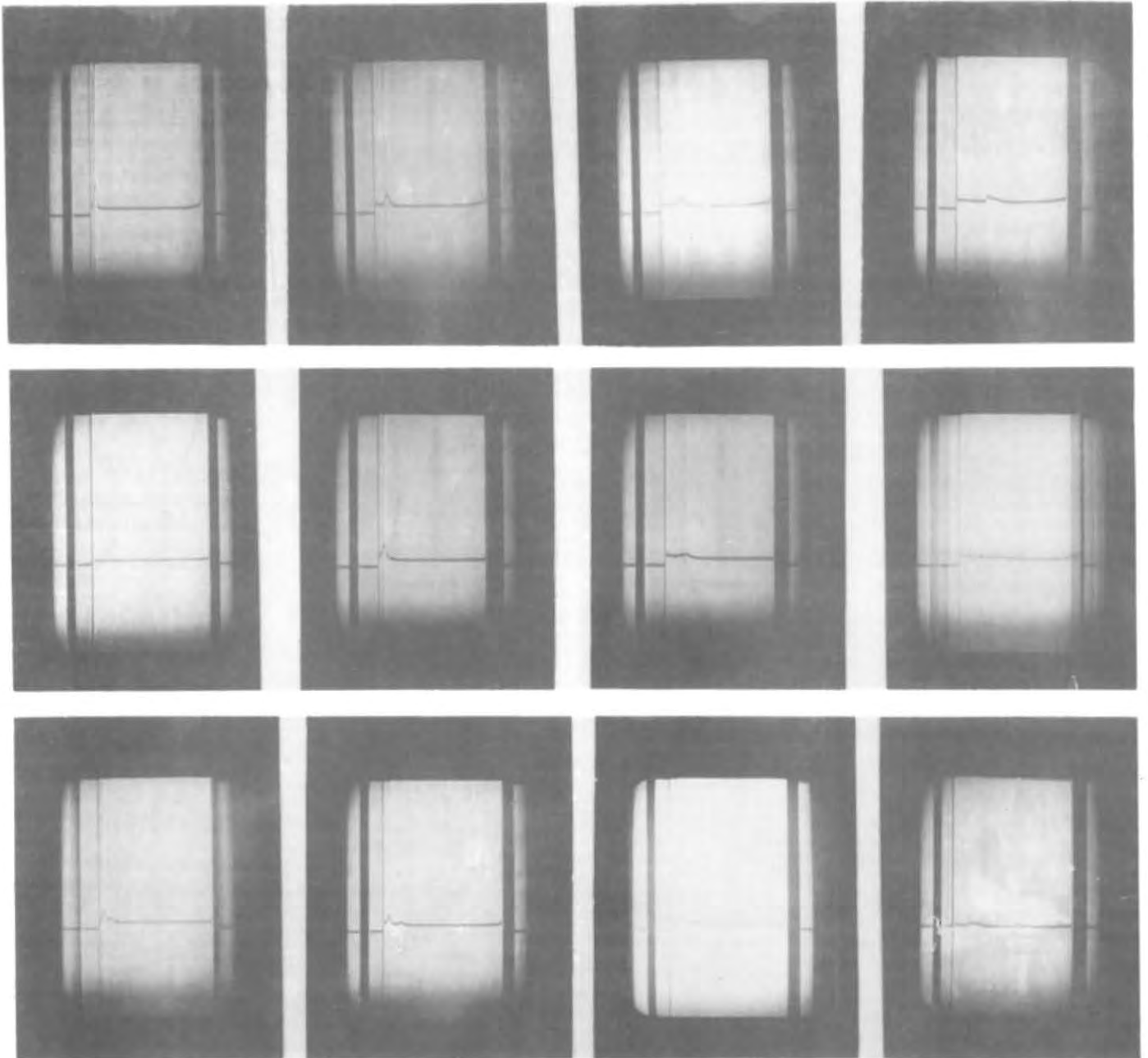
Plate IX



Ultracentrifuge Schlieren pictures showing the sedimentation of collagen at 60 000 rpm. at 20 minute intervals.

Top Row: Collagen in the absence of ligand (phosphate buffer pH 7)
 Centre Row: Collagen in 0.3×10^{-2} M (+)-catechin solution
 Bottom Row: Left to right, pictures 1 & 2: collagen in 0.11×10^{-2} M dihydroquercetin solution.
 Pictures 3 & 4: collagen in 0.5 M Urea

Plate X



Ultracentrifuge Schlieren pictures showing sedimentation of collagen (60 000 rpm.) at 20 minute intervals.

Top Row: Collagen in 0.4×10^{-2} M gallic acid solution.

Centre Row: Collagen in 0.11×10^{-2} M haematoxylin solution.

Bottom Row: Collagen in 0.2×10^{-3} M phenol solution

presence or absence of phenol. Phenol causes a reversal in the sign of the optical birefringence of collagen fibres (Gustavson, 1956), and this has been interpreted as being due to arrangement of the phenol molecules parallel to the fibre axis of the collagen. This interpretation supports the proposal of Otto (1940) that phenol binding to collagen involves the aromatic nucleus, presumably involving π -bonding, rather than the phenolic hydroxyl group. Thus it is possible that the binding of gallic acid and haematoxylin may also involve a mechanism similar to that of phenol-collagen binding, whereas the binding by the flavanoids is predominantly by hydrogen bonding.

The sedimentation patterns, in providing no indication of collagen association, are consistent with the observation (Roux et al., 1965) that tanning effects, such as shrinkage temperature increase, are evident only with plant phenolic compounds comprising of at least four monomeric subunits of the type investigated in this study.

In general, the results of the present study show low affinity, high capacity binding without evidence of site saturation over the experimentally accessible concentration range. The relatively weak binding inferred from the linear binding isotherms obtained is consistent with hydrogen bonding interactions through hydroxyl group substituents on the ligand. Collagen-ligand interaction appears to increase with structural complexity and polar group content of the ligand.

The estimated low values for the association constants of the interactions between these plant phenolic compounds and collagen confirm the findings of Shuttleworth et al. (1952) that "vegetable tanning appears to be a solvent reversible multipoint crosslinking mechanism in which hydrogen bonds provide the dominant forces and peptide links are probably the most powerful binding sites".

Chapter Eleven

General Discussion and Conclusion

A number of different methods for investigating protein-ligand interactions have been discussed in this dissertation. All methods used to study protein-ligand interactions have their strengths and weaknesses, advantages and disadvantages. The selection of a particular method will therefore often depend on the system under study, and the aims of the investigator. The continuous-flow dynamic dialysis method, which has been developed and described in this study, is a further application of a non-equilibrium kinetic dialysis method which correctly accounts for the effects of back-diffusion from the sink compartment. While sharing some of the limitations of subtractive methods in general, the flexibility of the CFDD method in permitting the adjustment of operational parameters should suit it to the study of the binding characteristics for a wide variety of protein-ligand systems. In particular, the method should be of considerable importance in the study of drug binding studies to plasma proteins, where unlike the fibrous proteins, limited solubility of the protein is not a restrictive factor. In particular, two major advantages of the CFDD method are:

- i the method, using a single protein-ligand solution, provides a very much larger number of data points for the establishment of the isotherm than previously reported dynamic dialysis techniques;
- ii the analysis of the dialysis data to extract the binding isotherm is independent of any *a priori* assumptions with respect to a protein-ligand binding model.

The large number of data points provided from a single experiment represents a considerable improvement over the equilibrium dialysis method, which requires the preparation of many protein-ligand samples, each sample providing but one data point of the isotherm. Thus the CFDD method makes possible the study of protein-ligand interactions over a wide range of protein and ligand concentrations, at a much lower cost in time, labour and chemicals in comparison with the equilibrium dialysis method. In addition, because the CFDD method requires less time for data collection than the equilibrium method, the associated risk of protein denaturation or destruction through microbial degradation is considerably reduced.

The independence of the method with respect to protein-ligand binding models permits a greater degree of objectivity in the interpretation of the results and avoids the potential hazards of unconscious biasing of data interpretation in accordance with an assumed binding model. This means that the binding isotherm provided by the method can be tested against a variety of binding models, and the selection of a particular model can be made solely on the basis of 'goodness of fit'.

Although it is believed that the CFDD method suffers no major pitfalls, other than those shared by all subtractive methods, certain precautionary measures must be adopted to ensure reliability of the results. Among the factors which can adversely affect the reliability of the method, membrane effects are probably the most important. These will similarly affect all dialysis methods. The possibility that the ligand can bind to the membrane must always be borne in mind, and it is imperative to establish that there is no appreciable source of error due to membrane binding, either by the ligand, protein or protein-ligand complex, for every protein-ligand system investigated by this method.

The ligand may bind irreversibly to the membrane, or alternatively the membrane may act as a competitive substrate to the protein (i.e., ligand binding to the membrane is reversible).

When the binding of the ligand to the membrane is irreversible, use of the CFDD method is still possible if due allowance is made for the loss of ligand due to membrane adsorption. However, if ligand is released from the membrane as the elution proceeds, an analysis of the data to differentiate between protein-ligand and membrane-ligand binding may be impossible.

It has been shown that for the phenol-red BSA system, as well as for the binding of low molecular mass tannin precursor materials to collagen, the conceptually simpler analysis utilizing a permeation constant is adequate, despite the necessity of having to discard some of the data collected during an initial transient phase until a more-or-less linear concentration gradient is established within the membrane.

The general method, based on the concept of a system transfer function, represents a more rigorous and unconstrained technique. This analysis, which incorporates the proportionality relationship of Fick's law of diffusion into the linearity of the dialysis system, is, from a theoretical point of view, a more fundamental approach. Thus apart from the readily verifiable assumption that the dialysis cell represents a linear system, the analysis makes no assumption with respect to the details of the diffusion process within the membrane. The relationship between the sample compartment and sink compartment ligand concentrations, established by means of the system transfer function, is therefore still valid over the initial transient phase, even though the concentration gradient of the ligand through the membrane during this interval is not linear.

In the case of the collagen-tannin precursor binding studies, it was not possible to obtain precise measures for the binding parameters by the CFDD technique. The inability to measure these quantities, however, was less the fault of the method than the nature of the collagen-ligand interaction. Collagen, with its limited solubility and rigid triple-helix molecular structure, is an unaccommodating substrate for protein-ligand binding studies. The linear relationship between ligand

uptake and ligand concentration precluded the determination of binding parameters by regression procedures. However, it is reasonable to conclude from this linear relationship that the binding of these ligands to collagen is non-specific. In addition, because of an inability to detect saturation limits for these ligands over the considerable range of ligand concentrations studied, it can be concluded that this binding probably involves hydrogen binding to the peptide links of the collagen backbone rather than to specific sequences of protruding amino acid side chains.

Intuitively it is anticipated that collagen-ligand binding will always be predominantly non-specific; a rigid triple helix does not readily undergo allosteric conformational changes to accommodate the ligand. Despite this assumption, however, there are aspects of collagen-tannin precursor binding which are intriguing. The observation (Kuttan et al., 1981) that (+)-catechin has the ability to render collagen resistant to mammalian collagenase degradation, but not to bacterial collagenase, has interesting implications. These investigators have reasoned that (+)-catechin modifies the collagen structure to make it resistant to enzymic degradation. However, in view of the very weak binding of (+)-catechin to collagen, and its inability to confer resistance to bacterial collagenase degradation, it must be presumed that any conformational change in the collagen structure is slight. Such conformational change may affect only the non-helical telopeptide portions of the molecule. It is of interest therefore to speculate whether the CFDD method is capable of detecting any differences between the binding of catechin to untreated collagen and collagen which has been enzymically treated to remove the telopeptides.

The disordered structure of gelatin offers greater scope for multipoint ligand attachment than collagen. Since the solubility of gelatin is greater than that of collagen, protein solubility above the collagen-gelatin transition temperature is no longer a restrictive factor for the CFDD method. Thus, the CFDD method can be used to study the binding of the tannin-precursor ligands

to gelatin at different pH. Comparative studies of the binding of these ligands to gelatin at different pH may provide insight into the role of ionic forces in the ability of collagen to bind to these ligands. In addition, binding studies at different temperatures, especially above the transition temperature, could provide measures of the enthalpy and entropy of binding. This would provide more information as to the nature of the protein-ligand interaction. The CFDD cell provides a very convenient means for investigating such aspects of ligand binding.

Appendix I

The Significance of Back-Diffusion in Continuous-Flow Dynamic Dialysis

If the back-diffusion of the ligand from the sink compartment to the sample compartment in the dialysis cell is neglected, the differential equations which describe the flow dialysis system (equations 5.3.1 and 5.5.2) reduce to:

$$-dC_1(t)/dt = D C_1(t)/V_1$$

.... A.I.1a

and

$$dC_2(t)/dt = \{D C_1(t) - F C_2(t)\}/V_2$$

.... A.I.1b

These equations for the dialysis of ligand in the control experiment have the analytical solutions:

$$C_1(t) = C_1(0)e^{-D/V_1 t}$$

.... A.I.2a

and

$$C_2(t) = [DC_1(0)/V_2\{D/V_1 - F/V_2\}](e^{-D/V_1 t} - e^{-F/V_2 t})$$

.... A.I.2b

An estimate of the diffusion coefficient, obtained from the natural log-linear plot of $C_2(t)$ vs t , is now given by $D = -V_1 b$ where b is the slope of the linear portion of the curve after it has passed through the maximum value. This results from the fact

that the last term in A.I.2b becomes negligible at long times with respect to the next-to-last term because the flow rate, F , is larger than the permeation constant, D .

The mass balance equation expression for D , when back-diffusion is neglected (equivalent to equation 5.8.8 in the analysis allowing for back-diffusion) is :

$$D = \frac{\{ V_2 dC_2(t)/dt + FC_2(t) \}}{\{ C_1(0) - (V_2 C_2(t) + F \int_0^t C_2(\tau) d\tau) \} / V_1}$$

.... A.I.3

The parametric equations for the binding isotherm are:

$$C_1^*(t) = \{ V_2 dC_2^*(t)/dt + FC_2^*(t) \} / D$$

.... A.I.4

and

$$p\bar{v}(t) = C_1^*(0) - C_2^*(t) [F/D + V_2/V_1] - [V_2/D] dC_2^*(t)/dt + F/V_1 \int_0^t C_2^*(\tau) d\tau$$

.... A.I.5

The magnitude of the effect of back diffusion on the permeation constant D can be determined as the difference between equations A.I.3 & equation 5.8.8.

This yields

$$\Delta D = \frac{[V_2 dC_2(t)/dt + FC_2(t)] C_2(t)}{Q [Q - V_1 C_2(t)]} \quad \dots \quad \text{A.I.6}$$

$$\text{where } Q = [C_1(0) - (V_2 C_2(t) + F \int_0^t C_2(\tau) d\tau)] / V_1 \quad \dots \quad \text{A.I.7}$$

ΔD converges to zero for large t (as is to be expected) when the effect of back-diffusion becomes less significant as the ligand concentration diminishes.

The effect of back diffusion on the binding isotherm, in particular the amount of ligand bound to the protein, is the difference obtained by subtracting equation 5.8.6 from equation A.I.5. This yields:

$$p\Delta\bar{v}(t) = V_1 C_2(t) \quad \dots \quad \text{A.I.8}$$

which again becomes less significant for large t , when $C_2(t)$ tends to small values.

Appendix II

Correction Factor for the Sink Compartment Volume to Correct for Membrane Distension

The determination of the permeation constant D using the mass-balance relationship (equation 5.8.8) at different eluting buffer flow rates indicates a dependence of D on the eluting buffer flow rate. This dependence does not reflect a departure of the diffusion process from first order kinetics, which would be indicated by a dependence of D on the initial ligand concentration. This dependence is most pronounced at high eluting buffer flow rates, and is the result of doming of the membrane under the influence of the dynamic pressure of the eluting buffer. A value for V_2 , the sink compartment volume, cannot be obtained directly from the physical dimensions of the dialysis cell, because the extent of doming of the membrane depends on the eluting buffer flow rate. It is, however, possible to obtain a value for this parameter indirectly.

The analytical expression for the elution profile of the control experiment, obtained from the solution of the differential equations describing the two-compartment dialysis model system, is:

$$C_2(t) = K\{e^{-bt} - e^{-at}\} \quad \dots \quad \text{A.II.1}$$

where $K = DC_1(0)/V_2(a-b)$ (see equation 5.4.2 page 90)

The parameters a and b are related to the permeation constant, D , the eluting buffer flow rate F , and the sink compartment and sample volumes V_2 and V_1 , respectively, by:

$$a + b = \{(V_1 + V_2)D + V_1F\}/V_1V_2 \quad \text{and} \quad ab = DF/V_1V_2$$

The relationship between V_2 and F , in terms of the parameters a & b , is obtained by eliminating D between these two equations. Thus

$$V_2^2 - [F(a + b)/ab - V_1]V_2 + F^2/ab = 0$$

.... A.II.2

The value for the parameter b is obtained from the slope of the linear portion of the log-linear plot of the elution profile. A value for the parameter a is derived from the value of b and the maximum absorbance value of the elution profile $C_2(t_m)$ at time $t = t_m$.

At $t = t_m$, $dC_2(t)/dt = 0$, and it is readily shown from equation A.II.1 that:

$$(a - b)t_m = \ln(a/b) \quad \text{.... A.II.3}$$

Equation A.II.3 is solved for a using Newton's method. (i.e., $a = a' - f'(a')/f(a')$ where a' is an initial estimate of a and $f'(a) = df(a)/da$)

Equation A.II.2 can be solved for V_2 in terms of the eluting buffer flow rate F and the estimated values obtained for the parameters a and b .

Thus, from a series of control dialysis experiments using the same initial ligand concentration, but different eluting buffer flow rates, it is possible to establish a calibration curve between the sink compartment volume and the eluting buffer flow.

Appendix III

The Special case: $n = 0$ in the Laplace Transform of the Mass Balance Relationship Between Sample and Sink Compartment Ligand Concentrations

The Fourier coefficients Q_0 and Q_0^t cannot be evaluated directly from the mass balance equations:

$$\beta T(Q_n - iP_n) = \{C_1(0) - F/V_1 L[C_2(t)]\}/(\alpha + i\omega) \\ - V_2/V_1 L[C_2(t)] \quad \dots \quad \text{A.III.1}$$

or

$$\beta T(Q_n^t - iP_n^t) = \{C_1^*(0) - F/V_1 L[C_2^*(t)]\}/(\alpha + i\omega) \\ - V_2/V_1 L[C_2^*(t)] \quad \dots \quad \text{A.III.2}$$

because of indeterminacy. These parameters may be obtained indirectly: (The same arguments apply to both the sample and control. The analysis is demonstrated for the control case)

The mass balance expression:

$$V_1[C_1(0) - C_1(t)] = V_2 C_2(t) + F \int_0^t C_2(\tau) d\tau \quad \dots \quad \text{A.III.3}$$

is differentiated and multiplied by t to yield:

$$-t dC_1(t)/dt = (V_2/V_1) t dC_2(t)/dt + (F/V_1) t C_2(t) \quad \dots \quad \text{A.III.4}$$

which is integrated by parts between the limits $t = 0$ and $t = \infty$, to give:

$$\int_0^{+\infty} c_1(t) dt = (F/V_1) \int_0^{+\infty} t c_2(t) dt - (V_2/V_1) \int_0^{+\infty} c_2(t) dt$$

but

$$Q_0 = 1/\beta T \int_0^{2\beta T} c_1(t) dt \quad \text{and} \quad V_0 = 1/\beta T \int_0^{2\beta T} c_2(t) dt$$

so that:

$$Q_0 = \{ F/\beta T \int_0^{+\infty} t c_2(t) dt - V_2 V_0 \} / V_1$$

..... A.III.5

Appendix IV

Techniques for Removing Oscillations due to to the Gibbs Phenomenon, from Step Functions generated by Summation of Fourier Series

The curve representing the sample compartment ligand concentration which is generated from the elution profile by means of the system transfer function and the summation of the Fourier components:

i.e.,

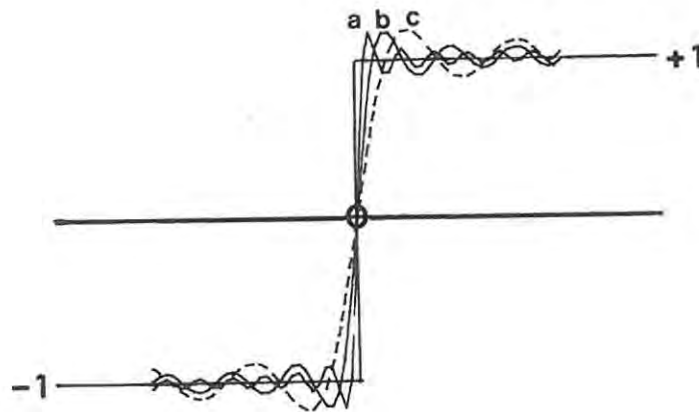
$$C_1(t) = \{Q_0/2 + \sum_{n=1}^N [P_n \sin(n\pi t/\beta T) + Q_n \cos(n\pi t/\beta T)]\}e^{\alpha t}$$

.... A.IV.1

contains oscillations occasioned by the step in the function at time $t = 0$. These oscillations decrease only gradually in amplitude for large t . Thus, the function represented by the summed Fourier series will only be a reliable approximation to the actual sample compartment ligand concentration for large t . A Fourier series representation of a function (as given by equation A.IV.1) represents the function exactly only if the sum contains an infinite number of terms. However, if the function satisfies the Dirichlet conditions (i.e., is piecewise continuous and piecewise monotonic) the frequency components will become vanishingly small for large n . The function obtained by the summation of a Fourier series containing only a finite number of terms will show its greatest deviation from the function it is meant to represent at the discontinuities (or sharp changes in the slope) of the latter. The Fourier series generated function,

intended to represent a function with a discontinuity or step, will (in the neighbourhood of the discontinuity) overshoot, pass through a maximum and oscillate about the correct value of the function (Stuart, 1966). This is the Gibbs phenomenon. The amplitude of the oscillations decreases with increasing distance from the discontinuity. The value of the overshoot does not depend on N , the number of terms used in the summation; it amounts to nearly 9% of the size of the discontinuity. The oscillations will decrease indefinitely in amplitude as N increases. The oscillations can thus be localized near the discontinuity by increasing the number of terms used in the summation. The maximum moves closer to the step as N increases (see Figure A.IV - I)

Figure A.IV - I



Oscillations in a Fourier series representation of a step function

- (a) Fourier series containing 50 terms
- (b) Fourier series containing 20 terms
- (c) Fourier series containing 10 terms

In the function representing the ligand concentration in the sample compartment of the dialysis cell as a function of time, there is a discontinuity at $t = 0$. This discontinuity arises from the rapid injection of the ligand into the cell at the commencement of the dialysis experiment. The analysis using Laplace transforms relies on the functions $C_1(t)$ and $C_2(t)$ being causal functions. However, because of the discontinuity at $t = 0$, the Fourier series representation of $C_1(t)$ will exhibit the Gibbs phenomenon.

A comparison of the total ligand concentrations in the sample compartment as a function of time is shown in Figure 9.8. The solid curve was generated from the analytical solutions of the system differential equations (equations 5.3.1a and 5.3.1b) and the broken curve obtained from the Fourier series representation of equation A.IV.1.

The analytical curve, which is the solution to the differential equations of the two compartment model dialysis cell, coincides with the curve generated from the elution profile by the mass balance relationship:

$$C_q(t) = C_1^*(0) - (V_2 C_2^*(t) + F \int_0^t C_2^*(t) dt) / V_1$$

.... A.IV.2

where

$C_q(t) = C_1(t)$ for the control dialysis ($C_2^*(t) = C_2(t)$
in equation A.IV.2)

and $C_1(t) = p\bar{v}(t) + C_1^*(t)$ for the sample dialysis

One method of smoothing out the oscillations in the function derived from the Fourier summation averages the oscillations by multiplying the Fourier components of the series by smoothing or weighting factors which have the form:

$$\frac{\sin[n\pi/(n-1)]}{\{n\pi/(n-1)\}} \quad (\text{Lanczos, 1953})$$

Thus, the Fourier summation becomes:

$$f(t) = \sum_{n=1}^N \frac{\sin(np)}{np} \{Q_n \cos(nqt) + P_n \sin(nqt)\} \quad \dots \quad \text{A.IV.3}$$

where $p = \pi/(n-1)$ and $q = \pi/\beta T$

The effect of including these weighting or σ factors into the analysis is shown in Figure 8.10. Although this method reduces the limiting value of the overshoot from 9% to about 1%, and effects a considerable reduction in the oscillations, it does not remove the initial rapid rise in the $C_q(t)$ vs t curves in the neighbourhood of $t = 0$.

An alternative method for eliminating the effect of the step, and increasing the rate of convergence of the Fourier coefficients with respect to n , is the technique of Krylov (Kantarovich & Krylov, 1964). These desirable results are achieved by removing from the Fourier series the slowly convergent parts which represent the step. The remainder is thus a rapidly convergent series, which does not display the Gibbs phenomenon. The slowly converging part which has been subtracted has an analytic sum to infinity which can be added back. It is necessary, however, when using this technique to determine how the Fourier coefficients converge for large n .

The Dirichlet conditions state that if the function represented by a Fourier series contains a discontinuity, either the Fourier coefficients of the sine series P_n or the Fourier coefficients of the cosine series Q_n (possibly both) will converge in inverse proportion to n . Thus P_n and/or Q_n (one of them at least) will converge as least as rapidly as g/n where g is a proportionality constant, for large n . Any remaining terms will converge as a higher order in n .

It was established for the sample compartment ligand concentration that the Fourier coefficients P_n of the sine series decrease in inverse proportion to n for large n . This was established from log-log, linear-log and reciprocal plots of the Fourier coefficients of $C_1(t)$, $C_1^*(t)$ and $C_1^t(t)$ with n . The decrease in the Fourier coefficients of the cosine terms is more rapid, and decreases inversely with the square of n for large n (cf. Figures A.IV.2a, b & c). The values for the proportionality constants can readily be established from the slope of the plot of P_n vs $1/n$ or by a regression procedure on the Fourier coefficients for fairly large n . A regression routine was incorporated into the computer program for processing the elution profile data, to provide the proportionality constant automatically.

Since the sine series decreases linearly with n for large n , the rate of convergence of the Fourier coefficients with n may be increased by subtracting g/n from the successive Fourier terms of the sine series. This corresponds to the subtraction of a ramp function from the function representing the sample compartment ligand concentration.

Thus the Fourier series for $C_1^t(t)$ is written as:

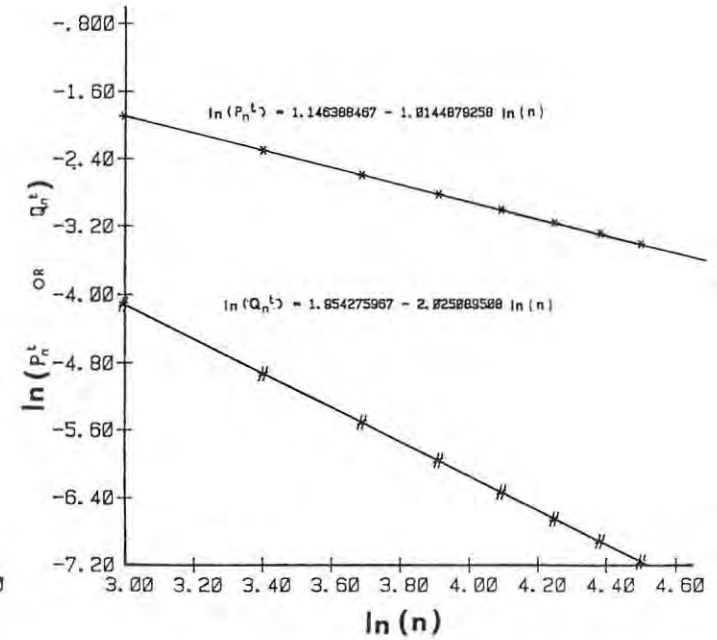
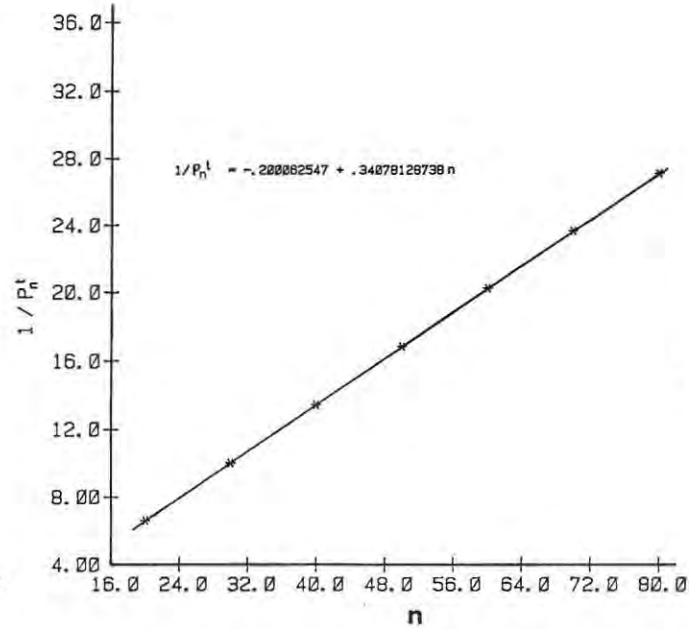
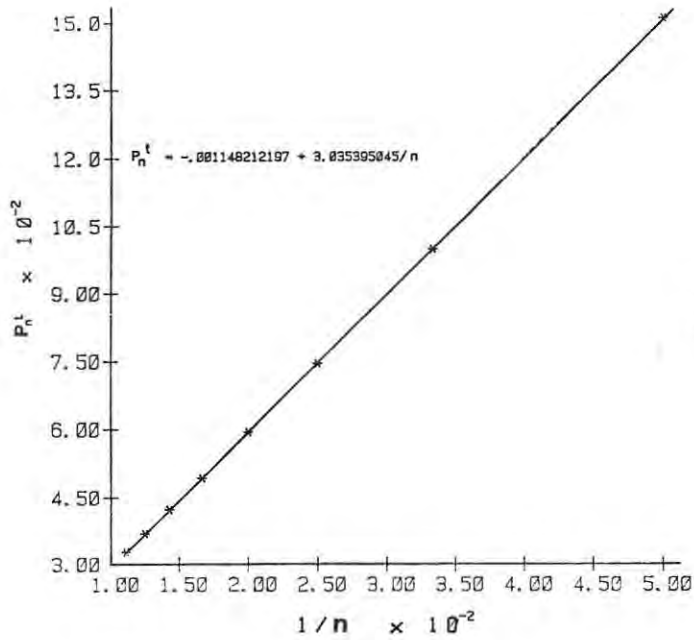
$$C_g(t) = \sum_{n=1}^N \{ [P_n - g/n] \sin(nqt) + Q_n \cos(nqt) \} + g \sum_{n=1}^N [\sin(nqt)]/n$$

..... A.IV.4

where $q = \pi/\beta T$ and the sum $\sum_{n=1}^N [\sin(nqt)]/n$ represents the

ramp function which has the values:

Figure A.IV-2



Semireciprocal and log-log plots of the sine series Fourier coefficients of $C_1^t(t)$ used to determine the rate of convergence with increasing n

$$R(t) = 0 \quad \text{for } t = -2\beta T, 0, +2\beta T$$

$$R(t) = g \pi(\beta T - t)/(2\beta T) \quad \text{for } 0 < t < 2\beta T$$

$$R(t) = -g \pi(\beta T - t)/(2\beta T) \quad \text{for } 0 > t > -2\beta T$$

The subtraction of the individual terms, g/n , from the Fourier coefficients of the sine components of the Fourier series is compensated for by the addition of the ramp $g \pi(\beta T - t)/2\beta T$ after summing the series:

$$C_1(t) = \sum_{n=1}^N \{ [P_n - g/n] \sin(nqt) + Q_n \cos(nqt) \} + g \pi(\beta T - t)/2\beta T$$

$$\text{for } 0 < t \leq 2\beta T$$

By this procedure, the Fourier coefficients of the ramp, which represent the slowly converging part of the Fourier sum, are effectively summed to infinity using the analytic expression for the sum. The remaining two series converge faster than the ramp. The errors introduced by truncating the summation of the remaining rapidly converging series after N terms, instead of summing an infinite number of terms, is thus greatly reduced. The term added in analytically is the full numeration to infinity of the ramp, and this therefore introduces no error. Since the slowly converging components of the Fourier series representation of $C_1(t)$ arise from the discontinuity, subtraction of the ramp also eliminates the initial rapid rise in $C_1(t)$ from the origin in the neighbourhood of $t = 0$.

It is possible to also speed up the convergence of the cosine components of the Fourier series by subtracting terms j/n^2 (here j is another proportionality constant) from the corresponding cosine terms in the Fourier series. However,

because of the relatively rapid decay of the cosine terms with increasing n (as $1/n^2$), this is not really necessary. Had the discontinuity in $C_1(t)$ not been at zero, a phase displacement would have occurred. This would have made it necessary to subtract corresponding terms from both the sine and the cosine components of the Fourier series (Wylie, 1975)

The effectiveness of the ramp subtraction in removing the step and oscillations from the Fourier series generated functions is demonstrated in figure 9.11a. The broken curve represents the sample compartment ligand concentration which was obtained from the mass balance relationship, while the solid curve is the function generated by the summation of the Fourier series which includes the ramp subtraction. The effectiveness of this procedure in smoothing the binding isotherm is shown by a comparison of figures 9.9 and 9.11.

Appendix VComputer Programs using FORTRAN #XFAE Compiler
for ICL 1900 Series Computer**Program ALPHA:** (not listed here)

A reformatting program, which reformats the elution profile data set from a linear array consisting of a single data entry per line to a block matrix array

Program BETA (not listed here)

An ICL graph plotting routine which is used to plot graphs of the data sets, the variation of the permeation constant with time, binding isotherms, etc.

Program GAMMA

An original program written to evaluate by means of the mass-balance relationship, and Fick's first law of diffusion, the permeation constant for the ligand from the elution profile of the control dialysis experiment. The program is also used to derive the binding isotherm from the elution profile of the sample dialysis data set, using the appropriate value for the permeation constant.

Program DELTA

An original program written to evaluate the system transfer function for the dialysis cell, and to evaluate the parametric equations of the binding isotherm (with time as a parameter) by means of this transfer function.

Program **EPSILON** (not listed here)

A program to provide equivalent transformations of the binding isotherm (e.g., the Bjerrum plot, the Scatchard plot, the Lineweaver-Burke plot, etc.)

Program **ZETA**

A non-linear least squares regression driver program for STEPIT (Chandler, 1965) to provide binding parameters by fitting the binding isotherm to an appropriate binding model.

Program **ETA**

A program to perform the step by step integration of the differential equations which describe the dialysis and elution processes in the dialysis system.

Appendix VI

```

1      PROGRAM GAMMA
2 C
3 C      THIS PROGRAM IS USED TO CALCULATE EITHER THE
4 C      PERMEATION CONSTANT FROM THE CONTROL ELUTION PROFILE
5 C      DATA SET, OR THE BINDING ISOTHERM FROM THE SAMPLE ELUTION
6 C      PROFILE DATA SET AND THE APPROPRIATE VALUE FOR THE
7 C      PERMEATION CONSTANT,
8 C
9      MASTER DIALYSIS
10     DIMENSION ITTL(40),CX(1200),DCX(1200),FCS(600)
11     DIMENSION CS(600),DCS(600),A(8),DD(600),CP(600)
12     COMMON CX,DCX
13 C
14 C      ITTL IS ALLOCATED FOR AN ALPHA-NUMERICAL TITLE
15 C
16     READ(5,100)ITTL
17     WRITE(6,100)ITTL
18 C
19 C      INPUT DATA
20 C
21 C      CIL IS THE INITIAL LIGAND CONCENTRATION (MOL)
22 C      CIP IS THE PROTEIN CONCENTRATION
23 C      F IS THE ELUTING BUFFER FLOW RATE
24 C      T IS THE SAMPLING INTERVAL (SECONDS)
25 C      V1 AND V2 ARE THE SAMPLE AND SINK COMPARTMENT VOLUMES
26 C      RESPECTIVELY
27 C      EPS IS THE MOLAR EXTINCTION COEFFICIENT OF THE LIGAND
28 C
29 C      THE ELUTION PROFILE DATA IS ENTERED AS NROW * 8
30 C      BLOCK MATRIX, WHERE NROW = NO. OF OBSERVATIONS/8
31 C      AND NOBS IS THE NUMBER OF DATA PINTS IN THE ELUTION
32 C      PROFILE
33 C      ZT IS THE ZERO TIME INTRVAL, I,E,, THE TIME LAPSING BETWEEN
34 C      THE INJECTION OF THE SAMPLE INTO THE CELL AND THE APPEARANCE
35 C      LIGAND IN THE SPECTROPHOTOETER FLOW CELL,
36 C      IDS IS THE PARAMETER FOR SELECTING THE OPTION OF
37 C      CALCULATING THE PERMEATION CONSTANT OR THE BINDING ISOTHERM
38 C      NIT IS THE PARAMETER FOR SELECTING THE QUANTITY OF
39 C      DATA OUTPUT - CALCULATION PERFORMED EVERY NIT DATA POINTS
40 C
41 C      NPTS IS THE NUMBER OF DATA POINTS USED IN THE
42 C      SAVITZKY-GOLAY RUNNING SMOOTH,
43 C      NPTS MUST 9,11,13,15,OR 17
44 C
45     READ(5,101)CIL,CIP,F,T,V1,V2,EPS
46     READ(5,102)NROW,ZT,IDS,NIT,NPTS
47     WRITE(6,100)ITTL
48     NOBS=8*NROW
49     NDATA=NOBS/2
50     IUVL=NDATA*7/8
51     JUVL=NOBS*7/8
52 C
53 C      PROGRAM SEGMENT TO REWRITE THE EXPERIMENT PRAMETERS
54 C
55     WRITE(6,70)CIL,CIP
56     70  FORMAT(5X,'LIGAND CONC. ',2X,E14,7,2X,'PROTEIN CONC. ',E14,7//)

```

```

57 WRITE(6,71)F,T
58 71 FORMAT(5X,'ELUTING BUFFER FLOW RATE '2X E14,7,1X'CC/SEC'/
59 * 5X,'SAMPLING INTERVAL',2X,F5,1/)
60 WRITE(6,72)V1,V2
61 72 FORMAT(5X,'SAMPLE COMPARTMENT VOLUME ',F6,3/
62 * 5X,'SINK COMPARTMENT VOLUME ',F6,3/)
63 WRITE(6,73)EPS
64 73 FORMAT(5X,' MOLAR EXTINCTION COEFFICIENT',2X,F10,2/)
65 100 FORMAT(40A2)
66 101 FORMAT(7G0,0)
67 102 FORMAT(10,F0,0,3I0)
68 IF(IDS,GT,0)READ(5,106)D
69 IF(IDS,GT,0)WRITE(6,73)D
70 75 FORMAT(5X,'PARAMETER OPTION SELECTED TO CALCULATE',
71 *1X,'THE BINDING ISOTHERM USING A VALUE OF ',E12,5,/
72 *5X,'FOR THE PERMEATION CONSTANT'/)
73 106 FORMAT(8G0,0)
74 DO 10 I=1,NROW
75 READ(5,103)A
76 DO 10 J=1,8
77 K=8*(I-1)+J
78 CX(K)=A(J)
79 10 CONTINUE
80 103 FORMAT(8G0,0)
81 TEMP=CX(1)
82 DO 12 J=2,NDATA
83 IF(TEMP=CX(J))11,11,12
84 11 TEMP=CX(J)
85 IMP=J
86 12 CONTINUE
87 TMAX=T*FLOAT(IMP)
88 WRITE(6,76)IMP,TMAX,TEMP
89 76 FORMAT(5X,'ELUTION PROFILE MAXIMUM IS DATA POINT'
90 *I4, /5X,'AT',1X,E11,4,1X,'SECONDS AFTER THE START'/
91 *5X,'AND HAS A VALUE OF',F6,3/)
92 C
93 DO 15 I=1,NOBS
94 IF(I,LE,1,OR,MOD(I,2),NE,1)GO TO 15
95 J=I/2+1
96 FCS(J)=SIMPSON(CX,I,T)
97 15 CONTINUE
98 FCS(1)=0,00
99 CALL SYSK(T,NOBS,NPTS)
100 600 FORMAT(1X,F6,1,2X,E14,7)
101 JLV=IMP*2,5
102 INVL=JLV/2
103 CALL SLOPEFIT(JLV,JUVL,NOBS,IDS,T)
104 C
105 C DO 17 IM=1,NDATA
106 C KM=2*IM
107 C DCS(IM)=DCX(KM)
108 C G=FLOAT(IM)
109 C 17 WRITE(6,600)G,DCS(IM)
110 C CONTINUE
111 DO 25 K=1,NDATA
112 JK=2*K
113 CS(K)=CX(JK)
114 DCS(K)=DCX(JK)
115 C FIX=FLOAT(JK)
116 C 25 WRITE(6,104)FIX,DCS(K)
117 IF(IDS)40,20,40

```

```

118      WRITE(6,77)
119      -77  FORMAT(5X,'PARAMETER OPTION SELECTED FOR CALULATION
120          *OF THE PERMEATON CONSTANT'/)
121  M 218
122      20  CONTINUE
123          N=0
124          DSM=0,0
125          DSQ=0,0
126          DO 30 I=1,NDATA
127              XT=ZT+2,0*FLOAT(I-1)*T
128              QL=V2*CS(I)+F*FCS(I)
129              CI=EPS*CIL=QL/V1
130              CP(I)=CI/EPS
131              DDNM=EPS*CIL=QL/V1-CS(I)
132              DNM=F*CS(I)+V2*DCS(I)
133              DD(I)=DNM/DDNM
134              IF(I,LT,INVL,OR,I,GT,IUVL)GO TO 28
135              N=N+1
136              DSM=DSM+DD(I)
137              DSQ=DSQ+DD(I)*DD(I)
138      28  CONTINUE
139          IF(MOD(I,NIT),NE,U)GO TO 30
140  C      WRITE(6,104)XT,DD(I),CI,CS(I),DCS(I),FCS(I),QL
141          WRITE(6,919)I,DD(I)
142  919  FORMAT(2X,I4,3X,E12,6)
143  C      WRITE(6,104)C1,FCS(I),DCS(I)
144      30  CONTINUE
145  C      WRITE(6,515)CP
146  515  FORMAT(5(2X,E10,4))
147  C      DO 32 I=1,NDATA
148  C          K=2+I-1
149  C          G=FLOAT(K)
150  C          WRITE(6,401)G,FCS(I)
151  C  32  CONTINUE
152  C      DO 33 K=1,NDATA
153  C          M=2+K-1
154  C          G=FLOAT(M)
155  C          WRITE(6,401)G,DCS(K)
156  C  33  CONTINUE
157  401  FORMAT(1X,F5,1,2X,E14,7)
158  C      STOP
159          DBAR=DSM/(FLOAT(N))
160          K=N-1
161          DVR=SQRT((DSQ=DSM*DSM/FLOAT(N))/FLOAT(K))
162          WRITE(6,500)N,DBAR,DVR
163  500  FORMAT(1X,'MEAN D FOR '1X,I3,1X,'VALUES IS ',E14,7/
164          *1X,'STD,DEV, ON D IS '1X,E14,7)
165  104  FORMAT(7(3X,E12,6))
166          GO TO 60
167      40  CONTINUE
168          DO 50 I=1,NDATA
169              XT=ZT+2,0*FLOAT(I)*T
170  45  CF=DCS(I)*V2/D+CS(I)*(1,0+F/D)
171              Q1=V1*CI*EPS
172              Q2=V1*CF
173              Q3=V2*CS(I)+F*FCS(I)
174              QB=Q1=Q2=Q3
175              CF=CF/(V1*EPS)
176  C      CP(I)=CF
177              CP(I)=CIL=Q3/(EPS*V1)
178              QB=QB/(V1*CIP*EPS)

```

```

179      NVL=INVL/2
180      IF(MOD(I,NIT),EQ,0,AND,I,GT,NVL)WRITE(6,108)CF,QB
181 C      IF(MOD(I,NIT),EQ,0)WRITE(6,108)XT,CF,QB,CS(I),DCS(I),PCS(I)
182      50 CONTINUE
183 C      WRITE(6,515)CP
184      108 FORMAT(6(2X,E10.4))
185      60 CONTINUE
186      STOP
187      END
188      SUBROUTINE SVSK(T,NOBS,NPTS)
189      DIMENSION CS(1200),DCS(1200),AMP(21)
190      COMMON CS,DCS
191      NUT=NPTS/2
192      NPO=NUT+1
193      NMO=NPTS-1
194      NNN=NPTS+1
195      DCS(1)=(CS(2)-CS(1))/T
196      DO 5 I=2,NUT
197      5 DCS(I)=(CS(I+1)-CS(I-1))/(2.0*T)
198      MOBS=NOBS-NPO
199      DO 6 J=1,NUT
200      K=MOBS+J
201      6 DCS(K)=(CS(K+1)-CS(K-1))/(2.0*T)
202      DCS(NOBS)=(CS(NOBS)-CS(NOBS-1))/T
203      M=NOBS-NMO
204      DO 10 I=2,NPTS
205      J=I-1
206      10 AMP(I)=CS(J)
207      DO 30 I=1,M
208      J=I+NMO
209      DO 15 K=1,NMO
210      KA=K+1
211      15 AMP(K)=AMP(KA)
212      AMP(NPTS)=CS(J)
213      SUM=0.0
214      SSM=0.0
215      DO 20 K=1,NUT
216      AM=FLOAT(NPO)-FLOAT(K)
217      SSM=SSM+AM*AM
218      N=NNN-K
219      BM=AM*(AMP(N)-AMP(K))
220      20 SUM=SUM+BM
221      SFC=2.0*SSM
222      KB=I+NUT
223      DCS(KB)=SUM/(SFC*T)
224      30 CONTINUE
225      RETURN
226      END
227      FUNCTION SIMPSON(F,N,H)
228      DIMENSION F(N)
229      SIMPSON=0.0
230      IF(N,LE,1,OR,MOD(N,2),NE,1)RETURN
231      SIMPSON=F(1)+4.0*F(2)+F(N)
232      J=N/2-1
233      IF(J,LE,0)GO TO 20
234      K=3
235      DO 10 I=1,J
236      SIMPSON=SIMPSON+2.0*F(K)+4.0*F(K+1)
237      10 K=K+2
238      20 SIMPSON=SIMPSON*H/3.0
239      RETURN

```

```

240      END
241      SUBROUTINE SLOPEFIT(INVL,IUVL,NOBS,IDS,T)
242      DIMENSION CS(1200),DCS(1200)
243      COMMON CS,DCS
244      SMX=0.0
245      SMY=0.0
246      SMXX=0.0
247      SMXY=0.0
248      N=0
249      DO 30 I=1,NOBS
250      IF(I,LT,INVL,OR,I,GT,IUVL)GO TO 30
251      N=N+1
252      II=I-1
253      DT=T*FLOAT(II)
254      SMX=SMX+DT
255      SMY=SMY+ALOG(CS(I))
256      SMXX=SMXX+DT*DT
257      SMXY=SMXY+DT*ALOG(CS(I))
258      30 CONTINUE
259      DNM=FLOAT(N)*SMXX=SMX*SMX
260      BN1=FLOAT(N)*SMXY=SMX*SMY
261      BN2=SMXX*SMY=SMX*SMXY
262      AYE=BN1/DNM
263      BEE=BN2/DNM
264      C WRITE(6,200)AYE,BEE
265      200 FORMAT(1X,2(1X,E14.7))
266      DO 40 I=INVL,NOBS
267      TIME=T*FLOAT(I-1)
268      DCS(I)=AYE*EXP(AYE*TIME+BEE)
269      40 CONTINUE
270      IF(IDS.NE.0) GO TO 50
271      ALPH=AYE
272      CFFT=EXP(BEE)
273      WRITE(6,300)CFFT,ALPH
274      300 FORMAT(/2X,'MONOEXPONENTIAL DECAY PARAMETERS'/5X,
275      *' AMPLITUDE = ',E14.7,5X,' EXPONENT, = ',E14.7/)
276      50 RETURN
277      END
278      FINISH

```

Appendix VII

```

1 C      PROGRAM DELTA
2 C
3 C      THIS PROGRAM PROVIDES THE BINDING ISOTHERM FROM THE
4 C      ELUTION PROFILE DATA SETS OF A CONTROL AND A SAMPLE
5 C      DILAYSIS EXPERIMENT BY MEANS OF THE SYSTEM TRANSFER
6 C      FUNCTION
7 C
8      MASTER DELTA
9      DIMENSION ROW(8),ALFA(2),CFFT(2),GNU(2),A(100),B(100),CNG(321)
10     DIMENSION CFRE(641),AMRT(100),ARLG(100),GEE(2)
11     DIMENSION PSTR(100),QSTR(100),PTOT(100),QTOT(100),CSMP(321)
12     DIMENSION TITLE(4,10),CSIN(3),CCS(3),CSNK(2,641),D(3)
13     DIMENSION U(2,100),V(2,100),PDSH(2),CFZ(2),CFX(2)
14     COMPLEX ESS,CPLC,ANMT,ADNM,ARTIO
15     DATA PI/3,141592654/
16 C
17 C      PROGRAM SEGMENT WHICH READS IN THE EXPERIMENTAL CONDITIONS
18 C      AND PARAMETERS
19 C
20     DO 2 I=1,4
21     2   READ(5,200)(TITLE(I,J),J=1,10)
22     READ(5,201)NOBS,NTRMS,ITEST
23     READ(5,202)CFZ(1),CFZ(2),PTN
24     READ(5,202)EPS,WVLN,TEMP
25     READ(5,202)FLW,OMEGA,DELTA
26     READ(5,202)V1,V2
27 C
28 C      DATA INPUT
29 C
30 C      LINES 1 - 4 RESERVED FOR NON-COMPUTABLE DATA
31 C      E,G. TITLE, DATE,LIGAND, PROTEIN
32 C      BUFFER PH AND CONCENTRATION ETC.
33 C
34 C      LINE 5  NOBS IS THE NUMBER OF DATA POINTS IN THE
35 C      ELUTION PROFILES (CONTROL & SAMPLE)
36 C      NTRMS IS THE NUMBER OF TERMS SUMMED IN THE
37 C      FOURIER SUMMATONS
38 C      ITEST IS AN OPTION PARAMETR
39 C
40 C      IF (ITEST.NE,0) THE PROGRAM CALCUATES THE SAMPLE COMPARTMENT
41 C      LIGAND CNCENTRATON BY A MASS-BALANCE, THE TRANSFR FUNCTION AND
42 C      THE POWER SERIES OF THE TRANSFER FUNCTION ARE ALSO
43 C      CALCULATED
44 C      IF (ITEST.EQ,0) THE BINDING ISOTHERM IS CALCULATED
45 C
46 C      LINE 6  LCFZ(1) IS THE INITIAL LIGAND CONCENTRATION IN THE
47 C      CONTROL DIALYSIS
48 C      CFZ(2) IS THE INITIAL LIGAND CONCENTRATON IN THE
49 C      SAMPLE DIALYSIS
50 C      PTN IS THE PROTEIN CONCENTRATON
51 C
52 C      LINE 7  EPS IS THE LIGAND EXTINCTION COEFICIENT
53 C      WVLN IS THE ABSORPTON WAVELENGTH FOR THE LIGAND
54 C      TEMP IS THE TEMPERATURE AT WHICH BINDING IS BEING STUDIED
55 C
56 C      LINE 8  FLW IS THE ELUTING BUFFER FLOW RATE
57 C      OMEGA IS THE FACTOR FOR THE HYPOTHETICAL EXTENSION
58 C      OF THE ELUTION PROFILE DATA SET
59 C      DELTA IS THE SAMPLING INTERVAL (SECONDS) (DELTA)
60 C
61 C      LINE 9  SAMPLE & SINK COMPARTMENT VOLUMES
62 C      (V1 & V2 RESPECTIVELY)

```

```

64 C   PROGRAM SEGMENT WHICH REWRITES EXPERIMENTAL PARAMETERS FOR
65 C   INSPECTION
66 C
67 C       GO TO 841
68 C
69 C       WRITE(6,300)(TITLE(1,J),J=1,10)
70 C       WRITE(6,301)(TITLE(2,J),J=1,4),(TITLE(3,J),J=1,4)
71 C       WRITE(6,302)TEMP,NOBS,DELTA
72 C       WRITE(6,303)
73 C       WRITE(6,304)(TITLE(2,J),J=1,4),CFZ
74 C       WRITE(6,304)(TITLE(3,J),J=1,4),PTN
75 C       WRITE(6,315)(TITLE(4,J),J=1,10)
76 C       WRITE(6,305)WVLN,EPS
77 C       WRITE(6,306)FLW
78 C       WRITE(6,325)V1
79 C       WRITE(6,326)V2
80 C       WRITE(6,307)NTRMS,OMEGA
81 C
82 C 841 CONTINUE
83 C   PROGRAM SEGMENT WHICH READS IN THE EXPONENTIAL DECAY
84 C   FACTORS AND CONVERGENCE FACTORS AND THE ELUTION
85 C   PROFILE DATA
86 C
87 C       NROW=NOBS/8
88 C       NGHT=8*NROW
89 C       NREM=NOBS-NGHT
90 C       CFX(1)=CFZ(1)*EPS
91 C       CFX(2)=CFZ(2)*EPS
92 C       J=1
93 C       5 CONTINUE
94 C       IF(J.NE.1)GO TO 10
95 C       WRITE(6,308)
96 C       GO TO 15
97 C 10 WRITE(6,310)
98 C
99 C       PARAMETRS USED FOR EXTENDING THE DATA STE BY A
100 C      ONOEXPONENTIAL DECAY FUNCTION (CONTROL)
101 C      ALFA: EXONENTIAL PARMETER
102 C      GNU: IS THE LAPACE CONVERGENCE PARAMETR
103 C 15 READ(5,202)ALFA(J),CFFT(J),GNU(J)
104 C      WRITE(6,309)ALFA(J),GNU(J)
105 C      WRITE(6,331)CFFT(J)
106 C      DO 20 I=1,NROW
107 C      READ(5,203)ROW
108 C      DO 20 IJ=1,8
109 C      K=8*(I-1)+IJ
110 C      CSNK(J,K)=ROW(IJ)
111 C 20 CONTINUE
112 C      IF(NREM.EQ.0)GO TO 26
113 C      READ(5,203)(KOW(K),K=1,NREM)
114 C      DO 25 L=1,NREM
115 C      M=NGHT+L
116 C 25 CSNK(J,M)=ROW(L)
117 C 26 CONTINUE

```

```

118 C
119 C   PROGRAM SEGMENT TO EVALUATE U(N) &V(N)
120 C
121     IF(MOD(NOBS,2),NE,0)GO TO 30
122     MOBS=NOBS+1
123     CSNK(J,MOBS)=2,0*CSNK(J,NOBS)-CSNK(J,NOBS-1)
124     GO TO 31
125 30  MOBS=NOBS
126 31  AYE=(ALFA(J)+GNU(J))
127     TDSH=FLOAT(MOBS)*DELTA/2,0
128     TEE=OMEGA*TDSH
129     XPNT=2,0*AYE*TDSH
130     EXX1=EXP(XPNT)
131     EXX2=EXP(OMEGA*XPNT)
132     ADE=AYE*AYE
133     E1=0,0
134     E2=0,0
135     DNTG=0,0
136     DO 60 NN=1,NTRMS
137     NN=NN-1
138     BEE=FLOAT(N)*PI/TEE
139     BEG=2,0*BEE*TEE/OMEGA
140     SNTG=0,0
141     CSTG=0,0
142     DEE=ADE+BEE*BEE
143     CS=COS(BEG)
144     SN=SIN(BEG)
145     ZN1=0,0
146     ZN2=0,0
147     CZ1=0,0
148     CZ2=0,0
149     DO 45 I=1,MOBS
150     TIME=DELTA*FLOAT(I-1)
151     GNUT=CSNK(J,I)*EXP(-GNU(J)*TIME)
152     E3=GNUT*TIME
153     ZN3=GNUT*SIN(BEE*TIME)
154     CZ3=GNUT*COS(BEE*TIME)
155     IF(I,EQ,1)GO TO 34
156     IF(I,EQ,2)GO TO 33
157     CSIN(1)=ZN1
158     CCS(1)=CZ1
159 33  CSIN(2)=ZN2
160     CCS(2)=CZ2
161 34  CSIN(3)=ZN3
162     CCS(3)=CZ3
163     ZN1=ZN2
164     ZN2=ZN3
165     CZ1=CZ2
166     CZ2=CZ3
167     IF(N,NE,0)GO TO 37
168     IF(I,EQ,1)GO TO 36
169     IF(I,EQ,2)GO TO 35
170     D(1)=E1
171 35  D(2)=E2
172 36  D(3)=E3
173     E1=E2
174     E2=E3
175 37  CONTINUE
176     IF(I,LT,3,OR,MOD(I,2),EQ,0) GO TO 45
177     IF(N,EQ,0)DNTG=(D(1)+4,0*D(2)+D(3))*DELTA/3,0+DNTG
178     IF(N,NE,0)SNTG=(CSIN(1)+4,0*CSIN(2)+CSIN(3))*DELTA
179     */3,0+SNTG
180 40  CSTG=(CCS(1)+4,0*CCS(2)+CCS(3))*DELTA/3,0+CSTG
181 45  CONTINUE
182     IF(N,EQ,0)PDSH(J)=CFFT(J)*EXX1*(1,0/ADE-2,0*TDSH/AYE)
183     */DNTG
184     UDSH=(EXX1*(BEE*CS-AYE*SN)-EXX2*BEE)/DEE
185 C   UDSH=EXX1*(BEE*CS+AYE*SN)/DEE
186     VDSH=(EXX2*AYE-EXX1*(AYE*CS+BEE*SN))/DEE
187 C   VDSH=EXX1*(AYE*CS+BEE*SN)/DEE
188 C
189 C400 WRITE(6,400)NN,SNTG,CSTG,DNTG,UDSH,VDSH,PDSH
190     IF(N,EQ,0) GO TO 50
191     U(J,NN)=SNTG+(CFFT(J)*UDSH)
192 50  V(J,NN)=CSTG+(CFFT(J)*VDSH)

```

```

193 C
194 C   PROGRAM SEGMENT TO EVALUATE A(N) & B(N)
195 C
196     IF(J,GE,2)GO TO 60
197     IF(N,NE,0)GO TO 55
198     Q0=FLW*PDSH(J)/(V1*TEE)-V2*CFX(J)/(FLW*TEE)
199     B(NN)=V(J,NN)/(Q0*TEE*TEE)
200     GO TO 60
201   55  ESS=CMPLX(-GNU(J),BEE)
202     CPLC=CMPLX(V(J,NN),-U(J,NN))
203     ANMT=ESS*CPLC
204     ADNMT=CFX(J)-ANMT*V2/V1=CPLC*FLW/V1
205     ARTIO=ANMT/ADNMT
206     A(NN)=-1,0*AIMAG(ARTIO)/TEE
207     B(NN)=REAL(ARTIO)/TEE
208   60  CONTINUE
209     WRITE(6,333)J,A(1),B(1),V(J,1),U(J,1),PDSH,Q0
210     WRITE(6,334)J,DNTG,PDSH(J),Q0
211   334  FORMAT(2X,12,3(2X,E14,7))
212   333  FORMAT(2X,12,3(2X,E14,7)/4X,3(2X,E14,7))
213     GO TO 840
214 C
215 C   PROGRAM SEGMENT TO PERFORM PRELIMINARY DIAGNOSTIC TESTS
216 C
217     IF(ITEST,EQ,0) GO TO 80
218     WRITE(6,311)
219 C
220 C   DIAGNOSTIC TEST #1
221 C
222 C   COMPARISON OF U(N) & V(N) WITH V(0)
223 C
224     WRITE(6,312)
225     WRITE(6,313)
226     DO 65 N=1,NTRMS
227     IF(N,EQ,1) U(J,N)=0,00
228     VZRO=V(J,1)
229     VEE=V(J,N)/TEE
230     EWE=U(J,N)/TEE
231     V3=V(J,N)/VZRO*100,0
232     U3=U(J,N)/VZRO*100,0
233     AMRT(N)=SQRT(U(J,N)*U(J,N)+V(J,N)*V(J,N))
234     AMRT(N)=AMRT(N)/TEE
235     ARLG(N)=ALOG10(AMRT(N))
236   65  CONTINUE
237 C 65  WRITE(6,330)N,EWE,U3,VEE,V3
238 C
239 C   GO TO 101
240 C
241 C   PROGRAM SEGMENT TO EVALUATE AND WRITE OUT THE
242 C   AMPLITUDE RATIO & LOG(AMPLITUDE RATIO)
243 C
244     WRITE(6,314)
245     DO 66 KK=1,NTRMS
246   66  WRITE(6,316)AMRT(KK)
247     WRITE(6,317)
248     DO 67 KM=1,NTRMS
249   67  WRITE(6,316)ARLG(KM)
250 C840  CONTINUE
251 C   GO TO 840
252 C

```

```

253 C   PROGRAM SEGMENT TO REGENERATE C2(T) FROM
254 C   V(N),U(N) & A(N),B(N)
255     WRITE(6,318)
256     WRITE(6,319)
257     WRITE(6,327)
258     WRITE(6,328)
259     WRITE(6,329)
260     V(J,1)=V(J,1)/2.0
261     KNOB=2*(MOBS=1)
262     DO 75 I=1,KNOB
263       TIME=FLOAT(I-1)*DELTA
264       TOTAL=0.0
265       DO 70 NN=1,NTRMS
266         FREQ=FLOAT(NN=1)*PI/TEE*TIME
267         EFF=U(J,NN)*SIN(FREQ)+V(J,NN)*COS(FREQ)
268     70  TOTAL=TOTAL+EFF
269         TOTAL=TOTAL*EXP(GNU(J)*TIME)/TEE
270 C     CDIFF=CSNK(J,I)-TOTAL
271         IF(CSNK(J,I).EQ.0)GO TO 75
272 C     CREL=CDIFF/CSNK(J,I)*100.0
273         ENI=FLOAT(I)
274 C     WRITE(6,330)I,CSNK(J,I),TOTAL,CDIFF,CREL
275         WRITE(6,332)ENI,TOTAL
276     75  CONTINUE
277         V(J,1)=2.0*V(J,1)
278     840 CONTINUE
279     80  CONTINUE
280         J=J+1
281         IF(J.LE.2.AND.ITEST.EQ.0)GO TO 5
282         J=J-1
283 C
284 C   PROGRAM SEGMENT TO EVALUATE P*(N) & Q*(N); P*TOTAL
285 C   AND Q*TOTAL
286 C
287         IF(ITEST.NE.0)J=1
288         DO 90 NN=1,NTRMS
289           DNM=A(NN)*A(NN)+B(NN)*B(NN)
290           IF(NN.NE.1)GO TO 85
291 C         V(J,NN)=0.5*V(J,NN)
292           QSTR(NN)=V(J,NN)/(B(1)*TEE+TEE)
293           PPST=QSTR(NN)
294           QSTR(NN)=QSTR(NN)/2.0
295           IF(J.EQ.1)GO TO 90
296 C         V(J,NN)=0.5*V(J,NN)
297           QTOT(NN)=FLW*PDSH(J)/(V1*TEE)-V2*V(J,NN)/(V1*TEE+TEE)
298           PPTT=QTOT(NN)
299           QTOT(NN)=QTOT(NN)/2.0
300           V(J,NN)=0.5*V(J,NN)
301 C         WRITE(6,330)NN,PPTT,PPST
302           WRITE(6,330)NN,V1,V2,EPS,FLW,TEE,CFX(J),J
303           WRITE(6,330)NN,PTOT(NN),PSTR(NN),QTOT(NN),QSTR(NN)
304 C         *      ,V(J,NN),U(J,NN)
305 C         *      WRITE(6,330)NN,PTOT(NN),QTOT(NN),V(1,NN),U(1,NN)
306 C         *      ,V(2,NN),U(2,NN)
307 C         GO TO 101
308         GO TO 90
309     85  CONTINUE
310           QSTR(NN)=(B(NN)*V(J,NN)+A(NN)*U(J,NN))/(DNM*TEE+TEE)
311           PSTR(NN)=(B(NN)*U(J,NN)-A(NN)*V(J,NN))/(DNM*TEE+TEE)
312           IF(J.EQ.1)GO TO 90
313           BEE=FLOAT(NN=1)*PI/TEE
314           ESS=CMPLX(-GNU(J),BEE)
315           ANMT=CMPLX(CFX(J)/TEE=FLW/V1*V(J,NN)/TEE,FLW/V1*U(J,NN)/TEE)
316           ADN=CMPLX(-V2/V1*V(J,NN)/TEE,V2/V1*U(J,NN)/TEE)
317           ARTIO=ANMT/ESS+ADN
318           QTOT(NN)=REAL(ARTIO)
319           PTOT(NN)=-AIMAG(ARTIO)
320           PPTT=SQRT(PTOT(NN)*PTOT(NN)+QTOT(NN)*QTOT(NN))
321           PPST=SQRT(PSTR(NN)*PSTR(NN)+QSTR(NN)*QSTR(NN))
322 C         WRITE(6,330)NN,PPTT,PPST
323 C         WRITE(6,330)NN,PTOT(NN),PSTR(NN),QTOT(NN),QSTR(NN),
324 C         *      V(J,NN),U(J,NN)
325 C         *      WRITE(6,330)NN,PTOT(NN),QTOT(NN),V(1,NN),U(1,NN),
326 C         *      ,V(2,NN),U(2,NN)
327     90  CONTINUE
328 C         GO TO 101

```

```

329 C
330 C PROGRAM SEGMENT TO REGENERATE C1(T)-- IF TEST OPTION HAS
331 C BEEN SELECTED-- OR C1*(T) AND THE BINDING ISOTHERM V'
332 C IF THE TEST OPTION HAS NOT BEEN SELECTED,
333 C
334 IF(ITEST, EQ, 0) WRITE(6, 320)
335 CNG(1)=0, 0
336 CSMP(1)=CFX(J)
337 MK=0
338 DO 94 IK=1, 2
339 INL=NTRMS=15
340 INU=INL+10
341 XRSM=0, 0
342 YRSM=0, 0
343 XRXR=0, 0
344 XRYR=0, 0
345 INDX=0
346 DO 93 ILL=INL, INU
347 INDX=INDX+1
348 XRN=1, 0/(FLOAT(ILL))
349 IF(IK, EQ, 1)YRN=PTOT(ILL)
350 IF(IK, EQ, 2)YRN=PSTR(ILL)
351 XRSM=XRSM+XRN
352 YRSM=YRSM+YRN
353 XRXR=XRXR+XRN*XRN
354 XRYR=XRYR+XRN*YRN
355 93 CONTINUE
356 XNDX=FLOAT(INDX)
357 GEE(IK)=(XNDX*XRYR-XRSM*YRSM)
358 GEE(IK)=GEE(IK)/(XNDX*XRXR-XRSM*XRSM)
359 94 CONTINUE
360 WRITE(6, 440)
361 WRITE(6, 430)GEE
362 WRITE(6, 440)
363 440 FORMAT(//)
364 C
365 C ESTABLISHMENT OF TIME FOR FOURIER SERIES
366 C
367 DO 99 I=1, NOBS
368 TIME=DELTA*FLOAT(I-1)
369 EXX=TIME*PI/TEE
370 FREE=0, 0
371 GNBR=0, 0
372 SMPL=0, 0
373 TOTL=0, 0
374 C IF(ITEST, EQ, 0)GO TO 95
375 IF(I, LT, 3, OR, MOD(I, 2), EQ, 0)GO TO 95
376 K=I/2+1
377 CNG(K)=(CSNK(J, I-2)+4, 0*CSNK(J, I-1)+CSNK(J, I))*DELTA/3, 0
378 CNG(K)=CNG(K)+CNG(K-1)
379 CSMP(K)=CFX(J)-(V2*CSNK(J, I)+FLW*CNG(K))/V1
380 95 CONTINUE
381 C GO TO 99
382 C

```

```

385 C      SUMMATION OF THE FOURIER SERIES
384 C
385 C      DO 97 NN=1,NTRMS
386 C      N=NN-1
387 C      FLN=FLOAT(N)
388 C      RHO=FLN*PI/TEE
389 C      PHI=RHO*TIME
390 C      ZIN=SIN(PHI)
391 C      COZ=COS(PHI)
392 C      EKS=PSTR(NN)*ZIN+QSTR(NN)*COZ
393 C      IF(J, EQ, 1) GO TO 96
394 C      ZED=PTOT(NN)*ZIN+QTOT(NN)*COZ
395 C      WHY=(PTOT(NN)-PSTR(NN))*ZIN
396 C      WHY=WHY+(QTOT(NN)-QSTR(NN))*COZ
397 C      PEE=V(J, NN)*COZ+U(J, NN)*ZIN
398 C      TOTL=TOTL+PEE
399 C      SMPL=SMPL+ZED
400 C      GNBR=GNBR+WHY
401 C      IF(N, EQ, 0) GO TO 96
402 C      SMPL=SMPL-GEE(1)*ZIN/FLN
403 C      GNBR=GNBR-(GEE(1)-GEE(2))*ZIN/FLN
404 C 96 CONTINUE
405 C      FREE=FREE+EKS
406 C      IF(N, EQ, 0) GO TO 97
407 C      FREE=FREE-GEE(2)*ZIN/FLN
408 C 97 CONTINUE
409 C      RAMP=(PI-EXX)/2.0
410 C      XXX=EXP(GNU(J)*TIME)
411 C      YHY=SMOOTHFOURIER(99, QTOT, PTOT, EXX)
412 C      YHY=YHY*XXX
413 C      IF(J, EQ, 1) GO TO 98
414 C      CTOT=(SMPL+GEE(1)*RAMP)*XXX
415 C      GNBR=(GNBR+(GEE(1)-GEE(2))*RAMP)*XXX
416 C      TOTL=TOTL+XXX/TEE
417 C 98 CFRE(I)=(FREE+GEE(2)*RAMP)*XXX
418 C      IF(J, EQ, 1, AND, ITEST, NE, 0) GO TO 99
419 C      CFRE(I)=CFRE(I)/EPS
420 C      VBAR=GNBR/(PTN*EPS)
421 C      WRITE(6, 321) CFRE(I), VBAR
422 C      IF(MOD(I, 2), NE, 0) MK=MK+1
423 C      IF(MOD(I, 2), NE, 0) WRITE(6, 330)
424 C      *I, CSNK(2, I), TOTL, CSMP(MK), CTOT, CFRE(I)
425 C      IF(MOD(I, 2), NE, 0) WRITE(6, 430) CSMP(MK), CTOT, TIME
426 C      IF(MOD(I, 2), EQ, 0) GO TO 99
427 C      WRITE(6, 430) CSMP(MK), CTOT
428 C 430 FORMAT(2(3X, E11, 5))
429 C 99 CONTINUE
430 C      IF(J, NE, 1, AND, ITEST, EQ, 0) GO TO 101
431 C      WRITE(6, 322)
432 C      WRITE(6, 323)
433 C      WRITE(6, 324)
434 C      NTWO=MOBS/2
435 C      DO 100 I=1, NTWO
436 C      K=2*I-1
437 C      WRITE(6, 321) CSNK(J, K), CSMP(I), CFRE(I)
438 C 100 CONTINUE
439 C 101 STOP
440 C

```

```

441 C   FORMAT STATEMENTS FOLLOW
442 C
443 200  FORMAT(10A8)
444 201  FORMAT(3I0)
445 202  FORMAT(3G0,0)
446 300  FORMAT(1H1, //10A8/)
447 301  FORMAT(5X, ' BINDING OF '4A8, /5X, ' TO '4A8/)
448 303  FORMAT(5X, 'EXPERIMENT PARAMETERS'//)
449 302  FORMAT(5X, 'ELUTION DIALYSIS CARRIED OUT AT ', F6.2,
450      *' DEGREES CENTIGRADE ' /
451      *5X, 'CONSISTING OF ', I4, ' DATA ENTRIES' /
452      *5X, 'RECORDED AT ', F6.2, ' SECOND INTERVALS'//)
453 304  FORMAT(5X, 4A8, 'CONCENTRATION ', G12.7, ' MM/ML, ' /)
454 305  FORMAT(5X, 'ABSORBANCE MEASUREMENTS RECORDED AT ', F5.1,
455      *' NM, ' /5X, 'EXTINCTION COEFFICIENT IS ', E12.6 /)
456 306  FORMAT(5X, 'ELUTION BUFFER FLOW RATE IS ', G11.5, ' MLS/SEC'//)
457 307  FORMAT(5X, 'NO. OF TERMS USED IN FOURIER SERIES = ', I4 /
458      *5X, 'LIMIT OF INTEGRATION = ', F5.2, ' TIMES THE ' /
459      *5X, 'DURATION OF THE DIALYSIS ' //)
460 308  FORMAT(1H1, //20X, ' CONTROL'//)
461 309  FORMAT(5X, 'EXPONENTIAL DECAY PARAMETER FOR ELUTION PROFILE' /
462      *5X, E11.5, ' /SEC ' /5X, 'CONVERGENCE PARAMETER ', E11.5, ' /SEC'//)
463 310  FORMAT(20X, 'ELUTION PROFILE WITH PROTEIN'//)
464 203  FORMAT(8G0,0)
465 311  FORMAT(1H1, //5X, 'PRELIMINARY TEST OPTION SELECTED'//)
466 312  FORMAT(//5X, 'COMPARISON OF U(N) & V(N) VALUES WITH V(0)'//)
467 313  FORMAT(7X, 'N', 7X, 'U(N)', 9X, 'U(N)/V(0)', 9X, 'V(N)',
468      *9X, 'V(N)/V(0)'//)
469 314  FORMAT(1H1, //5X, 'AMPLITUDE RATIOS'//)
470 315  FORMAT(4X, ' ELUTION BUFFER ', 2X, 10A8)
471 316  FORMAT(5X, E14.7)
472 317  FORMAT(1H1, //25X, 'LOG(AMPLITUDE RATIOS)'//)
473 318  FORMAT(1H1, //5X, 'REGENERATED ELUTION PROFILE'//)
474 320  FORMAT(1H1, //5X, 'FREE LIGAND CONC, '10X, 'BOUND LIGAND', 5X,
475      *'MML, LIGAND/MML, PROTEIN'//)
476 321  FORMAT(5X, G14.7, 5X, G14.7, 5X, G14.7)
477 322  FORMAT(1H1, //25X, 'SAMPLE COMPARTMENT LIGAND CONCENTRATION'//)
478 323  FORMAT(10X, 'GENERATED BY', 20X, ' GENERATED BY')
479 324  FORMAT(10X, 'MASS-BALANCE', 20X, 'TRANSFER FUNCTION'//)
480 325  FORMAT(5X, 'VOLUME OF SAMPLE USED ', F6.3, ' MLS, ' /)
481 326  FORMAT(5X, 'SINK COMARTMENT VOLUME ', F6.3, ' MLS, ' /)
482 319  FORMAT(5X, 'ORIGINAL ', 5X, 'REGENERATED ', 5X, 'DIFFERENCE ',
483      *5X, 'PERCENTAGE ' /)
484 327  FORMAT(5X, 'ELUTION ', 6X, 'ELUTION ', 6X, 'BETWEEN ',
485      *5X, 'ERROR ON' /)
486 328  FORMAT(5X, 'PROFILE ', 5X, 'PROFILE ', 6X, 'ORIGINAL & ',
487      *5X, 'ORIGINAL' /)
488 329  FORMAT(37X, 'GENERATED ', 5X, 'PROFILE' /38X, 'PROFILE' /)
489 330  FORMAT(2X, I3, 6(3X, E10.4), 2X, I3)
490 331  FORMAT(/5X, 'SCALING FACTOR FOR EXPONENTIAL DECAY EXPRESSION',
491      * /5X, E14.7 /)
492 332  FORMAT(5(2X, E12.5))
493      END
494      FINISH

```

Appendix VIII

```

1 C          PROGRAM ZETA
2 C
3 C          THE PROGRAM ZETA IS USED IN CONJUNCTION WITH THE PROGRAM
4 C          STEPIT ( BY J.P.CHANDLER 1965 ) TO OBTAIN BINDING
5 C          PARAMETERS BY FITTING THE OBSERVED BINDING ISOTHERM TO AN
6 C          APPROPRIATE BINDING MODEL, WHICH INCORPORATES THE
7 C          BINDING PARAMETERS, THE PROGRAM ENABLES THE DATA TO BE FITTED
8 C          TO A GENERALIZED BINDING MODEL (EQUATION 3.8.7), WHICH
9 C          CONTAINS BOTH REAL AND COMPLEX BINDING PARAMETERS,
10 C         THE PROGRAM PERMITS FIXED VALUES TO BE ASSIGNED TO
11 C         SELECTED PARAMETERS
12 C
13 C         MASTER PARAMETERS
14 C         DIMENSION X(20),XMAX(20),XMIN(20),DELTX(20),DELMN(20)
15 C         DIMENSION ERR(20,21),MASK(20)
16 C         DIMENSION A(250),B(250),TITLE(10)
17 C         COMMON /CSTEP/ X,XMAX,XMIN,DELTX,DELMN,
18 C         *      ERR,FOBJ,NV,NTRAC,MATRX,MASK,
19 C         *      NFMAX,NFLAT,JVARY,NXTRA,KFLAG,NOREP,KERFL,KW
20 C         COMMON /DTST/ A,B /PRMTRS/ IP
21 C
22 C         THE PARAMETERS IN THE COMMON DATA BLOCK /CSTEP/
23 C         ARE UTILIZED BY THE SUBROUTINE STEPIT
24 C
25 C         EXTERNAL FUNK
26 C
27 C
28 C         INPUT QUANTITIES..... FUNK,NV,NTRAC,MATRX,MASK,X,XMAX,XMIN,
29 C                               DELTX,DELMN,NFMAX,NFLAT,KW
30 C         OUTPUT QUANTITIES.... X,FOBJ,ERR,          KFLAG,NOREP,KERFL
31 C
32 C         FUNK      -- THE NAME OF THE SUBROUTINE THAT COMPUTES FOBJ
33 C                   GIVEN X(1),X(2),...,X(NV) (EACH SUCH
34 C                   SUBROUTINE MUST BE NAMED IN AN EXTERNAL
35 C                   STATEMENT IN THE CALLING PROGRAM)
36 C         NV        -- THE NUMBER OF PARAMETERS, X
37 C         NTRAC     -- =0 FOR NORMAL OUTPUT, =+1 FOR TRACE OUTPUT,
38 C                   =-1 FOR NO OUTPUT
39 C         MATRX     -- =0 FOR NO ERROR CALCULATION, =100+M FOR ERROR
40 C                   CALCULATION USING STEPS 10**M TIMES LARGER
41 C                   THAN THE LAST STEPS USED IN THE MINIMIZATION
42 C         FOBJ      -- THE VALUE OF THE FUNCTION TO BE MINIMIZED
43 C         MASK(J)   -- NONZERO IF X(J) IS TO BE HELD FIXED
44 C         X(J)      -- THE J-TH PARAMETER
45 C         XMAX(J)   -- THE UPPER LIMIT ON X(J)
46 C         XMIN(J)   -- THE LOWER LIMIT ON X(J)
47 C         DELTX(J)  -- THE INITIAL STEP SIZE FOR X(J)
48 C         DELMN(J)  -- THE LOWER LIMIT (CONVERGENCE TOLERANCE) ON THE
49 C                   STEP SIZE FOR X(J)
50 C         ERR(J,K)  -- RETURNS THE ERROR MATRIX IF -MATRX= IS NONZERO
51 C                   (ERR IS ALSO USED FOR SCRATCH STORAGE)
52 C         NFMAX     -- THE MAXIMUM NUMBER OF FUNCTION COMPUTATIONS
53 C         NFLAT     -- NONZERO IF THE SEARCH IS TO TERMINATE WHEN ALL
54 C                   TRIAL STEPS GIVE IDENTICAL FUNCTION VALUES
55 C         JVARY     -- STEPIT SETS JVARY NONZERO IF X(JVARY) IS THE ONLY
56 C                   X(J) THAT HAS CHANGED SINCE THE LAST CALL TO
57 C                   FUNK (THIS CAN BE USED TO SPEED UP FUNK)
58 C         NXTRA     -- USED BY SUBROUTINE SIMPLEX BUT NOT BY STEPIT
59 C         KFLAG     -- RETURNED ,GT, ZERO FOR A NORMAL EXIT,
60 C                   RETURNED ,LT, ZERO FOR AN ABNORMAL EXIT
61 C         NOREP     -- RETURNED ,GT, ZERO IF THE FUNCTION WAS NOT
62 C                   REPRODUCIBLE
63 C         KERFL     -- RETURNED ,LT, ZERO IF SUBROUTINE STERR
64 C                   TERMINATED ABNORMALLY
65 C         KW        -- THE LOGICAL UNIT NUMBER OF THE PRINTER
66 C
67 C         THE PARAMETERS IN THE COMMON DATA BLOCK /DTST/ ARE:
68 C         A      ARRAY OF FREE LIGAND CONCENTRATIONS
69 C         B      ARRAY OF QUANTITIES OF LIGAND BOUND
70 C               PER MOL OF PROTEIN,
71 C         IP IS THE NUMBER OF COMPLEX VARIABLES
72 C         USED IN THE BINDING MODEL

```

```

74 C      TITLE IS ALOCATED FOR AN ALPHANUMERIC TITLE (80 CHARACTERS)
75 C
76      READ(5,100)TITLE
77 100    FORMAT(10A8)
78      WRITE(6,100)TITLE
79      READ(5,110)(X(J),J=1,4)
80      READ(5,110)(XMAX(J),J=1,4)
81      READ(5,110)(XMIN(J),J=1,4)
82      READ(5,110)(DELT(X(J),J=1,4)
83      READ(5,110)(DELMN(J),J=1,4)
84 110    FORMAT(4G0,0)
85      READ(5,120)(MASK(J),J=1,4)
86      READ(5,120)NBS,NTRAC,MATRX,KW
87 120    FORMAT(4I0)
88      READ(5,130)NV,NFMAX,NFLAT,IP
89 130    FORMAT(4I0)
90      DO 10 K=1,NBS
91      READ(5,140)A(K),B(K)
92 10     CONTINUE
93 140    FORMAT(2G0,0)
94      CALL FUNK
95      CALL STEPT (FUNK)
96      STOP
97      END
98      SUBROUTINE FUNK
99 C
100 C      THIS SUBROUTINE EVALUATES THE SUM OF THE SQUARES
101 C      OF THE RESIDUALS BETWEEN THE OBSERVED B AND VBAR, THE
102 C      QUANTITY OF LIGAND BOUND TO THE PROTEIN, CALCULATED
103 C      ON THE BASIS OF THE MATHEMATICAL MODEL
104 C/
105      COMMON /CSTEP/ X(20),XMAX(20),XMIN(20),DELT(X(20),DELMN(20),
106 *          ERR(20,21),FOBJ,NV,NTRAC,MATRX,MASK,
107 *          NFMAX,NFLAT,JVARY,NXTRA,KFLAG,NOREP,KERFL,KW
108      COMMON /DTST/ A(250),B(250) / PRMTRS / IP
109      TOTL=0,0
110      DO 40 J=1,NOBS
111      CF=A(J)
112      PHI=0,0
113      IF(IP,Q,0)GO TO 20
114      DO 10 I=1,IP
115 10     PHI=PHI+CF*(X(2*I-1)+2,0*CF*X(2*I)/
116 *      (X(2*I)*CF+CF+2,0*X(2*I-1)*CF+1,0)
117 20     IP2=2*I
118      MM=(NV-IP2)/2
119      IF(MM,EQ,0)GO TO 50
120      DO 30 I=1,MM
121 30     PHI=PHI+X(IP2+2*I-1)*CF/(CF-X(IP2+I))
122      DFSQ=(B(I)-PHI)**2
123 40     TOTL=TOTL+DFSQ
124      FOBJ=TOTL
125 50     RETURN
126      END
127      SUBROUTINE STEPT (FUNK)

```

Appendix IX

PROGRAM ETA

```

MASTER DIFF
C
C
C PROGRAM TO PERFORM A STEP BY STEP INTEGRATION OF
C THE DIFFERENTIAL EQUATIONS WHICH DESCRIBE THE DIALYSIS OF
C A PROTEIN LIGAND SYSTEM FOR ONE OR TWO SITE BINDING
C MODELS
C DIMENSION Y(3),YP(3),XX(201),YY(201),ZZ(201)
C COMMON CFZ,PTN,NSTS
C READ(5,100)NSTS,IEQN
C
C *****
C NSTS = NO. OF DIFFERENT CLASSES OF BINDING SITES
C IEQN = OPTION PARAMETER TO SELECT EULER OR RUNGE KUTTA METHOD
C
C IEQN <= 0 FOR EULER METHOD
C IEQN > 0 FOR RUNGE KUTTA METHOD
C
C *****
105 FORMAT(2I0)
C READ(5,101)TSTS,TFNL,DELT
C
C *****
C TSTS = INITIAL TIME VALUE
C TFNL = FINAL TIME VALUE
C DELT = TIME INCREMENT OR SAMPLING TIME INTERVAL
C
C *****
C READ(5,102)CFZ,PTN
C
C *****
C CFZ = INITIAL TOTAL LIGAND CONCENTRATION
C PTN = PROTEIN CONCENTRATION.
C
C *****
C
M=1
Y(1)=TSTS
Y(2)=CFZ
Y(3)=0,0
XX(1)=Y(1)
YY(1)=Y(2)
ZZ(1)=Y(3)
TRNG=(TFNL-TSTS)/DELT
IRNG=IFIX(TRNG)
IF(IRNG.GT,200)GO TO 40
DO 30 N=2,IRNG
XX(N)=TSTS+FLOAT(N)*DELT
IF(IEQN)10,10,20
10 CALL EULER(Y,YP,F,IRNG,DELT)
GO TO 25
20 CALL RKG(Y,YP,F,IRNG,DELT)
25 YY(N)=Y(2)
ZZ(N)=Y(3)
30 CONTINUE
DO 35 IK=1,IRNG
WRITE(6,300)XX(IK),YY(IK),ZZ(IK)
35 CONTINUE
300 FORMAT(3(5X,F14,5))
GO TO 45
40 WRITE(6,200)
101 FORMAT(3G0,0)
102 FORMAT(2G0,0)
200 FORMAT(5X,'TOO MANY POINTS')
45 CONTINUE
STOP
END

```

SUBROUTINE EULER (Y,YP,F,N,H,M)

C ADVANCES INTEGRATION OF N FIRST ORDER AUTONOMOUS DIFFERENTIAL
 C EQUATIONS $Y'(J)=F(J)$ BY ONE STEP USING THE EULER
 C PROCESS. AN AUXILIARY ROUTINE DYBYDY (Y,F,N) MUST BE PROVIDED
 C TO EVALUATE F(J) FOR EACH EQUATION USING THE CURRENT VALUES OF
 C Y(J) AND F(J). OTHER PARAMETERS MUST BE HANDLED BY 'COMMON'
 C BLOCKS. IF THE EQUATIONS ARE NOT AUTONOMOUS, THE PROCEDURE IS
 C TO ADD AN EXTRA TRIVIAL EQUATION AT THE START OF THE SET, NAMELY
 C $F(1)=1.0$, AND TO TREAT Y(1) AS THE INDEPENDENT VARIABLE,
 C FOR EXAMPLE TO SOLVE THE EQUATION $Y'=X-2*Y$ WE WOULD DEFINE
 C $Y(1)=X$ $F(1)=1.0$
 C $Y(2)=Y$ $F(2)=Y(1)-2.0*Y(2)$
 C N IS THE NUMBER OF EQUATIONS. H IS THE STEP SIZE,
 C M=1 ON FIRST ENTRY, M=0 OTHERWISE, BUT TO 'RESTART' AT ANY OTHER
 C POINT WITH, E.G. ANOTHER STEP SIZE, M IS RESET TO 1 IN THE CALLING
 C ROUTINE. YP IS AN ARRAY CONTAINING THE RESULTS OF THE 'PREDICTOR' STEP

```

      DIMENSION Y(N),F(N),YP(N)
      CALL DYBYDY (Y,F,N)
      DO 10 I=1,N
        Y(I)=Y(I)+H*F(I)
10     YP(I)=Y(I)
      RETURN
      END
  
```

SUBROUTINE RKG (Y,YP,F,N,H,M)

C ADVANCES INTEGRATION OF N FIRST ORDER AUTONOMOUS DIFFERENTIAL
 C EQUATIONS $Y'(J)=F(J)$ BY ONE STEP USING THE RUNGE KUTTA GILL
 C PROCESS. AN AUXILIARY ROUTINE DYBYDY (Y,F,N) MUST BE PROVIDED
 C TO EVALUATE F(J) FOR EACH EQUATION USING THE CURRENT VALUES OF
 C Y(J) AND F(J). OTHER PARAMETERS MUST BE HANDLED BY 'COMMON'
 C BLOCKS. IF THE EQUATIONS ARE NOT AUTONOMOUS, THE PROCEDURE IS
 C TO ADD AN EXTRA TRIVIAL EQUATION AT THE START OF THE SET, NAMELY
 C $F(1)=1.0$, AND TO TREAT Y(1) AS THE INDEPENDENT VARIABLE,
 C FOR EXAMPLE TO SOLVE THE EQUATION $Y'=X-2*Y$ WE WOULD DEFINE
 C $Y(1)=X$ $F(1)=1.0$
 C $Y(2)=Y$ $F(2)=Y(1)-2.0*Y(2)$
 C N IS THE NUMBER OF EQUATIONS. H IS THE STEP SIZE,
 C M=1 ON FIRST ENTRY, M=0 OTHERWISE, BUT TO 'RESTART' AT ANY OTHER
 C POINT WITH, E.G. ANOTHER STEP SIZE, M IS RESET TO 1 IN THE CALLING
 C ROUTINE. YP IS AN ARRAY CONTAINING THE RESULTS OF THE 'PREDICTOR' STEP

```

      DIMENSION Y(N),F(N),YP(N),Q(20)
      IF (M,EQ,0) GO TO 20
      DO 10 I=1,N
        Q(I)=0.0
10     M=0
20     DO 90 J=1,4
          CALL DYBYDY (Y,F,N)
          DO 90 I=1,N
            A=Y(I)
            B=H*F(I)
            C=Q(I)
            GO TO (30,40,60,70) , J
30     D=.5
          E=D*B=C
          GO TO 80
40     D=.29289321881
          E=D*(B-C)
          GO TO 80
60     D=1.70710678119
          GO TO 50
70     D=.5
          E=.166666666667*(B-C=C)
80     E=E+A=A
          Y(I)=A+E
90     Q(I)=3.0*E-D*B+C
          DO 100 I=1,N
100    YP(I)=Y(I)
      RETURN
      END
  
```

```

SUBROUTINE DYBYDY(Y,F,N,NSTS)
DIMENSION Y(3),F(3)
COMMON CFZ,PTN,NSTS
N1=0
N2=0
K1=0.0
K2=0.0
F(1)=1.0
TERM=1.0
READ(5,103)V1,V2,D,F

C
C *****
C
C     V1 = SAMPLE COMPARTMENT VOLUME
C     V2 = SINK COMPARTMENT VOLUME
C     D  = PERMEATION CONSTANT,
C     F  = ELUTION BUFFER FLOW RATE,Z
C     IF(NSTS,EQ,0)GO TO 30
C     READ(5,151)N1,K1
C
C *****
C
C     N1 = NO. OF BNDG SITES IN FIRST CLASS OF BINDING SITES.
C
C     K1 = BINDING CONSTANT FOR FIRST CLASS OF BINDING SITES.
C
C *****
C
C     TERM=PTN*(N1*K1)*(1.0-K1*X/(1.0+K1*X))/(1.0+K1*X)
C     IF(NSTS,EQ,1)GO TO 30
C     READ(5,151)N2,K2
C
C *****
C
C     N2 = NO. OF BNDG SITES IN SECOND CLASS OF BINDING SITES.
C
C     K2 = BINDING CONSTANT FOR SECOND CLASS OF BINDING SITES.
C
C *****

SCND=PTN*N2*K2*(1.0-K2*X/(1.0+K2*X))/(1.0+K2*X)
TERM=TERM+SCND
30 F(2)=D*(Y-X)/(V1*TERM)
F(3)=D*(X-Y)-FLW*Y)/V2
RETURN
END

```

Bibliography

- Adair G.S. (1925) J. Biol. Chem. 63 529 -
- Alberty R.A. & Marvin H.H (1951) J. Am. Chem. Soc. 73 3220 -
- Allen J.B. (1970) J. Am. Inst. Aeronautics & Astronautics
8 414 - 423
- Amundsen A.R. Whelan J. & Bosnich B. (1977)
J. Am. Chem. Soc. 99 (20) 6370 -
- Anastassiadis R.A. & Common R.H. (1958) Canadian J. Biochem. 36 413
- André J.C. Vincent L.M. O'Conner D. & Ware W.R. (1979)
J. Phys. Chem. 83 (17) 2285 -
- Arridge R.C.G. (1977) Spectrum (U.K.) 15 (1) 47 -
- Ashgar K. & Roth L.J. (1971) Biochem. Pharmac. 20 3151 -
- Bailey A.J. (1968) Biochem. Biophys. Acta 160 447 -
- Bailey A.J. (1975) Colston Papers 26 115 -
- Bailey A.J. Peach C.M. & Fowler L.J. (1970) Biochem. J. 117 819 -
- Bancroft J.C. & Johnston R.H. (1973) Proc. IEEE 61 (4) 472 -
- Barnes C. (1934) Physics 5 4 -
- Barrie J.A. Spencer H.G. & Quig A. (1975)
J. Chem. Soc. Faraday Trans 1 71 (12) 2459 -
- Bazin S. & Delauney A. (1976) In "The Methodology of
Connective Tissue Research" (D.A. Hall Ed.)
Joynton-Bruvvers Ltd. London
- Bear R.S. (1952) Adv. Prot. Chem. 7 70 -
- Behm M.L. & Wagner J.G. (1979)
Res. Comm in Chem. Path. & Pharmacol. 26 (1) 145 -
- Bianci E. Rampone R. Tealdi A. Cifferri A (1970)
J. Biol. Chem. 245 (13) 2341
- Bjerrum N. (1923) Z. Physik. Chem. 1 45 -
- Bjerrum J. (1941) in 'Metal Ammine Formation in Aqueous Solution'
(P Haase & Sons Copenhagen) 660 -
- Blake C.C.F. & Oatley S.J. (1977) Nature (London) 268 115 -
- Bornstein P. & Nesse R. (1970) Arch. Biochem. Biophys. 138 443 -

- Bose S.M. Rao V.H. Verbruggen C. (1976)
J. Belg. Rhumatol. Med. Phys. 31 (3) 153 -
- Botherby A.A. & Gassend R. (1973) *Ann. N.Y. Acad. Sci.* 222 668 -
- Bowden J.K. Chapman J.A. & Wyman C.H. (1968)
Biochem. Biophys Acta 154 190 -
- Bowmer C.J. & Lindup W.E. (1978) *J. Pharm. Sci.* 67 (8)
- Bracewell R.N. Roberts J.A. (1954) *Aust. J. Physics*
7 615 - 640
- Bracewell R.N. (1965) 'The Fourier Transform and its
 Applications' McGraw-Hill N.Y. 179 - 181
- Bracewell R.N. (1978) 'The Fourier Transform and its Applications'
 Second Ed. McGraw-Hill N.Y.
- Braumbaugh E.E. Ackers G.K. (1971) *Anal. Biochem.* 41 543 -
- Brigham E.O. (1974) 'The Fast Fourier Transform' Prentice-Hall
- Bryson A.W. Glasser D. Karstaedt N.E. (1975)
 Unpublished
- Buchan T.J. Haggis G.H. Halstead J.B. & Robinson B.G. (1952)
Proc. Roy. Soc. A 213 379 -
- Bush M.T. Alvin J.D. (1973) *Ann. N.Y. Acad. Sci. (U.S.)* 226 36
- Byers P.M. Click E. Harper E. & Bernstein (1975)
Proc. Nat. Acad. Sci. 72 (8) 3009 -
- Campbell G.A. & Forster R.M. (1948)
 'Fourier Integrals for Practical Application' Wiley. N.Y.
- Cann J.R. (1978) In 'Methods in Enzymology' 48 299 -
- Carr C.W. (1953) *Arch. Biochem. Biophys.* 46 417 -
- Carr C.W. (1961) *Phys. Methods Chem. Anal.* 4 1 -
- Cassel J.M. (1966) *Biopolymers* 4 989 -
- Cassel J.M. Steinhardt J. (1969) *Biochemistry* 8 2603 -
- Chandler J. (1965) *Quant. Chem. Program Exchange* 11 307
- Chatterjee & Chatoraj (1979) *Indian J. Biochem. & Biophys.* 16 158 -
- Chignall C.F. (1969) *Molec. Pharm.* 5 244 -
- Chignall C.F. (1973) *Ann. N.Y. Acad. Sci.* 226 44 -
- Clark P. Rachinsky M.R. & Foster J.F. (1962)
J. Biol. Chem. 237 2509 -
- Cody V. (1980) *Proc. Intl. Thyroid Res.* 8 268 -

- Coleman J.E. (1968) *J. Biol. Chem* 243 4574 -
- Colowick S.P. Womack F.C. (1969) *J. Biol. Chem.* 244 774 -777
- Colowick S.P. Womack F.C. (1973) *Methods Enzymol.* 27
- Comisarow M.B. Melka J.D. (1979) *Anal. Chem.* 51 (13) 2198 -
- Cooley J.W. Tukey J.W. (1965) *Math. Comput.* 19 297 -
- Cooney D.O. (1980) *Anal. Chem.* 52 1068 -
- Craig L.C. Chen M.C. (1969) *Anal. Chem.* 41 590 -
- Craig L.C. Chen M.C. (1972) *Proc. Natl. Acad. Sci (USA)* A69 702 -
- Craig L.C. King T.A. & Stracher A (1957)
J. Am. Chem. Soc. 79 3729 -
- Crank J. (1956) 'The Mathematics of Diffusion' Second Ed.
Clarendon Press Oxford
- Crookes M.J. Brown K.F. (1973) *J. Pharm. Sci.* 62 1904 -
- Crookes M.J. Brown K.F. (1973) *Pharm. Acta Helv.* 48 494 -
- Dayhoff E. (1972) 'Atlas of Protein Chemistry' & Supplements
(1972 - 1976) Natl. Biomed. Research Foundation.
- Dearden J.C. Tomlinson E. (1970) *J. Pharm. Sci.* 22 Suppl. 53S -
- Debye P. Hückel E (1923) *Z Physik Chem* 24 198 -
- De Levie R. Srinivasan S. & Czekaj P. (1978)
Anal. Chem. 50 (1) 110 -
- Deshmukh K. & Nimni M.E. (1969) *J. Biol. Chem.* 244(7) 1787 -
- Deshmukh K. & Nimni M.E. (1971) *Biochemistry* 10 9 -
- Doluiso J.T. Crouthamel W.G. Tan G.H. Swintosky J.V. & Dittert L.
(1970) *J. Pharm. Sci.* 59 (1) 72 -
- Drake M.P. Davison P.F. Bump S. Schmit F.O. (1966)
Biochemistry 5 301 -
- Duggleby R.G. (1980) *Eur. J. Biochem.* 109 93 -
- Eastoe J.E. (1967) in 'Treatise of Collagen' Vol. I
(G.N.Ramachandran, Ed) Academic Press. N.Y. Chapter II
- Eastoe J.E. Courts A. (1963) 'Practical Analytical Methods for
Connective Tissue Proteins' F.N.Spon Ltd. London Chapter II
- Edsall J.T. & Wyman J. (1958) In 'Biophysical Chemistry' Vol.1
Academic Press N.Y. Chapters 5 & 8

- Eftink M. Biltonen R. (1980) *Biol. Microcalorium*
(A.E. Beezer Ed.) 343 -
- Einstein A. (1908) *Z.Elektrochem.* 14 235 239
- El Nimr A. Hardee G.E. & Perrin J.H. (1981)
J.Pharm. Pharmac. 33 (2) 117 -
- Fairclough G.P. Fruton J.S. (1966) *Biochemistry* 5 673 -
- Farrel P.C. Popovich R.P. & Babb A.L. (1971)
J. Pharm. Sci 60 (10) 1471 -
- Feldman H.A. (1972) *Anal. Biochem.* 48 (2) 317 -
- Ferguson-Miller S. Koppenol W.H. (1981) *Trends Biochem. Sci.* 6 (7) 4 -
- Ferry J.D. (1936) *Chem Rev.* 18 373 -
- Fessler L.I. Morris N.P. Fessler J.H. (1975)
Proc. Natl. Acad. Sci. (USA) 72 (12) 4905 -
- Fletcher J.E. (1977) *J. Phys. Chem.* 81 (25) 2374 -
- Fletcher J.E. Spector A. (1968) *Comput. Biomed. Res.* 2 164 -
- Fletcher J.E. Spector A. & Ashbrook J.D. (1970)
Biochemistry 9 (23) 4580 -
- Fletcher J.E. Spector A. & Ashbrook J.D. (1970)
Biochemistry 10 (17) 3229 -
- Fletcher J.E. Spector A.A. (1977a) *Molecular Pharmacology.*
13 387 -
- Fletcher J.E. Spector A.A. (1977b) *J. Phys. Chem.* 81 (25) 2374 -
- Friedman M.H. McCally R.L. (1972) *Science* 175 556 -
- Fujii K. Tanzer M.L. & Cooke M. (1976) *J. Mol. Biol.* 106 (1) 223 -
- Furthmayr H. Beil W. Timpl R. *FEBS Lett.* 12 341 -
- Gäbler E. Franke R. & Oehme P. (1976)
Beitrage zur Wirkstoffforschung 11 2 -
- Gäbler E. (1977) *Pharmazie* 32 m.12 739 -
- Gane R. & Ingold C.K. (1931) *J. Chem. Soc.* 2153 -
- Gilbert G.A. & Jenkins R.C.L (1960) *Proc. Roy. Soc. A-* 253 420 -
- Ginsburg M. & Ireland M. (1964) *J.Endocrinol* 30 131 -
- Goldstein A. (1949) In 'Pharmacological Review' Vol I 102 -
(H. Williams & J. Wilkins, Ed.) Baltimore
- Gonzales R.C. & Winz P. (1977) 'Digital Image Processing'
Addison-Wesley Reading Masachussets.

- Gould S. (1968) 'Treatise on Collagen' Part II
Academic Press London
- Grant M.E. & Jackson D.S. (1968) *Biochem. J.* 108 587 -
- Grassman W. Nordwig A. Hörmann H. (1961)
Hoppe Seyler's *Z Physiol. Chem.* 323 48 -
- Greenberg J. (1969) M.Sc. (Chem. Eng.) Dissertation
University of the Witwatersrand, Johannesburg S.A.
- Gross J. & Schmitt F.O. (1948) *J. Am. Leather Chem. Assn.* 43 658 -
- Gross J. Highberger J.H. & Schmitt F.O. (1954)
Proc. Natl. Acad. (USA) 40 679 -
- Gross J. Highberger J.H. & Schmitt F.O. (1955)
Proc. Nat. Acad. (USA) 41 1 -
- Gross J. (1958) *J. Exp. Med.* 107 247 -
- Grove W.E. (1966) In 'Brief Numerical Methods' Prentice-Hall N.J.
- Güntelberg A.V. & Linderstrøm-Lang K. (1949)
Compt. Rend, Trav Lab 15 (7) Carlsberg Ser. Chim 27 1
- Gustavson K.H. (1956) 'The Chemistry and Reactivity of
Collagen' Academic Press N.Y. Page 156 -
- Halfman C.J. & Nishida (1972) *Biochemistry* 11 (18) 3493 -
- Halfman C.J. & Steinhardt J. (1971) *Biochemistry* 10 (19) 3564 -
- Hamming R.W. (1973) In 'Numerical Methods for Scientists &
Engineers' Second Ed. McGraw-Hill Pg. 532 -
- Hannig K. Nordwig A. (1967) In 'Treatise on Collagen'
(Ed. G.N.Ramachandran) Academic Press London Chapter II
- Hanstein W.G. (1979) *J. Solid Phase Biochem.* 4 (3) 189 -
- Harborne J.B. Mabry T.J. & Mabry H. (1975) "The Flavanoids"
Chapman & Hall London
- Harlan J.W. Fairheller S.H. (1977) *Adv. Exp. Med. Biol.* 86A 425 -
- Harris F.J. (1978) *Proc. I.E.E.E.* 66 (1) 51 - 83
- Heald A.F. & Sampat M.S. (1978) *Annals. Clin. Libr. Sci.* 8 239 -
- Highberger J.H. Gross J. Schmitt F.O. (1950)
J. Am. Chem. Soc. 72 3321 -

- Highberger J.H. Gross J. Schmitt F.O. (1951)
 Proc. Natl. Acad. Sci. (USA) 37 286 -
- Hill T.L. (1955) Arch. Biochem. Biophys. 57 299 -
- Hill T.L. (1960) In 'Introduction to Statistical Thermodynamics'
 Addison-Wesley, Massachusetts
- Hoch H. & Williams (1958) Anal. Chem. 30 (7) 1258 -
- Hoch H. & Turner M.E. (1960) Biochem. Biophysica. Acta 38 410 -
- Hoch H. & Miller P.O. (1966) Anal Chem. 38 658 -
- Hodge A.J. & Schmitt F.O. (1960)
 Proc. Natl. Acad. Sci (US) 46 186 -
- Hodge A.J. Petrushka J.A. Bailey A.J. (1965)
 In 'Structure and Function of Connective and Skeletal Tissue'
 (S.Fitton-Jackson, R.Harkness, S.Partridge & G.Tristram, Eds.)
 Butterworths, London.
- Hodge A.J. (1965) In 'Treatise on Collagen'
 (G.Ramachandran, Ed.) Academic Press N.Y.
- Hoogervorst C.J.P. van Dyk J.A.P.P. & Smit J.A.M. (1978a)
 J. Phys. Chem. 82 (11) 1311 -
- Hoogervorst C.J.P. van Dyk J.A.P.P. & Smit J.A.M. (1978b)
 J. Phys. Chem. 82 (11) 1318 -
- Horlick G. Yuen W.K. (1976) Anal. Chem. 48 1643 -
- Hühnerman H.H. & Menzel N. (1979) Z. Naturforsch 34a 399 -
- Horejsi V. (1979) J. Chromatog. 178 (1) 1 -
- Hummel J.P. & Dreyer W.J. (1962) Biochem. Biophys. Acta 63 530 -
- Jackson S.D. (1978) Int. Rev. Biochem. 18 233 -
- Judis J. (1980) J. Pharm. Sci. 66 802 -
- Kanfer I (1975) Ph.D. Thesis, Rhodes University, Grahamstown S.A.
- Kanfer I & Cooper D.R. (1976) J. Pharm. Pharmac. 28 58 -
- Kantarovich L.V. & Krylov V.I. (1964)
 'Approximate Methods in Higher Analysis' Noordhof, Groningen
- Karush F. (1950) J. Am. Chem. Soc. 72 2705 -
- Karush F. (1952) J. Phys. Chem. 56 70 -

- Kauzman W. (1959) Adv. Protein Chem. 14 1 -
- Kelly P.C. & Horlick G. (1973) Anal. Chem. 45 (3) 519 -
- Kinget R. Bontinck A. Herbots H. (1979) Int. J. Pharm. 3 (2-3) 65
- Kirdani R.Y. Priore L. Murphy G.P. Sandberg A.A. (1979)
Prog. in Clinical & Biol. Res. 33 145 -
- Kirkwood J.G. Westheimer F.H. (1938) J.Chem. Phys. 2 331 -
- Kimura T. (1980) J. Pharm. Pharmac. 32 394 -
- Klotz I.M. (1946) Arch. Biochem. 9 109 -
- Klotz I.M. Walker F.M. & Pivan R.B. (1946)
J. Am. Chem. Soc. 68 1486 -
- Klotz I.M. & Urquhart J.M. (1949) J Am. Chem. Soc. 71 847 -
- Klotz I.M. (1953) In 'The Proteins' (H.Neurath & K.Bailey, Eds.)
Vol. I Academic Press N.Y. Pg 727 -
- Klotz I.M. (1953) Ann. N.Y. Acad. Sci. 226 18 -
- Klotz I.M. & Hunston D.L. (1971) Biochemistry 10 (16) 3065 -
- Klotz I.M. & Thompson C.J. (1971) Arch. Biochem. Biophys. 147 178 -
- Klotz I.M. Darnall D.W. & Langerman N.R. (1973) In 'The Proteins'
(H.Neurath & K.Bailey, Eds) Vol. I Academic Press N.Y. Pg. 727 -
- Klotz I.M. (1973) Ann. N.Y. Acad. Sci (US) 226 18 -
- Klotz I.M. (1974) Accounts of Chemical Research 7 162 -
- Klotz I.M. & Hunston D.L. (1975) J. Biol. Chem. 250 (8) 3001 -
- Klotz I.M. & Hunston D.L. (1979)
Arch. Biochem. Biophys. 193 (2) 314 -
- Koshland D.E. Nemethy G. & Filmer D. (1966) Biochemistry 5 364 -
- Kruger-Thiemer E. (1966) Arzneimittel-Forsch. 16 1431 -
- Kuchel P.W. Dalziel K. (1980) J. Theor. Biol. 85(3) 497 -
- Kühn K. Rautenburg J. Zimmerman B. & Tkocz C. (1968)
In 'Symposia on Fibrous Proteins'
(W.G. Crowther, Ed.) Plenum Press, N.Y. Pg. 181 -
- Kuntzel A. Schwenk M. (1940) Collegium 489
- Kuttan R. Donnelly P.V. & Di Ferrante N. (1981)
Experienta 37 (3) 221 -
- Lanczos C. (1967) 'Applied Analysis' (Pitman & Sons London)
Pg 272 - 280
- Langmuir J. (1918) J. Am. Chem. Soc. 91 162 -

- Lecureuil M. Lejeunne B. & Crouzat-Reynes G. (1973)
J. Chimie Physique 70 (5) 782 -
- Liao J.F. & Oehme K. (1980) *Vet. & Human Toxicol.* 22(3) 151 -
- Linderstrøm-Lang K. (1924) *Compt. Rend.* 15 (7)
- Lindup W.E. Rietbock N. & Woodcock B.G. (1980) In 'Methods in
 Chemical Pharmacology' (G. Neuhaus, Ed.)
 Vieweg & Sohn Wiesbaden.
- Lineweaver H. & Burke D. (1934) *J. Am. Chem. Soc.* 56 658 -
- Madden H.H (1978) *Anal. Chem.* 50 1383 - 1386
- Magar E.M. (1972) In 'Data Analysis in Biochemistry & Biophysics'
 Academic Press Chapter 13 Pg 401 -
- Makino S. Reynolds J.R. & Tanford C. (1973) *J. Biol Chem.* 248 4926 -
- McClain P.E. (1977) *Adv. Exp. Med. Biol.* 86B 603 -
- McElray J.C. D'Arcy P.F. (1980) *Int J. Pharm.* 6 3.4 205 -
- McPhie P. In 'Methods in Enzymology' (W.B. Jacoby Ed.) 22 23 -
- Mechanic G.L. (1975) *Colloq. Int. C.N.R.S.* 230 212 -
- Meyer M.C. & Guttman D.E. (1968) *J. Pharm. Sci.* 57 1627 -
- Meyer M.C. & Guttman D.E. (1970a) *J. Pharm. Sci.* 59 33 - 37
- Meyer M.C. & Guttman D.E. (1970b) *J. Pharm. Sci.* 59 37 - 43
- Michaelis L. (1925) *Z. Physik Chem.* 152 183 -
- Mihailova D. & Russeva V. (1978) *Proc. 11th Int. Symp. IUPAC
 Chemistry of Natural Products Series 1* 49 - 52
- Miller E.J. Matukas V.J. (1969) *Proc. Natl. Acad. Sci* 64 1264
- Miller E.J. Epstein E.H. & Piez K.A. (1971)
Biochem. Biophys Res. Commun. 42 1024 -
- Miller E.J. & Matukas V.J. (1974) *Fed. Proc.* 33 1197 -
- Miller S.C. (1979) *Comput. Biomed Res.* 13 52 -
- Mitchell A.D. Taylor I.E.P. (1970) *Analyst.* 95 1003 -
- Monad J. Changeaux J.P. & Jacob F. (1963) *J. Mol. Biol.* 6 306 -
- Monad J. Jacob F. & Changeaux J.P. (1965) *J. Mol. Biol.* 12 88 -
- Morgan P.H. Jacobs H.G. Segrest J.P. & Cunningham L.W. (1970)
J. Biol. Chem 245 5042 -
- Munson R.J. & Rodbard D. (1980) *Anal. Biochem.* 107 220 -

- Nakano N.I. Takayuki O. Sato N. Shimamori Y. & Yamaguchi S. (1979)
Chem. Pharm. Bull. 27 (9) 2048
- Nemethy G. & Scheraga H.A. (1962) J. Phys. Chem 66 1773 -
- Nichol L.W. & Ogsten A.G. (1965) J. Phys. Chem. 69 4365 -
- Nicolson A.M. Bennett C.L. Lamensdorf D. & Susman L (1972)
I.E.E.E. Trans. Microwave Theory & Techniques
MTT-20 (1) 3 - 9
- Nicolson A.M. (1973) Res.Paper - Sperry Res. Center SCRC-RP-73-16
- Noerby J.G. Ottolenghi P. & Jensen J.E. (1980)
Anal. Biochem. 102 (2) 318 -
- O'Halloran R.J. Smith D.E. (1978) Anal. Chem. 50 1939 -
- Olsen B.R. Alpwer R. & Kefalides N.A. (1973)
Eur. J. Biochem. 38 220 -
- Ollis W.H. (1961) Chemistry of Natural Phenolic Compounds
Pergamon Press London
- Orndorff W.R. & Sherwood F.W. (1923) J. Am. Chem. Soc. 45 486 -
- Ortung W.H. (1968) J. Am. Chem. Soc. 91 162 -
- Otto G. (1953) Das Leder 4 1 -
- Papoulis A. (1962) 'The Fourier Integral and its Applications'
McGraw-Hill N.Y.
- Parsons J.S. (1958) Anal. Chem. 30 (7) 1262 -
- Parsons D.L. Vallner J.J. (1980) Acta Pharm. 17 12 -
- Pasto D.J. & Johnson C.R. (1969)
in 'Organic Structure Determination' Pg. 101
Prentice-Hall N.J.
- Pedersen P.V. Crookes M.J. & Brown K.F. (1977)
J. Pharm. Sci. 66 1458 -
- Pedersen P.V. (1978) J.Pharm. Sci. 67 908 -
- Perutz M.F. (1965) J. Mol. Biol. 13 646 -
- Peters F. Pingoud A. (1979) Int. J. Biomed. Comput. 5 401 -
- Phillips D.C. (1967) Proc. Natl. Acad Sci. (US) 57 484 -
- Piez K.A. Eigner E.A. & Lewis M.S. (1963) Biochemistry 2 58 -
- Piez K.A. (1967) In 'Treatise on Collagen' Vol. I
(G.N. Ramachandran, Ed.) Chapter 8 Pg 207

- Piez K. Miller E.J. Lane J.M. & Butler W.T. (1970)
 In 'Chemistry and Molecular Biology of the
 Intercellular Matrix' (E.A. Balazs Ed.) Vol. I Pg 117
- Piez K.A. Trus B.L. (1979) J Am. Chem. Soc. 2 55 -
- Piez K.A. (1980) Dev. Biochem. 15 143 - 2 55 -
- Pinto J.S. Bentley J.P. (1974) Biochem. Biophys. Acta 354 254 -
- Pohl F.M. (1978) FEBS Symp. 58 3 -
- Polet H. & Steinhardt J. (1968) Biochemistry 7 1348 -
- Prockop D.J. Dehm P. Olsen B.R. Berg R.A. Grant M.E. (1973)
 'Biology of the Fibroblast' (E.Kulonen & J.Pikkerainen Eds.) Pg 311
- Prockop D.J. (1979) In 'Chemistry and Molecular Biology of the
 Intercellular Matrix' (Ed. E.A. Balazs) Vol. I Pg 335
- Proctor H.R. Wilson J.A. (1916) J. Am. Chem. Soc. 38 1982
- Rachidy E. Niazi S. (1978) J. Pharm. Sci. 67 (7) 967 -
- Ramachandran G.N. Kartha G. (1955) Nature (London) 176 593 -
- Ramachandran G.N. (1967) 'Treatise on Collagen' Academic Press London
- Ramachandran G.N. & Reddi A.H. (1976)
 'Biochemistry of Collagen' Plenum Press London
- Rautenburg J. Kühn K. (1968)
 Hoppe Seylers Z. Physik. Chem. 349 611 -
- Ray A. Reynolds J. A. Polet H. Steinhardt J. (1966)
 Biochemistry 5 2606 -
- Reed R. (1966) In 'Science for Students of Leather Technology'
 (A.G. Ward Ed.) Pergamon Press, N.J.
- Reed K.C. (1973) Biochem. Biophys. Res. Comm. 50 (4) 1136 -
- Reif R. Kamino T.I. & Sarawat K. (1978)
 J. Electrochem Soc. 125 (11) 1860 -
- Rencken E.M. (1955) J. Gen. Physiol. 38 225 -
- Reynolds J. (1967) Biochemistry 6 937 -
- Reynolds J.A. Herbert S. Polet H. & Steinhardt J. (1967a)
 Biochemistry 5 2606 -
- Reynolds J.A. Herbert S. Polet H. & Steinhardt J. (1967b)
 Biochemistry 6 937 -

- Reynolds J.A. Gallagher J.P. & Steinhardt J. (1970)
Biochemistry 9 1232 -
- Rich A. Crick F.H.C. (1955) *Nature (London)* 176 593 -
- Robertson J.S. Madsen B.W. (1974) *J. Pharm. Sci.* 62 234 -
- Rocha E. Silva M. (1960) *Arch. Int. Pharmacodyn.* 128 355 -
- Rodkey F.L. (1961) *Arch. Biochem. Biophysics* 94 38 -
- Romer J. Bickel M. (1979) *J. Pharm. Pharmac.* 31 (1) 7 -
- Rossotti F.J.C. & Rossotti M. (1961) 'The Determination of
 Stability Constants' McGraw-Hill N.Y.
- Rosenthal (1967) *Anal. Biochem.* 20 525 -
- Roux D.G. Drewes S.E. Saayman H.M. (1965)
J. Soc. Leather Tr. Chem. 49 416 -
- Russell A.E. Cooper D.R. (1969) *Biochemistry* 8 (10) 3980 -
- Russo S.F. Engel R.G. (1978) *Biopolymers* 17 (4) 837 -
- Savitzky A & Golay M.J.E. (1964) *Anal. Chem.* 36 1627 -
- Scatchard G. (1949) *Ann. N.Y. Acad. Sci.* 51 660 -
- Scatchard G. & Black E.S. (1949) *J. Phys. Colloid Chem.* 53 88 -
- Scatchard G. Coleman J.S. & Shen A.L. (1957)
J. Am. Chem. Soc. 79 12 -
- Scatchard G. Coleman J.S. & Shen A.L. (1959)
J. Am. Chem. Soc. 89 6104 -
- Schmitt F.O. Gross J. & Highberger J.H. (1953)
Proc. Natl. Acad. Sci. (USA) 34 459 -
- Schmitt F.O. Levine L. Drake M.P. Rubin A.L. Pfahl D. and
 Davison P.F (1964) *Proc. Natl. Acad. Sci.* 51 493
- Schutte J. (1981) *Rev. Sci. Instruments* 52 (3)
- Sharon N. Lis N. (1981) *Chem. Eng. News* 59 (13) 21 -
- Shen D. Gibaldi M. (1974) *J. Pharm. Sci.* 63 (11) 1698 -
- Shieh D. Feijen J. & Lyman D.J. (1975) *Anal. Chem.* 47 1186 - 1188
- Shuttleworth S.G. Russell A.E. Williams-Wynn W. (1952)
J. Leather Tr. Chem. 12 486 -
- Silhavy T.J. Smelcman S. Boos W. & Schwartz M. (1975)
Proc. Natl. Acad. Sci. (USA) 72 (6) 2120 -
- Simon W. (1972) 'Mathematical Techniques for Physiology &
 Medicine' Academic Press N.Y. Pp 77 - 88

- Sinanoglu O. (1968) In 'Molecular Associations in Biology'
(B. Pullman Ed.) Academic Press N.Y. pg 427
- Smith J.B. Jubiz W. (1980) Steroids 36 (4) 393 -
- Sprague E.D. Larabee C.E. Halsall H.B. (1980)
Anal. Biochem. 101 175 -
- Stark M. Rauterberg J. KÜhn K (1971) FEBS Lett. 13 101 -
- Stein H.H (1965) Anal. Biochem. 13 305 -
- Steinberg I.Z. & Schachman H.K. (1966) Biochemistry 5 3728 -
- Steiner R.F. (1953) Arch. Biochem. Biophys. 46 291 -
- Steiner R.F. (1980) Molecular and Cellular Biochemistry 31 5 -
- Steinhardt J. & Beychok S. (1964) Proteins 2 139 -
- Steinhardt J. & Reynolds J.A. (1969) In 'Multiple Equilibria in
Proteins ' Academic Press N.Y.
- Steinier J. Termonia Y. & Deltour J. (1972) Anal. Chem. 44 1906 - 1909
- Stewart K.K (1977) Adv. Prot. Chem. 31 135 - 185
- Stuart R.D. (1966) 'An Introduction to Fourier Analysis'
Chapman & Hall Ltd. London Pg 218 - 231
- Suarrez G. Veliz M. Nagel R.L. Arch. Biochem. Biophys. 205 (2) 422 -
- Sukow W.W. Sandberg H.E. & Lewis E.A. (1980)
Biochemistry 19 (5) 912 -
- Tanaka S. (1977) Thermochemica Acta 25 269 -
- Tanford C. & Kirkwood J.G. (1957) J. Am. Chem. Soc. 79 5333 -
- Tanford C. (1961) In 'Physical Chemistry of Macromolecules '
Wiley N.Y. Chapter 8 Pp 526 -
- Tanford C. (1969) J. Mol. Biol. 39 539 -
- Tanzer M.L. (1976) Proc. Biochem. Conf. Collagen 137 -
- Taylor G. (1953) Proc Roy. Soc. London A219 186 - 206
- Tejima K. Ozeki S. (1979) Chem. Pharm. Bull. 28 (2) 585 -
- Terry P. (1975) 'Special Scientific Subroutines for the ICL
1900 Series Computer' Computer Centre
Publication Rhodes University Grahamstown, S.A.
- Thakur A.K. Munson P.J. Hunsten D.L. & Rodbard D (1980)
Anal. Biochem. 103 240 - 254

- Tipping E. Moore B.P. Jones C.A. Cohen G.M. Ketterer B.
Bridges J. (1980) Chem.- Biol. Interactions 32 291 -
- Traub W. Piez K.A. (1971) Adv. Prot. Chem. 25 243 -
- Trueb B. Odermatt B.F. Sahu A.P. Spiess M. Ruettnen J.R.
and Winterhalf K.M. (1980) Renal Physiol. 3 23 -
- Tukamoto T. Ozeki S. Hattori F. Toshida T. (1974)
Chem. Pharm. Bull. 22 385 -
- Turner G.M.S. (1974) M.Sc (Chem. Eng.) Dissertation
University of the Witwatersrand, Johannesburg S.A.
- Turley H.G. (1926) J. Am. Leather Chem. Soc. 21 117
- Udenfriend S. (1970) In 'Chemistry and Molecular Biology of the
Intercellular Matrix' Volume I Pg 371 -
- Veis A. Anesy J. Mussel S. (1967) Arch. Biochem. Biophys. 98 104 -
- Viidick A. Vuust J. (1980) Proc. Aarhus Symposium on Fibrous
Proteins Academic Press London
- Von Hippel P.H. (1967) In 'Treatise on Collagen '
(G. Ramachandran Ed.) Vol. I Pg 253
- Von Hippel P.H. Scheich T. (1969)
In 'Structure and Stability of Biological Macromolecules'
(S.N. Timasheff & G.D. Fasman Eds.) Academic Press N.Y.
- Waldmann-Meyer H. (1980) Anal. Chem. Symp 3 125 -
- Wang C.A. Leavis B.C. Horrock W. Gergely J. (1981)
Biochemistry 20 2439 -
- Weber G. (1975) Adv. Prot. Chem. 29 1 - 83
- Weiss J.B. (1976) in "The Methodology of Connective Tissue Research"
(D.A. Hall Ed.) Joynson-Bruvvers Ltd. London.
- Whitehead E.P. (1980) J. Theor. Biol 86 (1) 45 -
- Whitehead E.P. (1980) J. Theor. Biol 87 (1) 153 -
- Whitlam J.b. & Brown R.F. (1980) Int. J. Pharmaceutics. 5 49 -
- Wolfenden R. Andersson L. Cullis P.M. Southgate C.C.B. (1981)
Biochemistry 20 (4) 849 -
- Woosely J.T. Muldoon T.G. (1977) J. Steroid Biochemistry 8 625 -
- Wylie C.R. (1975) in 'Advanced Engineering Mathematics'
McGraw-Hill N.Y.
- Wyman J. (1964) Adv. Protein Chem. 19 327 -